Marine sponges and their associated bacteria

as bioresource for the production of antimicrobial compounds

DISSERTATION

zur

Erlangung des Doktorgrades (Dr. rer. nat.)

der

Biologie und Chemie Fakultät

der

Justus-Liebig-Universität Gießen

vorgelegt von

RIYANTI

aus

Daerah Istimewa Yogyakarta, Indonesien

Gießen, 2021

Angefertigt mit Genehmigung der Biologie und Chemie Fakultät

der Justus-Liebig-Universität Gießen

1. Gutachter	: Prof. Dr. Till F. Schäberle
2. Gutachter	: Prof. Dr. Thomas Wilke

Erscheinungsjahr : 2021

In advance Publications of the Dissertation

Riyanti; Marner, M.; Hartwig, C.; Patras, M.; Wodi, S.; Rieuwpassa, F.; Ijong, F.; Balansa, W.; Schäberle, T. **Sustainable Low-Volume Analysis of Environmental Samples by Semi-Automated Prioritization of Extracts for Natural Product Research (SeaPEPR).** *Mar. Drugs* **2020**, *18*, 649, doi:10.3390/md18120649.

Riyanti; Balansa, W.; Liu, Y.; Sharma, A.; Mihajlovic, S.; Hartwig, C.; Leis, B.; Rieuwpassa, F.J.; Ijong, F.G.; Wägele, H.; et al. **Selection of sponge-associated bacteria with high potential for the production of antibacterial compounds**. *Sci Rep* **2020**, *10*, 19614, doi:10.1038/s41598-020-76256-2.

.

Selbstständigkeitserklärung

Hiermit versichere ich, die vorgelegte Thesis selbstständig und ohne unerlaubte fremde Hilfe und nur mit den Hilfen angefertigt zu haben, die ich in der Thesis angegeben habe. Alle Textstellen, die wörtlich oder sinngemäß aus veröffentlichten Schriften entnommen sind, und alle Angaben die auf mündlichen Auskünften beruhen, sind als solche kenntlich gemacht. Bei den von mir durchgeführten und in der Thesis erwähnten Untersuchungen habe ich die Grundsätze guter wissenschaftlicher Praxis, wie sie in der ‚Satzung der Justus-Liebig-Universität zur Sicherung guter wissenschaftlicher Praxis' niedergelegt sind, eingehalten. Gemäß § 25 Abs. 6 der Allgemeinen Bestimmungen für modularisierte Studiengänge dulde ich eine Überprüfung der Thesis mittels Anti-Plagiatssoftware.

07.06.2021	Riyanti
Datum	Unterschrift

Acknowledgments

First and foremost, Alhamdulillah, I am deeply grateful to the Almighty Allah SWT.

I offer my sincerest gratitude to my supervisor, Prof. Dr. Till F Schäberle, for allowing me to join his working group, his supervision, and constant support from the beginning in Bonn until the end in Gießen. His invaluable help of constructive comments suggestions throughout the experimental and thesis works have contributed to the success of this research. It was a great privilege and honour to work and study under his guidance. His dynamism, vision, friendship, empathy, and great sense of humour have deeply inspired me.

I would like to thank my supervisor Prof. Dr. Thomas Wilke for his help, support, and generous advice during my study.

I really appreciate Prof. Dr. Adriaan Dorresteijn and Prof. Dr. Ocky Karna Radjasa for their kind participation in the examination committee.

I would like to say thanks to my research colleagues from the previous and present working group of König and Schäberle: Luis Linares-Otoya, I Dewa Made Kresna, Lei Wang, Jil-Christine Kramer, Nils Böhringer, Abha Sharma, Katja Fisch, all lab mates and research team. Moreover, special thanks are conveyed as well to Zerlina G Wuisan who is together to be my best friend struggling to complete finish the study. I also thank Ms. Alexandra Bender for her genuine support throughout this study and her help during my time in Germany.

I am highly thankful to Dr. Ute Mettal, Dr. Yang Liu, and Christoph Hartwig for providing valuable assistance, helping me in mass spectrometry analysis, chemistry analysis, and their contribution in editing my publications.
I also appreciate all the support I received from Dr. Apisada Jiso, Dr. Aninditia Sabdaningsih, Dr. Zina Nasfi, and Dr. Diah Ayuningrum.

I am using this opportunity to express my gratitude to Prof. Dr. Heike Wägele, Dr. Maria A. Patras, Dr. Sanja Mihajlovic, Dr. Michael Marner and Dr. Walter Balansa for the support, great collaboration research, and publication.
I am extremely grateful to my husband, Mukti Trenggono, my three children, Nadiya, Zalfaa, Aksa, my parents, and the whole big family in Indonesia, for every effort and encourage me during this study. I am very much thankful for their love,

understanding, valuable prayers, and continuing support to complete this study. It was a wonderful experience going through PhD life with three lovely children.

My appreciation also goes to mas Purwanto for his help during sponge collections and the opportunity to join Reef Health Monitoring in Cenderawasih Bay National Park, Papua.

Then the great thank is presented for Indonesia Endowment Fund for Education (LPDP), for funding during the first four years of my PhD and *Programms zur Promotionsabschlussförderung im Rahmen des Gleichstellungskonzepts der Justus-Liebig-Universität Gießen* for financial support until the end of my PhD.

I am extending my thanks to my home University, Jenderal Soedirman University, Indonesia for permission to study abroad. I would express my gratitude to Dr.rer.nat Hamdan Syakuri whose guidance, support, and encouragement has been invaluable throughout this study. In addition, a thank you also to my colleagues for the constant support.

Finally, my thanks go to all the people who have supported me to complete the research work directly or indirectly.

Table of Contents

1. Introduction

1.1. Marine sponges as bioresource for marine natural products

The marine environment has been a source of bioactive compound discovery due to its enormous biodiversity, complex environmental parameters, and production of secondary metabolites by marine organisms and their associated microorganisms (Bibi et al., 2020). Marine sponges, jellyfish, sea anemones, corals, bryozoan, molluscs, echinoderms, tunicates, and crustaceans have all developed bioactive metabolites of interest for application in various fields, e.g. medicine, pharmacology, and nutraceuticals (Bhakuni and Rawat, 2005). More than 15,000 natural compounds isolated from marine invertebrates have already been reported, including bioactive compounds and antibiotics from sponges (Brinkmann et al., 2017). Sponges are sessile, ancient metazoans and belong to the phylum Porifera. Sponges are categorized into four classes with 25 orders, 128 families, and 680 genera (Van Soest et al., 2012). There are approximately 8,500 valid sponge species currently recognized.

Because of the longevity, abundance, and extraordinary survival, marine sponges are valuable components of the benthic community (Thakur and Singh, 2016). As compared to coral reefs, sponges are the second largest benthic community, and the diversity of sponge species outnumbers the total species diversity of all other organisms in the community (Anteneh et al., 2021). The fact that sponges have existed for so long in such diverse and extreme environments suggests that they are highly developed and successful organisms (Brinkmann et al., 2017). The sponges are remarkable in that they have no specialized organs or behaviours, but can be found in temperate, tropical, and polar environments. Most sponges have siliceous spicules, which give them an advantage over other calcareous species that are affected by ocean acidification and global warming (Thakur and Singh, 2016).

Allelopathy, or chemical defence, is most essential for all sessile invertebrates in the case of soft-bodied organisms like sponges, which lack physical defence strategies (Thakur and Singh, 2016). Many bioactive secondary metabolites have been observed in sponges in recent years, and more than 300 new and novel bioactive compounds had been identified from a single Porifera phylum and several compounds were tested in preclinical and clinical trials (Blunt et al., 2018).

The US Food and Drug Administration (FDA) and the European Medicines Agency (EMA) have licensed 14 marine-derived drugs, whereof three of them were discovered from sponges. First, Vidarabine (Vira-A®) is an antiviral compound obtained from the sponge *Cryptotethya crypta*. The two others have been certified for cancer treatment, i.e. (1) Cytarabine (Cytosar-U® and Depocyt®), reported in the sponge *Cryptotethya crypta* and (2) Eribulin mesylate (Halaven®), isolated from the sponge *Halichondria okadai* (Clinical Pipeline Marine Pharmacology; Izzati et al., 2021).

1.2. Interaction of sponges with other organisms

1.2.1. Interaction of sponges with macroorganisms

Allelopathy is described as the use of toxic chemicals to directly inhibit one species from another. These allelochemicals are secondary metabolites, meaning they are not directly involved in the organism's growth and reproduction. Allelochemicals may be released into the water column or transferred between donor and recipient cells by cell-to-cell contact.

Marine sessile invertebrates, especially soft-bodied sessile invertebrates like sponges that lack adequate physical defence mechanisms, produce allelochemicals as a chemical defence against rivals for resources during spatial competition (Sammarco et al., 1983; Thakur and Singh, 2016), preventing epibiosis and predator deterrence (Becerro et al., 1997). The chemical ecology of benthic species has revealed new information about the possible functions of secondary metabolites in these processes (Bakus et al., 1986; Hay, 1996). While sponges are slow-growing species, their morphological plasticity allows them to change their overall shape and size to keep up with other fast-growing sessile organisms. In areas where substratum is inadequate, sponges acquire living space through growth interactions and/or the production of allelochemicals (Singh and Thakur, 2016).

Since the structure of tropical reef ecosystems is influenced by both, competition for space and predation, there are numerous opportunities to investigate the various ecological functions of secondary metabolites. Thacker`s finding is the first to reveal that a secondary metabolite plays a role in the spatial competition between reef invertebrates, which it is likely to play a role in other sponge-based competitive interaction. Natural predators like reef fish (Pawlikl and Chanasl,

1995), starfish (Wulff, 1995), and the sponge itself have been recorded to be deterred by secondary metabolites from a wide variety of benthic species (Thacker et al., 1998).

According to various studies on sponge spatial competition, these chemicals aid sponges in preventing the overgrowth of other organisms, enabling the sponge to occupy more area (Engel and Pawlik, 2005). Allelochemicals produced by sponges may prevent other organisms' larvae from settling on their surfaces. This helps to keep their pores unclogged and their feeding rate at an optimum level (Singh and Thakur, 2016).

Marine sessile invertebrates such as sponges, bryozoans, cnidarians, and macroalgae are constantly stressed in complex environments such as rocky intertidal zones, due to restricted substratum availability (Singh and Thakur, 2016). Interactions between two or more different sponge species have previously been reported, including cases of mutualism, parasitism, and space competition.

For example, the Mediterranean sponge *Crambe crambe* does not allow other sponges to expand within a few centimeters of its borders, implying that their allelochemicals can play a role in establishing the zone of inhibition in the environment. In contrast, spatial interactions among sponge species, such as over-growth/out-growth, are symbiotic in nature, with the basal sponge serving as a suitable substratum and the overgrown sponge serving as an epizoic. Epizoic sponges were found to have a higher survival rate when they adhered closely to the supporting sponges (Singh and Thakur, 2016).

The majority of the research also focused on the interaction of sponges and corals. Sponge-coral interactions are common in coral reefs where there is fierce competition for space and aggressive sponges often overgrow the coral (Ávila et al., 2007). By drilling deeply into living coral heads, the bio-eroding sponge *Siphonodictyon* sp. has been confirmed to produce an allelochemical called siphonodictidine, which affects the growth and respiration rates of nearby coral polyps (Sullivan et al., 1983). The sponge produces mucus, which serves as a carrier for this allelochemical, which prevents coral growth around the base of these sponges' oscular chimneys. Sponges interact with corals by releasing active metabolites that weaken coral skeletal integrity and reduce photosynthetic efficiency and respiration, resulting in decreased coral growth (Sullivan et al., 1983; Pawlik et al., 2007).

Chemical-mediated interactions were also observed within sponges and micro-algae associated with corals. By inhibiting the photosynthesis of microalgal symbionts, some Caribbean sponges induce bleaching of the massive coral *Diploria labyrinthiformis*. The sponge was discovered to have two effects on coral microalgal symbionts (zooxanthellae): a) photosynthesis impairment with bleaching and b) photosynthesis impairment without significant bleaching. The allelochemicals pyrrole-imidazole alkaloids present in the sponge *Agelas clathrodes* led to the breakdown of the coral-zooxanthellae symbiosis (Pawlik et al., 2007).

The zoanthids and bryozoans are also reported to compete with the sponge. The sponge *Cinachyrella cavernosa* competed for space with *Zoanthus sansibaricus* in the intertidal regions of India's west coast. Allelochemicals released by both species to protect their occupied space seem to be mediating this impasse competition (Thakur and Singh, 2016). Furthermore, Jackson and Buss (1975) and Nandakumar et al.(1993) reported that allelochemicals detected in sponge extracts were found to be the cause of bryozoan mortality. Due to the use of whole organism extracts, these findings did not assist in estimating natural concentrations of allelochemicals released during such competitions. The toxic chemicals could be stored within the sponges and released at various concentrations depending on the level of competitive interactions (Jackson and Buss, 1975). Allelochemicals have been found to help sponges outgrow competitively dominant bryozoan organisms in a space-constrained environment (Thakur and Singh, 2016).

Production of allelochemicals of marine sponges is affected by biological and ecological factors. One of the most critical barriers for sessile invertebrates is the availability of nutrients, which affects both, their primary (growth and reproduction) and secondary functions (production of defensive chemicals). Because of its efficient filtration rate and nutrient availability, the abundance of a specific sponge will increase, potentially also resulting in the extinction of other sponge species. This emphasizes the significance of food as an energy source for a variety of energy-intensive processes, including overall growth and allelochemical production (Singh and Thakur, 2016).

1.2.2. Interaction between sponges and microorganisms

It has been discovered that marine sponges are home to rich and plentiful communities of symbiotic microorganisms (Kennedy et al., 2009; Mehbub et al.,

2014). The sponge mass contains 35-60% of microorganisms including cyanobacteria, heterotrophic bacteria, fungi as well as unicellular algae. Microorganisms live on the sponge`s outer layers and more permanently inside the sponge`s mesohyl (Brinkmann et al., 2017). Within the sponge, a series of feeding chambers are formed by specialized flagellated cells (choanocytes) (Taylor et al., 2007). The choanocytes are types of cells arranged in chambers that trap food particles in sea water, such as bacteria, unicellular algae, and viruses, then these are transported to the mesohyl, a thick connective tissue layer (Figure 1.1). Food particles are digested by another type of sponge cell, the archaeocytes, in the mesohyl through phagocytosis. Many sponges have dense colonies of microorganisms in their mesohyl (Taylor et al., 2007; Hentschel et al., 2012).

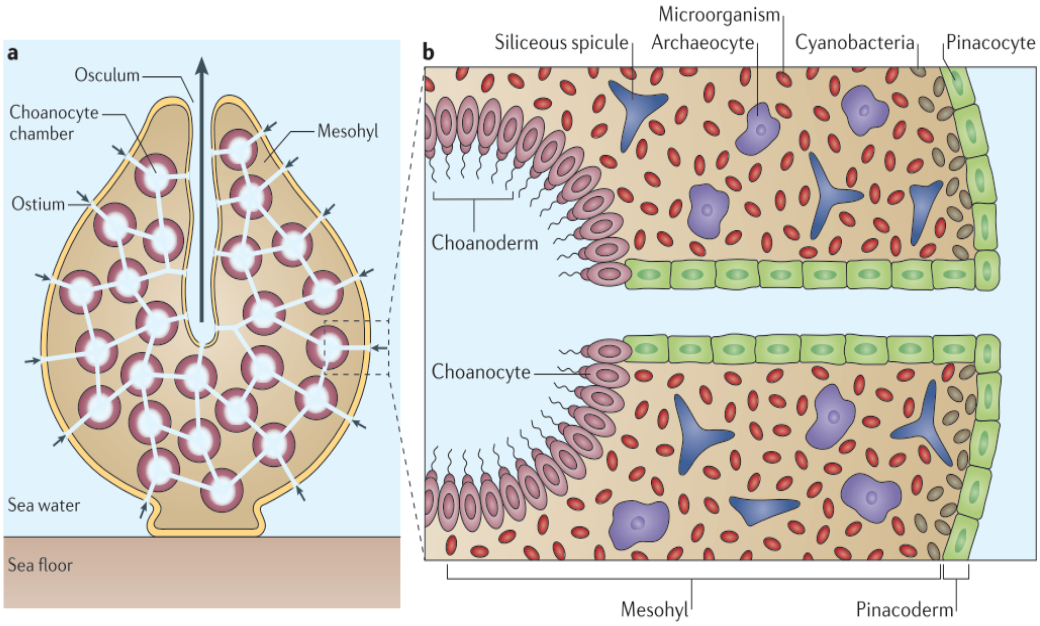

Figure 1.1. The body plan of marine sponges. A schematic overview of a typical demosponge (a) An enlargement of the internal structure of a typical demosponge (b) (Hentschel et al., 2012).

Microorganisms living inside sponge hosts, on the other hand, could become sponge specific, as demonstrated by the fact that distantly related sponges from various geographical locations harbor similar microbial groups that have not been found in nearby seawater or other marine environments (Webster and Taylor, 2012). Despite the fact that their sessile filter-feeding lifestyle exposes them to the microbes in the seawater, which are their primary food source, they have different symbiotic microbial communities (Pita et al., 2018). Sponge hosts may be

considered ecosystem engineers because they provide a specific environment that favors the presence and survival of certain microbes while excluding others (Wehrl et al., 2007).

The functions of the diverse microbes in sponge biology start from the microbe as the source of nutrition to mutualistic symbioses with the sponge (Kennedy et al., 2009; Mehbub et al., 2014). The sponge can recognize the difference between food bacteria and bacterial symbionts. They often gain control over their microbial inhabitants through distinguishing between foreign and symbiotic (Wilkinson et al., 1984; Wehrl et al., 2007), most likely through the innate immune system (Pita et al., 2018). The sponge *Aplysina aerophoba* was analyzed to assess bacterial isolate uptake rates, and it was revealed that the sponge could differentiate between phagocytized food bacteria and bacterial symbionts (Wehrl et al., 2007). Sponges may harbor photoautotrophic symbionts that not only benefit in host nutrition by transporting photosynthetically fixed carbon and nitrogen (Freeman and Thacker, 2011; Freeman et al., 2013) but also lead to ecosystem primary productivity (Wilkinson, 1987).

In a study on bacterial-eukaryote interactions, Dudler and Eberl (2006) found growing facts to justify the hypothesis that the secondary metabolites formed by symbiotic bacteria are the product of bacteria cell-to-cell signaling. Schmidt (2008) studied how species collaborate in the synthesis of natural products. They discovered that partners can share and alter natural products created by each other, as well as clarify how host organisms use these secondary metabolites.

Microbes that survive in these nutrient-poor and antagonistic habitats, such as marine sponges, often develop several secondary metabolites to counteract the harmful effects of the environment (Selvin et al., 2012). Figure 1.2 shows that the sponge microbiome also imparts protective abilities to the host, which have a significant impact on sponge-organism interactions in benthic communities. The sponge microbiome affects benthic population composition by affecting holobiont vulnerability to predation (Pita et al., 2018).

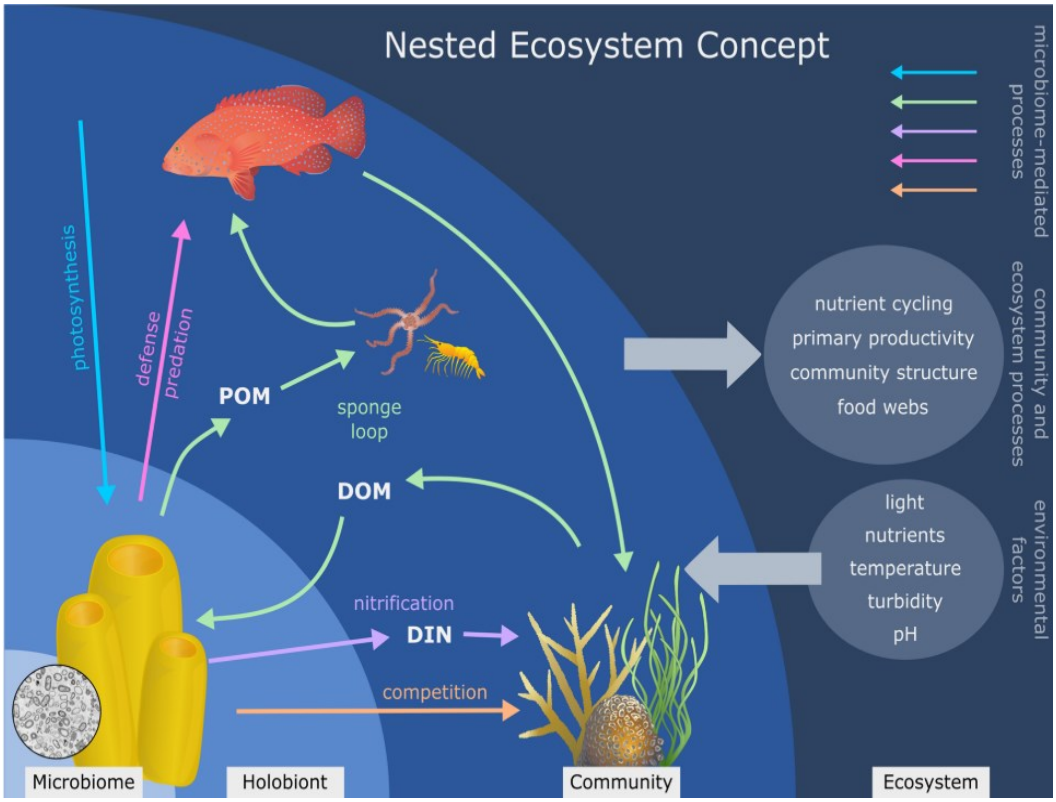

Figure 1.2. An example of a nested ecosystem is a sponge holobiont. The microbiome's key functions (colored arrows) affect holobiont function and, as a result of cascading impacts, population structure, and ecosystem function. DOM, dissolved organic matter; POM, particulate organic matter; DIN, dissolved inorganic nitrogen (Pita et al., 2018).

Sponge defences include the development of biologically active feeding deterrent compounds (Pawlikl and Chanasl, 1995; Rohde et al., 2015). In a variety of chemically defended sponge organisms, subsequent studies have found increasing evidence that the microbiome is actively responsible for the production of bioactive compounds with putative anti-predatory effects (Pita et al., 2018). Another crucial function of secondary metabolites biosynthesized by sponge-associated bacteria is their biological activity as antibiotics, antifungal, and anti-predation or antifouling compounds. Although the sponges' associated microbes produce secondary metabolites, each of these sponges may have its microbial symbiosis (Mehbub et al., 2014). Bioactive metabolites produced by microbes that can prevent sponges from infection and predation are evidence for the mutualistic relationship between microbes and sponges (Kennedy et al., 2009).

Another significant biotic aspect that influences benthic communities is spatial competition, and the sponge microbiome can mediate such interspecific interactions through a combination of metabolic and chemical defensive functions that strengthen the holobiont's competitive ability (Pita et al., 2018). Since microbial symbionts are critical to sponge health, disruptions in symbiosis as a consequence of climate change/environmental stress are likely to affect sponge health, growth rates, or their ability to protect themselves against predation, fouling, and disease (Webster and Taylor, 2012).

1.3. Antimicrobial compounds producing marine sponges from Indonesian waters

Considering the Caribbean, Mediterranean, and British Isles, for each 500-800 species are reported, while the sponge faunas of Australia, Papua New Guinea, and Indonesia, which have high biodiversity, are less described (Mehbub et al., 2014). Indo-Pacific regions, including Indonesia, are becoming targets in the ongoing quest for bioactive compounds that are abundant in marine invertebrates (Sabdono and Radjasa, 2008). According to the latest discovery trend, China, Australia, and Indonesia can be predicted to be the source of more new compounds. The coral reefs of Indonesia are among the most diverse in the world. About 850 species are thought to be present, the published literature on sponge taxonomy in Indonesia is still incomplete (De Voogd et al., 2006). As a result, Indonesian marine biodiversity has become a focus of global and domestic biodiscovery, especially in the field of marine natural product chemistry.

Many novel marine natural products (MNPs) have been discovered in Indonesian sponges including alkaloids, terpenoids, peptides, and polyketides. A review by Izzati et al. (2021) covering the period from 2007-2020 showed that sponges were found to be involved in the production of 105 novel compounds, the major components were alkaloids. The majority of sponges were collected from the east area of Indonesia, i.e. Sulawesi islands (Figure 1.3, Table 1.1). Manzamines are the sponge alkaloids that have been isolated and shown a wide variety of biological activities (Sakai and Higa, 1986; Furusato et al., 2014). The marine sponge *Acanthostrongylophora ingens* yielded 21 alkaloids, five of these were new manzamine alkaloids, acanthomanzamines A-E. The majority of the sponge alkaloids were discovered in the genera *Aplysinella* and *Acanthosrongulophora*. Terpenes and peptides were the next two major classes of metabolites reported

from Indonesian sponges. The order Dictyoceratida, in which the dominant genera are *Lamellodysidea* and *Carteriospongia*, yielded nearly all the sponge terpenoids.

Furthermore, Mehbub et al. (2014) reported that on average one individual species contributed 3 – 5 compounds. Of all the sponge orders investigated, the order Dictyoceratida was observed as being the most prolific producer of new compounds. Because of the ability to produce new bioactive compounds, *Dysidea* sp. and *Ircinia* sp. can be regarded as the most promising genera for future bioprospecting campaigns.

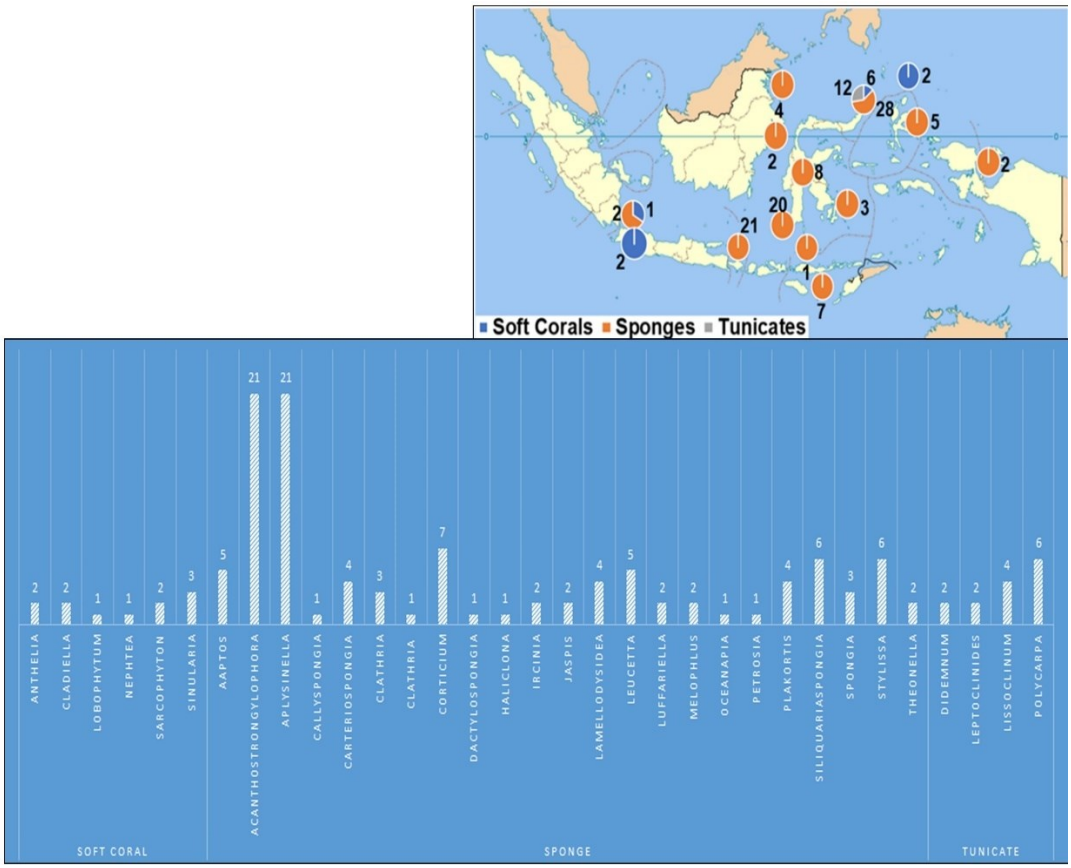

Figure 1.3. The distribution of the sample is produced by the origin of sponges (Porifera), tunicates (Chordata), and soft corals (Cnidaria) (Izzati et al., 2021).

Table 1.1. Summary of the marine natural products isolated from marine sponges derived from Indonesian oceans reported from 2007 to 2020 (Review in Izzati et al., 2021).

Group of compounds (number)	Sponge species	Location
Alkaloids (21)	*Acanthostrongylophora ingens*	-Mantehage, North Sulawesi -Bajotalawaan, North Sulawesi -Wakatobi Marine National Park in Southeast Sulawesi -South Sulawesi
Bromopyrrole alkaloids (2)	*Stylissa massa*	Papua
Alkaloids (4)	Genus *Stylissa*	Derawan Island, Berau, Northeast Kalimantan
Guanidine alkaloids (3)	*Clathria bulbotoxa*	Samalona Island, South Sulawesi
Imidazole alkaloids (4)	*Leucetta chagosensi* *Leucetta microraphis*	-Kapoposang Island, South Sulawesi -North Sulawesi
β-carboline alkaloids (2)	Luffariealla variabilis	North Sulawesi
Pyridoacridine alkaloid (1)	*Oceaniapia* sp.	Ambon, Maluku Islands
Steroidal alkaloids (7)	*Corticium simplex*	Flores Island, East Nusa Tenggara
Aaptamine derivates (5)	*Aaptos suberitoides* *Aaptos* sp.	Kupang, East Nusa Tenggara
Psammaplysin derivatives (21)	*Aplysinella strongylata*	Tulamben Bay, Bali
Terpenes (4)	*L. herbacea*	Manado, North Sulawesi
Terpenoids (3)	*Spongia* sp.	Bunaken Marine Park, North Sulawesi

Scalarane-based sesterterpenoids (4)	*Carterospongia foliascens*	Palau Barang Lompo, near Makasar, South Sulawesi
Sesquiterpenoid aminoquinone (1)	*Dactylospongia elegans*	Tahuna, Sangihe Islands, North Sulawesi
Meroditerpene (1)	Genus *Haliclona*	Baubau, Southeast Sulawesi
Triterpene galactosides (2)	*Melophlus sarassinorum*	Siladen, North Sulawesi
Cycoldepsipeptide jaspamide derivatives (2)	*Jaspis splendens*	East Kalimantan
Tridecapeptides (2)	*Theonella swinhoei*	Bunaken Marine Park in Manado, North Sulawesi
Depsipeptides (6)	*Siliquariaspongia mirabilis*	Sulawesi
Polyhalogenated peptides (1)	*Ircinia* sp.	Thousand Islands
Endoperoxyketal polyketides (4)	*Plakortis* cfr. *simplex*	Bunaken Marine Park of Manado, North Sulawesi
Macrolide (1)	*Calyspongia* sp.	Ambon, Indonesia
A-nor steroid (1)	*Clathria* sp.	Bintang Samudra Marine Education Park, Southeast Sulawesi
Nortriterpenoid saponin (1)	*Petrosia* sp.	North Sulawesi

1.4. The sponge as host for a bacterial community

Sponges are filter feeders that come into contact with several microorganisms that are either extracellularly or intracellularly stored within the sponge (Brinkmann et al., 2017). The microbial communities are species-specific, but they are comprised of both generalist and specialist microbes that can be found in the majority of sponge species from all over the world, as well as specialists that are abundant in some species but uncommon or absent in most others. Microbial communities that

produce bioactive compounds may live in symbiotic relationships with their hosts or bind transiently (Pita et al., 2018).

Sponges are divided into two types based on the number and density of microbes found in their tissues. Microbe densities are 2-4 orders of magnitude higher in high microbial abundance (HMA) sponges than in low microbial abundance (LMA) sponges. The phyla Proteobacteria (primarily Gamma- and Alphaproteobacteria), Actinobacteria, Chlorofexi, Nitrospirae, Cyanobacteria, and candidatus phylum Poribacteria are the most dominant bacterial symbiont species, while *Thaumarchaea* is the most dominant archaeal community. The composition of sponge-associated microbiota might have been influenced by temporal variation, depth, and habitat type (Pita et al., 2018).

It is crucial to classify and distinguish sponge and symbiotic microbial species from marine sponges in order to understand how they communicate. Many recent works, using both culture-dependent and independent techniques, have established bacterial communities associated with host sponges, resulting in the identification of more than 39 distinct phyla from marine sponges (Figure 1.4) (Pita et al., 2018). In order to isolate and screen bacteria from marine sponges for the development of bioactive metabolites, several studies have been conducted (Indraningrat et al., 2016).

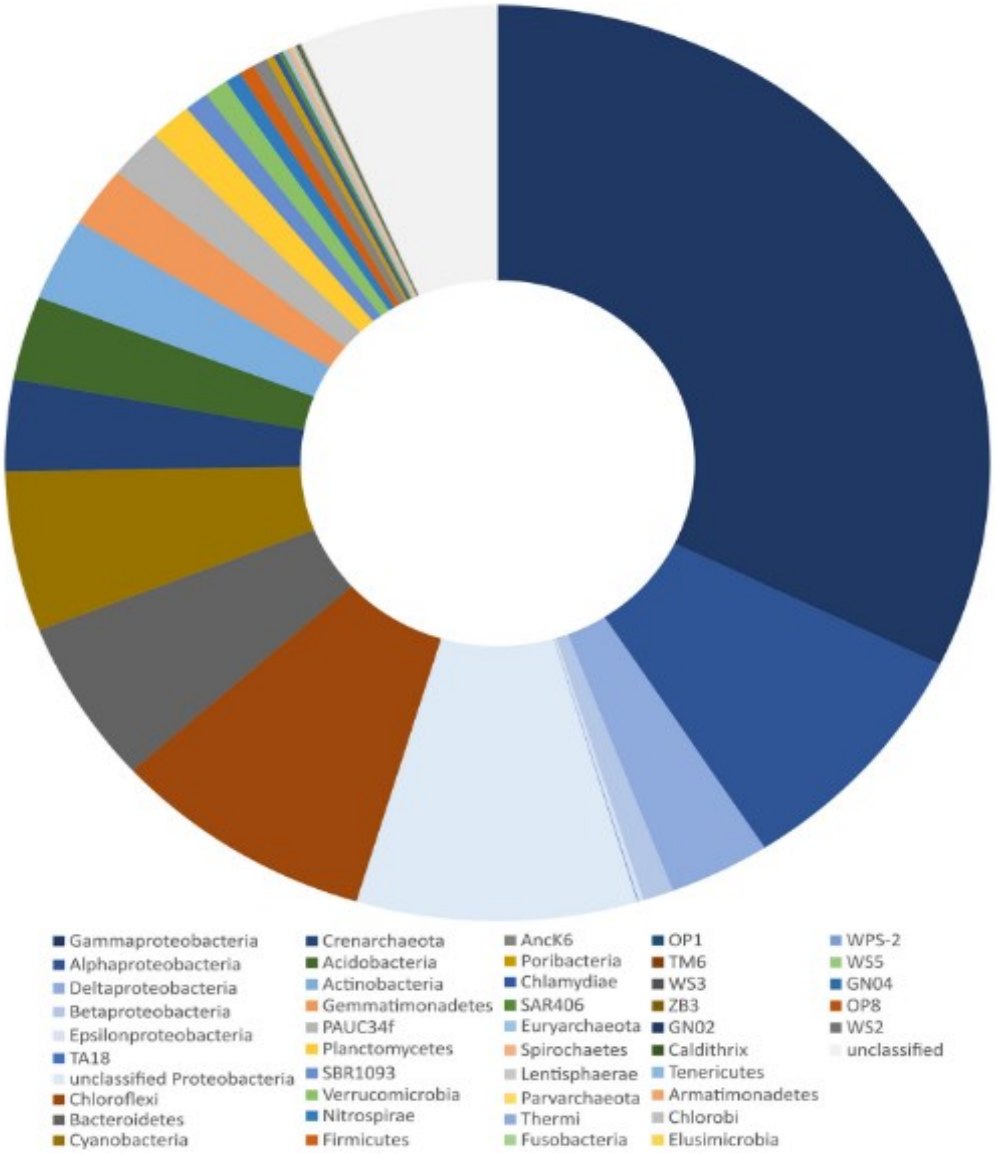

Figure 1.4. Microbial Operational Taxonomic Unit (OTU) richness in sponge-associated microbial communities at the phylum level (Pita et al., 2018).

1.5. Bioactive compounds from sponge symbiotic bacteria

The symbiotic microorganisms generate a broad variety of bioactive compounds that might be particularly useful for the development of new drugs. The large number of secondary metabolites found in the marine environment are microbially produced and have a variety of functions, including antiviral, antifungal, immunosuppressive, anti-inflammatory, antitumor, and other biotechnological and pharmaceutical applications (Taylor et al., 2007; Imhoff et al., 2011). The chemical defence of the sponge host against various predators relies heavily on symbiotic microbial species. The isolation of secondary metabolite-producing bacteria from

sponges, as well as microbial secondary metabolism gene clusters from sponge metagenomes, has led to widespread recognition that these metabolites are, in many instances, the product of microbial symbionts rather than the sponge's microbial diet (Kennedy et al., 2009).

The survival of sponges in the marine environment is dependent on their symbiotic microbes strategy (Hay, 2009). The most common phyla that produce bioactive compounds are Actinobacteria, Cyanobacteria, Proteobacteria, Firmicutes, and Bacteroidetes in various marine sponge species, i.e. *Haliclona, Petrosia, Theonella, Dysidea, Xestospongia, Callyspongia, Halicondria*, *Aplysina*, and *Sarcophyton* sp. (Bibi et al., 2020). Thomas et al. (2010) reported that actinobacteria, followed by Proteobacteria, is the phylum that produces the most compounds that might become interesting as therapeutic leads. Firmicutes and Cyanobacteria have yet to be fully investigated in terms of their bioactivity.

It has long been recognized that metabolites generated by sponge-associated marine microorganisms could become a major source for drug discovery, not only because biological diversity in marine environments such as coral reefs and deep-sea floors is likely higher than in the rainforest, but also because marine microorganisms provide a renewable resource for the scaling-up and production of new drugs (Mehbub et al., 2014). Many sponge metabolites are identical to bacterial natural products or belong to compound groups found in the microorganisms (Mehbub et al., 2014). The two main structural classes of MNPs formed by marine sponge-associated microorganisms are nitrogen compounds and polyketides (Wang et al., 2019). Almost all bioactive polyketides and peptides found in the marine sponge *Theonella swinhoei* can be traced to a single bacterial phylotype, *Entotheonella* spp., which is widely distributed in sponges (Wilson et al., 2014). The Great Barrier Reef of Australia, the South China Sea, the Mediterranean Sea, Indonesia, Papua New Guinea, and the Indo-Pacific area have all revealed clinically important bioactive compounds from marine sponge-associated microbes (Thomas et al., 2010; Anteneh et al., 2021).

In the Demospongiae, microbial associations are known as the richest sources of pharmacologically important bioactive compounds. There are 26 out of 92 families in the Demospongiae class that possess medicinally essential bioactive compounds of microbial origin (Thomas et al., 2010). The wide range of locations (Okinawa, the Philippines, Indonesia, the Red Sea, Italy, South Africa, and Papua

New Guinea) and genera of sponges (*Amphimedon* sp. and *Acanthostrongylophora*) responsible for the production of manzamine alkaloids is commonly thought to be the result of a symbiotic relationship between these sponges and common or closely related microorganisms (Mehbub et al., 2014). In the here presented thesis, the bioactive compounds from bacteria belonging to three phyla, i.e. Firmicutes, Actinobacteria, and Bacteroidetes, were observed.

1.5.1. Bioactive compounds from Firmicutes

The Firmicutes phylum, specifically the genus *Bacillus*, is the most studied genus of bacterial producers of antimicrobial substances. Members of marine *Bacillus* are common in the ocean and can withstand extremes in temperature, pressure, salinity, and pH (Rampelotto, 2010). Marine organisms develop potent bioactive compounds to fend off competitors or avoid micropredation due to the diluting effect of the ocean drives (Sayem et al., 2011). Since marine strains vary metabolically from their terrestrial counterparts, they can produce specific bioactive compounds not present in terrestrial strains (Feling et al., 2003). *Bacillus* spp. have been shown in many genomic studies to be capable of producing a wide range of antibiotics (Mondol et al., 2013). The genome sequence of widely distributed *Bacillus* strains demonstrated that up to ~8% of the genome is attributed to the production of compounds with antibacterial activity (Chen et al., 2007). Lipopeptides, polypeptides, macrolactones, fatty acids, polyketides, lipoamides, and isocoumarins are among the structurally diverse groups of secondary metabolites produced by marine *Bacillus* isolates. The genus *Bacillus* contains a significant number of cyclic lipopeptides from three families: iturins, fengycins, and surfactins (Mondol et al., 2013).

There are many reports of marine drugs from marine sponge association of *Bacillus* strains (Nagai et al., 2003; Pabel et al., 2003; Suzumura et al., 2003; Thomas et al., 2010). Associated with *Haliclona simulans* from the west coast of Ireland, 52 bacteria isolated belonged to the genera *Pseudoalteromonas, Pseudomonas, Halomonas, Psychrobacter, Marinobacter, Sulfitobacter, Pseudovibrio, Salegentibacter, Bacillus, Cytophaga, Rhodococcus,* and *Streptomyces*. These strains were discovered to be abundant in biological activities, with more than half of them displaying antimicrobial activity. *Bacillus* strains with polyketide synthase (PKS) and non-ribosomal peptide synthetase (NRPS) genes have been found to produce substances that are active against

drug-resistant pathogenic bacteria, indicating that these species have a high potential for secondary metabolite synthesis (Thomas et al., 2010).

Bacillus subtilis strains A184, A190, and A202 from the sponge *Aplysina aerophoba* collected from the Mediterranean coast of France displayed high antifungal activity against *Candida albicans*. According to an analysis by MALDI MS which was used to confirm the production of the secondary metabolite of *Bacillus*, it was detected that strain A184 produced surfactins, iturins, and fengycins, while strain A190 produced surfactin and strain A202 produced iturin (Pabel et al., 2003). Another species, *Bacillus pumilus* A586 produced plumilacidin, a lipopeptide containing a hydroxyl fatty acid and which is structurally comparable to surfactin, demonstrated high activity against *Staphylococcus aureus* (Thomas et al., 2010).

Novel thiopeptide antibiotics, YM-266183 and YM-266184, were isolated from the sponge *Halichondria japonica* associated strain *Bacillus cereus* QN03323, (Table 1.2). These two compounds revealed antibacterial activities against staphylococci and enterococci, including multiple drug-resistant strains but did not show activity against Gram-negative bacteria (Nagai et al., 2003; Suzumura et al., 2003). The diglucosyl-glycerolipid GGL11, isolated from *Bacillus pumilus* AAS3 associated with the Mediterranean sponge *Acanthella acuta*, demonstrated strong growth-inhibition of the tumor cell lines HM02 and Hep G2. The other identified and unidentified bioactive compounds with antibacterial activity from sponge-associated *Bacillus* are shown in Table 1.2 (Reviewed by Indraningrat et al. 2016).

Table 1.2. Bioactive compounds with antibacterial activity from sponge-associated microbes (Reviewed by Indraningrat et al., 2016).

Sponge	Microorganism	Compound	Target
Halichondria japonica	*Bacillus* cereus QNO3323	Thiopeptide YM-266183 Thiopeptide YM-266184	*Staphylococcus aureus,* Methicillin resistant *Staphylococcus aureus* (MRSA), Methicillin-Resistant *Streptococcus epidermidis* (MRSE), *Bacillus subtilis* ATCC 633, *Enterococcus faecalis* CAY 04_1, *Enterococcus faecium* CAY 09_1, Vancomycin-Resistant *E. faecium* CAY 09_2, and *Escherichia coli* JCM 5491
Aplysina aerophoba	*Bacillus subtilis A184*	Surfactin Iturin Fengycin	*S. aureus, S. epidermidis, Bacillus megaterium,* and *E. coli*
Aplysina aerophoba	*Bacillus subtilis A190*	Surfactin Indole	*S. aureus, S. epidermidis, B.megaterium,* and *E. coli*
Halichondria sp.	*Bacillus licheniformis* SAB1	Indole 3-Phenylpropionic	*S. aureus*
Haliclona simulans	*Bacillus subtilis* MMA7	Subtilomycin	*S. aureus*, heterogeneous vancomycin intermediate *Staphylococcus aureus* (hVISA), and *E. faecium*
Dragmacidon reticulatus	*Bacillus pumilus* Dr31	Unidentified	*S. aureus, S. epidermidis,* and *E. faecium*
Sigmadocia fibulatu	*Bacillus* sp. SC3	Unidentified	*B. subtilis*

Petromica citrina	*Bacillus pumilus* Pc31 *Bacillus pumilus* Pc32	Unidentified	*S. aureus*, community-associated MRSA, *S. epidermidis*, *S. epidermidis* 57s, *Staphylococcus haemolyticus*, *S. haemolyticus* 109s, *Staphylococcus hominis*, *S. hominis* 79s, *E. faecium*, *Enterobacter cloacae* AE, *Enterobacter hafniae,* and *E. coli*
Mycale sp.	*Bacillus* sp. HNS004, HNS010, HNS005	Unidentified	*S. aureus*
Aplysina aerophoba	*Bacillus* SB8, SB17	Unidentified	*S. aureus*
Halichondria sp.	*Bacillus licheniformis* SAB1	Indole 3-phenylpropionic	MRSA and *Streptococcus pyogenes*
Haliclona simulans	*Bacillus subtilis* MMA7	Subtilomycin	MRSA
Aplysina aerophoba	*Bacillus subtilis* A202	Iturin	Multi drug-resistant *S. aureus*, Multi drug-resistant *S. epidermidis, B. megaterium,* and *E. coli*
Mycale sp.	*Bacillus* sp. HNS004 HNS015	Unidentified	*Bacillus* subtilis
Mycale sp.	*Bacillus* sp. HNS005, HNS010,	Unidentified	*B. subtilis*

In addition, besides as the source of antibacterial compounds, *Bacillus* species are well known as producers of metabolites with antifungal, antialgal, plant growth regulator, or anticancer activities. Bogorol A, a novel peptide antibiotic, was isolated from a marine *Bacillus* sp. isolated from a tropical reef habitat in Papua New Guinea. It had strong activity against methicillin-resistant *S. aureus* (MRSA) (MIC 2 µg/mL), vancomycin-resistant enterococcus (VRE) (MIC 10 µg/mL), and moderate activity against *E. coli* (MIC 35 µg/mL), but no activity against *Stenotrophomonas maltophilia* (>200 µg/mL) (Mondol et al., 2013).

Mondol et al. (2013) provided a summary of important compounds isolated from marine *Bacillus* species (Table 1.3). For example, halobacillin, a cyclic acylpeptide, the first novel acylpeptide of the iturin class close to surfactin was isolated from *Bacillus* sp. CND-914 culture broth. The CND-914 strain was isolated from a deep-sea sediment core collected near the Guaymas Basins in Mexico. Halobacillin prevents the growth of HCT-116 human colon tumor cells (IC_{50} 0.98 µg/mL), but it does not have antimicrobial activity like surfactin even it showed antibacterial activity in high concentrations (Table 1.3) (Mondol et al., 2013).

At least 32 macrolactins were identified, including macrolactins A–Z, 7-O-succinyl macrolactin A, 7-O-succinyl macrolactin F, 7-O-malonyl macrolactin A, and three ether-containing macrolactin A derivatives, from marine sediment isolates and a few derivatives were identified from soil-derived Bacilli (Zheng et al., 2007; Lu et al., 2008). Because of its biological activities, macrolactin A was of great interest. It showed antibacterial activity against *S. aureus* and *B. subtilis* at concentrations of 5 and 20 µg/disc, respectively, and an inhibiting effect against B16-F10 murine melanoma cancer cells (IC_{50} 3.5 µg/mL) and mammalian Herpes simplex viruses (type I virus (strain LL) and type II virus (strain G) with IC_{50} 5.0 and 8.3 µg/mL, respectively) was shown. Furthermore, it also prevented lymphoblast cells from HIV infection by avoiding virus replication (maximum protection at 10 µg/mL) (Gustafson et al., 1989).

Table 1.3. Selected important bioactive compounds from marine Bacilli (Review Mondol et al., 2013)

Compounds	Producing strains	Test organisms/cell line	Nature of bioactivities
Halobacillin	*Bacillus* sp. CND-914	Human HCT-116 cancer cells	Anticancer
Mixirin	*Bacillus* sp.	Human HCT-116 cancer cells	Anticancer
Bogorol A	*Bacillus* sp.	MRSA	Antibacterial
Loloatin B	*Bacillus* sp.	MRSA, Vancomycin-resistant enterococcus (VRE)	Antibacterial
Bacillistatins 1 and 2	*Bacillus silvestris*	Human cancer cell line	Anticancer
Bacillamide	*Bacillus* sp.	*Cochlodinium polykrikoides*	Antialgal
Bacilosarcin A	*Bacillus subtilis*	Barnyard millet sprouts	Plant growth regulator
Macrolactin S	*Bacillus amyloliquefaciens*	*Escherichia coli* and *S. aureus*	Antibacterial
Macrolactin V	*B. amyloliquefaciens*	*E. coli, B. subtilis* and *S. aureus*	Antibacterial
Basiliskamides A and B	*Bacillus laterosporus*	*Candida albicans* and *Aspergillus fumigatus*	Antifungal

1.5.2. Bioactive compounds from Actinobacteria

Microorganisms have been found to produce approximately 23,000 antibiotically active metabolites, of which actinobacterial classes have produced 10,000. Furthermore, actinobacteria possess unique biosynthetic processes not found in other microbial groups (Kamala et al., 2020). Actinobacteria are very abundant and biosynthesize compounds with bioactivity, e.g. antibacterial and cytotoxicity (Kim et al., 2006; Izumikawa et al., 2010; Thomas et al., 2010; Schinke et al., 2017; Tawfike et al., 2019). Many polyketide genes have been discovered in

actinobacteria, especially sponge-associated marine actinobacteria (Schirmer et al., 2005; Kim and Fuerst, 2006).

The genus *Streptomyces*, in particular, is capable of producing a wide range of bioactive primary and secondary metabolites, including antibiotics. The main species of *Streptomyces* among all other genera of actinobacteria represents about 500 species in nature (Kamala et al., 2020). Motohashi et al. (2010) obtained and described two new anthracyclines from the sponge *Haliclona* sp. Sponge-associated *Streptomyces* sp. Sp080513GE26: tetracenoquinocin and 5-iminoaranciamycin. Furthermore, tetracenoquinocin revealed weaker cytotoxicities with IC_{50} values of 120 μM and 210 μM against HeLa and HL60 cells, respectively. While 5-iminoaranciamycin did not show activity against these cancer cells (IC_{50} > 200 μM). Mayamycin was discovered in the marine *Streptomyces* sp. associated with the sponge *Halichondria panacea*. The naphthacene glycoside SF2446A2 isolated from *Streptomyces* sp. RV15, which was previously obtained from the marine sponge *Dysidea tupha*, is one example of a Gram-negative bacterium inhibitor (Reimer et al., 2015). JBIR31, a teleocidin analog isolated from the marine sponge *Haliclona* sp. associated *Streptomyces* sp. NBRC 105896, showed a weak cytotoxic activity against HeLa cells (Izumikawa et al., 2010).

Nocardiopsis sp. HB383, an actinobacterium associated with the marine sponge *Halichondria panacea* yielded four new pyrones, nocapyrones A–D. Antibacterial activity was found in nocapyrones A and B against *Bacillus subtilis* and *Staphylococcus lentus*, respectively (Schneemann et al., 2010). The new potential thiazolyl peptide kocurin was isolated from the sponge-derived marine actinobacteria *Kocuria* sp. and *Micrococcus* sp. and showed potential antimicrobial activity against human bacterial pathogens (Palomo et al., 2013).

Abyssomicin C, a novel polycyclic polyketide was derived from the marine *Verrucosispora* sp., as a major inhibitor of para-aminobenzoic acid biosynthesis (Riedlinger et al., 2004). Furthermore, abyssomicin C demonstrated antimicrobial activity against Gram-positive bacteria, including vancomycin-resistant *Staphylococcus aureus* and several resistant clinical isolates (Rath et al., 2005). The strain *Nocardiopsis dassonvillei* MAD08 was isolated from the marine sponge *Dendrilla nigra* and demonstrated activity against the multidrug-resistant pathogens tested (Selvin et al., 2009).

The latest discovery of the obligate marine actinobacterium *Salinispora* in marine sediments and sponges has demonstrated that the marine environment continues to be a rich source of pharmaceutically important natural compounds that have yet to be fully explored (Ng et al., 2014). The marine actinomycete genus *Salinispora* comprises three closely related species (Freel et al., 2013; Maldonado et al., 2005) with 99% sequence identity in the 16S rRNA gene, i.e., Sa*linispora tropica, Salinispora arenicola,* and *Salinispora pacifica*. In research on *Salinispora* biogeography, *S. arenicola* was discovered to be the most widely distributed and abundant species, accounting for 86 percent of all strains (Jensen and Mafnas, 2006).

Salinispora species have been found in marine sediments as well as marine sponges (Mincer et al., 2002; Kim et al., 2005; Sun et al., 2010) and have been shown to produce a variety of bioactive compounds (Fenical and Jensen, 2006). *S. arenicola* and *S. pacifica* strains have also been found in the Great Barrier Reef marine sponges *Pseudoceratina clavate*, *Subera clavata*, *Cinachyrella australiensis*, *Dercitus xanthus*, *Hyattela intestinalis*, and *Amphimedon queenslandica* (Kim et al., 2005; Izumi et al., 2010; Vidgen et al., 2012).

Due to its ability to produce a diverse range of biologically active natural products, *Salinispora* has sparked a lot of interest (Fenical and Jensen, 2006). Secondary metabolites of potential biopharmaceutical significance are known to be produced by *Salinispora* strains, including the antibiotic rifamycin (Kim et al., 2006), which derivatives are especially effective against pathogenic mycobacteria that cause tuberculosis. Antitumor compounds like the proteasome inhibitor salinosporamide A (Williams et al., 2005; Fenical and Jensen, 2006), as well as other natural products of potential interest, namely staurosporine, saliniketal A and B (Williams et al., 2007), lomaiviticin A, sporolides, and arenicolide, are currently being investigated (Fenical and Jensen, 2006).

Applying molecular networking, (Duncan et al., 2015) investigated 35 *Salinispora* strains and dereplicated known compounds and the derivatives thereof (Fig. 1.5). This revealed a wide range of metabolites, made it easier to identify media components to select new compounds prioritized for structure elucidation. Dereplicated previously known *Salinispora* metabolites included cyclomarins, cyanosporasides, rifamycins, saliniketal, lomaiviticins, desferrioxamines, staurosporines, and 7-OH staurosporine.

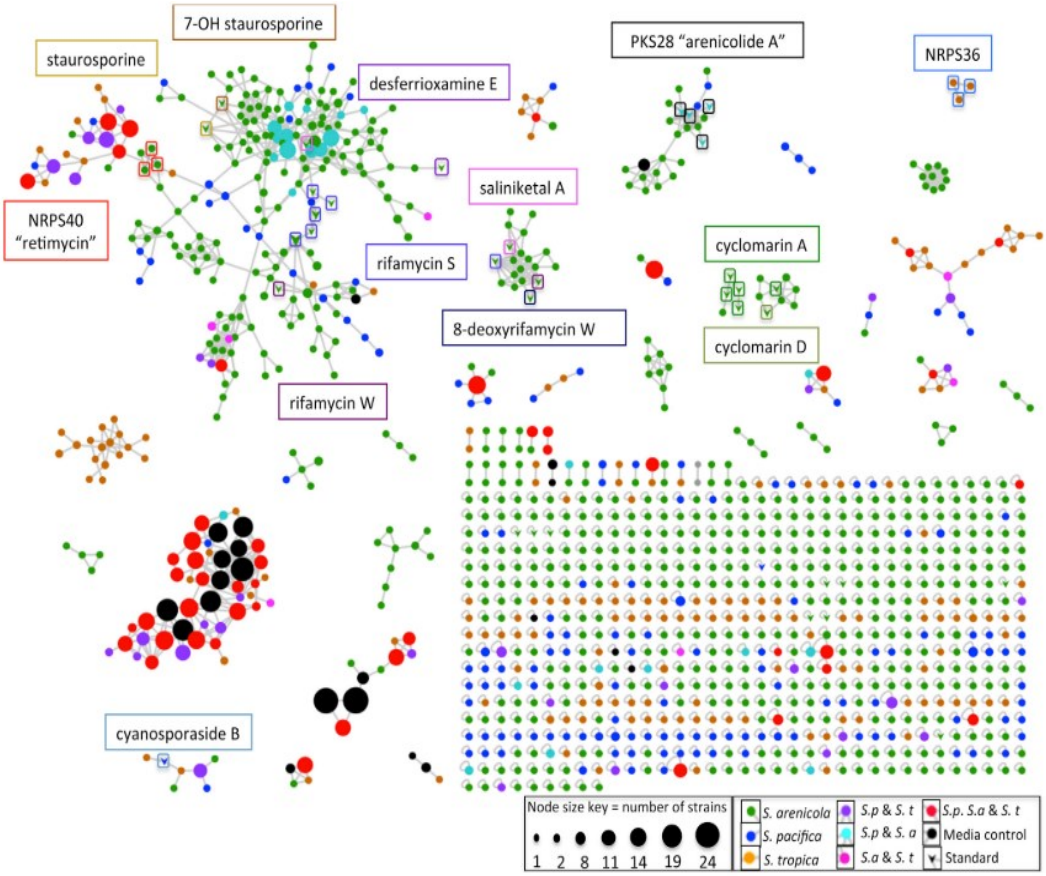

Figure 1.5. *Salinispora* molecular network. Molecular networking of 35 *Salinispora* strains, including 30 for which draft genome sequences exist. The MS/MS data revealed the presence of 1,137 parent ions, which were represented as nodes in a molecular network. The number of strains generating each parent ion is represented by the size of the node, which ranges from strain specific (one strain), which represents the vast majority of nodes, to the most ubiquitous metabolites, which were found in a maximum of 24 of the 35 strains (Duncan et al., 2015).

1.5.3. Bioactive compound from Bacteroidetes

Bacteroidetes, previously known as Cytophaga-Flavobacteria-Bacteroides (CFB), is the phylum of marine heterotrophic bacterioplankton that is generally located on macroscopic organic matter particles (marine snow) (Bauer et al., 2006). Each year, an increasing number of new Bacteroidetes species are identified, the majority of which are found in marine environments (Oku et al., 2008). Members of

the phylum Bacteroidetes are the most numerous bacteria in the ocean after Proteobacteria and Cyanobacteria (Glöckner et al., 1999; Kirchman, 2002). They can be found in a variety of marine habitats (Pommier et al., 2006) including coastal, offshore, sediments, and hydrothermal vents (Pommier et al., 2006; Alonso et al., 2007). Bacteriodetes are common in the aquatic environment during and after algal blooms, preferring to consume polymers rather than monomers. Bacteriodetes are thought to live in the oceans by attaching to particles and degrading polymers (Cottrell and Kirchman, 2000).

Kennedy et al. (2009) reported that the majority of the bacteria previously identified had been isolated from other marine sponges, with two Bacteroidetes isolates FB1 (*Mesonia* sp.) and CP1 (*Cytophaga* sp.) having 99% identity on 16S rRNA gene level. According to Jensen et al. (1996), low-nutrient media enhanced the cultivation of algae-associated marine bacteria. Choi et al. (2013) identified two new families of marine bacteria, the Mooreiaceae and Catalimonadaceae, within the phylum Bacteroidetes, using a similar method and longer agar plate incubation times. Organic extracts of some of these bacterial cultures were found to have antibiotic activity and contributed to the discovery of new alkaloidal secondary metabolites, some of which have new carbon skeletons (Choi et al., 2015a).

At present, the number of isolated compounds from this phyla is limited; these include N-(3-acyloxyacyl) glycines from *Cytophaga* sp., neoverrucosane diterpenoids from *Saprospira grandis*, an algal morphogen thallusin from a strain belonging to the genus *Zobellia*, a hydroxamate siderophore from *Tenacibaculum* sp. and an acetylcholinesterase (AChE) inhibitor marinoquinoline from *Rapidithrix thailandica* (Oku et al., 2008). Furthermore, Oku et al. (2008) also reported the isolation of ariakemicin A and B, which showed activity against Gram-positive bacteria, from the marine gliding bacterium *Rapidithrix* sp.

One of the strains that was investigated in this thesis belongs to the genus *Flammeovirga*. *Flammeovirga* is a genus of the Cytophagia class that belongs to the Flammeovirgaceae family. *Flammeovirga aprica, Flammeovirga arenaria, Flammeovirga yaeyamensis, Flammeovirga kamogawensis,* and *Flammeovirga pacifica* are five species in this genus that have been identified (Dong et al., 2017). This genus has been isolated from the surface of algae, in deep-sea, coastal sediments, and the innards of marine biota (Han et al., 2016a). Sodium chloride or seawater are needed for growth members of this genus (Takahashi et al., 2006).

They are all marine bacteria with the ability to digest complex polysaccharides found in the sea, such as agar and carrageenan. (Dong et al., 2017). *Flammeovirga* sp. strain MY04 was able to liquefy and grow solely on agarose as the carbon source, suggesting that MY04 is capable of producing effective agarose-degrading enzymes (Han et al., 2012). With the increasing need for novel drug discovery and the diverse species of Bacteriodetes that have still been unexplored, a high potential for the identification of novel compounds can be anticipated.

2. Scope of the study

Marine sponges and their associated bacteria are highly interesting marine organisms to be explored for the discovery of promising new bioactive natural products. However, the rediscovery of known compounds is considered a major problem in natural product discovery projects. Therefore, this study aims to establish a rapid screening method based on the antimicrobial properties of sponge extracts to fast identify the most active fractions and, most importantly, to dereplicate known compounds early in the workflow.

In parallel, it is projected to isolate and identify bacteria from marine sponges. The samples will be derived from different locations in Indonesia, i.e., Bunaken National Park (Campaign 1), Sangihe Islands (Campaign 2), and Cenderawasih Bay National Park (Campaign 3). To isolate taxonomically different isolates, different isolation methods will be applied. Then, axenic marine bacterial isolates will be screened for their capacity to produce antimicrobial compounds and already known molecules will be dereplicated.

Due to the fact that many bioprospecting campaigns start in remote areas and not every laboratory in every country has access to modern cost-intensive instrumentation, classical microbiological approaches will be applied for the selection of the most promising bacterial isolates. This phenotypic-based approach will be evaluated by metabolomics approaches based on LC-MS/MS analyses in combination with molecular networking. This should give insights into how different the metabolic profile of the selected bacteria is and if this can be linked to the previously observed biological activity. The selected bacteria, which show the highest antimicrobial activities and unique metabolite profiles, will be chosen for further isolation of new compounds.

In a nut shell, this study focuses on (i) the dereplication of bioactive compounds present in crude extracts obtained from Indonesian marine sponges, (ii) the isolation and discovery of marine sponge-associated bacteria, and (iii) the isolation of new bioactive compounds from these new bacterial isolates.

3. Materials and Methods

3.1. Materials

3.1.1. Chemicals and solvents

Table 3.1. Chemical substances and solutions used in this work.

Substance	Manufacturer
Agar	Fischer BioReagents (Geel, Belgium)
Agarose	Cleaver Scientific (Warwickshire, United Kingdom)
GoTag Flexi Buffer 5x	Promega (Promega, USA)
dNTP	Promega (Promega, USA)
$CaCl_2.2H_2O$	abcr GmbH (Karlsruhe, Germany)
Celite 545	Serva Electrophoresis GmbH (Heidelberg, Germany)
$CoCl_2$	Th. Geyer GmbH & Co. KG (Renningen, Germany)
Dichloromethane	Julius Hoesch (Düren, Germany)
Dimethyl sulphoxide (DMSO)	Carl Roth GmbH (Karlsruhe, Germany)
Dimethylsulfoxide-d6 99.8%	Deutero (Kastellaun, Germany)
EDTA-Na+2-dihydrate	Applichem GmbH (Darmstadt, Germany)
Ethanol 99.8%	Fisher (United Kingdom)
Ethidium bromide	Carl Roth GmbH (Karlsruhe, Germany)
Ethylacetate	Julius Hoesch (Düren, Germany)
$FeSO_4.7H_2O$	ThermoFisher (Kandel, Germany)
Gel Loading Dye	New England Biolabs, Inc.
Glucose	Carl Roth GmbH (Karlsruhe, Germany)
Glycerol	Carl Roth GmbH (Karlsruhe, Germany)
H_3BO_3	Carl Roth GmbH (Karlsruhe, Germany)
KBr	Fisher Scientific (UK)
KCl	Carl Roth GmbH (Karlsruhe, Germany)
K_2HPO_4	VWR International GmbH (Leuven, Belgium)
KI	VWR International GmbH (Leuven, Belgium)
KNO_3	Carl Roth GmbH (Karlsruhe, Germany)
LiCl	Carl Roth GmbH (Karlsruhe, Germany)

Malt extract	Carl Roth GmbH (Karlsruhe, Germany)
Marine broth	Carl Roth GmbH (Karlsruhe, Germany)
Methanol	Julius Hoesch (Düren, Germany)
Methylalcohol-d4 99.8%	Deutero (Kastellaun, Germany)
$MgCl_2.6H_2O$	ORG Laborchemie (Bunde, Germany)
$MgSO_4.7H_2O$	VWR International GmbH (Leuven, Belgium)
$MnCl_2$-tetrahydrate	Acros (New Jersey, USA)
Mueller Hinton II medium	Becton Dickinson (Sparks, NV, USA)
NaCl	Carl Roth GmbH (Karlsruhe, Germany)
$NaHCO_3$	Sigma Aldrich Chemie GmbH (St.Louis, USA)
Na_2MoO_4-dihydrate	Th. Geyer GmbH & Co. KG (Renningen, Germany)
Na_2SO_4	Carl Roth GmbH (Karlsruhe, Germany)
Nystatin	Sigma Aldrich Chemie GmbH (St.Louis, USA)
Paper disc	Carl Roth GmbH (Karlsruhe, Germany)
Peptone	Carl Roth GmbH (Karlsruhe, Germany)
$SnCl_2$-dihydrate	Fischer Chemical (Schwerte, Germany)
Sodium formate	Sigma Aldrich Chemie GmbH (St.Louis, USA)
$SrCl_2.6H_2O$	Carl Roth GmbH (Karlsruhe, Germany)
Starch	Unilever (Hamburg, Germany)
Tryptone/Peptone Casein	Sigma Aldrich Chemie GmbH (St.Louis, USA)
Vitamin B12	Tokyo Chemical Industry (Tokyo, Japan)
Yeast extract	VWR International GmbH (Leuven, Belgium)
$ZnCl_2$	Merck KGaA (Darmstadt, Germany)

Table 3.2. Technical equipment and other material used in this project.

Equipment	Manufacturer
ATP quantification	BacTiter-Glo™ Promega (Madison, WI, USA)
Autoclave	MMM Münchener Medizin Mechanik GmbH (Stadlern, Germany)
Biometra TRIO Thermal Cycler	Analytik Jena (Jena, Germany)
Bio Spectrometer	Eppendorf (Hamburg, Germany)

Centrifugal concentrator HT12-II	Genevac (Ipswitch, Suffolk, GB)
Centrifuge 5424 R	Eppendorf (Hamburg, Germany)
Centrifuge 5804 R	Eppendorf (Hamburg, Germany)
Cybi Liquid handling system	Analytic Jena (Jena, Germany)
Eppendorf tubes 1.5, 2 mL	Starstedt (Nümbrecht, Germany)
Fraction collector	Zinsser–Analytik (Eschborn, Germany)
Gel chambers power basic	Biorad (California, USA)
HPLC Dionex Ultimate 3000	Thermo Scientific (Darmstadt, Germany)
HPLC	Shimadzu Deutschland GmbH (Duisburg, Germany)
Incubator	Memmert GmbH (Schwabach, Germany)
Incubation shaker	Infors HT (Bottmingen, Switzerland)
Intas Imager	Intas Science Imaging Instruments GmbH (Göttingen, Germany)
Laminar Airflow Clean Bench BSB Safe 2020 (Safety cabinet, class II)	Thermo Scientific (Langendelbold, Germany)
MicrOTOF-QII mass spectrometer	Bruker (Billerica, MA, USA)
Microplate spectrophotometer	LUMIstar® Omega BMG Labtech (Ortenberg, Germany).
Milli-Q Water System	Millipore (Eschborn, Germany)
Nalgene®system 100TM cryogenic tubes	Thermo Scientific Inc. (Rochester, New York)
NMR spectrometer	Brucker (Ettlingen, Germany)
Nucleodur C18 EC 250/4.6 Gravity-SB, 5 µm column	Macherey-Nagel (Düren, Germany)
Nucleodur C18 VP 250/10 Gravity-SB, 5 µm column	Macherey-Nagel (Düren, Germany)
pH paper	Merck (Darmstadt, Germany)
Puriflash 4125 chromatography	Interchim (Montluçon Cedex, France
Puriflash C18-HP 30µm F0040 Flash column	Interchim (Montluçon Cedex, France)

Puriflash C18-HP 30µm F0080 Flash column	Interchim (Montluçon Cedex, France)
Rotary evaporator Interface I-100	Buchi (Flawil, Switzerland)
Scale	Sartorius Lab Instruments GmbH (Goetingen, Germany)
Sephadex LH-20	GE Healthcare Europe GmbH (Freiburg, Germany)
Sterile filter	Hahnemühle FineArt GmbH (Düsseldorf, Germany)
Thermomixer	Eppendorf (Hamburg, Germany)
UV cuvettes	Sarstedt (Nümbrecht, Germany)
Water bath	Witeg (Wertheim, Germany)
1290 UHPLC	Agilent (Santa Clara, CA, USA)
384 well microtiter plates	Greiner (Kremsmünster, Austria)

3.1.2. Enzymes

The enzymes used in the scope of this study are listed in Table 3.3. The enzymes were used according to the instructions given by the manufacturer. Lysozyme and Proteinase K were performed as stock solutions with concentrations of 50 mg/ml and 10 mg/ml, respectively.

Table 3.3. Enzymes used in the scope of this study.

Enzyme	Manufacturer
GoTag® G2 Flexi DNA Polymerase	Promega (Madison, USA)
Lysozyme	Aplichem GmbH (Darmstadt, Germany)
Proteinase K	Analytik Jena (Jena, Germany)

3.1.3. Molecular biological kits

Commercial molecular kits that were used in this study are listed in Table 3.4. The application of the kits was applied according to the manufacturer's instruction manuals.

Table 3.4. Molecular biological kits.

Molecular biological kit	Manufacturer
Bacterial Genomic DNA Kit	Analytik Jena (Jena, Germany)
Wizard®SV Gel and PCR Clean-Up System	Promega (Madison, USA)

3.1.4. Molecular weight marker

The following DNA standards listed in Table 3.5 were used for gel electrophoresis.

Table 3.5. Molecular weight marker applied for size estimation.

Molecular weight marker	Manufacturer
Gene Ruler 1kb Plus DNA Ladder	Thermo scientific (Vilnius, Lithuania)

3.1.5. Water

Demineralized water was provided by Stakpure GmbH (Niederahr, Germany). A Milli-Q® Academic Water Purification System (Millipore (Eschborn, Germany) was used to generate ultra-pure water prepared.

3.1.6. Culture Media

Culture media were prepared with demineralized water before sterilization. The following table shows the composition of the used media (Table 3.6).

Table 3.6. List of media culture and the composition.

Artificial Sea Water (ASW)
0.1 g KBr
23.48 g NaCl
10.61 g $MgCl_2.6H_2O$
1.47 g $CaCl_2.2H_2O$
0.66 g KCl
0.04 g $SrCl_2.6H_2O$
3.92 g Na_2SO_4
0.19 g $NaHCO_3$
0.03 g H_3BO_3

Add 1 L H_2O
International Streptomyces Project (ISP) 2 Medium
4 g glucose
10 g malt extract
4 yeast extract
Add 2% / 20 g NaCl
Add 1 L H_2O or 100 % ASW without NaCl
Luria-Bertani (LB) Medium
10 g tryptone
5 g yeast extract
10 g NaCl
Add 1 L H_2O or 100 % ASW
M1 Medium
10 g starch
4 g yeast extract
2 g peptone
Add 1 L 100 % ASW
Malt Yeast Extract (MYE) medium
10 glucose
3 g malt extract
3 g yeast extract
5 g peptone
Nutrient Agar (NA) medium
5 g peptone
3 g malt extract
5 g NaCl
Starch Nitrate (SN) medium
20 g starch
1 g KNO_3
0.5 g K_2HPO_4
0.5 g $MgSO_4.7H_2O$
0.5 g NaCl
0.01 g $FeSO_4.7H_2O$

Trace element solution
0.02 g $ZnCl_2$
0.1 g $MnCl_2$-tetrahydrate
0.01 g H_3BO_3
0.01 mg $CoCl_2$
0.005 g $SnCl_2$-dihydrate
0.005 g LiCl
0.02 g KBr
0.02 mg KI
0.01 g Na_2MoO_4-dihydrate
5.2 g EDTA-Na_2-dihydrate
Add 1 L H_2O then the solution was filtered
Tryptic soy broth (TSB) medium
17 g casein peptone
2.5 g K_2HPO_4
2.5 g glucose
5 g NaCl
Tryptone and yeast extract medium
4 g casein peptone
2.5 g yeast extract

3.1.7. Antibiotics

The antibiotics mentioned in Table 3.7 were used as positive controls on assays and as additives in culture media for bacteria selection. The antibiotics were used as antibiotic stock solutions, which were solved in autoclaved Milli-Q water.

Table 3.7. List of antibiotics used as an additive in culture media and positive control.

Antibiotics	Manufacturer
Carbenicillin	(Carl Roth GmbH + Co., Karlsruhe, Germany)
Chloramphenicol	Merck (Darmstadt, Germany)
Cycloheximide	Carl Roth GmbH (Karlsruhe, Germany)
Gentamycin	Sigma Aldrich, St. Louis, MS, USA
Nalidixic acid	Thermo Fisher (Kandel, Germany)

3.1.8. Buffers and solutions

All buffers and solutions (Table 3.8) were prepared with Milli-Q water.

Table 3.8. Buffers and solutions.

Buffer for DNA extraction
TE Buffer
10 mM Tris-HCl
1 mM EDTA
pH 8.0
Buffer for gel electrophoresis
50 x TAE buffer
2 M Tris-acetate
50 mM EDTA (pH 8)

3.1.9. Software and databases

Basic Local Alignment Search Tool (BLAST)

BLAST (Basic Local Alignment Search Tool) searches for regions with the local similarity between sequences. The program compares nucleotide or protein sequences to databases of sequences and calculates the statistical importance of matches. BLAST can be used to infer functional and evolutionary associations between sequences as well as classify gene family members.

Cytoscape 3.7.2

Cytoscape is an open-source software framework for visualizing molecular interaction networks and biological pathways, as well as integrating them with annotations, gene expression profiles, and other state information. This platform can also be used to analyze and visualize dynamic networks. The cytoscape core distribution provides a basic set of features for data integration, analysis, and visualization.

Global Natural Products Social Molecular Networking (GNPS)

Global Natural Products Social Molecular Networking (GNPS, https://gnps.ucsd.edu/) is a web-based mass spectrometry network that is intended to serve as an open-access knowledge base for community-wide organisation and exchange of raw, refined, or specified tandem mass (MS/MS) spectrometry results.

GNPS helps with the discovery and exploration of data during the data life cycle, along with the initial data.

For high-resolution mass spectrometry, molecular networks use parent ion fragmentation data (MS/MS). According to the chemical architecture of the drug, these parent ions are intertwined. Similar compounds have similar patterns of parent ion fragmentation, as determined by a cosine score ranging from 1 (identical fragmentation spectra) to 0 (different fragmentation spectra) (completely different parent ions).

Molecular Evolutionary Genetic Analysis (MEGA) X

Molecular Evolutionary Genetics Analysis (MEGA) software was created to provide tools for the study, identification, and analysis of DNA and protein sequences from an evolutionary viewpoint. MEGA includes programs for assembling sequence alignments, inferring evolutionary trees, measuring genetic distances and diversities, inferring ancestral sequences, calculating timetables, and checking selection (Kumar et al., 2016).

3.2. Methods

3.2.1. Marine sponge collection

Marine sponge as sources samples were collected 4 times in 3 different locations during SCUBA diving in Bunaken National Park, Sangihe Islands, and Cenderawasih Bay National Park. The first sampling was collected at the Bunaken National Park in August 2015, located near Manado, North Sulawesi, Indonesia. Then, the sponge samples were freeze-dried for further bacterial isolation (Table 10.1).

The second sponge sampling was collected by scuba diving in Enepahembang East Tahuna, Sangihe Islands, North Sulawesi Indonesia at a depth of ~1-9 m during July 2017 at the geographical position around 3°36′00.7′′N, 125°29′44.5′′E. All specimens were photo-documented under water (GoPro Hero 4.0), transferred to the laboratory in Politeknik Nusa Utara (Polnustar), then cut and kept in a sterile plastic bag at -16°C. Small pieces were used for subsequent morphological identification (Table 10.2). All specimens (labeled EP1 to EP15, each ~500 g wet weight) were individually sliced into small pieces, dried in the oven at 45°C for 3

days, and blended to give either powder or mash of sponges (on average ~30% of the wet weight).

The third sponge samples collection was done in Cenderawasih Bay National Park, Papua, Indonesia (Figure 3.1). Sponge samples were cut with a dive knife while wearing latex gloves and the individual sample was put into the sterile plastic bag. Collected samples from Cenderawasih Bay National Park were brought to the surface, kept at ambient seawater temperature, and transferred for processing within 2 h of sampling for in situ bacteria isolation.

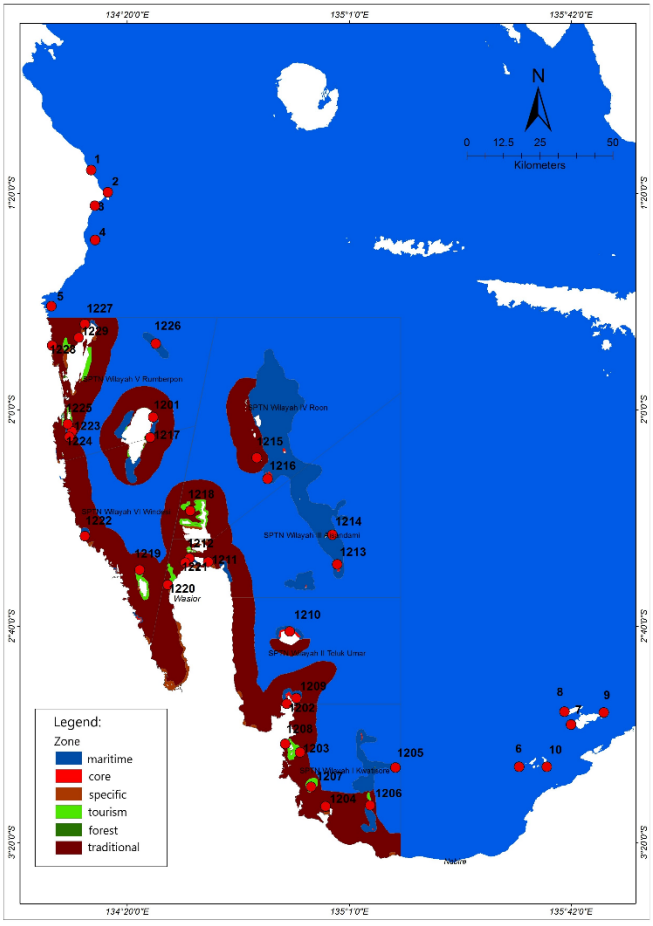

Figure 3.1. Map of sampling points and sponge collection in Cenderawasih Bay National Park, Papua, Indonesia

The fourth sponge samples were collected from Paniki (2°42′31.4″ N, 125°21′36.8″ E), Pehe (2°44′03.3″ N, 125°21′33.3″ E), and Ulu (2°43′53.4″ N, 125°24′42.8″ E) of Siau Islands Regency and from Batulewehe (3°36′00.7″ N, 125°29′44.5″ E), Kolongan (3°38′11.4″ N, 125°25′28.9″ E), and Kuma (3°34′51.2″ N, 125°34′28.2″ E) of Sangihe Islands Regency North Sulawesi Indonesia at a depth between ~4 and ~20 m May 2019 (Figure 3.2). After morphological

description and underwater documentation by the photograph (GoPro Hero 4.0, except for specimens from Kolongan which were taken by GroPro Hero 7.0), each specimen was cut and kept individually in a plastic bag. Samples were transferred to the laboratory in Politeknik Negeri Nusa Utara Tahuna Indonesia where the specimens were stored at −16°C until used. From each specimen, a small portion (1 cm^3) was taken for taxonomic identification using a slightly modified bleach digestion method (Hooper and Van Soest, 2002). All specimens (Table 10.3) were individually sliced into small pieces, dried in the oven at 45°C for 3 days, and blended to give either powder or mash of sponges. This drying step was performed, since the infrastructure available at the islands is limited and the material prepared in this way was then ready to be sent by normal post. Sponges of 2 to 5 g were packed individually in a small plastic bag separately secured in 76 sample bottles and sent to Justus-Liebig-University Giessen, Germany in October 2019.

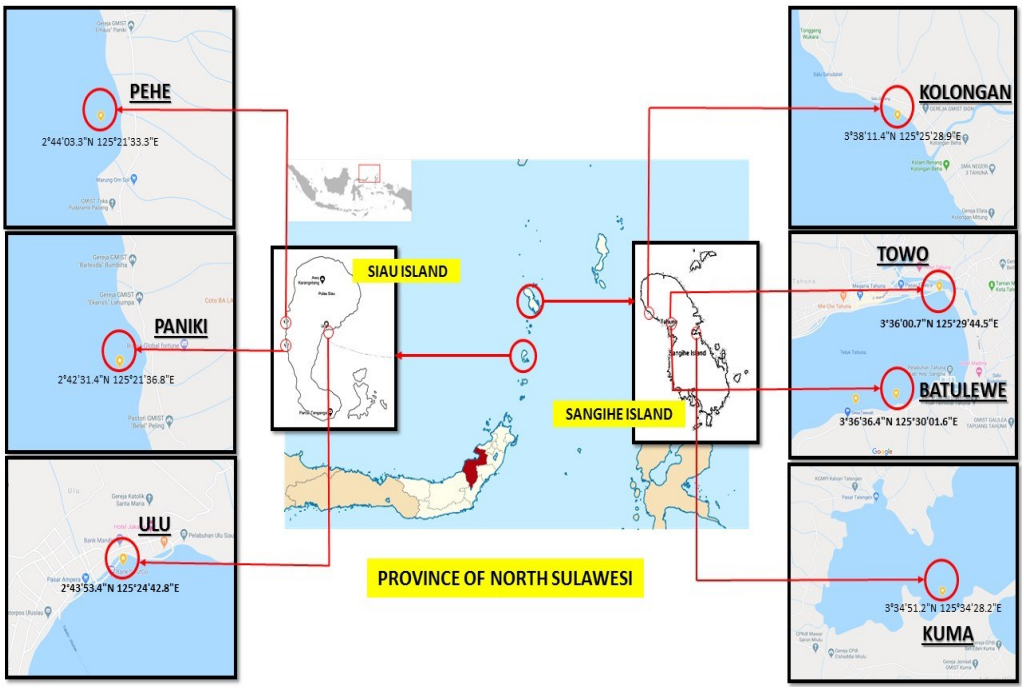

Figure 3.2. Sampling sides of sponge specimen. Samples were retrieved by SCUBA in a depth of 4–20 m below the surface.

3.2.2. Marine sponge extraction and screening new antimicrobial compounds

3.2.2.1. Marine sponge extraction

We analyzed only the fourth sponge sample for new antimicrobial compounds screening. From the sponge samples, a portion of 5 mg dry weight was solved in

500 µL of methanol. The sample was cut into small pieces and subsequently macerated in a shaker (140 rpm, 30°C overnight). In the next step, the debris was pelleted by centrifugation in a tabletop centrifuge at full speed for 5 min. The supernatant was taken and the remaining material (pellet) was extracted one more time with 500 µL methanol. The supernatants were combined and evaporated under a flow of N_2, before storage at −20°C. The dry weight of the extract was determined and extraction efficiency was calculated. The crude extract was dissolved in dimethyl sulfoxide (DMSO, final concentration 1 mg/mL) for the antimicrobial assays and methanol (1 mg/mL) for LC-HRMS measurement.

3.2.2.2. Antibacterial susceptibility tests

Antimicrobial activity of the crude sponge extracts was determined by micro broth dilution assays in 384 well microtiter plates (Greiner, Kremsmünster, Austria). A Cybi Liquid handling system (Analytic Jena, Jena, Germany) was used to distribute 0.5, 0.25, and 0.125 µL (in duplicate, corresponding to 10.0, 5.0, and 2.5 µg/mL extract concentration) of each extract to the assay plates. A dilution series of gentamycin (64 - 0.002 µg/mL, Sigma Aldrich, St. Louis, MS, USA) was added to the antibacterial assays as the positive control, while wells containing only medium or only bacterial suspension were used as sterile and growth control respectively. Pre-cultures of *Escherichia coli* ATCC35218*, Staphylococcus aureus* ATCC33592, and *Pseudomonas aeruginosa* ATCC27853 were incubated (overnight, 37°C, 180 rpm) in cation adjusted Mueller Hinton II medium (Becton Dickinson, Sparks, NV, USA) before the cell density was adjusted to 2×10^4 cells/mL and 50 µL bacterial suspension was added to each well (except the sterile control) using a multi-well dispenser (Multidrop; Thermo Labsystems*,* Waltham, MA, USA). After incubation (18 h, 37°C, 180 rpm, 80% relative Humidity (rH)), cell growth was assessed by turbidity measurement with a microplate spectrophotometer at 600 nm (LUMIstar® Omega BMG Labtech, Ortenberg, Germany).

The pre culture of *Candida albicans* FH2173 was incubated for two days at 27°C. Cell density was diluted to 1×10^5 cells/mL in Mueller Hinton II medium before the assay plates were incubated for 48 h at 37°C, 180 rpm, and 80% rH. For *Septoria tritici* MUCL45407, a previously prepared spore solution was used to adjust the assay inoculum to 1×10^5 spores/mL in YM medium (yeast extract 4 g × L^{-1}, malt extract 4 g × L^{-1}, sucrose 4 g × L^{-1}). *Septoria* assay plates were incubated for 72 h at 24 °C, 180 rpm, and 80% rH. Nystatin (Sigma Aldrich) was used as a positive

control for both, yeast and mold assays. Cell viability was evaluated via ATP quantification (BacTiter-Glo™, Promega, Madison, WI, USA) according to the manufacturer's instructions.

3.2.3. Prioritization sponge samples and dereplication of antimicrobial compounds

3.2.3.1. UPLC-HRMS/MS and microfractionation

UHPLC-HR-MS analysis was performed on a 1290 UHPLC system (Agilent, Santa Clara, CA, USA) equipped with DAD, ELSD, and maXis II™ (Bruker, Billerica, MA, USA) ESI-qTOF-UHRMS with the following gradient: 0 min: 95% A; 0.30 min: 95% A; 18.00 min: 4.75% A; 18.10 min: 0% A; 22.50 min: 0% A; 22.60 min: 95% A; 25.00 min: 95% A (A: H_2O, 0.1% formic acid (FA); B: Acetonitrile, 0.1% FA; Flow: 600 µL/min). Column oven temperature: 45°C. Column: Acquity UPLC BEH C18 1.7 µm (2.1 x 100 mm) with Acquity UPLC BEH C18 1.7 µm VanGuard Pre-Column (2.1 × 5 mm).

For microfractionation, the flow path was changed, so that 90% of the flow was collected with a custom-made fraction collector (Zinsser–Analytik, Eschborn, Germany) while the rest was analyzed in MS/MS mode in maXis II™. Collision induced fragmentation was performed at 28.0–35.05 eV using argon at 10^{-2} mbar. Depending on the potency observed in the primary screening, microfractionation assay plates were prepared by injecting 1 and 2 µL or 2 and 5 µL of extract. A total of 159 fractions were generated per extract and collected on one 384 well plates (fraction length is 7 s, starting immediately after injection) (Figure 10.1). Plates were dried in vacuo using a HT12-II centrifugal concentrator (Genevac, Ipswitch, Suffolk, GB) at 35°C before screening. Microfractionation assay volume of *S. aureus* and *C. albicans* was 20 µL, while volume of *S. tritici* assays was 50 µL.

3.2.3.2. Metabolic Fingerprinting

MS Data processing was performed with DataAnalysis 4.4 (Bruker, Billerica, MA, USA) using recalibration with sodium formate (Sigma Aldrich), RecalculateLinespectra (threshold 10,000), and FindMolecularFeatures (0.5–25 min, S/N = 0). Bucketing was performed using ProfileAnalysis 2.3 (Bruker, Billerica, MA, USA) (30–1080 s, *m/z* 100–1600, Advanced Bucketing with Δ12 s and Δ5 ppm, no transformation, Bucketing basis = H^+). The bucket table was subsequently used as input for analysis via R.R (version 3.6.0) (Team, 2019), with libraries readr

(Wickham et al., 2020b), coop (Schmidt and Heckendorf, 2019), gplots (Warnes et al., 2020), data.table (Dowle and Srinivasan, 2021), parallelDist (Eckert, 2018b), and devtools (Wickham et al., 2021) were used. For heatmap-generation with several sidebars, a variation of heatmap.2 by Griffith (Griffith, 2016) was used. The script used in this publication is deposited on GitHub [https://github.com/christoph-hartwig-ime-br/cosine-V3; https://dx.doi.org/10.5281/zenodo.4320539]. For sample comparison, the cosine similarities (dot product of vectors) between samples were calculated. Samples were sorted according to clustering results and pairwise similarities were used to determine metabolic groups. If the pairwise similarity between subsequent clustered samples is 0.7 or higher, they were assigned to one metabolic group.

3.2.3.3. Dereplication

MS and MS/MS Data analysis was performed with DataAnalysis 4.4 (Bruker, Billerica, MA, USA). Molecular formula assignment was done manually for all compounds present in the active fractions, allowing a mass accuracy tolerance of ± 2 ppm. Annotation of the MS/MS spectra was performed manually for all the compounds present in active fractions, whenever no hits against our pure compound library were observed. Molecular formula searches were performed on AntiBase 2017 (Laatsch, 2017), Dictionary of Natural Products (Dictionary of Natural Products 29.2 Chemical Search) and SciFinder® (SciFinder).

3.2.3.4. Molecular Networking

The UHPLC-QTOF-MS/MS data of the prioritized extracts were visualized and subsequently analyzed using molecular networking. Established parameters (Yang et al., 2013; Allard et al., 2016) were used for the experiment. MSConvert (ProteoWizard package32) was used to convert the raw data (*.d files) into plain text (*.mgf) files, wherein all detected fragment ions are expressed as a list of mass/intensity value pairs sorted according to their parent ions (peak picking: vendor MS level = 1-2; threshold type = absolute intensity, value = 1000, orientation = most-intense). The networking algorithm itself, thus the calculation of cosine similarity values between parent ion vectors, was computed offline, using an in-house server (Marner et al., 2020).

3.2.4. Isolation bacteria from sponge samples

Sponge samples collected from Bunaken National Park (Campaign 1) and Sangihe Islands (Campaign 2). To sponge material 500 µL of sterile distilled water was added; afterwards diluted 1:100 and plated on agar plates. Seven different agar media (Campaign 1, media 1-7) and ten different media (Campaign 2, media 1-10) were used for isolation, the compositions per 1 L were: **(1) Marine Broth** (Carl Roth GmbH, Germany) with 12.5 µg/mL chloramphenicol added; **(2) Marine Broth** with 25 µg/mL nalidixic acid added; **(3) Marine Broth** with 25 µg/mL cycloheximide added; **(4) International Streptomyces Project (ISP) 2** with 2% NaCl: glucose (4 g), malt extract (10 g), yeast extract (4 g); **(5) ISP2** with artificial sea water (ASW); **(6) Nutrient Agar (NA)**: peptone (5 g), malt extract (3 g), NaCl (5 g); **(7) ASW** agar (20 g) with *Escherichia coli* as prey bacteria. 25 µL of an *E. coli* overnight culture in LB medium was dropped onto ASW agar. Then, 10 µL of diluted sponge sample was dropped onto that spot on the agar; **(8) M1** with ASW: starch (10 g), yeast extract (4 g), peptone (2 g); **(9) Malt Yeast Extract (MYE)** with ASW: glucose (10 g), malt extract (3 g), yeast extract (3 g), peptone (5 g); **(10) Starch Nitrate (SN)** with ASW: starch (20 g), KNO_3 (1 g), K_2HPO_4 (0.5 g), $MgSO_4.7H_2O$ (0.5 g), NaCl (0.5 g), $FeSO_4.7H_2O$ (0.01 g). In order to minimize fungal growth, the media were supplemented with cycloheximide (25 µg/mL). The composition of 100% ASW per 1 L was: KBr (0.1 g), NaCl (23.48 g), $MgCl_2.6H_2O$ (10.61 g), $CaCl_2.2H_2O$ (1.47 g), KCl (0.66 g), $SrCl_2.6H_2O$ (0.04 g), Na_2SO_4 (3.92 g), $NaHCO_3$ (0.19 g), H_3BO_3 (0.03 g). The plates were incubated at 30°C for 4 weeks. Colonies were selected based on different morphological characteristics and re-streaked on new plates until axenic cultures were obtained.

Sponge samples collected from Cenderawasih Bay National Park (Campaign 3). To remove the temporary and tightly bacteria, each sponge sample was rinsed with sterile seawater, then directly cut into small pieces using sterile scalpel. *Bacillus* sp. 438, *Eschericia coli* K12, *Micrococcus luteus* ATCC 4698, *Nocardiopsis synnemataformans* 290 and *Salinispora arenicola* 301 were used as prey bacteria. 25 µL of an bacteria overnight culture in proper medium was dropped onto ASW agar. Then washed and cut sponge tissue was dropped onto that spot on the agar. In order to minimize fungal growth, media were supplemented with cycloheximide (25 µg/mL). For further use purified bacterial strains were stored at -80°C in 25% (v/v) glycerol.

3.2.5. Screening the antibacterial activity of sponge-associated bacteria

Isolated bacteria campaign 1 and 3. The isolated marine bacteria were cultivated on appropriate liquid medium at 30°C for 1-7 days, depending on the growth rate of the respective strain. The fermented broths were extracted once using ethyl acetate (1:1). The antibacterial testing using the agar diffusion method and the plates were incubated at 30°C for 24 - 48 h. Methanol and carbenicillin were used as negative and positive control, respectively.

Isolated bacteria campaign 2. The isolated marine bacteria were cultivated on appropriate solid medium at 30°C for 1-7 days, depending on the growth rate of the respective strain. Then, an agar-plug (diameter 6 mm) was punched out and transferred to the test plate. On the latter, cultures of *E. coli* K12 or *M. luteus* ATCC 4698 were swabbed on to the surface of Luria-Bertani agar (tryptone (10 g/L), yeast extract (5 g/L), NaCl (10 g/L), and agar (20 g/L)) before plug assembly. The test plates were incubated at 30°C (24 - 48 h), depending on the growth of the screening strain) and the inhibition zones were measured.

3.2.6. Identification of active strains

3.2.6.1. 16S rRNA gene sequencing analysis

All active bacteria campaign 1-3. The active isolates were identified by 16S rRNA gene sequencing. Genomic DNA of the isolates was extracted using the genomic DNA kit (Analytik Jena). PCR amplification was carried out using the primer pair pA (5'-AGAGTTTGATCCTGGCTCAG-3') and pH (5'-AAGGAGGTGATCCAGCCGCA-3'). The PCR was performed in a total volume of 40 µL including 2 µL of DNA template, 2 U of Taq Polymerase (Promega, Madison, USA), 1X green buffer, 0.2 mM dNTPs, 0.5 µM primer pA, 0.5 µM primer pH, 1.25 mM $MgCl_2$ and 5% of DMSO. PCR was performed in a Biometra TRIO Thermal Cycler (Analytik Jena) using the amplification conditions as follows: 95°C 5 min (denaturation), 50°C 45 sec (annealing), 72°C 1 min (elongation), and 72°C 5 min (final elongation). Amplified 16S rRNA gene fragments were purified using the Promega SV Gel and PCR Clean Up System kit. Purified PCR products were sequenced (Eurofins Genomics). The obtained forward and reverse sequences were assembled. Then, BLAST analysis was done to identify the closest homologues. Sequences with >98% sequence similarity (over an average of 1372-1400 bases) to their closest phylogenetic neighbour were assigned to the species

level. Sequences with <98.0% sequence similarity were identified to the genus level (Hentschel et al., 2001). The 16S rRNA gene sequences of the isolates have been deposited in GenBank with the accession numbers MT314037-MT314061 (Table 10.4). Phylogenetic tree based on the 16*S* rRNA gene was constructed in MEGA X by using the Maximum Likelihood method (default settings, 1000 bootstraps) based on the Tamura 3-parameter model. The percentage of trees in which the associated taxa clustered together is shown next to the branches. Initial tree(s) for the heuristic search were obtained automatically by applying Neighbor-Joining and BioNJ algorithms to a matrix of pairwise distances estimated using the Maximum Composite Likelihood (MCL) approach (Kumar et al., 2018).

3.2.6.2. BOX PCR

Preparation of samples and PCR conditions.

The selected bacterial strains campaign 2 were analyzed using BOX PCR. The bacterial strains were grown on ISP2 agar plate at 30°C overnight. Several bacterial colonies were transferred into the collection micro tubes (Cat.No.19560, Qiagen) with 2 Zirconia beads (2.3 mm Carl Roth, Art.: N036.1) and resuspended in 200 µL of sterile water. The mechanical cell disruption was performed by TissueLyser II for 2x 1 minute at 30 Hz. The samples were centrifuged for 2 min at 3220 x g. One microliter of supernatant was used as a DNA template for the repetitive element palindromic-polymerase chain reaction (rep-PCR) analysis with BOXA1R oligonucleotide (CTACGGCAAGGCGACGCTGACG) (Versalovic, 2005). The rep-PCR was carried out in a total volume of 25 µL including 1 µL of DNA template, 0.625 U of Dream Taq™ Polymerase, 1X Dream Taq buffer, 200 µM each dNTP, 1 µM primer, and 0.4 µg/µL BSA. The following PCR conditions were used: 95°C for 3 min followed by 30 cycles of 94°C for 30 s, 53°C for 1 min and 70°C for 8 min, and a single final extension step at 70°C for 16 min. The PCR products were analyzed by Lab Chip GX Touch HT microfluidics technology using 5K DNA Assay (Cat.No. CLS760675, PerkinElmer, Inc.).

Statistical analysis/ Rep-PCR DNA fingerprint analysis.

Gel image was normalized, bands were identified and data were statistically analysed by using GelCompare II software version 6.5 (Applied Maths, Belgium). The positions of bands on the gel were normalized using the DNA 5K ladder (PerkinElmer, Inc.) from 100 to 7000 bp as an external reference standard.

Similarity coefficient was calculated by band-based method of Dice, while unweighted pair group method with arithmetic averages (UPGMA) was used for cluster analysis.

3.2.7. Competition assays the active bacteria

The selected bacteria from campaign 2 were tested for competition assays. Initially, all strains to be tested were cultured on agar and in liquid medium 1-7 days. Liquid cultures represented the pre-culture for the test strain. Therefore, cells were separated by centrifugation at 6010 x g, 5 min, 20°C; then, inoculated into soft agar medium (10% agar), which was used to overlay the test plates. The tested bacteria were also inoculated and incubated until growth was visible on separate plates. The competition assay started afterwards; therefore, agar-plugs were prepared from the solid medium cultures and placed on the test plates.

3.2.8. Optimization of active bacteria culture conditions

The five most promising strains from the competition assay were fermented in ten different liquid media: ISP2, ISP2+NaCl, LB, LB with ASW, marine broth, malt yeast extract, nutrient broth, starch nitrate with ASW, tryptic soy broth (TSB), tryptone and yeast extract medium with ASW. TSB medium consists of casein peptone (17 g/L), K_2HPO_4 (2.5 g/L), glucose (2.5 g/L), NaCl (5 g/L), soya peptone (3 g/L); tryptone and yeast extract medium with ASW consists of casein peptone (4 g/L) and yeast extract (2.5 g/L); the other media compositions are given above. Strains were inoculated from cryoculture into a preculture (20 mL in a 50 mL flask), which was incubated at 140 rpm at 30°C overnight. Then, 1 mL of this preculture was transferred into the main culture (100 mL new medium in 300 mL flask). Fermentation was done at 140 rpm, 30°C for 2 days.

The fermented broths were extracted once using ethyl acetate (1:1). The resulting organic layer was collected and evaporated to dryness under reduced pressure using a rotary evaporator. Therefrom resulting organic extracts were used for antibacterial testing using the agar diffusion method. Extracts were dissolved in methanol (final concentration 10 mg/mL) and 10 µL were applied onto a 6 mm paper disc that was allowed to dry at room temperature. Plates were pre-incubated for 1 h at 4°C and subsequently transferred to 30°C for 24 - 48 h. Methanol and carbenicillin were used as negative and positive control, respectively.

3.2.9. MS measurements and molecular networking active bacteria

To compare the various extracts and to dereplicate the compounds therein, molecular networking was carried out. The sixty-crude extract samples were dissolved in MeOH at the final concentration of 10 mg/mL and subjected to LC-HRMS measurement. Mass spectra were detected on a micrOTOF-QII mass spectrometer (Bruker, Billerica, MA, USA) with ESI-source combined with a HPLC Dionex Ultimate 3000 (Thermo Scientific, Darmstadt, Germany) utilizing an EC10/2 Nucleoshell C18 2.7 µm column (Macherey-Nagel, Düren, Germany) at 25°C. MS data were obtained in positive mode over a range from 100 to 1000 *m/z*. For all ions above a threshold of 100, auto MS/MS fragmentation was performed with increasing collision energy (35–50 kV over a gradient from 500 to 2000 *m/z*) at a frequency of 4 Hz. The injection volume was 2 µL with a concentration of 1 mg/mL.

MS/MS data were converted from MassHunter data files (.d) to mzXML file format using MS Convert. The data were uploaded to the Global Natural Products Social (GNPS) molecular networking (https://gnps.ucsd.edu/). Network files were visualized using the program Cytoscape 3.7.2. Dereplication was done by comparing the MS^2 spectra with the reference spectra in GNPS spectral libraries (Wang et al., 2016).

3.2.10. Metabolic fingerprinting

Bacteria were inoculated from cryoculture in ISP2 liquid medium supplemented with 2% NaCl and incubated overnight at 30°C and 140 rpm. Then, ISP2 agar plates (2 per strain) were inoculated each with 50 µL of preculture and incubated at 30°C for 2 days. The agar plates were cut into small pieces, macerated with ethyl acetate, and placed on a shaker overnight. The solution was filtered and the resulting organic extract was dried in a rotary evaporator under vacuum. The concentration of this crude extract was adjusted to 50 mg/mL and subjected to LC-HRMS measurement (procedure done in triplicates).

MS-analysis was performed on 1290 UHPLC system (Agilent, Santa Clara, CA, USA) equipped with DAD, ELSD and maXis II (Bruker, Billerica, MA, USA) ESI-qTOF-UHRMS with the following gradient: A=H_2O, 0.1% formic acid (FA); B=acetonitrile, 0.1% FA; Flow: 600 µL/min; 0 min: 95% A; 0.30 min: 95% A; 18.00 min: 4.75% A; 18.10 min: 0% A; 22.50 min: 0% A; 22.60 min: 95% A; 25.00 min: 95% A. Column oven: 45°C. Column: Acquity UPLC BEH C18 1.7 µm (2.1 x 100 mm) with Acquity UPLC BEH C18 1.7 µm VanGuard Pre-Column (2.1 x 5 mm).

Data processing was performed with DataAnalysis 4.4 (Bruker, Billerica, MA, USA) using sodium formate for recalibration, RecalculateLinespectra (threshold 10000) and FindMolecularFeatures (0.5-25 min, S/N=0). Bucketing was performed using ProfileAnalysis 2.3 (Bruker, Billerica, MA, USA) (30 s-1080 s, 100 *m/z*-1600 *m/z*, Advanced Bucketing with 24 s 5 ppm, no transformation, Bucketing basis= H+). The bucket table was subsequently used as input for analysis via R. R (version 3.6.0) (R Core Team, 2019) with libraries tidyverse (Wickham, 2017), coop (Schmidt and Heckendorf, 2019), gplots (Warnes et al., 2019), data.table (Dowle and Srinivasan, 2019), parallelDist (Eckert, 2018a) and devtools (Wickham et al., 2020a) were used. Hierarchical clustering in the heatmap is performed with function “hclust” based on “complete linkage” of the cosine similarity results. The complete R-script is deposited here: Cosine-V2. R GitHub repository https ://githu b.com/chris toph-hartw ig-ime-br/cosin e-V2; https ://dx.doi.org/10.5281/zenod o.39329 68. For sample comparison, the cosine similarities (dot product of vectors) between samples were calculated. Samples were sorted according to clustering results and pairwise similarities were used to determine metabolic groups. If the pairwise similarity between subsequent clustered samples is at the threshold (e.g., 0.9) or higher, they belong to the same metabolic group. Cosine similarity data was also analyzed inside of triplicates and between strains. For outlier in triplicates MS-data were inspected. If the differences could be explained due to large concentration differences, outliers were included in the same metabolic group as the rest of the strain.

3.2.11. Antibacterial compounds isolation

3.2.11.1. Co-cultivation

Selected bacteria (one representative of closely related strains of the 108 active ones with a different species) were cultured in liquid media in a co-cultivation approach. Bacterial strain 1 and bacterial strain 2 were inoculated separately in a 150 mL Erlenmeyer flask as pre-culture. Then, the experiment was conducted as follows: (a) Strain 1 was inoculated as single strain control, (b) strain 2 was inoculated as single strain control, (c) strain 1 was inoculated first and strain 2 was inoculated after 1 day in the same flask, (d) strain 2 was inoculated first and strain 1 was inoculated after 1 day in the same flask, (f) strain 1 and strain 2 were inoculated at the same day in the same flask, (e) medium was used as the negative control.

The activity was measured based on the zone of clearance around the paper discs. The co-cultivation experiments that showed the highest activities were selected to perform the large scale cultivation: (1) *Bacillus* sp. EP6-817 and *Lysinibacillus sphaericus* EP6-121 inoculated at the different day in NB medium (Peptone 5 g/L, Malt extract 3 g/L, NaCl 5 g/L) and co-cultivated for 1 day at 30°C with shaking at 140 rpm; (2) *Verrucosispora* sp. EP6-325 and *Bacillus* sp. EP6-454 inoculated at the same day in M1 medium (Starch 10 g/L, yeast extract 4 g/L, peptone 2 g/L) and cultivated for 3 days at 30°C with shaking at 140 rpm.

3.2.11.2. Fractination and purification

Cultures (12 L) were extracted with ethyl acetate by liquid-liquid separation (1:1). The generated crude extract (4.6 g) from the co-cultivation of *Bacillus* sp. EP6-817 and *Lysinibacillus sphaericus* EP6-121 was first submitted onto a reverse phase silica C-18 column (Puriflash C18-HP 30 µm F0080 Flash column). The gradient was increased from 10% MeOH to 100% MeOH in 40 min, then kept at 100% MeOH for 10 min with flowrate of 25 mL/min. This yielded 4 fractions which were collected according the UV absorption of the substance. By bioassay-guided isolation, fraction 4 was purified by Sephadex LH 20 (mobile phase 100% MeOH) to yield one active fraction (32.4 mg) which was further purified using a Shimadzu HPLC (Shimadzu Deutschland GmbH, Duisburg, Germany) with a reverse phase column (column EC 250/4.6 Nucleodur C18 Gravity-SB, 5 µm) at a flowrate of 1 mL/min. Gradient increased from 75% MeOH to 90% MeOH in 25 min. One active compound was identified as macrolactin A (5.2 mg) according to the 1D and 2D NMR spectra as well as the LC-HRMS spectra (Figure 10.2-10.7). The crude extract from the co-cultivation of *Verrucosispora* sp. EP6-325 and *Bacillus* sp. EP6-454 generated 6 fractions via Sephadex LH 20 (mobile phase 100% MeOH). Then, the active fraction 1 was loaded on a reverse phase silica C-18 (Puriflash C18-HP 30 µm F0040 Flash column; gradient increased from 50% MeOH to 90% MeOH in 20 min) to yield 2 active subfractions. Subfractions 1 and 2 were further purified by semi-prep HPLC (subfraction 1: gradient increased from 80% MeOH to 95% MeOH in 30 min; subfraction 2: gradient increased from 85% MeOH to 100% MeOH in 38 min) to isolate four compounds. C14 surfactin (7.2 mg) and C15 surfactin (4.3 mg) were identified by 1D NMR spectra together with LC-HRMS (Figure 10.8-10.10), while C16 surfactin (1.2 mg) and C17 surfactin (1.5 mg) were identified by LC-HRMS (Figure 10.11).

NMR spectra (1D and 2D) of isolated compounds were recorded in CD3OD (Aldrich, St. Louis, MO, USA) using a Bruker Avance II 400 MHz NMR spectrometers (Bruker, Ettlingen, Germany).

3.2.12. Minimal inhibitory concentration and synergistic effect of isolated compounds

The minimal inhibitory concentration (MIC) and fractional inhibitory concentration (FIC) were determined as previously reported (Hirsch et al., 2019). In brief, a panel of Gram-negative *E. coli* ATCC 25922 (wild-type and Δ*tolC* mutant), Gram-positive *B. subtilis* DSM 10, *S. aureus* ATCC 25923 (methicillin-sensitive), and *S. aureus* ATCC 33592 (methicillin-resistant, MRSA) were grown in cation-adjusted Mueller-Hinton II broth (CAMHB, Becton Dickinson) over-night, *Listeria monocytogenes* DSM 20600 was grown in brain heart infusion (BHI) medium supplemented with 1% (v/v) Tween 80 over 2 days of incubation at 37°C, until the 30 mL preculture was turbid. Next, the preculture was adjusted to McFarland 0.5-1 turbidity standard (approx. 1.5 – 3.0 x 10^8 cfu per mL) and diluted 1:600 in fresh media as seeding cell suspension for the growth inhibition assay. Purified macrolactin A and surfactins were dissolved in DMSO (12.8 mg/mL final concentration), spotted onto 96 well plates and 1:2 dilution series in a volume of 100 µL of the seeding cell suspensions were prepared on 96 well plates to obtain a final compound concentration of 128 – 0.0625 µg/mL. Growth and sterility controls were added (DMSO as solvent control), and gentamycin served as positive control. Endpoint MIC values were measured after 18±2h at 180 rpm shaking speed and 37°C at 85% rH. Readout was obtained by turbidity absorption measurement at 600 nm and chemiluminescence-based ATP-quantification using BacTiter Glo Microbial Cell Viability Assay (Promega) according to the manufacturer's recommendations on a LUMIstar Omega plate reader (BMG Labtech). MIC values were calculated as growth inhibition (I%) ≥ 80% from at least three independent measurements (n ≥ 3). Synergistic interaction of purified surfactin and macrolactin A was tested using the chequerboard assay in 96 well plate format (Hirsch et al., 2019). In brief, fractional inhibitory concentration (FIC) values for macrolactin A and the C14 surfactin were calculated for each compound concentration combination using the equation FIC_{cpd} = $Conc._{cpd}$ / MIC_{cpd}. The fractional inhibitory concentration index (FICI) values were calculated as FICI = $FIC_{Macrolactin\ A}$ + $FIC_{Surfactin}$, whereas FICI ≤

0.5 indicated synergistic effects between both compounds and FICI values > 4 antagonism.

3.2.13. Antibacterial screening and active compound isolation from *Flammeovirga yaeyamensis* 2b

The bacteria *F. yaeyamensis* 2b was chosen for further antibacterial compound isolation from campaign 3 bacteria isolation because it has the highest activity against tested bacteria.

3.2.13.1. Media culture and optimization *F. yaeyamensis* 2b

An initial antibacterial screening, the strain *F. yaeyamensis* 2b was cultured in MB agar as the general medium from marine bacteria. The cultures were shaken 140 rpm at 30°C for 15 days. 20 mL culture was harvested on the day 1, 2, 6, 10, 12, 14 and 15. The culture was extracted with ethylacetate (1:1) for further antibacterial screening. Antibacterial screening was tested using *E. coli* K12 and *Bacillus megaterium* DSM32.

For optimization of culture conditions, eight media i.e., ISP2, LB, M1, Marine broth, MYE, NB, TSB, tryptone and yeast extract medium with 100% ASW (except marine broth with water) were used. Trace element and Vitamin B_{12} solutions were added after sterilization. 20 mL of the preculture was inoculated from cryoculture. Then overnight preculture was transferred into 200 mL culture in 500 mL flask. The cultures were shaken 140 rpm at 30°C for 15 days. The culture was extracted with ethylacete (1:1) for further antibacterial screening.

3.1.13.2. Antibacterial screening *F. yaeyamensis* 2b

Antibacterial screening was tested using *E. coli* K12 and *B. megaterium* DSM32. The cultures of *E. coli* and *B. megaterium* were swabbed on to the surface of Luria-Bertani. The crude extract was dissolved in methanol at a concentration of 10 mg/mL and 10 µL were applied onto a 6 mm paper disc. The test plates were incubated at 30°C (24 - 48 h, depending on the growth of the screening strain) and the inhibition zones were measured. The highest inhibition zones from certain medium dan time were chosen as next large-scale cultivation. The crude metabolites were further obtained in large scale in 30 L culture NB medium. The preculture was prepared from cryoculture at 140 rpm at 30°C for 1 day. Inoculum was transferred to 1.5 L of growth media containing 5 L flask and cultured with

shaking (140 rpm) for 14 days at 30°C. Ethyl acetate was applied to the cultivation broth at a ratio of 1:1 (v/v) and shaken for 1 h to complete extraction. The organic phase was separated from the aqueous phase and dried under vacuum. The crude extract at concentration 10 mg/mL was tested again to confirm the antibacterial activity. On every plate were included negative (methanol) and positive control (carbenicillin).

3.2.13.3. Fractination active compounds from *F. yaeyamensis* 2b

The active crude extract (3.2 g) was subjected to flash chromatography (Puriflash C18-HP 30µm F0080 Flash column), gradients: 0–30 min, 30% MeOH; 30-45 min, 50% MeOH; 45-60 min, 70% MeOH; 60–90 min, 100% MeOH, to yield 16 fractions. To assess the antibacterial activity, all fractions were performed against tested bacteria. Ten active fractions against *B. megaterium* and *M. luteus* were further purified using HPLC (VP 250/10 Nucleodur C18 Gravity-SB, 5 µm). Analysis of the active crude extract, fractions, and pure compounds was done by HPLC (column EC 250/4.6 Nucleodur C18 Gravity-SB, 5 µm) with the following conditions: gradient 0–10 min, 10% MeOH; 10–40 min, 10%-100% MeOH; 40–50 min, 100%; 50–60 min, 10% MeOH, flowrate 1mL/min.

3.2.13.4. Purification of active compounds from *F. yaeyamensis* 2b

From 16 fractions, ten fractions showed activity against Gram-negative bacteria. Due to of low amount the samples, only 2 fractions that to be continued for further purification. Fraction 6 (74.7 mg) with antibacterial activity was further subjected to semipreparative HPLC (VP 250/10 Nucleodur C18 Gravity-SB, 5 µm) using gradient 40-60% MeOH 40 min, flowrate 3 mL/min, to yield 2 compounds i.e., **6.4** (4.5 mg) and **6.5** (2.5 mg). The structures were identified by analyzing the NMR data.

Fraction 12 was further purified a Shimadzu HPLC system (Shimadzu Deutschland GmbH, Duisburg, Germany) equipped with a reverse phase column (EC Gravity C18, 250 × 10 mm) at a flowrate of 3 mL/min The gradient increased from 35% ACN/H_2O+ 0.01% TFA to 75% ACN/H_2O + 0.01% TFA, over 25 min. This purification procedure yielded 6 compounds i.e. (**1**)1.5 mg, (**2**) 5.6 mg, (**3**) 3.6 mg, **4** (3.1 mg), **5** (1.5 mg), and **6** (1.5 mg).

4. Result I: Sustainable low-volume analysis of environmental samples by semi-automated prioritization of extracts for natural product research (SeaPEPR)

This chapter was already published as articles in marine drugs (*Mar. Drugs* 2020, *18*(12), 649; https://doi.org/10.3390/md18120649).

marine drugs

MDPI

Article

Sustainable Low-Volume Analysis of Environmental Samples by Semi-Automated Prioritization of Extracts for Natural Product Research (SeaPEPR)

Riyanti [1,2,3,†], Michael Marner [3,†], Christoph Hartwig [3], Maria A. Patras [3], Stevy I. M. Wodi [4], Frets J. Rieuwpassa [4], Frans G. Ijong [4,5], Walter Balansa [4,*] and Till F. Schäberle [1,3,6,*]

1 Institute for Insect Biotechnology, Justus-Liebig-University of Giessen, 35392 Giessen, Germany; riyanti@bio.uni-giessen.de
2 Faculty of Fisheries and Marine Science, Jenderal Soedirman University, Purwokerto 53122, Indonesia
3 Fraunhofer Institute for Molecular Biology and Applied Ecology (IME), Branch for Bioresources, 35392 Giessen, Germany; Michael.Marner@ime.fraunhofer.de (M.M.); Christoph.Hartwig@ime.fraunhofer.de (C.H.); Maria.Patras@ime.fraunhofer.de (M.A.P.)
4 Department of Fisheries and Marine Science, Politeknik Negeri Nusa Utara, Tahuna Sangihe Islands, North Sulawesi 95812, Indonesia; wodiimelda@gmail.com (S.I.M.W.); frets.jr@gmail.com (F.J.R.); ijongfrans@yahoo.com (F.G.I.)
5 Faculty of Fisheries and Marine Science, Sam Ratulangi University, Manado 95115, Indonesia
6 German Center for Infection Research (DZIF), Partner Site Giessen-Marburg-Langen, 35392 Giessen, Germany
* Correspondence: walterbalansa@polnustar.ac.id (W.B.); till.f.schaeberle@agrar.uni-giessen.de (T.F.S.); Tel.: +49-641-99-37140 (T.F.S.)
† These authors contributed equally.

Received: 23 October 2020; Accepted: 11 December 2020; Published: 17 December 2020

check for updates

4.1. Background

Natural products (NPs) are the oldest form of medicine utilized by humans. Technologies and methods improved and NPs remained one of the most important source for the development of medicinal drugs. Today, NPs and their derivatives make up a significant percentage of approved drugs worldwide. Especially in the antibiotics sector, almost all lead structures were identified from bio-resources (~75% either unaltered or semi-synthetically modified; 1981–2014) (Newman and Cragg, 2007, 2016). Although being a traditional source for antimicrobial compounds, the pool of NP-derived structural novelty is not exhausted as exemplified by the discovery of teixobactin (Ling et al., 2015) and darobactin (Imai et al., 2019).

Besides clinical application, specialized natural products are drivers of socio-economic stability by finding application in food preservation, livestock and aquaculture treatment, as well as crop protection (Meek et al., 2015). In all fields, humans benefit from the evolutionary shaped intrinsic antimicrobial activity of NPs. In the 1940s, the “Waksman antibiotic discovery platform” was the first systematical approach to identify antimicrobial NPs and led to the isolation of the first aminoglycosides (Schatz et al., 1944).

However, high rediscovery rates make classical discovery campaigns unattractive and pose an unreasonable financial risk for the private sector. This might partly be circumvented by implementing chemo-informatics in systematic, routine processes. Data mining processes such as automatic annotation of bucket matrices (Forner et al., 2013) or MS/MS networks (Yang et al., 2013) against public databases help to identify signals and interest, even in gigantic datasets.

Besides discovery of novelty, repurposing of already known structures to different fields of application seems an encouraging approach, but high expense or no commercial availability of many natural products reduce feasibility substantially. In this context, SeaPEPR represents a methodology allowing a preliminary determination of specific bioactivity of single compounds within crude environmental extracts. Application allows us to evaluate the bio-economical value of large sets of low volume sample on the metabolite level in a standardized manner and finally facilitates decision making on downstream processes such as isolation of unknown metabolites or repurposing studies.

Here, we chose a promising and likewise challenging bio-resource as a case study to present our approach of crude environmental extract analysis. Sponges, as

sessile filter feeders without physical defense, are believed to depend on chemical defense or deterrence mechanisms mediated NPs, biosynthesized either by themselves or by associated microorganisms. Due to ethical reasons, straightforward isolation and characterization of compounds by harvesting sponges from nature should be discouraged. Limited availability of material usually prohibits extensive information retrieval from a given environmental sample. Frequently, scaffolds initially discovered in environmental samples are subject to delicate chemical synthesis without a clear product application. MS/MS coupled microfractionation of environmental extracts facilitates semi-automatic dereplication and allows attributing bioactivity observed in crude extract primary screens to single compounds without the necessity of cost and time-consuming isolation or synthesis.

4.2. Sample collection and extract generation

Sponges are a well-known bioresource for bioactive molecules and can be regarded as a complex environmental sample, since the holobiont (consisting of the sponge and its associated microbes) is extracted as a whole. Furthermore, the taxonomic classification of sponges, which is based on both, genetic barcoding and morphology, is time consuming and challenging. In this project, 76 sponge samples from seven different dive sites at the coastal area of Sangihe and Siau Island (Pacific Ocean, Indonesia) were obtained (Figure 3.2). At each diving site, around 11–15 sponge samples were collected, except sponge sample T_5, which was the only one obtained from the site named Towo. Hence, it can be expected that the sample set represents a survey of the biodiversity around the islands. How this translates into chemical diversity was investigated in the following. As starting material, 5 mg of dried sponge, which is approximately equivalent to the size of a thumbnail, was used. From all samples, crude extracts were prepared. The extraction yield (based on dry mass) using methanol was between 12 and 86% (Figure. 10.12).

The generated extracts represent the material further analyzed for NP discovery. The general workflow of SeaPEPR is depicted in Figure 4.1.

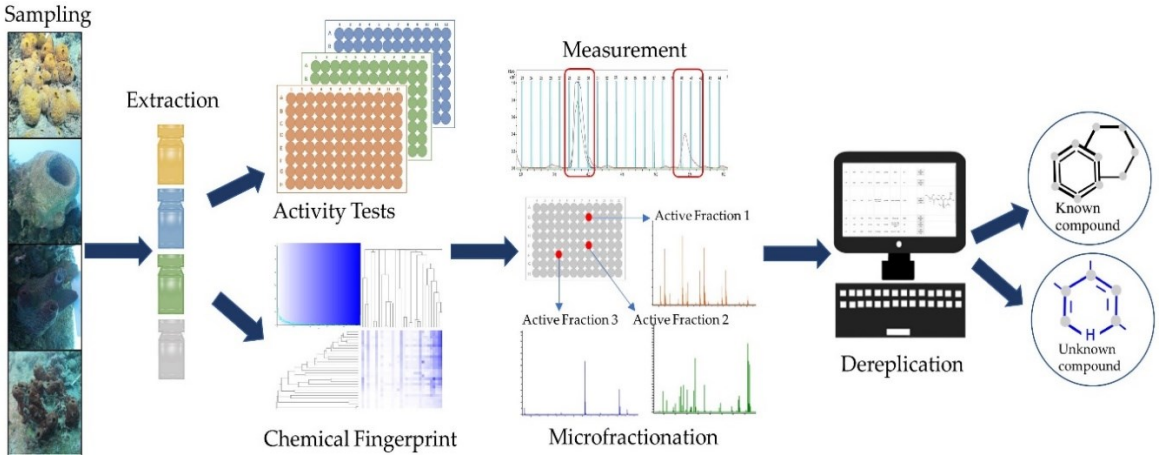

Figure 4.1. Schematic overview of the SeaPEPR pipeline. In a first step, crude environmental extracts are subject of bioactivity assessment. At the same time, the chemical diversity of the entire set of samples is determined by cosine similarity calculation ("chemical fingerprints"). Prioritized samples are microfractionated to identify the causative agent responsible for the initially observed bioactivity. If desired, dereplicated compounds of interest can be selected for isolation.

4.3. Bioactivity assessment - microbroth dilution assays

In order to determine the antimicrobial potency, the generated extracts were screened against a diverse panel of pathogenic microorganisms including *E. coli* ATCC35218, *S. aureus* ATCC33592, *P. aeruginosa* ATCC27853, as well as *C. albicans* FH2173 and the phytopathogenic fungus *S. tritici* MUCL45407. In total, seven of the 76 tested sponge extracts exhibited growth inhibitory effects of at least 85% across 3 dilution steps against one or more test strains and were thereby considered bioactive. Essentially, samples KOL_8, KOL_16, KOL_18, and ULU_13 were active against *S. aureus*, *C. albicans*, and *S. tritici*, PEHE_5 against *S. aureus* and *S. tritici*, and extracts PANIKI_4 and ULU_16 showed activity only against *S. tritici*. In addition, two extracts (ULU_11 and ULU_17) showed weak activity against *C. albicans* by inhibiting the cell viability of the test strain only in the highest concentrations. No growth inhibition of the selected Gram-negative test strains was observed.

4.4. Prioritization-metabolic fingerprinting

Results from metabolic fingerprinting and bioactivity screening were combined to allow prioritization of samples and are summarized in Figure 4.2. The detailed grouping results with pairwise similarities are presented in Table 10.5. While a total of 45 distinct metabolic groups was generated, extracts sharing the same activity pattern (KOL_8, KOL_16, KOL_18, and ULU_13) were assigned to the same group (Figure 4.2), strongly suggesting a similar metabolite composition of the extracts (see also Figure 4.3). Similarly, extracts ULU_11 and ULU_17 formed one group, while extracts PEHE_5, PANIKI_4, and ULU_16 appeared to consist of unique metabolite mixtures. From each metabolic group containing bioactive extracts, one representative was selected for microfractionation. Samples selected for microfractionation are marked.

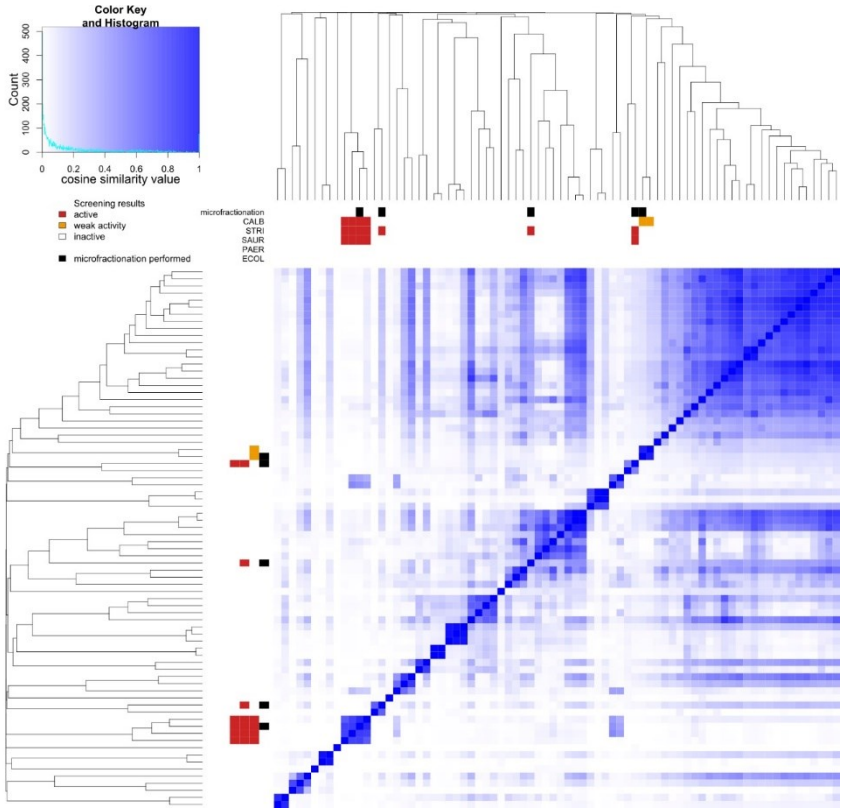

Figure 4.2. Cosine similarity heatmap of all 76 extracts. Blue color indicates a high degree of similarity among compared extracts (see color key histogram). Flags in sidebar mark selected samples for microfractionation (black) and screening results (red = active, orange = weak activity, white = inactive) of the respective extract against the indicator strains (CALB = *C. albicans*, STRI = *S. tritici*, SAUR = *S. aureus*, PAER = *P. aeruginosa*, ECOL = *E. coli*).

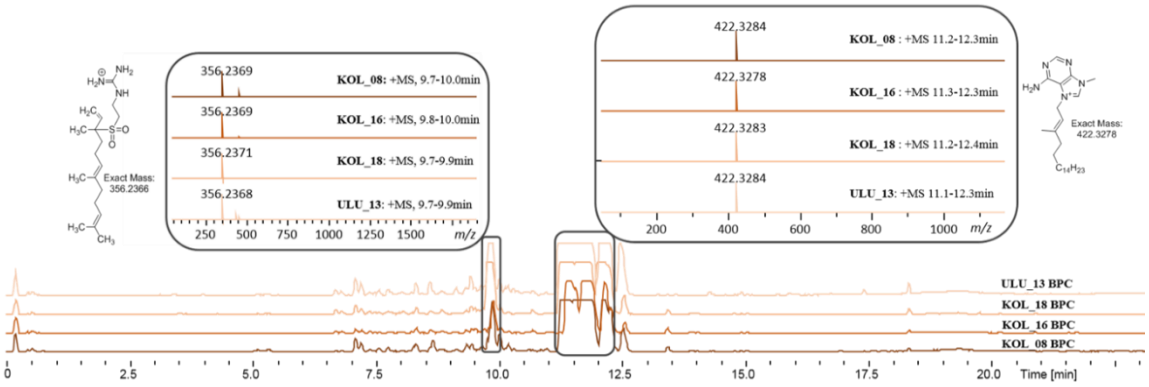

Figure 4.3. Base peak chromatogram (BPC) of the extracts KOL_08, KOL_16, KOL_18, and ULU_13 obtained from different *Agelas nakamurai* organisms. Most intense peaks within the similar BPCs correspond to the agelasines groups (box, top right) and agelasidine A (box, top left).

4.5. Dereplication of bioactive compounds—microfractionation

4.5.1. KOL_18 (TSRR0002_D-07) *Agelas nakamurai*

Extract KOL_18 was selected as representative of the group of the four extracts exhibiting an identical bioactivity pattern and similar metabolite composition (Figure 4.3). Based on the primary activity of the crude extract against *S. aureus*, the corresponding crude extract (1 mg/mL in MeOH) was fractionated in 1 and 2 µL injection volume replicates and rescreened against the same indicator strain. The active fractions were reproduced in both dilutions. The two activity zones, namely fractions 80–81 and 83–84 (Figure 10.13), could be assigned to partly co-eluting isomeric compounds with an *m/z* 422.3283 $[M]^+$, corresponding to the molecular formula $[C_{26}H_{40}N_5]^+$. The compounds showed an UV absorption at 220 and 272 nm. Based on the MS/MS fragmentation pattern, the compounds could be assigned as members of the agelasine A-F family (Figure 4.4) (Nakamura et al., 1984); since MS/MS fragmentation does not allow for distinction between the different isomeric structures of the diterpene unit. As the name indicates, agelasines are known metabolites of the sponge *A. nakamurai*.

The same extract was fractionated against *S. tritici* (injection volume 2 and 5 µL). Both of the replicates showed activity, corresponding to the above-described agelasines. The 5 µL injection volume replicate showed an additional activity zone, namely fraction 69 (Figure 10.14), which could be assigned to a compound of *m/z* 356.2370 $[M+H]^+$, corresponding to the molecular formula $C_{18}H_{33}N_3O_2S_1$. The

compound shows UV absorption at 220 nm. Based on the MS/MS fragmentation pattern (Figure 10.14.d), the compound was dereplicated as agelasidine A (Nakamura et al., 1985) (Figure 4.4), also a known metabolite of *A. nakamurai* (Stout et al., 2012). The extract was also fractionated against *C. albicans* (2 mg/mL solution, injection volume 2 and 5 µL). Both injection replicates showed activity in the fractions corresponding to the above described agelasines A-F and agelasidine A (Figure 10.15).

Molecular networking analysis revealed the presence of several derivatives (minor compounds) including oxo-agelasines A-F of *m/z* 436.3073 $[M]^+$ with a molecular formula of $C_{26}H_{38}N_5O_1$, hydroxy-agelasines of *m/z* 438.3231 $[M]^+$ with a molecular formula of $C_{26}H_{40}N_5O_1$, and dihydro-hydroxy-agelasines of *m/z* 440.3389 $[M]^+$ with a molecular formula of $C_{26}H_{42}N_5O_1$, each present in the extract as a complex mixture of isomers (Figures 10.16 and 10.17).

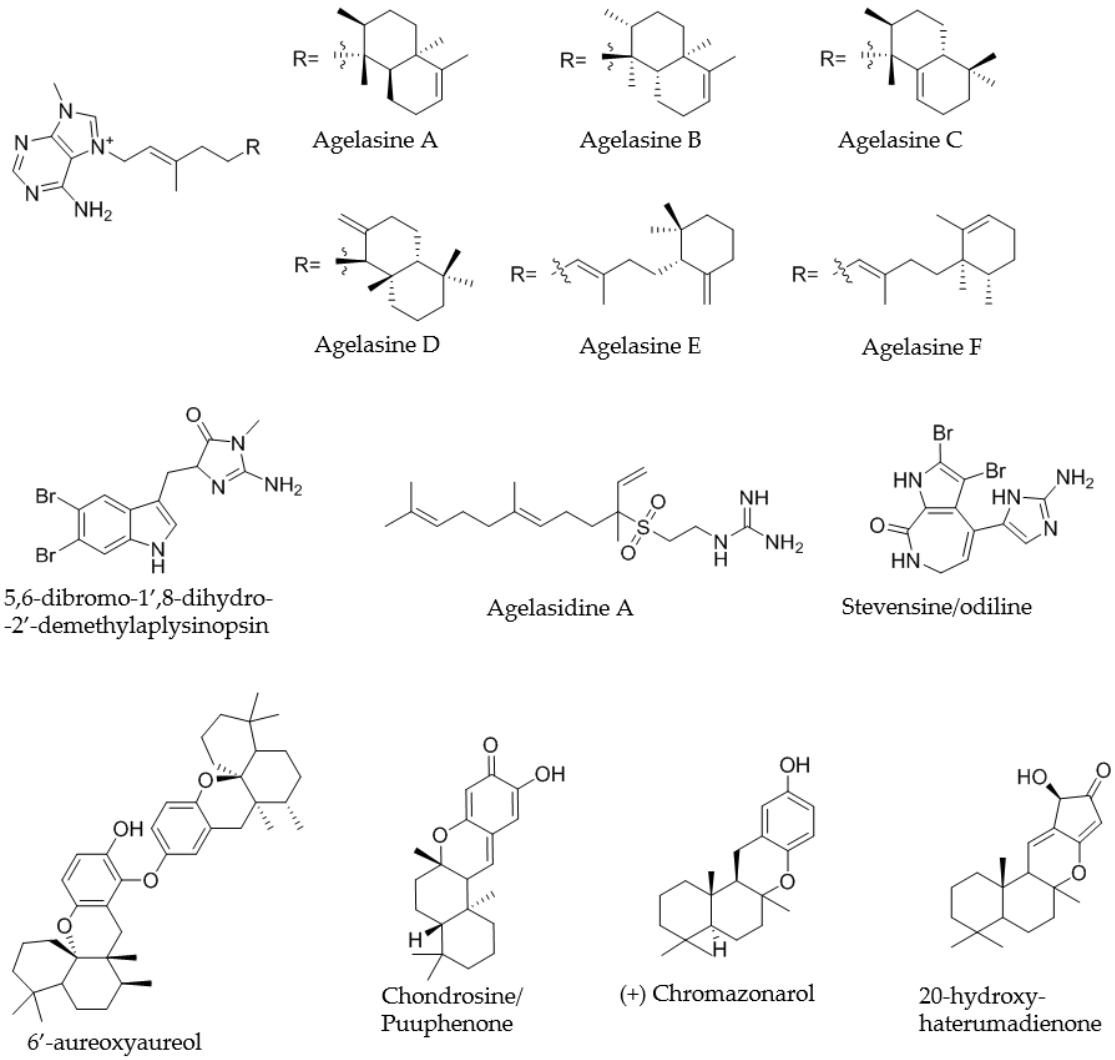

Figure 4.4. Chemical structures of the dereplicated compounds responsible for the activity of the microfractionated samples.

4.5.2. PEHE_5 (TSRR0002_F-08) *Haliclona* sp.

Based on the results of the primary screening against *S. aureus*, the corresponding crude extract (1 mg/mL in MeOH) was fractionated in 2 and 5 µL injection volume replicates and rescreened against the same indicator strain. Only the 5 µL replicate showed active fractions, namely fractions 47,48 and 108 (Figure 10.18 and 10.19). Activity of fractions 47-48 was assigned to a compound of *m/z* 398.9449 $[M+H]^+$ showing the specific isotope pattern of a dibrominated compound (Figure 10.18.b) corresponding to a molecular formula of $C_{13}H_{13}Br_2N_4O_1$. The compound shows UV absorption maxima at 220 and 292 nm. The fragmentation pattern is indicative of a dibrominated triptamine framework as structural subunit. A substructure search on SciFinder retrieved no hits corresponding to the assigned molecular formula,

however, one candidate, namely 5,6-dibromo-2′-demethylaplysinopsin ($C_{13}H_{11}Br_2N_4O_1$ - one additional degree of unsaturation compared to the compound in the extract), was found to fit the fragmentation pattern observed for the compound in the extract. Therefore, the active compound was putatively assigned the structure of 5,6-dibromo-1′,8-dihydro-2′-demethylaplysinopsin (Bialonska and Zjawiony, 2009) (Figure 4.4), which is in agreement with the molecular formula, fragmentation pattern, and observed UV spectrum. Aplysinopsins are a family of indole alkaloids isolated from sponges (Balansa et al., 2013), scleractinian corals (Guella et al., 1989; Mancini et al., 2003) and sea anemones (Murata et al., 1986). The tentative 5,6-dibromo-1′,8-dihydro-2′-demethylaplysinopsin is, to our knowledge, not reported in literature.

Activity of fraction 108 was assigned to a mixture of co-eluting compounds of *m/z* 627.4414 $[M+H]^+$, *m/z* 315.2321 $[M+H]^+$, *m/z* 329.2115 $[M+H]^+$ (Figure 10.19b–d; proposed structures in Figure 4.4), corresponding to the molecular formulae $C_{42}H_{58}O_4$, $C_{21}H_{30}O_2$, and $C_{21}H_{28}O_3$, respectively. The compounds showed UV absorption maxima at 223 and 299 nm. The MS/MS fragmentation pattern of all three compounds showed a base peak ion of *m/z* 191.1798, corresponding to the molecular formula of $C_{14}H_{23}^+$, which was assigned to the retro Diels–Alder fragmentation product ion of sesquiterpene hydroquinone frameworks. Based on the MS/MS data for $C_{21}H_{30}O_2$, no distinction between the two-literature known isomeric sponge metabolites, aureol and chromazonarol (Cimino et al., 1975; Gordaliza, 2010), could be made. The same holds true for $C_{42}H_{58}O_4$ (putatively 6′-aureoxyaureol or 6′-aureoxychromazonarol). The bissesquiterpene 6′-aureoxyaureol was reported together with several dibrominated aplysinopsin derivatives in the sponge *Smenospongia* sp., whereas the hypothetical chromazonarol stereoisomer was not described (Prawat et al., 2012). Finally, literature query of $C_{21}H_{28}O_3$, produced a range of hits corresponding to algal metabolites, while only one compound, chondrosine (a.k.a. puupehenone) (Ravi et al., 1979), was previously reported from sponges. The structures of 6′-aureoxyaureol, chondrosine, and chromazonarol (Figure 4.4) were chosen as representative examples for each of the ions of *m/z* 627.4414, *m/z* 329.2115, and *m/z* 315.2321, respectively.

The same extract was fractionated against *S. tritici* (injection volume 2 and 5 µL), however, no active fractions could be observed.

4.5.3. ULU_16 (TSRR0002_H-07) *Neopetrosia* sp.

To investigate the observed antifungal activity of ULU_16, the extract was fractionated in 2 and 5 µL injection volume replicates and rescreened against *S. tritici*. The activity zone was reproduced in the two replicates and could be assigned to a compound of *m/z* 385.9249 $[M+H]^+$ showing the specific isotope pattern of a dibrominated compound (Figure 10.20) with the molecular formula $C_{11}H_9Br_2N_5O_1$. The compound showed UV absorption maxima at 220 and 340 nm. Based on the MS/MS fragmentation pattern, the compound was dereplicated as stevensine, also known as odiline (Figure 4.4), a metabolite reported in various sponge species (Albizati et al., 1985).

4.5.4. PANIKI_4 (TSRR0002_D-12) *Halichondria* sp.

The microfractionated extract PANIKI_4 (injection volume 1 and 2 µL, 1 mg/mL) was rescreened against *S. tritici*. Only the 2 µL injection volume replicate produced one active zone (Figure 10.21), which could be assigned to a compound of *m/z* 317.2112 $[M+H]^+$ corresponding to the molecular formula of $C_{20}H_{28}O_3$. The fragmentation pattern of the compound does not allow for clear assignment of substructural frameworks. The UV absorption maximum was detected at 220 nm. A database search of the molecular formula retrieved a sesquiterpene compound, namely 20-hydroxyhaterumadienone (Figure 4.4), as plausible candidate for tentative structure assignment. 20-hydroxyhaterumadienone is a cytotoxic compound reported from the sponge *Dysidea* sp. (Ueda et al., 2007).

4.5.5. ULU_11 (TSRR0002_H-03)

The extract ULU_11 was selected as a representative of extracts exhibiting weak *C. albicans* activity and highly similar metabolite composition (together with ULU_17, Figure 4.2). The crude extract was fractionated in 2 and 5 µL injection volume replicates and rescreened against *C. albicans*. However, no active fractions could be identified.

4.6. Discussion

In this study, we used a set of 76 sponge samples to present our Semi-automated Prioritization of Extracts for natural Product Research (SeaPEPR) pipeline. Primary bioactivity assessment led to the identification of nine sponge extracts exhibiting bioactivity against at least one of the selected indicator strains. Simultaneously, unsupervised chemical diversity visualization by cosine similarity

heat map construction facilitated the overall data interpretation and prioritization of extracts for downstream processes.

During prioritization, four bioactive extracts (KOL_08, KOL_16, KOL_18, and ULU_13) were grouped together, indicating highly similar metabolite composition. In fact, orthogonal data obtained from sponge identification by morphological features, such as spicule identification (Figure 4.5, Table 10.3), indicated taxonomic uniformity of the organisms (i.e., all specimens were identified as *A. nakamurai* based on spicule morphology*).* In this case, taxonomic uniformity translated into chemical uniformity. Consequently, agelasines and agelasidines (dereplicated in the active fractions of the representative extract KOL_18) were found in all members of this metabolic group (Figure 4.2).

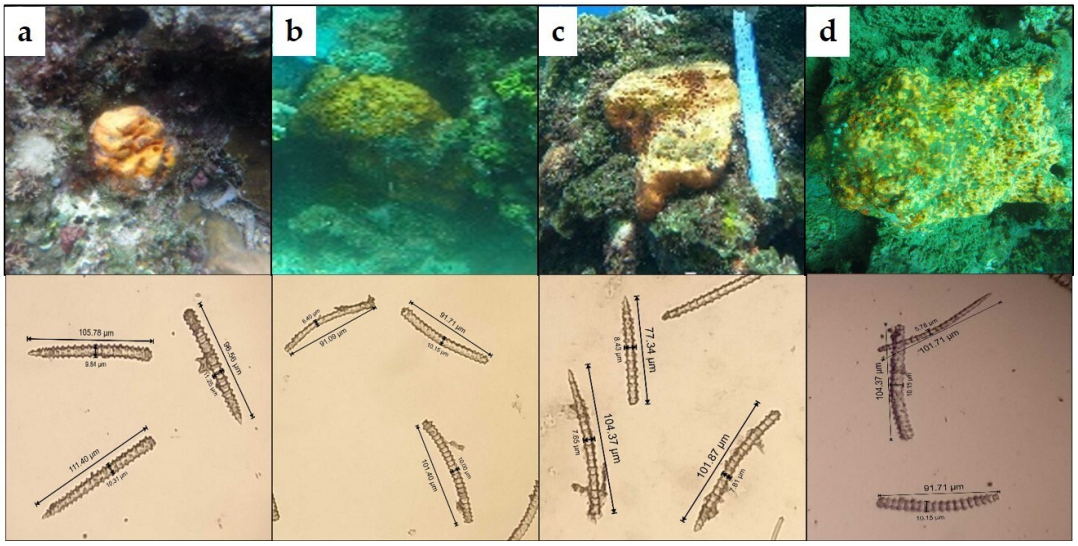

Figure 4.5. Underwater pictures and isolated spicules of the *Agelas nakamurai* cf specimens (**a**) Sample KOL_8, (**b**) Sample KOL_16, (**c**) Sample KOL_18, and (**d**) Sample ULU_13. It can be seen that the specimens are thick encrusting orange sponges and the type of spicule is megascleres acanthostyle for all four samples. This suggested the assignment as *Agelas nakamurai* cf.

On the other hand, PEHE_5 and PANIKI_4 were initially taxonomically classified as members of the genus *Haliclona*. In contrast, the metabolite fingerprinting of these two sponges clearly indicated distinctiveness of organisms. A focused investigation on morphological level finally revealed that PANIKI_4 belongs to the genus *Halichondria*. Six other sponges were morphologically identified as *Haliclona* sp. However, only two pairs of high metabolic similarity could be observed in the heat map, indicating different *Haliclona* species. Within this genus,

speciation seems to be tightly linked to chemical diversification, as *Haliclona* extracts did not cluster, but were distributed throughout the heat map. It is known that besides species affiliation of the holobiont, the chemical profile could also be shaped by the associated microbial communities (Noyer et al., 2011), the habitat (El-Demerdash et al., 2019), as well as stress associated to predation and wounding (Koopmans et al., 2009).

Both observations, chemical uniformity within a species (*A. nakamurai*) and interspecies metabolic diversity (*Haliclona* sp.) can be explained by the well-accepted assumption that taxonomic, thus genetic, diversity is often expressed by chemical diversity. Broad chemical diversity is generally desired in natural product discovery campaigns and thereby careful selection of the source material is crucial. In this context, the prioritization of extracts based on the similarity of their chemical composition helps to maximize metabolite diversity in downstream processes. Especially for samples for which reliable species identification in the field (e.g., sponges) is challenging, chemotyping (e.g., cosine similarity heatmaps) as interface between primary screenings and follow up experiments seems useful to decrease workload. Besides, it has to be kept in mind that even different intra-species samples have the potential for the detection of new and even novel compounds, since analysis of the same species could result in different metabolomes due to the dynamic environmental factors (Malve, 2016). Independent from the sample set, it demands a straightforward downstream pipeline to mine the vast amount of data. While other microfractionation platforms are suitable to acquire detailed information about extracts obtained from precisely selected samples such as different medicinal plants (Bohni et al., 2013; Mohotti et al., 2020), one benefit of the herein presented pipeline is the potential to characterize extracts (and not necessarily the source organism) in detail without processing replicates and yet account for most drivers of metabolic diversity. After prioritization, extract components (ions) are directly linked to the observed bioactivity. Other elegant strategies (e.g., bioactive molecular networking (Nothias et al., 2018)) establish this connection by calculation of the Pearson correlation between the relative abundance of ions across chromatographic fractions (usually 18–20) and the observed bioactivity. Our alternative dereplication approach aims to screen fractions containing only a very limited number of, if not single, ions or ions all belonging to the same molecular feature against the indicators strain (Figures 10.14, 10.18–10.21). Because fraction collection in assay plates is

coupled to MS/MS, a direct, experimental connected between candidate molecule and bioactivity can be established. By using this workflow, five out of initially 76 extracts were prioritized based on bioactivity and unique metabolic fingerprint, before the causative metabolites were determined by microfractionation.

Bioactivity of extracts obtained from *A. nakamurai* could be assigned to agelasines and agelasidine A. Synthetic access to the agelasines was already established (Roggen and Gundersen, 2008) and broad compound profiling was carried out: Reported bioactivities include Na,K-ATPase inhibition (Nakamura et al., 1984), cyto-toxicity, ichthyotoxicitiy, antiprotozoal (Roggen et al., 2011), and antifouling activity, as well as growth inhibition of *M. tuberculosis*, Gram-positive and negative pathogenic bacteria (Balansa et al., 2020), as well as yeast (reviewed by Gordaliza, 2009). Likewise, agelasidines were observed to exhibit activity against *S. aureus* and *C. albicans* (Stout et al., 2012). Broad screening of aplysinopsins demonstrated a modulating activity against the glycine-gated chloride channel receptor (Balansa et al., 2013), antineoplastic, antiplasmodial, anti-bacterial, as well as anti-fungal activities. The latter included growth inhibition of *Penicillium atrovenetum* and *Trichophyton mentagrophytes* (reviewed by Bialonska and Zjawiony, 2009). Besides aplysidine A, a mix of several cytotoxic (Cimino et al., 1975; Gordaliza, 2010) sesquiterpene hydroquinones was dereplicated in the extract PEHE_5 obtained from *Haliclona* sp. The bioactivity of *Neopetrosia* sp. extract ULU_16 was attributed to stevensine (odiline). Reported activity of stevensine comprises fish deterrence (Wilson et al., 1999) and weak antimicrobial growth inhibition (e.g., *Deleya marina*, a common fouling bacterium) (Newbold et al., 1999). The compound 20-hydroxyhaterumadienone (here dereplicated from PANIKI_4 a putative *Halichondria* sp.) is known to possess cytotoxic effects (Ueda et al., 2005, 2007), and exhibit weak interaction with human lipoxygenase (5-hLO) (Robinson et al., 2009).

While these results indicate a generally robust transfer of primarily observed growth inhibitory effects to microfractionated assays, two extracts did not show bioactivity in any fraction. These findings emphasize a general challenge in bioactivity driven NP research (in contrast to cheminformatics inclined discovery projects (Marner et al., 2020). Microbial crude extracts are composed of a mixture of various substances at dramatically different concentrations and potencies. It is important to realize that almost each substance (or a combination of several metabolites) becomes unspecifically toxic at high concentrations, hence producing

a positive assay read out. As discrimination between specific and unspecific effects might come at the price of insensitivity, we chose a trade off in favor of false positive instead of false negative results. Consequently, initially moderately active crude extracts (e.g., ULU_11 against *C. albicans*) might not produce positive microfractionation read outs. Given suitable chromatography parameters, members of compound families are separated and tested individually at lower overall concentration. In the case of PEHE_5, the microfractionated extract was unsuccessfully rescreened against *S. tritici.* Potentially, the sum of compounds presents in the extract (di-brominated aplysinopsins; aureol/chromazonal) possessed additive, however unspecific, growth inhibition of the test strain, while individual compounds did not show the effect. Although the reduction of unspecific effects caused by high concentration of compounds seems to be an advantage, separation and individual testing of metabolites might also prohibit identification of synergistic effects.

Another limitation of rapid MS/MS-based annotation approaches, including the herein presented methodology, is the reduced identification confidence of target molecules (as defined by the Metabolite Annotation Task Group of the Metabolomics Society) (Salek et al., 2013; Creek et al., 2014) compared to full structure and stereochemistry assignment studies. In that sense, no distinction between the isomeric sponge metabolites aureol and chromazonarol or between putatively 6′-aureoxyaureol and 6′-aureoxychromazonarol could be made. Besides these challenges, SeaPEPR has proven its value as prioritization strategy allowing data-based decision making on follow-up projects early in the discovery process. This study gave insight into the metabolites of four morphologically seemingly different specimens of *A. nakamurai*, preventing an otherwise very daunting task of molecular structure elucidation.

If a compound exhibits the desired properties such as structural novelty or repurposing potential, the metabolite should undergo further analysis, including confirmation of the 3-dimensional structure and extensive activity profiling. For repurposing studies of small molecules, the required amount (~ 1 mg) to carry out experiments required for hit characterization might be generated by straightforward chemical synthesis as shown for the agelasines (Roggen and Gundersen, 2008). While an unknown and likewise bioactive metabolite is scientifically most intriguing, it initially requires more sample material; hence, detailed metadata should be recorded in the field (Table 10.3) to allow resupply. Collection of specimens with

the same chemotype might be challenging, but not per se, as observed by the robust metabolic fingerprint of *A. nakamurai* across sampling sites (>60 km distance between Kolongan and Ulu sampling sites). Before isolation from animal tissue is conducted, metabolite access via fermentation of the cultivable microbiome should be investigated. If this route is obstructed, authorities should decide case by case whether a targeted isolation campaign from animal tissue, towards new and urgently needed antibiotic or agrochemical lead structures, is ethically justifiable. Selection of promising projects might be facilitated by data obtained from prioritization processes, such as SeaPEPR.

Finally, yet importantly, to the best of our knowledge, no bioactivity against the common plant pest *S. tritici* was reported for any of the herein dereplicated sponge compounds. The ascomycete *S. tritici*, which is the causative agent of blotch disease on wheat, is responsible for serious losses in cereal yields and quality in Western European countries. In 2014, an estimated $1.3 billion worth of fungicides was used to control *Septoria*-induced crop rust (Torriani et al., 2015). Resistance development, strict EU regulations, and increased public awareness against the use of petrochemicals drive the continuous demand for new agents with potency against *S. tritici*. The herein presented data indicate that marine-derived natural products pose potential solutions for current challenges in plant pest control.

5. Results II: Isolation and screening of antibacterial compounds producing bacteria associated with marine sponge

5.1. Background

Marine invertebrates, e.g. sponges (Porifera), are a well-known bioresource for natural products (Laport et al., 2009; Perdicaris et al., 2013; Melander et al., 2016; Bertrand and Munoz-Garay, 2019), which have the potential to advance into lead structures for drug discovery and development. For several of these compounds, in the meanwhile, evidence exists that the molecule of interest isolated from these sponges is actually produced by (endo)-symbiotic or otherwise associated bacteria, leading to the assumption that sponge-associated bacteria produce a multitude of novel bioactive molecules (Fuerst, 2014). Sponges associated with many microorganisms have been termed high microbial abundance (HMA) sponges and low microbial abundance (LMA) sponges. HMA sponges have bacterial population densities of 10^8–10^{10} bacteria per gram of sponge wet weight, surpassing seawater concentrations by 2–4 orders of magnitude, whereas LMA sponges have bacterial population densities that are comparable to natural seawater (10^5–10^6 bacteria per gram of sponge wet weight) (Hentschel et al., 2006). Up to now, seven bacterial phyla were isolated and brought into culture from marine sponges, i.e., Actinobacteria, Bacteroidetes, Cyanobacteria, Firmicutes, Planctomycetes, Proteobacteria, and Verrucomicrobia. However, it is reported that at least 16 bacterial phyla are present in sponges, as observed by culture independent methods (Taylor et al., 2007).

The host sponges and their bacterial microbiome constitute a mutualistic symbiosis, in which sponges provide space for the bacteria and the bacteria offer metabolites, e.g. nutrients of nitrogen and carbon fixation and specialized metabolites (Imhoff and Stohr, 2003; Taylor et al., 2007). Furthermore, bacteria are involved in the chemical defence of the sponge by providing bioactive molecules (Hentschel et al., 2002; Imhoff and Stohr, 2003; Taylor et al., 2007; Laport et al., 2009). In this thesis, three isolation campaigns of bacteria associated with marine sponges are reported. The samples were collected at three different locations around Indonesian islands. In this chapter, the isolation results of campaign 1 and 3 are stated, while campaign 2 is reported separately in chapter 6.

5.2. Isolation of bacteria associated with marine sponges

5.2.1. Bacteria isolation campaign 1

Five sponge samples from around Bunaken National Park (Table 10.1) were used to obtain 396 pure bacterial isolates using seven different media. The sponge Phva16Sa-43,44-S, was identified as *Haliclona amboinensis* based on cytochrome oxidase subunit I (COI) gene sequencing. This specimen was the only one that was identified by COI sequencing, since most bacterial strains were isolated from this sponge. It should be mentioned that it was not easy to get the sequence. PCR reactions were not successful in amplifying any partition of the COI region for some reasons. Future work on providing fresh tissue, designing better primer sets, and optimizing the PCR program could help reduce the effect of the sample age on the success of PCR and improve COI barcoding efficiency and selectivity. This sponge yielded the highest number of isolates (170). The sponge Phpu16Sa-47S yielded the second-highest number of isolates (78) and from sponge Phva16Sa-49 the lowest number of bacteria (11) was isolated. Seven different media including three times medium marine broth (MB) using three different antibiotics each were used to obtain bacterial isolates. The isolated bacteria were chosen based on the difference in the morphology and colour. The isolation medium generating the highest number of isolates was marine broth medium with nalidixic acid (101), followed by marine broth medium with cyclohexamide (98) and the lowest number of bacteria were isolated from medium MB with chloramphenicol (7) (Figure 5.1). In total 396 isolates were tested for antibacterial activities. The bacteria that showed antibacterial activities were chosen for 16S rRNA gene sequencing.

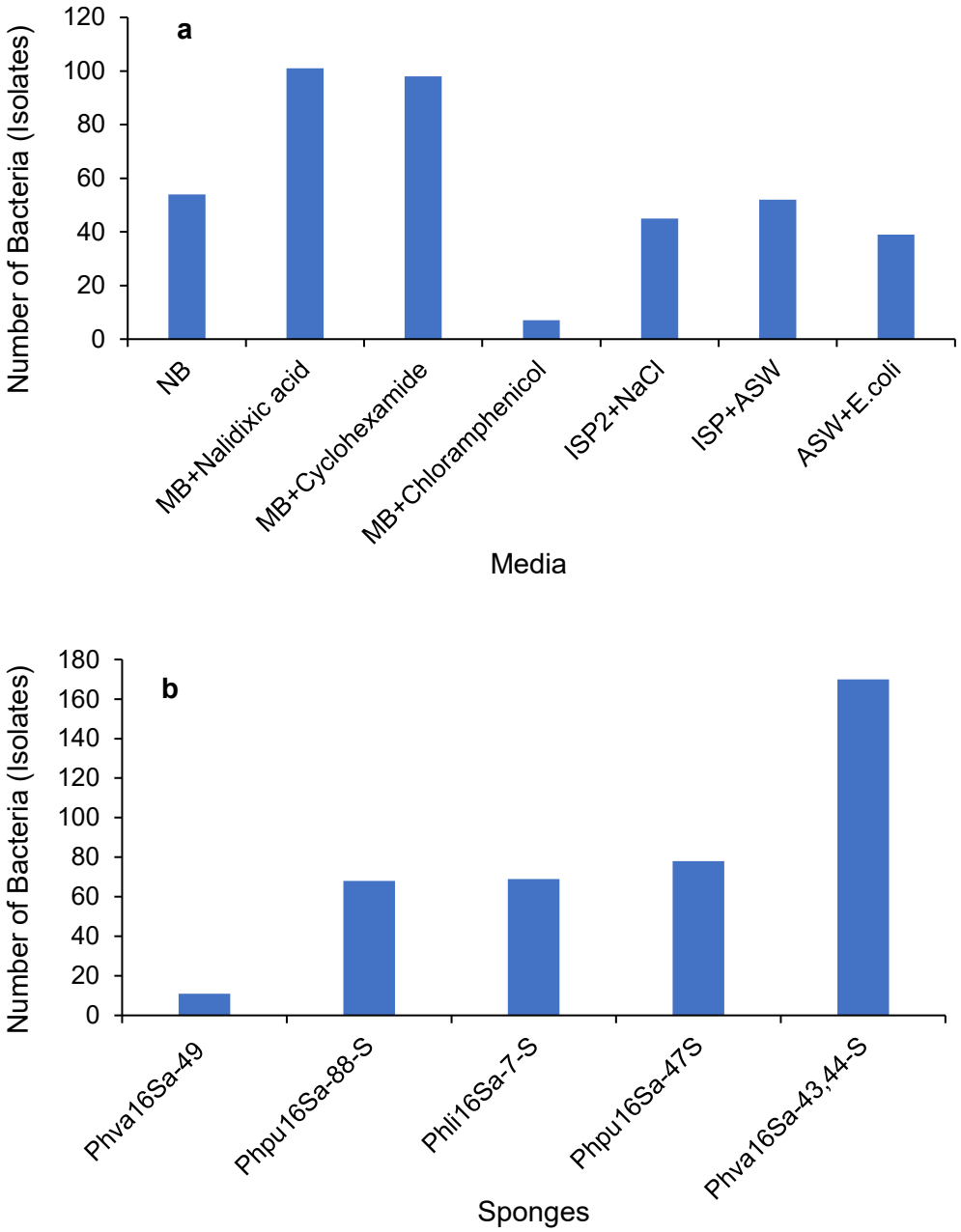

Figure 5.1. Number of bacterial isolates from five sponges collected from around Sangihe Island, Indonesia based on media (a) and host sponges (b).

5.2.2. Bacteria isolation campaign 3

More than 99% of bacteria from environmental samples remain unculturable in the laboratory. A different isolation strategy with low nutrient-medium, prey bacteria and long incubation times was applied to get rare bacteria. The rational was that the before uncultured marine bacteria can be a promising candidate source of new secondary metabolites. A total of 54 marine sponges and four marine sediment

samples were collected from Cenderawasih Bay National Park, Papua, Indonesia. Until this thesis is written, I isolated 135 pure bacteria from ten sponge samples using artificial sea water (ASW) agar medium with several prey bacteria. The artificial seawater agar medium was used that is low in nutrients, since the only ingredient beside ASW is the agar used for solidification. On this medium several prey bacteria were applied. The idea was that some bacteria can feed on the prey bacteria and thereby the chance to isolate bacteria that could produce antibacterial metabolites, since they have to weaken or even kill their prey should be enhanced.

Table 5.1. Number of identified strains isolated from sponges and marine sediment Cenderawasih Bay National Park

Phyla	Genus	Occurrence (%)
Proteobacteria	*Thalassospira*	13.04
Bacteroidetes	*Flammeovirga*	11.11
Bacteroidetes	*Algoriphagus*	8.70
Bacteroidetes	*Sinomicrobium*	6.52
Bacteroidetes	*Tenacibaculum*	6.52
Bacteroidetes	*Cytophaga*	4.35
Bacteroidetes	*Fabibacter*	4.35
Bacteroidetes	*Flexibacter*	4.35
Bacteroidetes	*Galbibacter*	4.35
Proteobacteria	*Marinobacter*	4.35
Proteobacteria	*Pseudovibrio*	4.35
Proteobacteria	*Salinicola*	4.35
Proteobacteria	*Labrenzia*	4.35
Actinobacteria	*Streptomyces*	2.17
Bacteroidetes	*Euzebyella*	2.17
Bacteroidetes	*Flavobacterium*	2.17
Bacteroidetes	*Meridianimaribacter*	2.17
Bacteroidetes	*Sufflavibacter*	2.17
Proteobacteria	*Alcanivorax*	2.17
Proteobacteria	*Alteromonas*	2.17
Proteobacteria	*Halomonas*	2.17
Proteobacteria	*Microbulbifer*	2.17

Then, 46 isolates were selected for further 16S rRNA identification on the basis of the colour and morphological group on the marine broth medium. Based on 16S rRNA gene sequencing of the cultured isolates, three different bacterial phyla were most abundant: Bacteroidetes (58.70%), Proteobacteria (39.13%), and Actinobacteria (2.17%), whereby 12, 9 and 1 genera/genus were proposed on sequence similarity, respectively (Table 5.1). Alignments of the generated one side-length 16S rRNA gene sequences revealed that most of the bacterial isolates shared 99-100% identity with known species. However, the strain in genus *Cytophaga*, *Salinicola,* and *Sinomicrobium* showed 98% 16S rRNA similarity. Furthermore, the genus *Galbibacter* had a sequence identity of 95% in 16S rRNA.

5.3. Primary screening of antibacterial compounds producing bacteria

In this paragraph, the screening for antibacterial activity of bacterial isolates derived from campaign 1 will be described. More details about the strains isolated during campaign 2 will be explained in detail in chapter 6. Campaign 3 is still in process, strain collection and maintenance and antibacterial activities screening are not finished yet. Preliminary screening of 135 isolated bacteria was performed using disk diffusion assay. Strain *Flammeovirga yaeyamenisis* 2b showed highest antibacterial activity based on preliminary screening. Analysis of this active strain *F. yaeyamenisis* 2b is detailed in chapter 7.

All bacterial isolates obtained from campaign 1 were initially tested for antibacterial activity using paper disc assays. The sponge-derived bacterial isolates were assayed for inhibitory activity against Gram-positive *M. luteus* and Gram-negative *E. coli* test strains. Among 396 marine bacterial isolates derived from five sponges, 6.1 % showed antibacterial activity against at least one of the test organisms. About half of the active isolates inhibited both, and the other half displayed activity against Gram-positive bacteria. None of the isolates showed activity against the Gram-negative bacterium without activity against the Gram-positive under these assay conditions (Figure 5.2, Table 10.6).

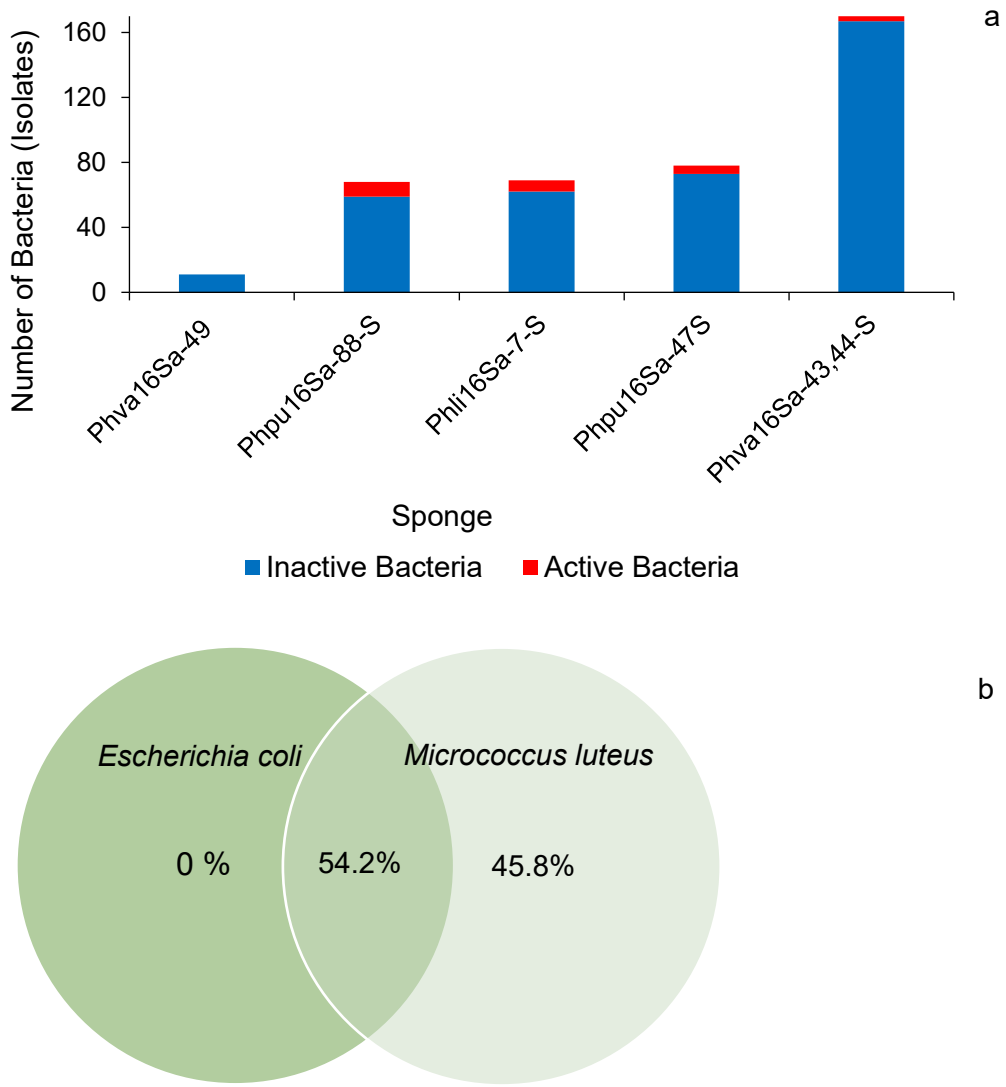

Figure 5.2. Bacterial isolates (active strains in red) isolated from each sponge specimen (a) Percentage of the 396 isolated active bacteria that showed activity solely against Gram-positive *M. luteus*, Gram-negative *E. coli* and both test strains (b).

Twenty-four active isolates were chosen for molecular identification. Analysis of the 16S rRNA gene revealed that the 24 active strains belonged to the three phyla Actinobacteria (54.2%), Firmicutes (41.7%), and Proteobacteria (4.2%). Photographs of axenic culture representatives of each active genus are shown in Figure 10.22. Most of the active strains belonged to the genus *Bacillus*. Further antimicrobial activities were observed for *Salinispora* and *Microbacterium* species (Table 5.2).

Table 5.2. Phyla and genera of the active bacterial strains based on 16*S* rRNA gene sequencing

Phyla	Genus	Occurrence (%)
Firmicutes	*Bacillus*	41.7
Actinobacteria	*Salinispora*	37.5
Actinobacteria	*Microbacterium*	12.5
Actinobacteria	*Nocardiopsis*	4.2
Proteobacteria	*Psychrobacter*	4.2

To get an idea about which compounds might contribute to the observed activities, crude extracts of these strains were generated and analyzed. Ethyl acetate extracts were investigated using tandem high-resolution mass spectrometry of fermentation extracts, accompanied by metabolite dereplication using molecular networking. A molecular networking on the Global Natural Product Social (GNPS; www.gnps.ucsd.edu) platform was utilized for data analysis purposes. The resulting molecular network (Figure 5.3) was visualized in Cytoscape 3.7.2. Using molecular networking, known compounds can be dereplicated by automatized comparison with mass spectrometry profiles available in databases (Mohimani et al., 2018). The resulting metabolite mass spectra of the 24 bacterial strains were visualized in a molecular network that contained 275 parent ions (nodes); whereby, the medium nodes were already omitted (Figure 5.3). The node with the precursor ion *m/z* 467.211 $[M + H]^+$ revealed a hit for the MS/MS spectrum, since a matching spectrum was identified in the GNPS spectral library. This was annotated as staurosporine, and was produced by *Salinispora* sp. 238.1 and *Salinispora* sp. 239.2 in ASW medium. (For this experiment, the bacteria were cultured solely in the same medium as they were isolated from). After the identification of this library hit, manual inspection of the additional nodes of this small sub-network (Figure 5.3) revealed the precursor ion *m/z* 481.184 $[M + H]^+$ to be staurosporine M1, *m/z* 483.204 $[M + H]^+$ to be staurosporine-7-OH and *m/z* 486.163 $[M + H]^+$ to be a derivative of staurosporine-7-OH.

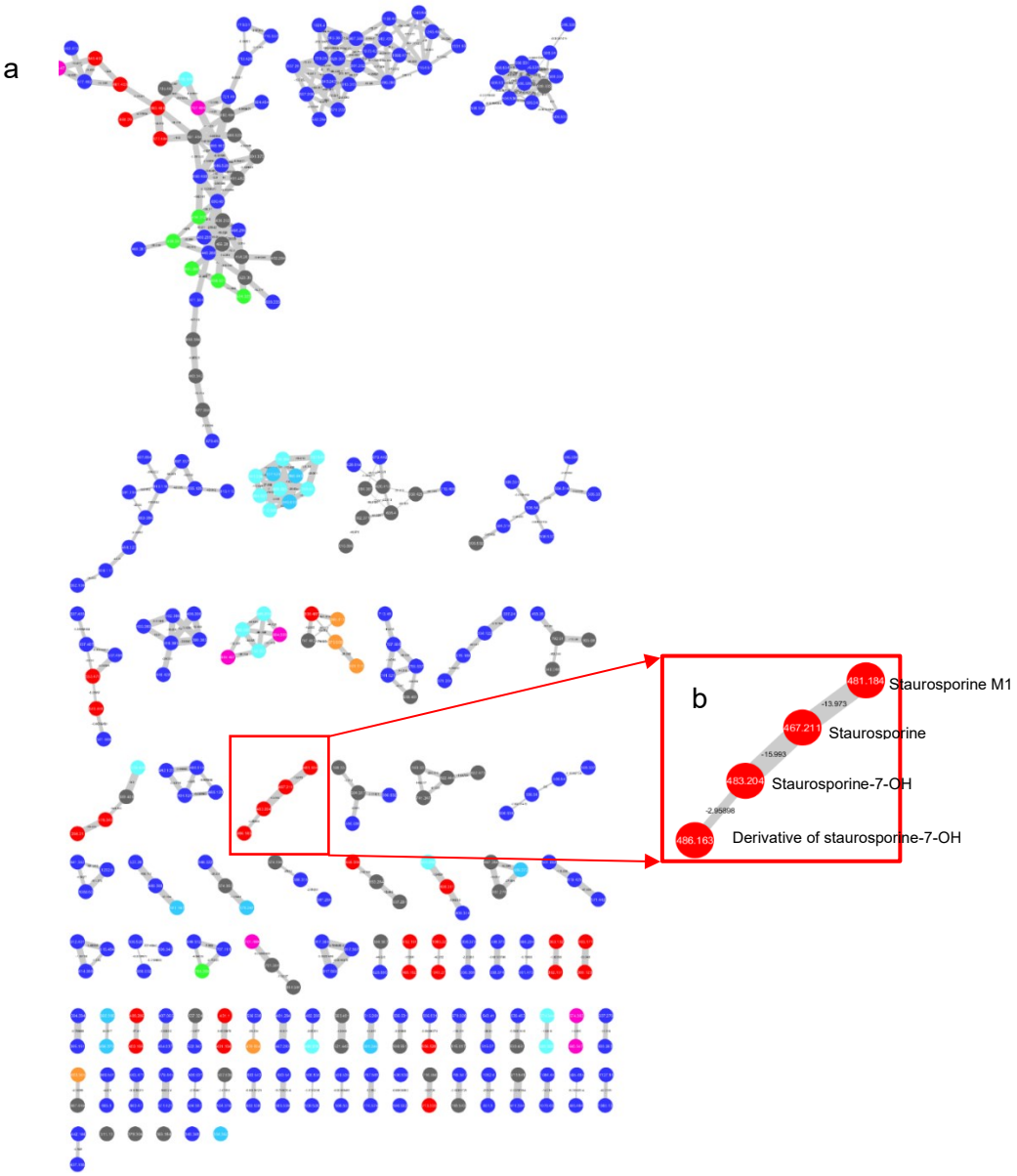

Figure 5.3. Molecular networking of 275 parent ions produced by 24 bacterial strains. Node's colors are based on each genus of bacteria, where the media are excluded. Dark blue: *Bacillus* sp.; red: *Salinispora* sp.; light blue: *Nocardiopsis synnemataformans*; orange: *Microbacterium arborescens*; green: *Psychrobacter pasificensis*; purple: *Salinispora* sp. and *M. arborescens*; grey: all strains (a). Nodes highlighted in the colored box represent parent ion that were dereplictaed as staurosporine M1 (*m/z* 481.184), staurosporine (*m/z* 467.211), staurosporine -7-OH (*m/z* 483.204) and derivative of staurosporine-7-OH (*m/z* 486.163) (b).

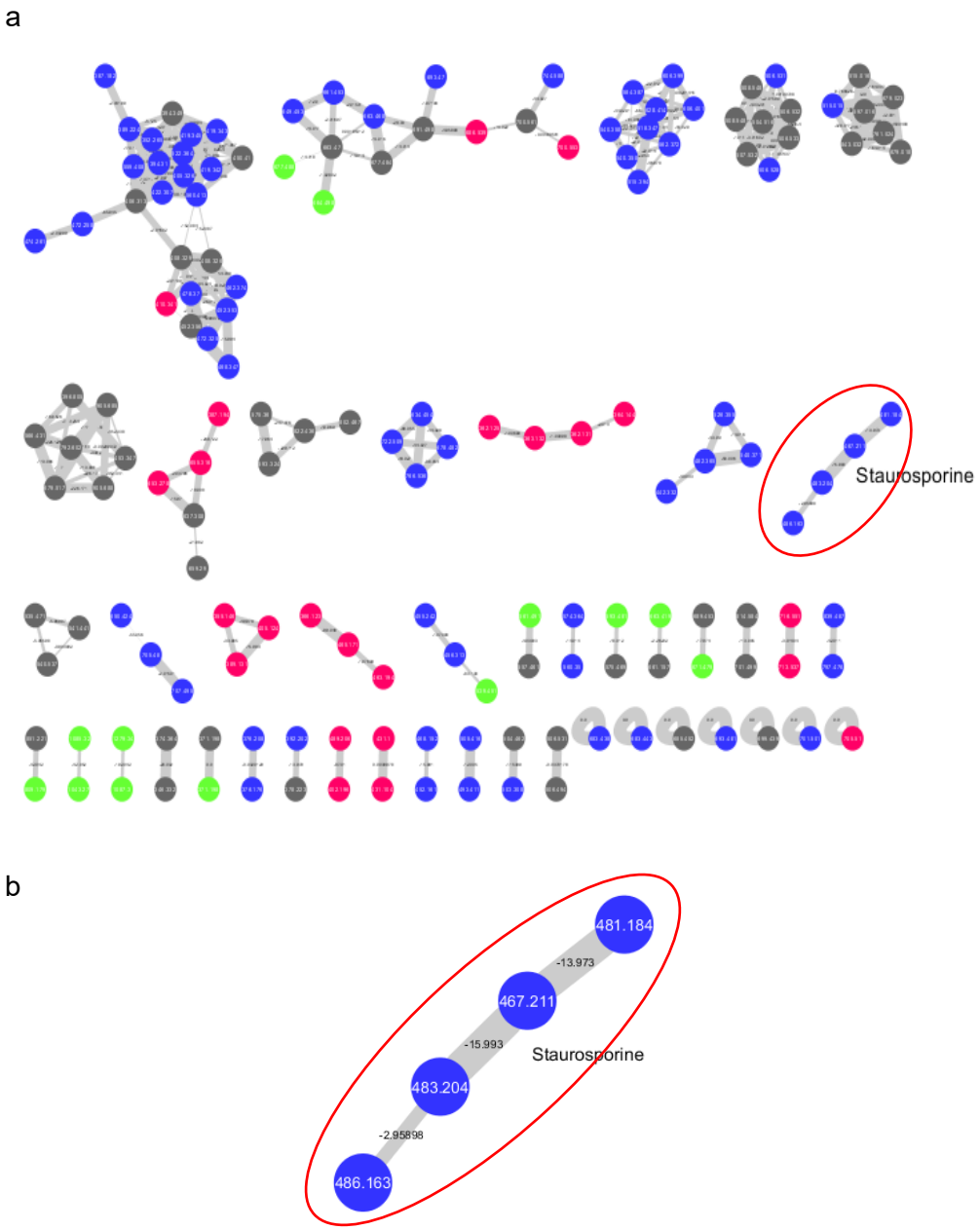

Figure 5.4. A molecular network obtained combining the LC-MS/MS analyses from *Salinispora* sp. cultured using 3 different based media. Nodes are represented as the source of the compound (blue: *Salinispora* sp. cultured in ASW; green: in starch nitrate; red: in M1; grey: in all media. Numbers within nodes reflect parent ions, and edge thickness reflects cosine similarity between nodes (a). The red circle node represents staurosporine (*m/z* 467.211) which was produced by *Salinispora* sp. cultured in ASW medium (b).

Salinispora sp. are known to be proliferative producers of bioactive compounds and due to the fact that these extracts generated the biggest zones of inhibition in the here performed screening, these strains were fermented in bigger scale. *Salinispora* sp. 238.1, 239.3, and 240.1 were cultured, each in three different media, i.e., ASW, starch nitrate, and M1. The metabolite profile of the crude extracts was observed by molecular networking (Figure 5.4). The staurosporins that were dereplicated before could be shown to be produced by *Salinispora* sp. 238.1 and *Salinispora* sp. 239.2 only if cultured in ASW medium.

To find new compounds with antibacterial activity, starch nitrate medium was chosen for further fermentation. 10% Tryptic soy broth (TSB) was also used as a comparative medium to optimize the antibacterial activity.

Table 5.3. Antibacterial activity of *Salinispora* sp. against *Micrococcus luteus*

***Salinispora* strain experiment**	**Activity against *M. luteus***
238.1 S SNB 15 d	+++
238.1 P SNB 15 d	-
238.1 S SNB 30 d	++++
238.1 S TSB 15 d	+++++
238.1 P TSB 15 d	+++
238.2 S SNB 14 d	++++
238.6 S SNB 19 d	++++
238.6 S SNB 22d	++++
239.2 S SNB 14d	+++
239.2 P SNB 14 d	-
239.2 S TSB 14 d	+
239.2 S TSB 14 d	+
239.3 S SNB 14 d	++
239.3 P SNB 14 d	-
239.3 S TSB 9 d	++
239.3 P TSB 9d	-
239.3 P TSB 14d	-
301 S SNB 14d	++++
301 P SNB 14d	+
302 S SNB 14d	++++
302 P SNB 14 d	-
302 S TSB 14 d	++++
302 P TSB 14d	+
303 S SNB 22 d	+

S: Supernatant extraction using ethyl acetate

P: Pellet extraction using methanol
SNB: Starch nitrate broth TSB: 10% Tryptic soy broth d: days
-: no activity ++ until +++ : moderate activity
+: weak activity ++++ until +++++ : high activity

The methanol extracts were obtained from the pellet as the intracellular extract, whereas the ethyl acetate extracts from the supernatant as the extracellular extract. Both extracts were tested against test organisms. All eight *Salinispora* sp. revealed various activity against the Gram-positive bacterium *M. luteus* extracted either from SNB or TSB culture. The ethyl acetate extracts obtained from the culture that were incubated for a longer time period (day 14 – day 30) exhibited the highest activity (Table 5.3, Figure 10.23). Besides the activity testing, all the crude extracts were subjected to LC-MS/MS analysis. The MS/MS dataset was used to generate a molecular network (Figure 5.5). Initially, the automated dereplication by comparison of MS^2 fragmentation profiles with the GNPS library resulted in the annotation of four compounds, i.e. desf-05 (*m/z* 575.38 $[M + H]^+$), desferrioxamine B *m/z* 585.32 $[M + H]^+$ desferrioxamine E *m/z* 601.36 $[M + H]^+$ and ferrioxamine D1 (*m/z* 627.33 $[M + H]^+$). These known compounds were annotated entirely from pellet extract *Salinispora* sp. cultured in 10% TSB medium. Bacteria produce structurally distinct siderophores with various forms of Fe (III) binding functional groups including hydroxamic acids due to competition for limited iron. Desferrioxamine B and desferrioxamine E are iron chelators from the hydroxamic acid class produced by *S. tropica* CNB-440 (Ejje et al., 2013) as well as desf-05/ desferrioxamine N and ferrioxamine D1 (Jarmusch et al., 2021).
However, it could be expected that more compounds could be dereplicated from *Salinispora* species, since these bacteria are well-investigated. Therefore, a manual dereplication was also performed by comparison of the *m/z* of the nodes with reported *Salinispora* compounds (the list was based on the internal database of the Center for Marine Biotechnology and Biomedicine, Scripps Institution of Oceanography, United States). This manual dereplication allowed the identification of four additional compounds based on the mass, i.e., saliniketal A, rifamycin S, staurosporine, and staurosporine-7-OH (Table 5.4).

a

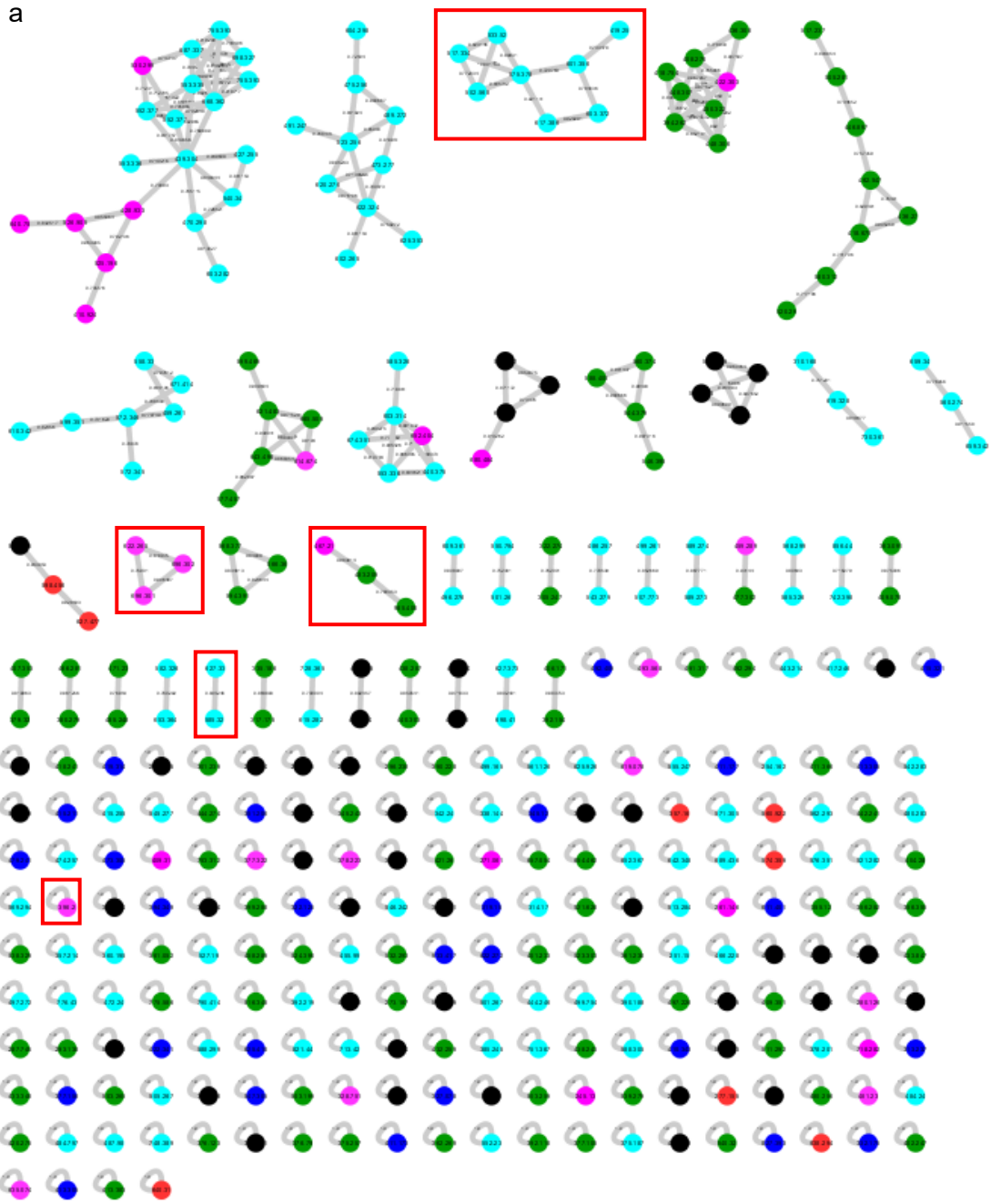

b

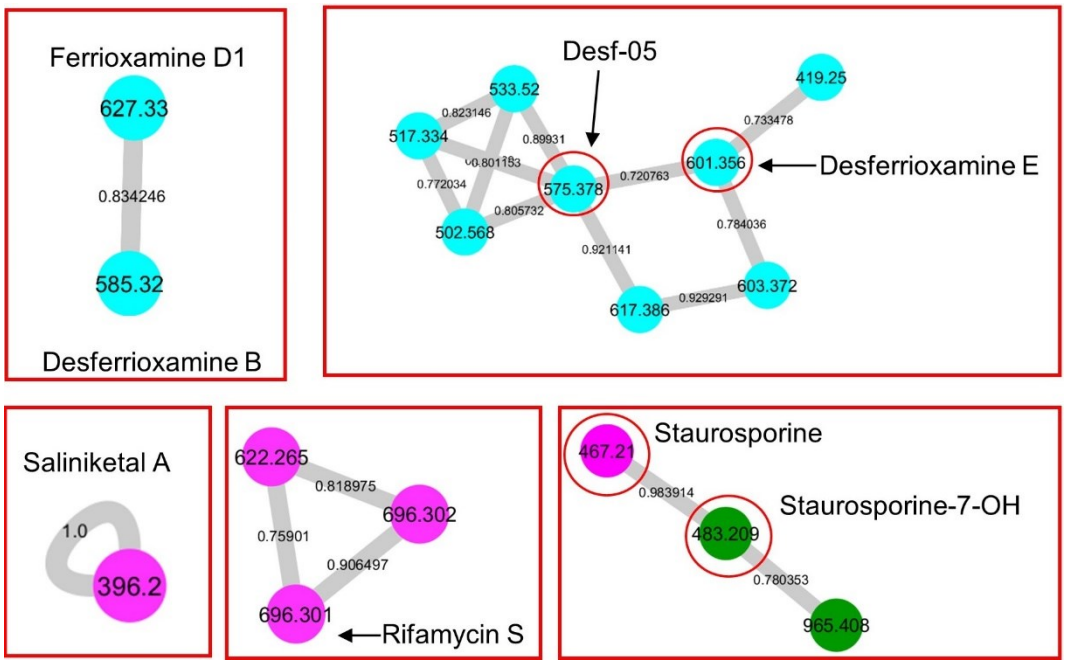

Figure 5.5. Molecular networking Salinispora strains obtained from supernatant (S) and pellet (P) extraction. Each node represents medium, day period of culture and extraction source of *Salinispora* strains. Red nodes are TSB, day 9 - 15, S; dark blue nodes are SNB, day 9 – 15, S; green nodes are SNB, day 19 – 30, S; light blue nodes are TSB, day 9 – 15, P; purple nodes are all conditions; and black nodes are media (a).

Table 5.4. Compounds detected in *Salinispora* strains by manual LC-MS analysis

Compound	*m/z*	Name	Producer (Strain Extraction-Medium- Day)
1	396.2737	Saliniketal A	*Salinispora* sp.238.1 S TSB 14 d *Salinispora* sp.238.1 S SNB 14 d
2	696.3011	Rifamycin S	*Salinispora* sp.238.1 S TSB 14 d
3	467.2093	Staurosporine	*Salinispora* sp.238.1 S SNB 15 d *Salinispora* sp.238.1 S SNB 30 d *Salinispora* sp. 238.2 S SNB 14 d *Salinispora* sp. 239.3 S SNB 15 d
4	483.2	Staurosporine-7-OH	*Salinispora* sp.238.1 S SNB 30 d

5.4. Discussion II

Due to the increased incidence of multi-drug resistance among pathogenic bacteria, the discovery of new antibiotics from marine bacteria is crucial. About 99% of marine sponge-associated bacteria are estimated to have yet to be cultivated. In this project (campaign 1), 396 bacteria were isolated from 5 sponges, whereby a high variation within the number of isolates was observed between the sponges. The range was between 11-170 isolates, which almost half of them were isolated from the sponge *H. amboinensis* Phva16Sa-43,44-S. The use of different sections of the sponge body known to be populated by different bacterial communities, may be a potential explanation for this result. Observation on two clearly differentiated sample regions, i.e. cortex and endosome, of the sponge *Tethya aurantium* proved that they also differ in bacterial communities (Thiel et al., 2006).

Here, the isolation of bacteria from 5 sponges allowed 24 active bacteria belonging to phyla Actinobacteria, Firmicutes, and Proteobacteria. Similarly, Graça et al. (2013); Graça et al. (2015); and Rajasabapathy et al. (2020) also observed that these phyla were the most abundant high antimicrobial sponge isolated bacteria. Furthermore, Webster and Taylor (2012) reported that those phyla are commonly present in sponges.

Several bioactive genera isolated in this study have been described to possess antimicrobial activity. *Bacillus* is a well-known bioactive compounds producer (Devi et al., 2010; Indraningrat et al., 2016; Mohan et al., 2016; Kuo et al., 2019; Freitas-Silva et al., 2020) as well as *Salinispora* (Kim et al., 2006; Asolkar et al., 2010; Jensen et al., 2015; Da Silva et al., 2019; Wang et al., 2020), and *Microbacterium* (Kanagasabhapathy et al., 2008; Liu et al., 2019). The antibacterial activity produced by *Nocardiopsis* has been previously found (Liu et al., 2019; Wang et al., 2020). *Psychrobacter,* according to Graça et al., 2015 revealed antimicrobial activity.

Bacteria isolation campaign 3 revealed 135 isolates, which were dominated by the phyla Proteobacteria and Bacteroidetes. Proteobacteria and Bacteroidetes were dominant bacteria isolated from sponges belonging to genus *Mycale* (Cárdenas et al., 2018), eight different sponges from King George Island, South Shetland Islands (Maritime Antarctica) (Rodríguez-Marconi et al., 2015). Using low nutrient medium, only consisting of ASW, the isolates were targeted for searching new active

metabolites. Choi et al. (2015) encouraged the use of low-nutrient media and long incubation periods to explore for new antibiotics from previously uncultivated Gram-negative marine bacteria. Some active compounds were isolated from the phylum Bacteroidetes. Marinoquinoline A, flexirubin and carotenoids were isolated from *Rapidithrix thailandica* (Choi et al., 2015), *Flexibacter*, and *Rhodonellum psychrophilum* (Schmidt et al., 2006) respectively. This phylum also produced new alkaloid secondary metabolites, representing new carbon skeletons and revealed antibacterial activities.

Furthermore, *Salinispora* strains were chosen for further analysis because they exhibited potential antibacterial activities. In this study, *Salinispora* strains were detected to produce staurosporine, stauroporine M1, staurosporine 7-OH and a further derivative, rifamycin S and saliniketal A. The detected compounds can explain the high activities of the *Salinispora* crude extracts in comparison to other bacteria. From the genus *Salinispora* alone, 150 metabolites were detected and their chemical and biological activities characterized since 2001, when lomaiviticins A and B were reported (Kim et al., 2020). Staurosporine, rifamycin, and saliniketal A were previously observed in *S. arenicola* and proved their biological activities as anticancer, antibiotic and cancer chemoprevention, respectively (Jensen et al., 2007).

Staurosporine, rifamycin S and saliniketal A were detected merely from supernatant derived of *S. arenicola* strain samples. However, there are three other staurosporine derivatives, i.e., staurosporine M1, staurosporine 7-OH, and a derivative of staurosporine-7-OH. This means that the *Salinispora* strains produced secreted the compounds into the medium. Marine sponge-associated bacteria produced molecules provide the host chemical defence against predation and microbial infection. Izumi et al. (2010) proved this spesific role of rifamycin-producing *S. arenicola* strains isolated from a marine sponge against other bacteria. Rifamycin could inhibit *Mycobacterium* strains isolated from the same sponge, indicating that rifamycins might work in competition against members of the sponge microbial community.

Staurosporine was first isolated from a *Streptomyces* strain (Furusaki et al., 1978) and thereafter reported in *S. arenicola* as a renowned class of protein kinase inhibitors (Freel et al., 2011). Already earlier, staurosporine was dereplicated from strains belonging to another actinomycete, i.e., *Saccharothrix* (ŌMura et al., 1995).

Furthermore, rifamycin and saliniketal were produced by *Salinispora*, as described by Jensen et al., (2007a and Jensen et al., 2015). Hereafter, rifamycins are antibacterial drugs targeting RNA polymerase against Gram-positive bacteria and Gram-negative bacteria to a lesser level (Kim et al., 2020). *Amycolatopsis mediterranei* was first published as a rifamycin producer (Krishna et al., 1998; Floss and Yu, 2005), while rifamycins were first identified in *Salinispora* M403 isolated from the sponge *Pseudoceratina clavata*, which was revealed to produce both rifamycin B and SV. The first reported source of rifamycin from marine bacteria is the *Salinispora* group of actinobacteria (Kim et al., 2006).

In this study, *Salinispora* sp.238.1 produced rifamycin S at the 14 days. Most of the inhibitory activity of *S. arenicola* occurred early in its growth cycle and was related to the production of antibiotics (Patin et al., 2016). Rifamycin S has been shown to be produced during the complete growth cycle of *S. arenicola*, but the amount produced was time-dependent with the detection starting at 14 days and maximum concentrations after 29 days (Bose et al., 2015). Rifamycin S had antibacterial activities against Gram-positive bacteria as well as mycobacteria. (Kim et al., 2020). Saliniketals A has been isolated from *S. arenicola* strains CNR-005 and CNR-059, which was reported to have potential as cancer chemoprevention (Williams et al., 2007). Jensen et al. (2015) reported several compounds were produced in taxonomic-specific patterns when trying to isolate novel compounds from *Salinispora* species using conventional bioassay-guided techniques. This definition was explained in more depth and led to the inference that certain compounds are species specific, i.e., members of the same species have continuously produced them. Rifamycin S and saliniketal A were produced 100% by *S. arenicola* strains, indicating that the gene cluster of this biosynthetic pathway is strongly conserved in this species (Bauermeister et al., 2018).

Furthermore, the environment appears to have an important effect in microbial metabolite synthesis (Costa-Lotufo et al., 2018). Bauermeister et al. (2018) found that several *S. arenicola* strains from the same location can produce species-specific metabolites when cultivated under the same parameters. One *S. arenicola* strain from a different location had also more profile metabolite, indicating that their metabolic expression is influenced by the environment.

S. arenicola strains produce some species-specific compounds including saliniketal, rifamycin, and staurosporines. Interestingly, it should be noted that

these rifamycin and staurosporines, repeatedly observed from *S. arenicola*, represent some of the most potent biologically active compounds in this genus (Jensen et al., 2007, 2015). Saliniketal A may be a chemical marker for *S. arenicola* (Bauermeister et al., 2018) since other genera, such as *Nocardia mediterranei*, also produce rifamycin and derivatives (Kim et al., 2020). 108 more metabolites were detected from *S. arenicola* strains than from *S. pacifica* strains (Bauermeister et al., 2018). Letzel et al. (2017) also reported that *S. arenicola* had in average a significantly higher number of biosynthetic gene clusters (BGCs) per genome than the other two species.

There are not so many publications related to staurosporine M1. This staurosporine derivative was reported by Xiao et al. (2018) to be produced by heterologous expression using an engineered spc BGC in *Streptomyces coelicolor* M1146. The spc BGC involved in staurosporine production was discovered and described previously from marine-derived *Streptomyces sanyensis* FMA (Li et al. 2013). The spc BGC involved in staurosporine biosynthesis in *S. coelicolor* M1146 was analyzed. The expression cosmids pWLI624 and pWLI626 were designed to carry the modified spc gene clusters, spcN deletion and spcMA spcMB double-deletion, respectively. It proved to the isolation of two new (staurosporine M1 and staurosporine M2) and five known staurosporine derivatives (Xiao et al., 2018).

In the pellet extracts of the investigated *Salinispora* strains here were cultured in 10% TSB medium, four compounds belonging to the class of siderophores were detected. The low concentration of nutrients might trigger production of these compounds. Siderophores are only formed in very small quantities under conditions of iron deficiency. For example, it is described that *S. tropica* CNB-440 is capable to produce eight siderophores of the desferrioxamine (DFO) class, the largest number of derivatives produced by a single species of actinomycetes. Simulation complex marine environment parameters was design at several concentrations according to various laboratory culture conditions to produce the DFOs. This would mean that *S. tropica* CNB-440 can adapt to changing habitat conditions in the marine life through its ability to adapt the production level and type of siderophores (Ejje et al., 2013).

Roberts et al. (2012) reported that that DFOs are the primary siderophores of *Salinispora* species. As a competitive advantage, some bacteria generate several siderophores by offering alternative ferric-uptake pathways not used by

neighboring microbes (Challis and Hopwood, 2003). Multiple siderophore-like biosynthetic loci were indicated by genome analysis of the obligate marine actinomycetes *S. arenicola* (Penn et al., 2009).

Another strain of *Salinispora* was observed, i.e., *S. arenicola* CNS-205, which produced two iron chelators DFOB and DFOE. DFOE was the most abundant siderophore detected from *Salinispora*. *S. tropica* CNB-440 showed a high abundance of the siderophore DFOE, i.e. 7 mg/L which is ten-fold higher than its DFOB production (Roberts et al., 2012). DFOE biosynthesis will be up-regulated under more severe iron deficiency conditions (Ejje et al., 2013). Due to its nontoxicity and ability to treat acute iron poisoning and chronic aluminium overload, DFOB has been clinically approved for medicinal usage (Kim et al., 2020).

The other sideropohore also produced in this study by *Salinispora* was ferrioxamine D1 (Figure 5.4). Ferrioxamine D1, a relatively hydrophilic family member, structurally related to hydroxamate-containing siderophores. The production of ferrioxamine D1 was reported for the soil-dwelling *Streptomyces coelicolor* M145. Ferrioxamines are actually the most frequently produced siderophores among terrestrial Actinomycetes (Barona-Gómez et al., 2004; Yamanaka et al., 2005). The siderophores observed were only produced at detectable levels when the organism was grown at high temperatures, indicating that their synthesis is triggered in response to stress (Sidebottom et al., 2013).

6. Results III: Selection of sponge-associated bacteria with high potential for the production of antibacterial compounds

This chapter was already published as articles in scientific reports (*Sci Rep* 10, 19614 (2020). https://doi.org/10.1038/s41598-020-76256-2).

www.nature.com/scientificreports

scientific reports

Check for updates

OPEN

Selection of sponge-associated bacteria with high potential for the production of antibacterial compounds

Riyanti[1,2], Walter Balansa[3], Yang Liu[1], Abha Sharma[1], Sanja Mihajlovic[4], Christoph Hartwig[4], Benedikt Leis[4], Frets Jonas Rieuwpassa[3], Frans Gruber Ijong[3], Heike Wägele[5], Gabriele M. König[6] & Till F. Schäberle[1,4,7]✉

The potential of sponge-associated bacteria for the biosynthesis of natural products with antibacterial activity was evaluated. In a preliminary screening 108 of 835 axenic isolates showed antibacterial activity. Active isolates were identified by 16S rRNA gene sequencing and selection of the most promising strains was done in a championship like approach, which can be done in every lab and field station without expensive equipment. In a competition assay, strains that inhibited most of the other strains were selected. In a second round, the strongest competitors from each host sponge competed against each other. To rule out that the best competitors selected in that way represent similar strains with the same metabolic profile, BOX PCR experiments were performed, and extracts of these strains were analysed using metabolic fingerprinting. This proved that the strains are different and have various metabolic profiles, even though belonging to the same genus, *i.e. Bacillus*. Furthermore, it was shown that co-culture experiments triggered the production of compounds with antibiotic activity, *i.e.* surfactins and macrolactin A. Since many members of the genus *Bacillus* possess the genetic equipment for the biosynthesis of these compounds, a potential synergism was analysed, showing synergistic effects between C14-surfactin and macrolactin A against methicillin-resistant *Staphylococcus aureus* (MRSA).

The oceans house highly dynamic and diverse microbiological habitats with an inherent high potential to discover species that are completely new, unique and highly adapted[1]. Furthermore, it can be assumed that this diversity represents a driving force for chemical novelty, opening up the chance to identify novel natural products with biological and pharmaceutical activities from this still underexplored part of the world[2,3]. Marine invertebrates, e.g. sea slugs (marine Heterobranchia), tunicates (Chordata) and sponges (Porifera), are a well-known bioresource for natural products[4–10], which have the potential to advance into lead structures for drug discovery and development. Due to the fact that natural product research on sponges has been performed for many decades, various compounds with biological effects had already been discovered. For several of these compounds, evidence exists that the molecule of interest isolated from these sponges is actually produced by (endo)-symbiotic or otherwise associated bacteria, leading to the assumption that sponge-associated bacteria produce a multitude of novel bioactive molecules[11]. The host sponges and their bacterial microbiome constitute a mutualistic symbiosis, in which sponges provide space for the bacteria and the bacteria offer metabolites, e.g. nutrients of nitrogen and carbon fixation and specialized metabolites[12,13]. Furthermore, bacteria are involved in the chemical defence of the sponge by providing bioactive molecules[5,12–14]. Although the detailed mechanisms involved in shaping a sponge microbiome are unknown, it is clear that being able to influence potential competitors or predators represents an advantage for the producing microorganism(s), as well as for the host[13]. However, the interaction between

[1]Institute for Insect Biotechnology, Justus-Liebig-University of Giessen, 35392 Giessen, Germany. [2]Faculty of Fisheries and Marine Science, Jenderal Soedirman University, 53122 Purwokerto, Indonesia. [3]Department of Fisheries and Marine Science, Politeknik Negeri Nusa Utara, 95021 North Sulawesi, Indonesia. [4]Fraunhofer Institute for Molecular Biology and Applied Ecology (IME), Branch for Bioresources, 35392 Giessen, Germany. [5]Centre of Molecular Biodiversity, Zoological Research Museum Alexander Koenig, 53113 Bonn, Germany. [6]Institute for Pharmaceutical Biology, University of Bonn, 53115 Bonn, Germany. [7]German Center for Infection Research (DZIF), Partner Site Giessen-Marburg-Langen, Giessen, Germany. ✉email: till.f.schaeberle@agrar.uni-giessen.de

6.1. Background

The oceans house highly dynamic and diverse microbiological habitats with an inherent high potential to discover species that are completely new, unique, and highly adapted (Fenical and Jensen, 2006). Furthermore, it can be assumed that this diversity represents a driving force for chemical novelty, opening up the chance to identify novel natural products with biological and pharmaceutical activities from this still underexplored part of the world (Hughes and Fenical, 2010; Montaser and Luesch, 2011). Marine invertebrates, e.g. sea slugs (marine Heterobranchia), tunicates (Chordata) and sponges (Porifera), are a well-known bioresource for natural products (Reyes et al., 2008; Laport et al., 2009; Perdicaris et al., 2013; Melander et al., 2016; Fisch et al., 2017; Palanisamy et al., 2017; Bertrand and Munoz-Garay, 2019), which have the potential to advance into lead structures for drug discovery and development. Due to the fact that natural product research on sponges has been performed for many decades, various compounds with biological effects had already been discovered. For several of these compounds, evidence exists that the molecule of interest isolated from these sponges is actually produced by (endo)-symbiotic or otherwise associated bacteria, leading to the assumption that sponge-associated bacteria produce a multitude of novel bioactive molecules (Fuerst, 2014). The host sponges and their bacterial microbiome constitute a mutualistic symbiosis, in which sponges provide space for the bacteria and the bacteria offer metabolites, e.g. nutrients of nitrogen and carbon fixation and specialized metabolites (Imhoff and Stohr, 2003; Taylor et al., 2007). Furthermore, bacteria are involved in the chemical defence of the sponge by providing bioactive molecules (Hentschel et al., 2002; Imhoff and Stohr, 2003; Taylor et al., 2007; Laport et al., 2009). Although the detailed mechanisms involved in shaping a sponge microbiome are unknown, it is clear that being able to influence potential competitors or predators represents an advantage for the producing microorganism(s), as well as for the host (Taylor et al., 2007). However, the interaction between different bacteria within the host is not known. Therefore, it is highly interesting to test and use the antibiotic effect of molecules that inhibit other bacteria also for pharmaceutical applications.

In recent years, antimicrobial resistance (AMR) has become a severe threat to global health systems. The antibiotic development pipeline is drying out and the number of antibiotic resistant bacteria is steadily increasing (Schäberle and Hack,

2014; Banin et al., 2017; Tangerina et al., 2017; Tacconelli et al., 2018). There are projections that by 2050 around 10 million people will die from antibiotic resistant infections per year (O'Neill, 2014). Hence, novel targets and novel antibiotics represent an unmet medical need.

To fill the antibiotic development pipeline from the very beginning, natural products are still a highly promising resource. In recent years, it has been shown that there is still potential in the fraction of culturable bacteria for the identification of novel antibiotic compounds. In bioprospecting projects, hundreds of bacterial strains can easily be isolated, and approximately 10% of them possess antibacterial activities in preliminary screens. For example, Kuo *et al.* (Kuo et al., 2019) reported 15% of bacterial isolates from the marine sponge *Theonella swinhoei* to show antibacterial activity. From the marine sponges *Isodictya compressa* and *Higginsia bidentifera* 415 isolates were retrieved and 35 of them (8.4%) showed antibacterial activity (Matobole et al., 2017). Using the marine sea slugs *Chromodoris annae*, *Chromodoris dianae*, *Chromodoris* sp. 30, *Chromodoris willani*, *Doriprismatica stellata*, *Hexabranchus sanguineus* egg mass and *Phyllidiella* cf *pustulosa* as bioresource, out of 49 isolated bacteria, 35 demonstrated antibiotic activity (Böhringer et al., 2017). In addition, even well-investigated habitats and species proved themselves as most valuable, as shown by the identification of teixobactin from a bacterium isolated from a soil sample (Ling et al., 2015), and of darobactin from *Photorhabdus* species (Imai et al., 2019).

If it can be accepted that the potential for finding novel antibiotics is still high, it is of importance to select the most promising strains for further investigations. The technological development in the last years offers great tools for the dereplication of compounds and activities. Mass-based analyses using sensitive mass spectrometers in combination with molecular networking, or even genome sequencing to get insights into the metabolic potential of a strain will be applied in the future (Wang et al., 2016). However, such research and development pipelines are costly, need highly trained researchers and are not accessible to every lab. Therefore, in this study, we tested if a classical microbiology-based approach could be suitable to perform first prioritization without the need of expensive state-of-the-art laboratories. This is of special interest as bioresources like sponges are very often accessible in regions with poor biotech infrastructure. We report here about our bioprospecting project, in which 835 marine bacterial isolates were retrieved from 10 different sponges and 108 of these showed antibacterial activity in a

preliminary screening. The prioritization of these active strains, which were identified by 16S rRNA gene sequencing, was done using a competition assay. In a championship like assay, the isolates were challenged with each other. The strongest competitors, i.e., isolates that won most of the matches against other isolates, were selected for further analysis. In that way, 25 isolates were prioritized and analysed further. To validate if only identical isolates were selected by this approach and the strong inhibitory effect was based on the same compound, BOX PCR and chemical fingerprinting was performed. This revealed that different bacteria made it to the top places. Furthermore, antibacterial active molecules were isolated and positively tested for their synergistic effects against clinically relevant methicillin-resistant *Staphylococcus aureus* (MRSA).

6.2. Selection high potential bacteria producing antibacterial compounds

6.2.1. Sponge collection and bacteria isolation

During our continuous efforts to identify natural products from marine bioresources, 10 sponge specimens covering 10 different Demospongia species, were collected from Sangihe Island, Indonesia (a description of the specimens with a preliminary genus or species identification is provided in the Table 10.2). From these samples, associated bacteria were isolated using classical agar plate-based methods with various media. In total, 835 marine bacteria were isolated as axenic culture. From most sponge samples, approximately 100 cultures were isolated. However, from two sponge samples, i.e., specimen EP10 (cf. *Aaptos suberitoides*) and EP15 (cf. *Agelas nakamurai)*, only about 20 isolates were retrieved in this study. Comparing the isolation efficiency of the different media, the highest number of isolates (143) was obtained from SNA medium (consisting of starch and salts); while from NB medium (complex medium) only 23 isolates were retrieved (Figure 10.24).

6.2.2. Screening for antibacterial activity

Concerning a biological activity of the isolates, we focussed on antibacterial activity. The 835 isolates were screened for activity against the Gram-positive bacterium *M. luteus* ATCC 4698 and the Gram-negative bacterium *E. coli* K12 using a growth inhibition assay on agar plates. This primary screening revealed that 12.9 % (108) of the isolates showed antimicrobial activity against at least one of the bacteria tested (Table 10.7). Among the 108 isolates active in the primary

screening, 4.6% inhibited solely Gram-negative *E. coli* bacteria, 78.7% inhibited Gram-positive *M. luteus* and 16.7% inhibited both test strains (Figure 6.1). Thereby, the highest number of active isolates originated from the sponge EP6 (22 out of 104 isolates showed activity) and the lowest number from sponge EP14 (2 out of 112 isolates showed activity). From sponge sample EP15 no active isolates were isolated. However, it must be considered that from this sponge only a very low number of bacteria was isolated in total (Figure 6.1).

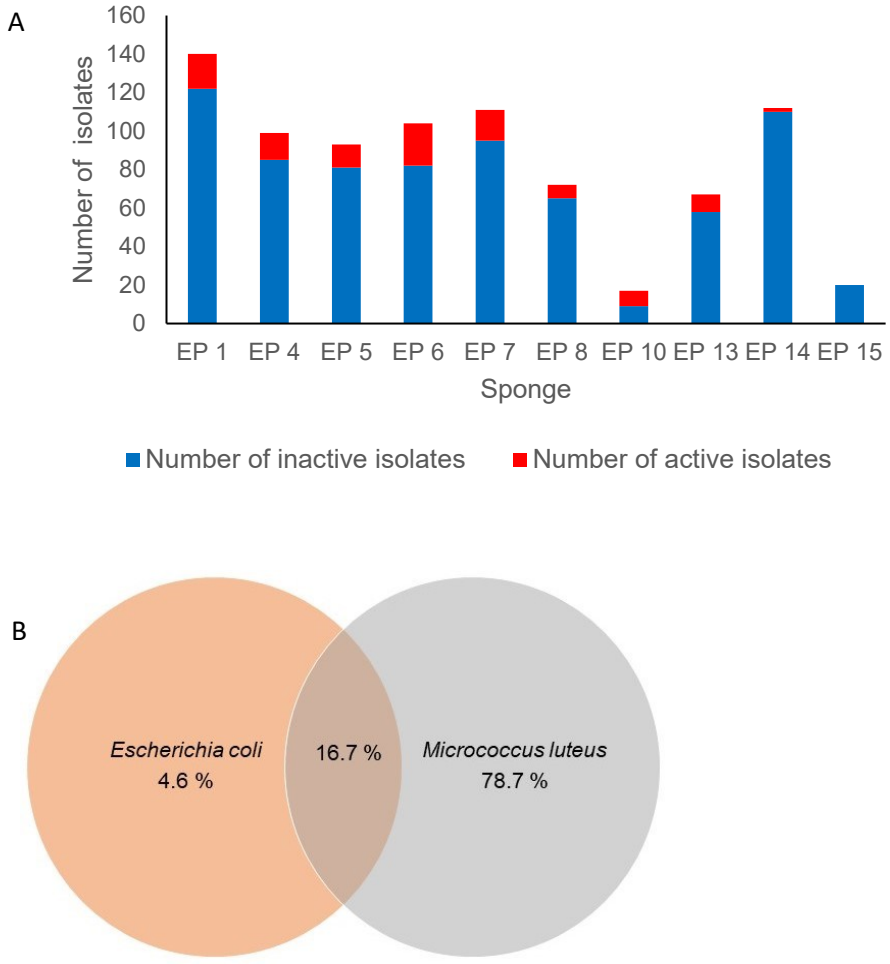

Figure 6.1. Number of active isolates

A) Bacterial isolates (active isolates in red) retrieved from each sponge specimen (for description of sponges see Table 10.2). **B)** Percentage of the 108 isolated active bacteria that showed activity solely against Gram-positive *M. luteus*, Gram-negative *E. coli* and against both test strains.

6.2.3. Identification the active strains

In a next step, the active isolates were identified using 16*S* rRNA gene sequencing. Identified strains belonged to the phyla Firmicutes (76.9%), Proteobacteria (17.6%) and Actinobacteria (5.6%), respectively. On genus level, 12 genera were present, whereby two third of the strains belonged to *Bacillus* (66.7%), followed by *Pseudomonas* (6.5%), *Staphylococcus* (5.6%), *Lysinibacillus* (4.6%), and *Solwaraspora* (3.7%). The other seven genera had a share below 3% (Table 6.1).

Table 6.1. Phyla and genera of the active bacterial strains based on 16*S* rRNA gene sequencing

Phyla	Genus	Occurrence (%)
Firmicutes	*Bacillus*	66.67
Proteobacteria	*Pseudomonas*	6.48
Firmicutes	*Staphylococcus*	5.56
Firmicutes	*Lysinibacillus*	4.63
Actinobacteria	*Solwaraspora*	3.70
Proteobacteria	*Citrobacter*	2.78
Proteobacteria	*Enterobacter*	2.78
Proteobacteria	*Serratia*	2.78
Proteobacteria	*Cronobacter*	1,85
Proteobacteria	*Leclercia*	0.93
Actinobacteria	*Brevibacterium*	0.93
Actinobacteria	*Verrucosispora*	0.93

6.2.4. Competition assay

An important step in natural product research is the prioritization of bacterial strains for further investigation. Therefore, a strong dereplication platform, mostly based on MS analyses of the extracts derived from the strains, is key. Another option is the in silico analysis of the strains following genome sequencing. However, both platforms are relatively costly and not available at all laboratories. The goal of this project was to test if a prioritization of strains is possible depending on agar plate-

based competition assays. This methodology can be done by microbiologists in virtually every lab, also in remote areas without expensive instrumentation.

The underlying hypothesis is that the strongest competitors should be selected, since these strains have a higher probability of success for the identification of compounds with antibacterial activity. Strong competitors were regarded as the strains that inhibited most of the other strains originating from the same host sponge (Figure 6.2). Hence, in a preliminary round, the strains were challenged in bilateral agar plate-based inhibition assays. Strains were incubated as axenic cultures on agar plates during 2 – 7 days depending on the growth rate of the respective strain. Then, plugs were punched out and transferred to a test plate inoculated with the test strain. After 24 h incubation, the inhibition zone was measured. In that way, the strongest inhibitors (in total 25 strains) were selected and qualified themselves for the next round, i.e. the competition assay between the strains selected from the different sponge hosts. In the final round, the number of inhibited strains, inhibition zones,and the number of strains inhibiting each strain were documented (Figure 6.3 and Table 10.8).

Bacillus sp. EP1-654 was the winner of this challenge, since this strain inhibited 16 of the 24 other strains (67%). Thereby, it showed inhibitory activity against at least one bacterium from each host sponge, except the bacterial strain derived from sponge EP8, *Bacillus* sp. EP8-203. The latter strain was also a high competitor, like *Bacillus* sp. EP7-200, EP5-815 and EP6-816; it inhibited 12 out of 24 strains of the test set, respectively. Furthermore, *Bacillus* sp. EP8-203 showed the lowest sensitivity, since it was only inhibited by one competitor. *Brevibacterium* sp. EP14-508 was the weakest strain in the challenge. It did inhibit none of the other strains and in turn it was inhibited by 16 of the competitors (Figure 6.3 and Table 10.8)

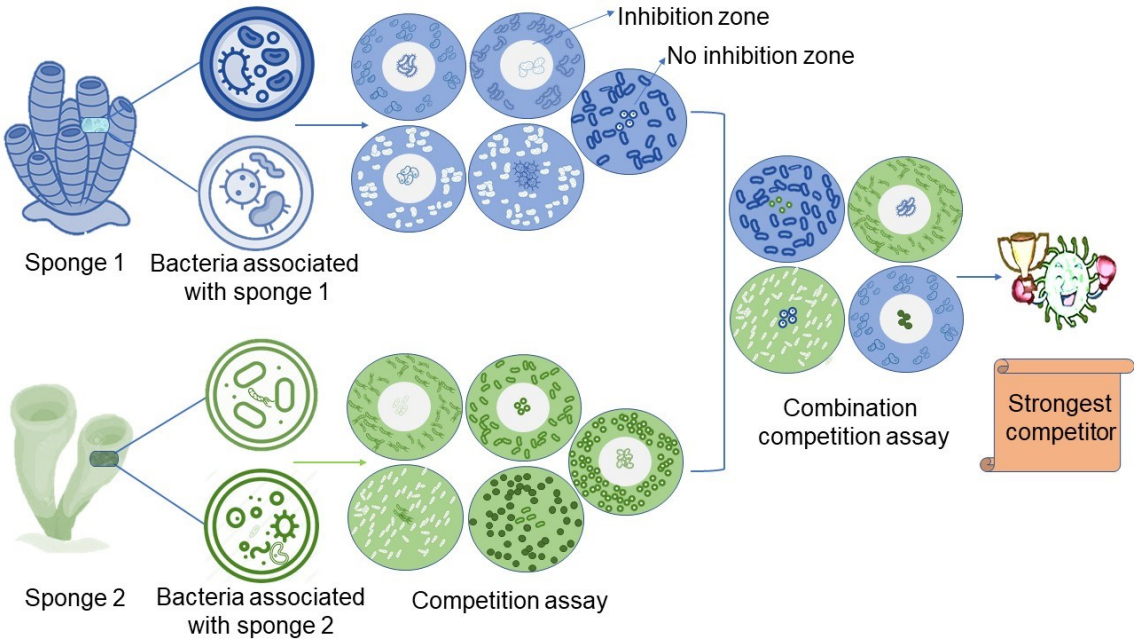

Figure 6.2. Scheme of the competition assay

Bacteria were isolated from the sponge specimens. As example a blue and green coloured sponge are shown. All axenic cultures derived from one sponge were tested against all the others from one sponge. Therefore, bacteria were cultured and agar plugs were transferred to agar plates inoculated with the test strain. Best competitors (inhibiting most of the test strains, which was observed by inhibition zone) were selected and tested against best competitors derived from other sponges.

6.2.5. Correlation of marine bacterial taxonomy and chemical fingerprint

As mentioned before, the top five competitors belonged to the genus *Bacillus*, which was also the most abundant genus in this collection. To get an idea about the phylogenetic relationship and if other genera could also be found among the strong competitors, a phylogenetic tree based on the 16*S* rRNA gene sequences was built (Figure 6.3). The activity and sensitivity pattern were plotted to this tree and showed that the highest competitors belonged to a branch of closely related strains. This holds also true in different media (Figure 6.3). This trend was observed (i) when all strains were fermented in the same medium (which gives a better comparability) and (ii) when the strains were fermented in the medium, they were originally isolated from. Since it is known that variation of the growth conditions, e.g., medium applied, results in a changed metabolome, the isolation media was also used (Figure 6.3). Since this could be an indication that the strains

selected by the competition assay would be highly redundant, a BOX PCR was performed (Figure 6.4).

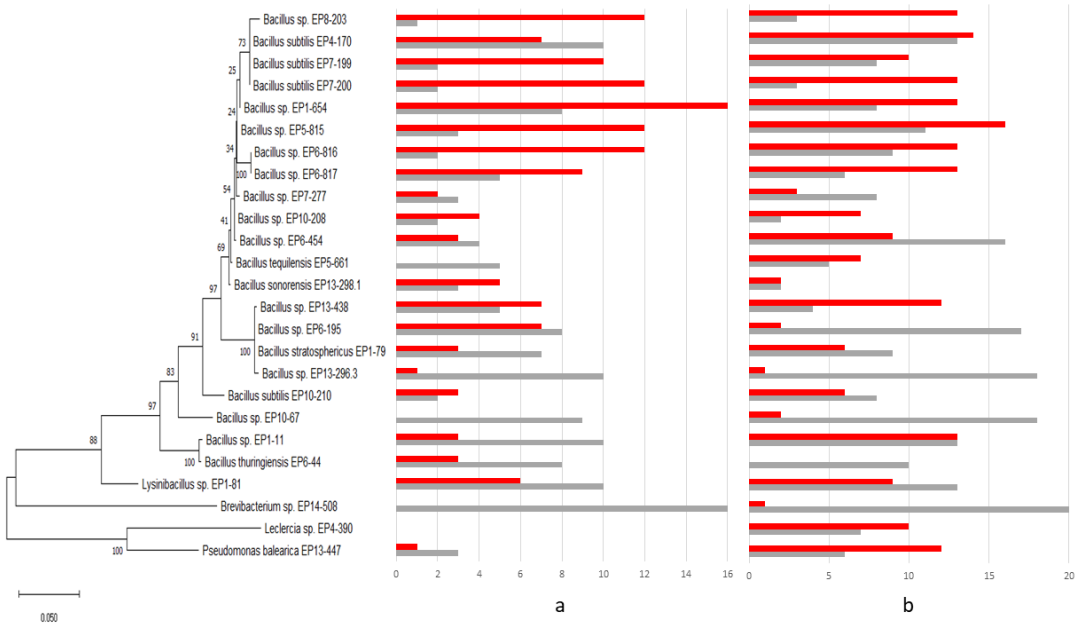

Figure 6.3. Phylogenetic tree and the activity/sensitivity profile of the 25 high competitor strains. (a) Phylogenetic tree based on 16S rRNA gene sequences. (b) Activity/sensitivity profile of the strains, which were cultivated in the medium they were originally isolated from. Therefore, different media were used. (c) All strains fermented in ISP2 medium supplemented with NaCl. The bar diagram indicates for each strain how many competitors were inhibited (red) and by how many itself was inhibited (grey). The blue bar indicates the branch of high competitors. Bootstrap values are given at the branches of the phylogenetic tree.

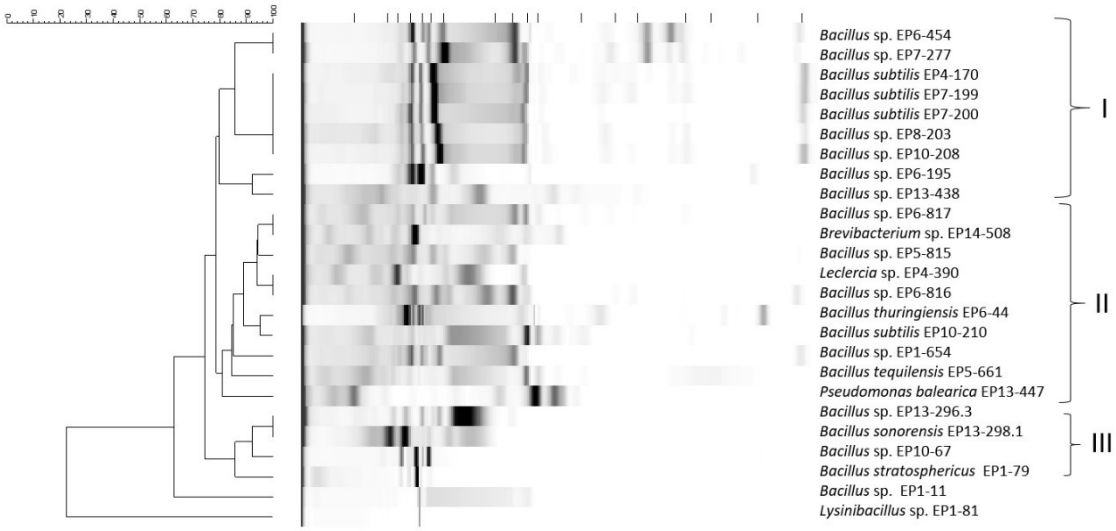

Figure 6.4. Dendrogram showing the relatedness of the isolated strains as determined by a PCR DNA fingerprint analysis with BOXA1R. Relationships were determined by using Dice similarity coefficient and UPGMA clustering method. The number gives the internal identifier of the respective strain; cluster groups with a similarity higher than 75% are indicated by brackets.

A dendrogram based on BOXA1R fingerprint data was constructed by using Dice similarity coefficient and the UPMGA cluster analysis method to determine the phylogenetic relationship of the strains with higher resolution. This revealed that a few strains show a high similarity of the band pattern, but in general, a quite diverse pattern was observed. Taking into account the similarity higher than 75%, the strains are grouped in three major clusters (Figure 6.5). The first group includes solely *Bacillus* strains. The average similarity coefficient among these strains was 93% while the strains EP4-170, EP7-199, EP7-200, and EP8-203 appeared to be identical. The second group represents the most heterogeneous group involving the species from different genera but with the average similarity of 90%. The third group includes four *Bacillus* strain isolated from EP 1, 10, and 13. They had the same similarity coefficient as group I.

In a next step, the 25 high competitors were subjected to a metabolomics analysis. The taxonomic similarity based on housekeeping genes does not necessarily reflect the similarity of strains in regard to their metabolome, since also closely related strains might carry different biosynthetic gene clusters (BGCs) encoding for antibacterial active natural products. Therefore, the crude extracts of these strains were analysed by chemical fingerprinting. The chemical fingerprint enables to

judge the similarity of metabolomes, visualized in a dendrogram (Figure 6.5 complete dataset is shown in Figure 10.25). Grouping of extracts using a cosine similarity threshold of 0.9 resulted in 36 groups (cosine 0.8 in 18 groups).

Analysis of cosine similarity between strain triplicates was performed and outliers were sorted to the rest of the triplicates if large differences in concentration led to the deviation while the Base Peak Chromatogram pattern was identical (Table 10.9, metabolic variations are shown in Figure 10.26). After inspection, 19 metabolic groups (excluding media controls) remained (Table 10.10, corresponding chromatograms Figure 10.26). While strain EP14-508 is most dissimilar to all other profiles (Figure 6.5), it closely groups to other strains in the DNA analysis. The strains EP7-199 and EP7-200 showed even 100% identity in their 16S rRNA sequence; however, in the chemical fingerprint differences were detectable. This result matches the results of the BOX PCR, that already indicated slight differences, and of the competition assay, since in the latter strain EP7-200 inhibited more strains than EP7-199. Furthermore, the strains of metabolic group 1 are partly from different clades based on the DNA fingerprint (Figure 6.4).

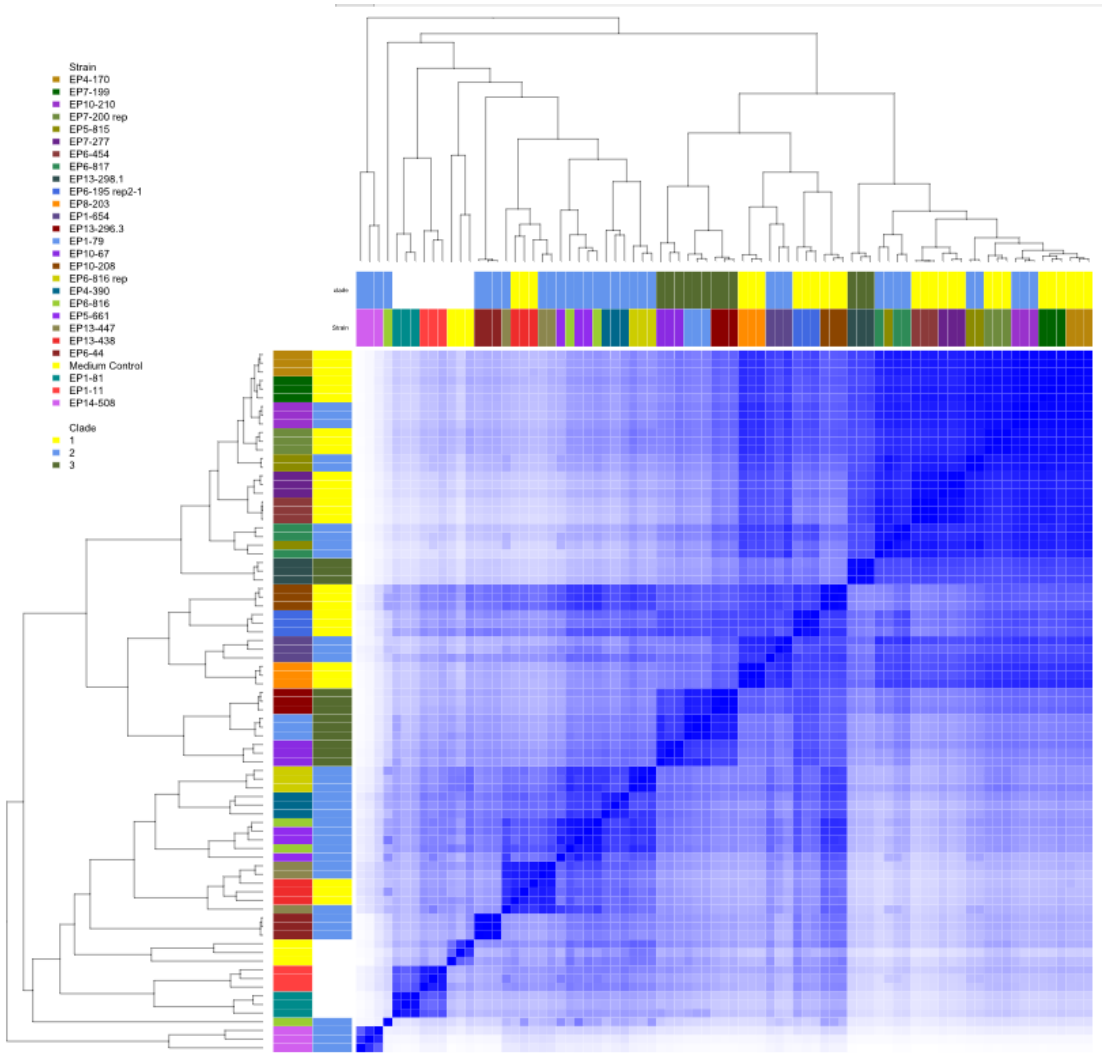

Figure 6.5. Cosine similarities of chemical fingerprints from 25 strains and medium control (n=3 for all strains represented). The different samples are color-coded.

6.2.6. Natural products produced by selected strains

The strongest competitors belonged all to the genus *Bacillus*. The top five (*Bacillus* sp. EP7-200, EP8-203, EP1-654, EP5-815, and EP6-816) were selected and fermented in ten different liquid media to test the crude extracts for antibacterial activity against *E. coli* and *M. luteus*. Extracts of nearly all strains were active against both Gram-positive and Gram-negative test bacteria. *Bacillus* sp. EP6-816 was the only exception, since the extract showed only activity against *M. luteus*. However, the results differed depending on the cultivation medium. For example, *Bacillus* sp. EP7-200 and EP8-203 displayed activity against Gram-negative and Gram-positive bacteria only, if grown on ISP2 medium. Instead, *Bacillus* sp. EP1-

654 and EP5-815 were active against both tested bacteria after fermentation in MYE and NB medium. Furthermore, the results of the activity screening varied between solid and liquid cultivation. *Bacillus* sp. EP7-200 showed activity against both of the tested bacteria in the agar plug assay when cultivated on ISP2 medium supplemented with NaCl. However, this activity was not observed by testing the ethyl acetate extract obtained from liquid broth. Then, only activity was observed against *M. luteus* (Table 10.11).
In addition to the activity tests, the extracts from the five selected strains in ten media, as well as the medium controls were subjected to LC-MS/MS analysis. Thereby, some compounds could be dereplicated based on the GNPS natural products library, e.g., C12 surfactin, C14 surfactin, C15 surfactin and lichenysin A (Figure 10.27-10.29).

The production of surfactins was a common feature for many of the here isolated bacteria when cultivated on solid medium. In liquid medium, it was observed that especially in co-culture experiments the production of this compound series was induced. The C14 - C17 surfactins were successfully isolated from a co-culture, in which *Verrucosispora* sp. EP6-325 and *Bacillus* sp. EP6-454 were inoculated at the same day in M1 medium (Figure 10.8-10.11).

The experiments with axenic cultures do not reflect the conditions of the microbiome of a sponge in nature. Therefore, further co-culture experiments were performed, to challenge the strain with the presence of a competitor. A co-culture of *Bacillus* sp. EP6-817 and *Lysinibacillus sphaericus* EP6-121 was tested in a way that the one strain was incubated for one day before the other strain was added, as well as inoculation on the same day in one flask. A clear increase in the production of one compound was observed when *Bacillus* sp. EP6-817 was cultured for 1 day, before the culture was inoculated with *L. sphaericus* EP6-121 (Figure 6.6, Figure 10.30). This peak was not detected in *L. sphaericus* EP6-121 extracts, and in much lower abundance if *Bacillus* sp. EP6-817 was cultivated alone. From the co-culture, this peak was purified and its structure elucidated using NMR experiments, proving it to be macrolactin A (*m/z* 425.2308 $[M+Na]^+$, Figure 10.2-10.7).

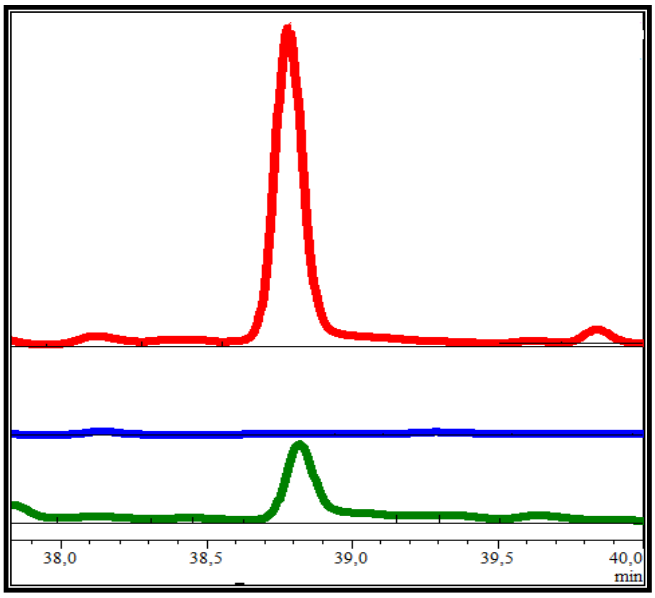

Figure 6.6. High performance liquid chromatography (HPLC) profiles of ethylacetate extracts. The extract of pure cultures of *Bacillus* sp. EP6-817 is depicted in green, of *L. sphaericus* EP6-121 in blue, and of the co-culture in red. It can be seen that the production of macrolactin A is induced in the co-culture.

6.2.7. Synergistic effect of isolated compounds

Surfactin and macrolactin appeared to be compounds of which the production is increased by the presence of a competitor strain. Furthermore, both corresponding BGCs can be detected in many sequenced genus *Bacillus* genomes. Therefore, their antibacterial effects were analysed as single compounds and in combination. First, the minimal inhibitory concentration (MIC) values of the single compounds were determined against a panel of bacteria in broth microdilution assays, i.e., Gram-negative *E. coli* ATCC 25922, *E. coli* ATCC 25922 ΔTolC and Gram-positive *B. subtilis* DSM 10, *S. aureus* ATCC 25923 (methicillin-sensitive), *S. aureus* ATCC 33592 (methicillin-resistant, MRSA), *L. monocytogenes* DSM 20600. However, none of the surfactins were active against these strains (MIC > 128 µg/mL). Instead, macrolactin A was active against the Gram-positive test strains, except *B. subtilis* DSM 10 (Table 10.12). In addition, combination effects between macrolactin A and C14 surfactin were assessed by chequerboard assays (Table 10.13), using *E. coli* ATCC 25922, *B. subtilis* DSM 10 and *S. aureus* ATCC 33592 (methicillin-resistant, MRSA) as test strains. In this experiment, the fractional

inhibitory concentration indices (FICI) for each compound concentration and compound combination were calculated, whereas FICI values ≤ 0.5 indicated synergism for the combination of macrolactin A and C14 surfactin. The presence of sub-MIC concentrations of C14 surfactin (as low as 0.5–2 µg/mL) in combination with macrolactin A (sub-MIC dosing between 1-2 µg/mL) showed a synergistic antimicrobial effect (FICI ≤ 0.5). As compared to macrolactin A without any supplement, the percentage of growth inhibition is enhanced by factor >10 at 1 µg/mL macrolactin A and surfactin dosing ≥ 0.5 µg/mL, whereas at 2 µg/mL macrolactin A the percentage of growth inhibition is doubled by surfactin (Figure 6.7 and Figure 10.31). At higher macrolactin A concentrations (≥ 4 µg/mL), the synergistic effect cannot be resolved anymore.

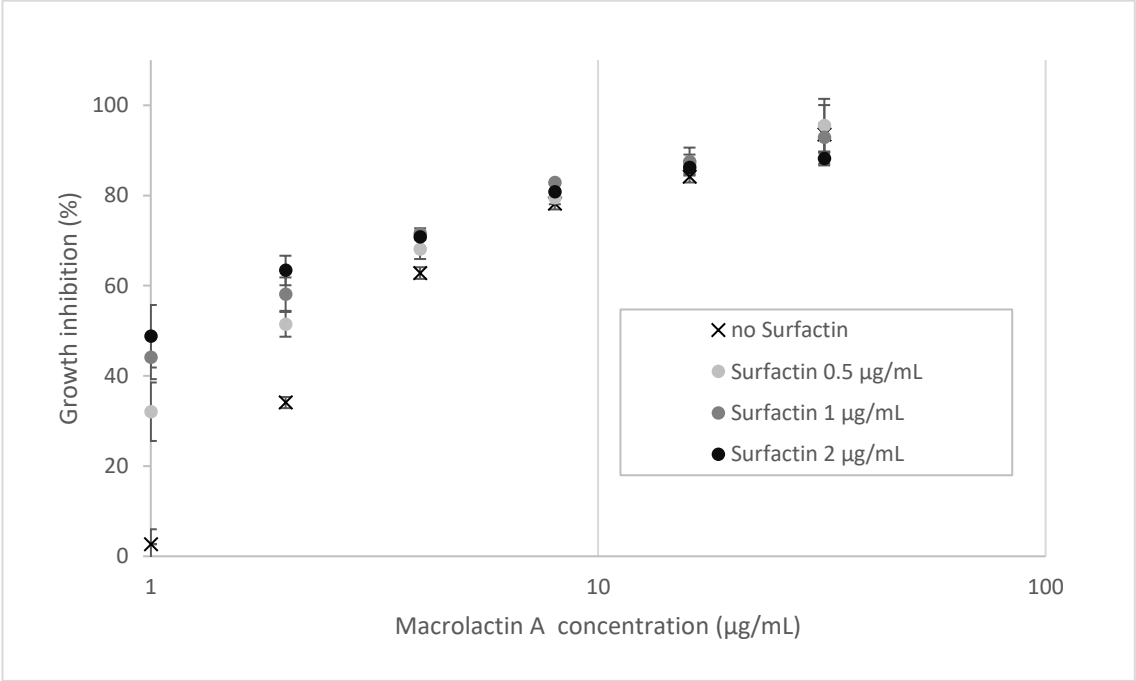

Figure 6.7. Synergistic combination effect of macrolactin A and C14 surfactin against *S. aureus* ATCC 33592 (methicillin-resistant MRSA strain). Dose-response of macrolactin A without surfactin (black cross) is compared with increasing sub-MIC concentrations of C14 surfactin (0.5-2 µg/mL surfactin, light grey to black dots). Data is depicted as average values ± standard deviations from four independent experiments, n = 4.

6.3. Discussion

Sponge-associated bacteria represent an important bioresource for antibiotic compounds. In this study, 12.9% of isolated bacteria exhibited antimicrobial activity

against at least one test organism. This number of active isolates is in the range reported for other bioprospecting projects, which was in the range of 2 - 34% (Anand et al., 2006; Haber and Ilan, 2014; Matobole et al., 2017). e.g., 8 of 400 isolates (2%) from the coastal marine sponges *Amphilectus fucorum* and *Eurypon major* revealed activity against *E. coli* and *B. subtilis* (Margassery et al., 2012). In our study, Firmicutes is the phylum with the highest share (77%) on antibacterial activity, thereby especially genus *Bacillus* contributing to this, which is consistent with other reports (Kanagasabhapathy et al., 2008; Santos et al., 2010). However, several of these projects, aiming to isolate bacteria with antibiotic activity started with a lower number of isolates and selected the most promising isolate. For example, from 92 bacteria isolated from red algae, 33% showed antibacterial activity. Of the ten selected isolates, seven were of the genus *Bacillus* (Kanagasabhapathy et al., 2008). A total of 158 isolates were isolated from a sponge, thereunder 12 were active isolates, five of them belonging to Firmicutes (Santos et al., 2010). In general, *Bacillus* have to be regarded as proliferative producers of natural products with various biological effects. Together with their sporulation efficiency this can be regarded as a significant advantage for survival in different environments (Dimkic et al., 2017). However, this is also providing a bias in isolation projects, since the spore-formers easily survive different sampling and storage procedures and are fast growers on many standard media. Based on metagenomic approaches, the most dominant groups of sponge holobionts belong to the phylum Proteobacteria (Kennedy et al., 2008; Webster and Thomas, 2016; Moreno-Pino et al., 2020). Therefore, it is obviously hard to compare the cultured communities from marine sponges directly, since variations in media and cultural conditions can have a huge impact on the isolation and cultivation success (Santos et al., 2010). Furthermore, the great plate count anomaly was also reported for sponge-derived bacteria, e.g. less than 1% of bacteria observed by microscopic analysis in sponge tissues could be cultured using standard medium (De Rosa et al., 2003), and only a low number of bacteria within a sponge grew under laboratory conditions (Imhoff and Stohr, 2003).

In this study, the fraction of isolated bacteria from different sponges varied. However, the low number of 20 isolates originating from sponge EP 15 (*Agelas nakamurai)* can be explained by the presence of agelasines in this sponge (Balansa et al., 2020). Agelasines are sponge-derived compounds that show antibacterial, as well as cytotoxic properties. Hence, it might be that either

associated bacteria were killed during storage and processing of the samples due to the active compounds present, or that due to the presence of these effective compounds the sponge does not need dedicated antibiotic producers in its microbiome.

To evaluate the approach of prioritizing strains active in a preliminary screening, based on their ability to inhibit other isolates from the same holobiont, the metabolomic fingerprints were analysed. The method was reported to provide a high-resolution strain discrimination, as shown for a group of closely related Streptomycetes (Forner et al., 2013). Here, experiments were performed in triplicates, which grouped together; however, a few triplicate samples did not cluster together; they rather formed a group with other strains. This might indicate that these strains, that cannot be clearly differentiated by chemical fingerprinting, are very similar in their metabolome. Furthermore, three strains (strain code EP4-170, EP7-199 and EP7-200) that are highly similar on their metabolic fingerprint showed high identity in the BOX PCR band pattern, and formed a monophyletic clade in the 16*S* rRNA gene-based phylogenetic tree. However, even these three strains, which are closely related to *Bacillus subtilis*, did not show an identical activity and sensitivity pattern in the competition assay. Therefore, it can be concluded that analysis of the activity and sensitivity pattern of a strain allows differentiation and therewith prioritization, even between highly similar strains. This result is consistent with another study (Betancur et al., 2017), which reported significant differences in bioactivity and chemical diversity between strains of the same species. It might even be that strains, which are identical on the genetic level, could show a different reaction in strain interactions. The background of different hosts could have resulted in different fine tuning of the regulation mechanisms that in turn lead to the production of different (levels of) metabolites (Kuo et al., 2019).

In addition, the activity/sensitivity pattern of the five strongest competitors (all taxonomically related *Bacillus* species) was different. These bacteria should be prioritized for further analysis, because they can inhibit most of the competitors. The strains were isolated from five different sponges, which might point toward the fact that in each microbiome a high competitor *Bacillus* strain is selected. It is obvious that isolates from different sponges could produce varying active compounds. At present, most of the activities observed cannot be directly linked to a corresponding compound. However, sponge-derived Firmicutes (particularly the

genus *Bacillus*), are well known for the production of antimicrobial compounds (Bibi et al., 2016). In this project, the dereplication of the extracts resulted in the identification of 'classic' *Bacillus* compounds, e.g., C12, C14, C15 surfactins and lichenysin A. Based on the fact that genus *Bacillus* in general possess many BGCs, which reflects the potential to produce various secondary metabolites, it can be expected that in nature a cocktail of compounds is used to tackle competitors. In terms of biological fitness, the ability to produce relatively low (sub-MIC) amounts of single antimicrobial compounds in combination, while maintaining or even exceeding the growth inhibition effects against competing microorganisms is of major importance. Synergy of at least two different molecules with different mode of action is given, if the effect of the combination at low dosage is larger than the additive effect of both compounds alone. This principle has shaped natural-product producing bacteria in their specialized ecological niches, whereas the classic medicinal approach is currently antibiotic treatment with one specific drug. In a historical retrospective, this has been a dead-end strategy that has assisted the emergence of antibiotic resistance, reducing effective treatment options in the future. The analysis of surfactin, which is sometimes reported as antibiotically active, did not show activity in our MIC tests, but showed synergistic effects combined with macrolactin A. The production of both compounds was clearly triggered by the presence of another strain, since in a bioactivity-guided isolation approach none of the compounds would have been caught from single cultures. The co-culture approach, based on the interaction of microbes can be regarded as an effective approach for the induction of secondary metabolites. Many studies in mixed microbe fermentation cultures have described triggered metabolite production. The co-culture of the marine-derived fungi *Emericella* sp. (strain CNL-878) and the marine actinomycete *Salinispora arenicola* (strain CNH-665) revealed markedly enhanced production of emericellamide A and emericellamide B (Oh et al., 2007). A number of secondary metabolites were induced by co-culture of two sponge-derived Actinomycetes, *Actinokineospora* sp. EG49 and *Nocardiopsis* sp. RV163 (Dashti et al., 2014). Yu *et al.*(Yu et al., 2019) detected the chromone derivative 7-methoxy-2,3-dimethylchromone-4-one produced by *Streptomyces rochei* MB037. Co-culture with the gorgonian-derived fungus *Rhinocladiella similis* 35 stimulated its production significantly. It can be speculated that increased natural product production is caused by microbial competition for nutrients or space.

Surfactins are cyclic lipopeptides with surfactant-like properties, interfering with many kinds of cell membranes. They were reported to show antibacterial activity in agar diffusion assays against various test strains if used at high concentrations (Kim et al., 2009; Sudarmono et al., 2019). However, these results must be interpreted with caution, since the MICs determined were >1024 µg/mL (Sudarmono et al., 2019), indicating no activity. The debate on the antimicrobial effect of surfactins remains active, but may be accounted to the non-specific mode of action on the cell layer, e.g. cation transport through the bilipid layer (Heerklotz et al., 2004), pore-formation on the cell wall (Deleu et al., 2003), and distortion of the membrane integrity by detergent-like properties of surfactins that induce membrane depolarization events in the host (Arjes et al., 2019). In consequence the cell's energy balance is affected by compromising the cell wall potential, which results in reduced cell proliferation fitness and inactivation of transport processes into and out of the cell. Furthermore, deficient cell ultrastructure integrity may no longer block diffusion of large molecules, while its efflux efficiency may be severely reduced. A synergistic combination of sub-MIC surfactin and macrolactin A may be explained by this route. Synergistic effects of lipopeptides are described in some studies, i.e. surfactin with iturin , surfactin with fengycin, and iturin with fengycin (Jacques, 2011). In another study, synergistic effects between C15 surfactin and ketoconazole were described against *Candida albicans* SC5314 (Liu et al., 2012).

Macrolactins are macrolide compounds containing a 24-membered lactone ring, which are well known for their broad bioactivity spectrum like antiviral and anticancer properties, as well as activity against multi-resistant and clinically relevant pathogenic bacteria such as MRSA (Romero-Tabarez et al., 2006; Yoo et al., 2006). However, information about the common mode of action of this macrolide antibiotic remains scarce. A bacteriostatic mode of action against staphylococci and MRSA could be inferred from morphological changes during cell septum formation, which indicated cell wall synthesis inhibition as in the case of 7-*O*-malonyl macrolactin A (Romero-Tabarez et al., 2006). As known for macrolide antibiotics, macrolactin N targets protein biosynthesis by inhibition of peptide deformylase in *S. aureus* (Yoo et al., 2006).

7. Results IV: Antibacterial screening and active compound isolation from *Flammeovirga yaeyamensis* 2b

7.1. Background

Flammeovirga is one of the genera belonging to the family Flammeovirgaceae of the class Cytophagia. The genus is known for its ability to degrade polysaccharides. Five species of this genus have been reported so far, namely *Flammeovirga aprica*, *Flammeovirga arenaria*, *Flammeovirga yaeyamensis*, *Flammeovirga kamogawensis,* and *Flammeovirga pacifica* (Gao et al., 2017). Cells are Gram-negative, aerobic, chemo-organotrophic, and motile by gliding (Takahashi et al., 2006). In the exponential growth phase, colonies are reddish-orange and turn white in the late stationary growth phase (Hosoya and Yokota, 2007). *Flammeovirga* species were isolated from coastal seawater (Hosoya and Yokota, 2007), deep-sea sediment (Xu et al., 2012; Cai et al., 2018), and scallop (Jeong et al., 2020). All cultured and investigated strains of *Flammeovirga* are successful in the enzymatic degradation and usage of multiple polysaccharides, e.g. agarose, alginate, and starch (Han et al., 2016a). Herein, we report a *Flammeovirga* species isolated from a marine sponge that was collected from campaign 3. *Flammeovirga* was chosen for natural product isolation, as it is a so far underexplored genus, which increases the likelihood of finding new interesting compounds. In the preliminary investigation, ethyl acetate crude extracts of *Flammeovirga* species revealed antibacterial activity.

7.2. Phenotypic appearance of *F. yaeyamensis* 2b

The strain was cultured on marine broth agar medium plates and incubated at 30°C for 24 h. The observed cell mass was orange in appearance (Figure 7.1). The colonies spread and produced large gelase fields and deep craters in agar plates.

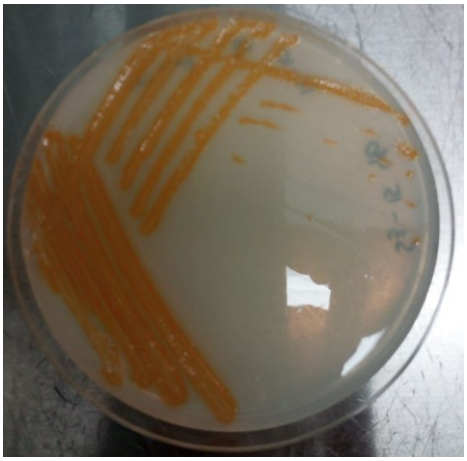

Figure 7.1. Colonies of *F. yaeyamensis* 2b on marine broth agar after 24 h incubation at 30°C

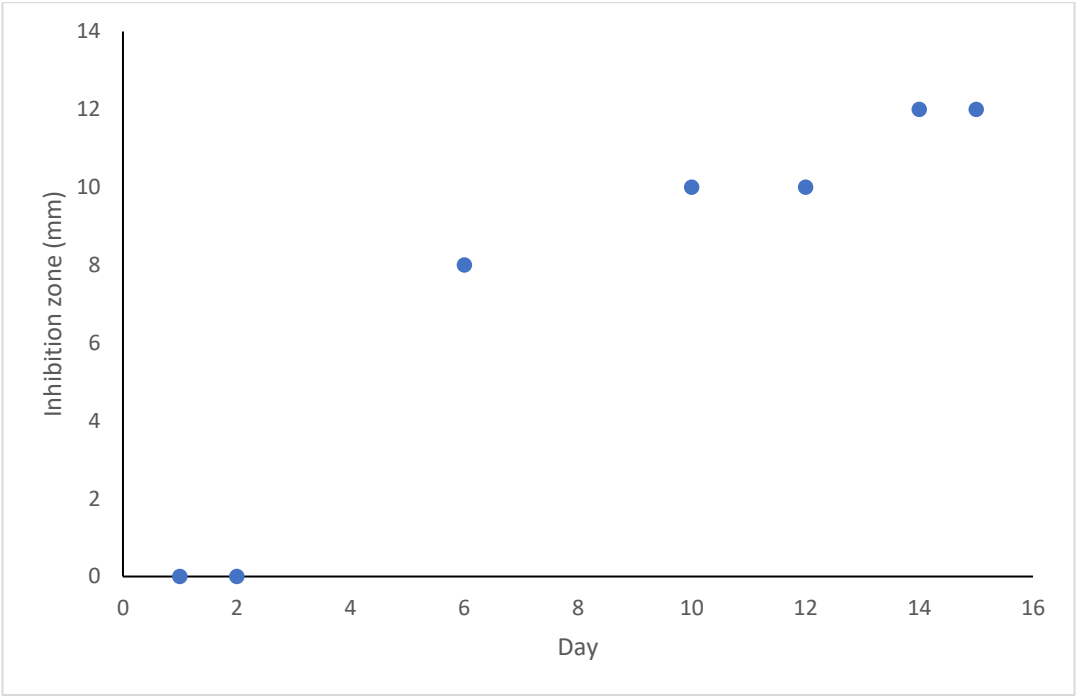

Figure 7.2. Antibacterial activity of *F. yaeyamensis* 2b grown in liquid marine broth medium during 1-15 days at 30°C against *B. megaterium* as assessed by inhibition zone assay. The culture was harvested on day 1, 2, 6, 10, 12, 14, and 15 days and extracted using ethyl acetate. The crude extracts were tested against Gram-positive bacteria (including *B. megaterium* as shown above). The highest inhibition zone was used to determine the harvesting time for large scale fermentation.

To determine the kinetics of the antibacterial activity against *B. megaterium*, the crude extract of strain *F. yaeyamensis* 2b was tested by disk diffusion assay from

day 1 until day 15. The extracts of the first and second day did not show any activity in this assay. Therefore, it might be that no active compound is produced in the beginning. The highest activity was exhibited on the days 14 and 15 when no overall population growth seemed to occur, possibly indicating the late stationary phase has been reached on this day while the early stationary phase started on the days 10 and 12 (Figure 7.2). Day 12 was chosen to determine harvesting time for further OSMAC (one strain many compounds) experiment.

7.3. Antimicrobial screening of the crude extract of *F. yaeyamensis* 2b

In an initial screening, the antibacterial activity of the crude extracts from various fermentations of *F. yaeyamensis* 2b was tested against two test organisms, i.e., *E. coli* and *B. megaterium*. The OSMAC approach was applied in this study to obtain various metabolites from the sponge-associated bacteria *F. yaeyamensis* 2b. The strain was fermented on eight different media. Among the crude extracts of the eight different media tested, one showed a moderate and two exhibited a high antibacterial activity, as assessed by inhibition zone assay (Dash et al., 2009). These three crude extracts were obtained from *F. yaeyamensis* 2b cultured in the media ISP2, MYE, and NB during 12 days, and showed inhibition of the Gram-positive test bacterium (Table 7.1). The cultivation condition yielding the most active extract was chosen for further large-scale fermentation. However, none of the crude extracts revealed activity against the Gram-negative test bacterium.

Table 7.1. Antibacterial activity of *F. yaeyamensis 2b* crude extracts.

Media	Activity	
	E. coli	*B. megaterium*
ISP2	-	++
LB	-	-
Marine broth	-	-
M1	-	-
MYE	-	+++
NB	-	+++

TSB	-	-
Tryptone and yeast extract	-	-

10 mg/mL during 12 days culture in 8 different media

- : No activity ++ : moderate activity

+ : low activity +++ : high activity

In total 3.2 g crude extract was obtained from three large scale cultivation batches (33 L in total) in NB medium for 14 days. A first purification step by medium pressure chromatography yielded 15 fractions, which were tested against 2 Gram-positive bacteria. The antibacterial activities of these 15 fractions against the Gram-positive bacteria *B. megaterium* and *B. subtilis* are shown in Table 7.2. Ten out of 15 fractions collected from flash chromatography demonstrated activity.

Table 7.2. Antibacterial activity against *B. megaterium* and *B. subtilis* as assessed by the percentage of bacterial growth for the 15 fractions obtained by flash chromatography. The activity was interpreted as a percentage, for which high percentages (100%) values represent increased and low percentage (0%) values decreased growth of the test strain. An extract can be marked as assay active if the observed growth inhibition is under 40%.

	Activity	
Fraction	*B. megaterium* (%)	*B. subtilis* (%)
2	-	-
3	-	-
4	-	-
5	21.35	0.46
6	1.26	0.85
7	26.97	0
8	15.31	-1.183
9	21.91	1.71
10	-	0.66
11	6.32	34.11
12	-	2.50
13	-	0.60

14	28.51	8.87
15	-	-
16	-	-
Negative control (medium)	90.22	106.82
Positive control (carbenicilin)	2.57	0.00

- : no activity observed

7.4. Active compound isolation of *F. yaeyamensis* 2b

The ten fractions showing activity in the above-mentioned assay were analyzed by HPLC for their potential for further separation with the aim of obtaining pure active compounds. Antibacterial activity was detected by measuring the optical density using Gram positive bacteria as test organisms. Based on the aforementioned assay, fractions displaying the same activity pattern were combined. Those combined fractions were subjected to HPLC in the attempt to isolate the pure compounds. Moreover, single fractions displaying unique activity patterns were also further purified by HPLC. Fractions 11 and 12 were combined into one fraction (total 39.8 mg) in consideration of the similar activity pattern and the similarity of their chromatograms. Six compounds were collected after purification i.e. (**1**) 1.5 mg, (**2**) 5.6 mg, (**3**) 3.6 mg, **4** (3.1 mg), **5** (1.5 mg), and **6** (1.5 mg) (Figure 10.32). Compounds **2**, and **3** revealed activity against Gram-positive bacterium with the percentage of bacterial growth being 19.7 % and 18.6 %, respectively. Further analysis of these compounds by HPLC revealed the pure compounds **2** and **3** being in fact several peaks (Figure 10.33). The results indicated the compounds might be decomposing. Compounds can be decomposed into simpler compounds, e.g., into two or more simpler substances or their elemental components by breaking bonds. The decomposition was suspected due to the acidity of 0.01% TFA during purification. Based on these findings, the purity and integrity of the purification results should be monitored in the further experiments. The HPLC purification of fractions 5, 7, 9, 10, 13, and 14 resulted in very less amount of the purified fractions.

Purification of fraction 8 resulted in 3 impure subfractions i.e., **8.1** (5.3 mg), **8.2** (1.5 mg) and **8.3** (5.4 mg). The analysis of LCMS chromatogram exhibited that each fraction was detected more than three compounds (Figure 10.34-10.36). Considering the amount of each subfraction, it was estimated difficult to obtain

enough amount of pure compound, so in this case no further purification was attempted.

Purification of fraction 6 yielded 2 pure compounds i.e., **6.4** (4.5 mg) and **6.5** (2.5 mg). NMR-analysis of compounds **6.4** and **6.5** and comparison with the literature (Pelter et al., 1976; Murthy et al., 1986; Sung et al., 2004; Li et al., 2008, 2009) revealed those compounds to correspond to daidzein (*m/z* 255.0659 $[M+H]^+$) and glycitein (*m/z* 285.0795 $[M+H]^+$) respectively (Figure 7.3, Figure 10.37-10.38, Tabel 10.14-10.15).

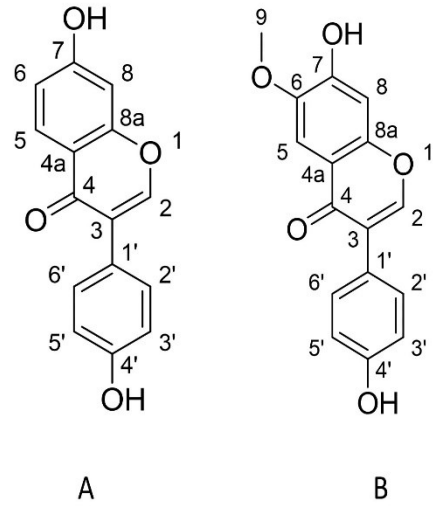

Figure 7.3. Chemical structure of (A) compound **6.4** (daidzein) and (B) compound **6.5** (glycitein).

To obtain a profound dereplication of the identified compounds, data from fraction 6 were analyzed using molecular networking (Figure 7.4). The red nodes show parent ions detected from fraction 6 only. The parent *m/z* 591.106 ($[M+Na]^+$) was dereplicated as tanikolide dimer by dereplicator. This compound was observed alongside compound **6.4** (daidzein) which the peak belonging to tanikolide dimer was a minor compound (Figure 10.39). Considering the low amount of the isolated sample (4.5 mg) and the even lower percentage of the tanikolide dimer in the sample, it seemed too hard to isolate this compound.

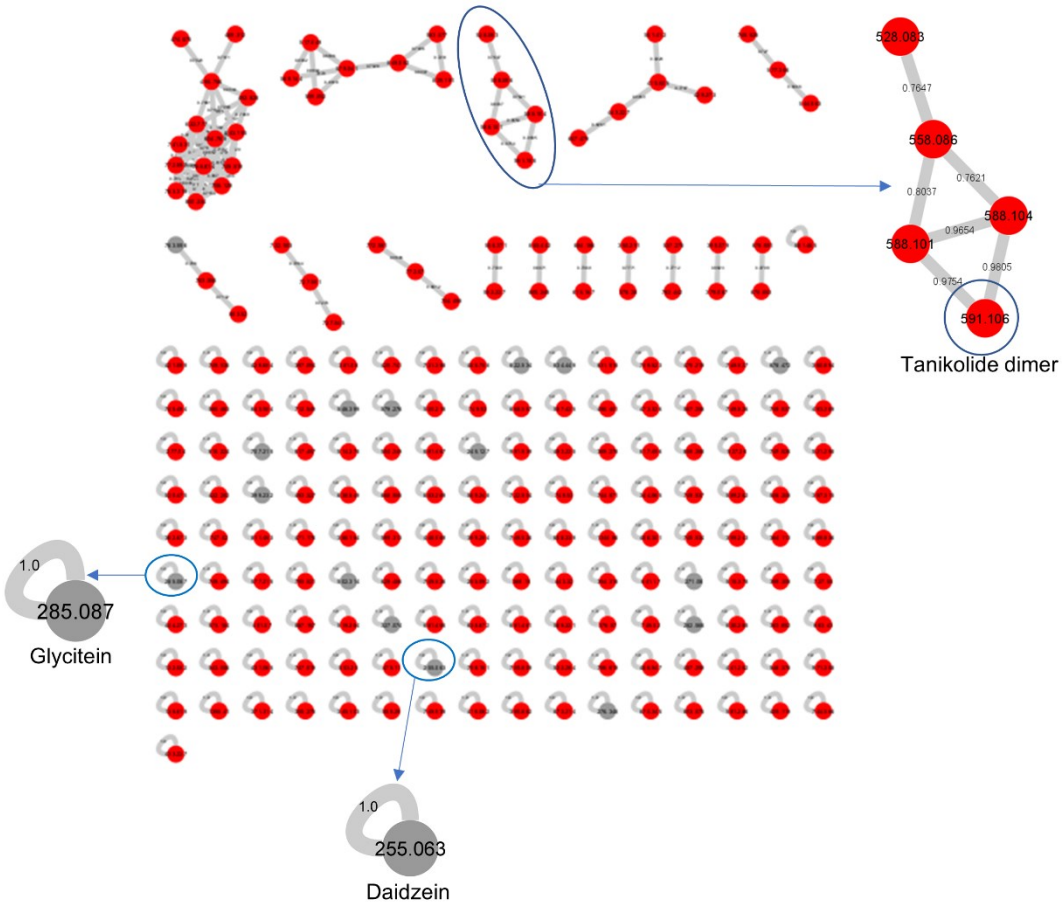

Figure 7.4. Molecular network of fraction 6 isolated from *F. yaeyamensis* 2b. Each node is labelled with the parent mass. The red nodes correspond to the parent ions from fraction 6 and grey nodes represent the medium. Arrows indicate ions that matched the isolated compounds (daidzein and glycitein) and dereplicated known compound tanikolide dimer.

7.5. Discussion

Like the majority of *Flammeovirga*, our isolated organism had a high agar-degrading ability. When the bacterium was streaked onto an agar surface, an orange region could be observed and the cells are in this region. Dong et al. (2017) describe it as an agar-degrading bacterium with effective agarose liquefying capacity and at least 14 agarases in its extracellular agarase system. Takahashi et al. (2006) reported that the color of the cell mass of *F. yaeyamensis* is orange. Colonies spread through agar plates, resulting in vast gelase fields and deep craters.

F. yaeyamensis 2b was initially selected for compound isolation based on its high activity against the Gram-positive bacterium *B. megaterium*. The cultivation optimization with respect to medium composition and cultivation time was performed with the aim of finding appropriate conditions for large scale fermentation. The one-strain-many-compounds (OSMAC) approach is one of the most effective ways to increase the chemical diversity of bacterial metabolites. According to this strategy, new compounds can be stimulated by cultivating microorganisms in various fermentation conditions. Crüsemann et al. (2017) emphasize that, based upon observations from the OSMAC method, the cultivation medium is a significant factor in secondary metabolite biosynthesis. Using a variety of seawater-based media, the screening of active compounds produced by *F. yaeyamensis* 2b was performed. From eight crude extracts obtained from eight different media, three of them showed moderate to high activity against the Gram-positive bacterium *B. megaterium*. Multiple growth variables can be adjusted between tests to induce antibiotic development using the OSMAC method, which allows simultaneous testing of several variables deciding metabolite production (English et al., 2017).

The duration of culturing before extraction can be applied as another dimension to the investigations. This is particularly helpful in experiments aimed at determining the best time to isolate compounds and observing changes in compound patterns over time. The incubation period determination for *F. yaeyamensis* 2b can be an essential factor for the cultivation of this underexplored bacterium. The analysis of activity during days 1-15 represented increasing production of an antibacterial compound by the strain. The antibacterial activity increased from day 10 until 15 which indicates the stationary phase was started from days 10-12 and end on days 14-15. Secondary metabolite production in bacterial cultures is frequently linked to a specific growth stage (Esikova et al., 2002) and typically occurs during the stationary growth phase (Robinson et al., 2001; Patakova, 2013). Furthermore, Andryukov et al. (2019) stated that the production of molecules of microorganisms was discovered to occur at the end of the exponential and beginning of the stationary phases.

Since no isolated compounds were previously reported from *F. yaeyamensis* 2b, this paragraph provides examples for compounds isolated at different time points from bacteria of the phylum Bacteroidetes for comparison. After three days of

fermentation, marinoquinoline A, as well as the novel marinoquinolines B-F, were isolated from the gliding bacterium *Ohtaekwangia kribbensis*. These compounds demonstrated activity against tropical parasites *Plasmodium falciparum* K1 with IC_{50} values between 1.7 and 15 µM (Okanya et al., 2011). Similarly, marinoquinoline A was obtained from the gliding bacterium *Rapidithrix thailandica* TISTR 1742 after a 7-day incubation (Sangnoi et al., 2008). A gliding marine bacterium in the genus *Rapidithrix* was cultivated for 4 days as the source of antibiotics ariakemicin A and B (Oku et al., 2008). Both strains *Mooreia alkaloidigena* CNX-216T and *Catalinimonas alkaloidigena* CNU-914T belonging to the order of *Cytophagales* yielded the new compounds marinopyrazinones A and B after 7 days of cultivation (Choi et al., 2015). Another strain from the order *Cytophagales*, the gliding marine bacterium *Saprospira grandis* led to the isolation of four new diterpenoids after 7 days of cultivation (Spyere et al., 2003).

Compared to the relatively short incubation times described above, our large-scale fermentation of *F. yaeyamensis* 2b was cultivated for 14 days. The activity was analyzed based on the percentage of growth of the test bacteria. Ten active fractions were acquired from the low amount of crude extracts. Purification of those ten fractions proved challenging, as the yields were low and some compounds even appeared to be decomposing. An exception was fraction 6, from which the two compounds daidzein and glycitein could be isolated and identified. These compounds were reported from soybean paste (Sung et al., 2004). This result suggests that these compounds derived from the medium and no compound could be isolated from strains *F. yaeyamensis* 2b itself.

Interestingly, one known compound, tanikolide dimer was dereplicated by molecular networking from fraction 6. The tanikolide dimer, a novel human sirtuin type 2 SIRT2-selective inhibitor was isolated from the marine cyanobacterium *Lyngbya majuscula* collected from Madagascar (Gutiérrez et al., 2009). This result implies that *F. yaeyamensis* 2b might be able to produce the same compound as *L. majuscula.* Yet, due to its low amount of sample, further purification could not be continued.

To the best of my knowledge, no reported compounds were isolated from the genus *Flammeovirga*. According to reports, all bacteria in the *Flammeovirga* genus can degrade complex polysaccharides, especially agar and carrageenan (Dong et al., 2017), that derived from the cell wall of red seaweeds (Gao et al., 2017)

indicating that the strains have a lot of enzymes involved in carbohydrate metabolism (Han et al., 2016b). Furthermore, the genome information of *Flammeovirga* bacteria is still largely unknown (Gao et al., 2017). Among them, only three draft genome sequences have been published, namely *Flammeovirga* sp. OC4 (Liu et al., 2015), *F. pacifica* WPAGA1 (Chan et al., 2015), and *Flammeovirga* sp. SJP92 (Dong et al., 2017). To discover new active compounds, genome mining and further investigation of the underexplored *Flammeovirga* are needed.

8. Summary and Outlook

The discovery of novel natural products (NPs) that can serve as lead structures has to be an ongoing effort to fill the respective development pipelines. However, identification of NPs, which possess a potential for application in e.g., the pharma or agro sector, must be as cost effective and fast as possible. Furthermore, the amount of sample available for initial testing is usually very limited, not least because of the fact that the impact on the environment, i.e., the sampled biosystem, should be kept minimal. Here, the pipeline SeaPEPR was implemented, in which a primary bioactivity screening of crude extracts is combined with the analysis of the corresponding metabolic fingerprint. This enables prioritization of samples for subsequent microfractionation and dereplication of the active compounds early in the workflow. As a case study, 76 marine sponge-derived extracts were screened against a microbial screening panel. Thereunder, human pathogenic bacteria (*Escherichia coli* ATCC35218 and *Staphylococcus aureus* ATCC33592) and yeast (*Candida albicans* FH2173), as well as the phytopathogenic fungus *Septoria tritici* MUCL45407. Overall, nine extracts revealed activity against at least one test organism. Metabolic fingerprinting enabled assigning four active extracts into one metabolic group; therefore, one representative was selected for subsequent microfractionation. Dereplication of the active fractions showed a new dibrominated aplysinopsin and a hypothetical chromazonarol stereoisomer derivative. Furthermore, inhibitory activity against the common plant pest *Septoria tritici* was discovered for NPs of marine origin. The pipeline represents a valuable tool for further bioprospecting projects, since only low sample volumes are needed that in turn renders an extensive collection of limited bioresources for screening purposes (e.g., slow-growing macroorganisms like sponges) obsolete.

The potential of sponge-associated bacteria for the biosynthesis of natural products with antibacterial activity was evaluated. Out of all 396 marine bacteria from campaign 1, which were isolated from five sponges, 6.1% showed antibacterial activity against at least one of the test organisms. Most of the active isolates belonged to the genus *Bacillus*. Further antimicrobial activities were observed for *Salinispora* and *Microbacterium* species. The automatic and manual analysis of LC/MS^2 data allowed dereplication of ten compounds, i.e., saliniketal

A, rifamycin S, staurosporine, staurosporine M1, and staurosporine-7-OH, derivatives of staurosporine-7-OH, desf-05, desferrioxamine, desferrioxamine E, and ferrioxamine D1.

In a preliminary screening, bacteria isolation campaign 2 revealed that 108 of 835 axenic isolates showed antibacterial activity. Active isolates were identified by 16S rRNA gene sequencing and selection of the most promising strains was done in a championship like approach, which can be done in every lab and field station without expensive equipment. In a competition assay, strains that inhibited most of the other strains were selected. In a second round, the strongest competitors from each host sponge competed against each other. To rule out that the best competitors selected in that way represent similar strains with the same metabolic profile, BOX PCR experiments were performed, and extracts of these strains were analysed using metabolic fingerprinting. This proved that the strains are different and have various metabolic profiles, even though belonging to the same genus, i.e., *Bacillus*. Furthermore, it was shown that co-culture experiments triggered the production of compounds with antibiotic activity, i.e., surfactins and macrolactin A. Since many members of the genus *Bacillus* possess the genetic equipment for the biosynthesis of these compounds, a potential synergism was analysed. It was shown that molecules with assumed antibacterial effects, e.g., surfactins, are inactive alone (at the concentrations tested), but can have synergistic effects combined with other molecules produced by *Bacillus* species.

From the third isolation campaign, one bacterium belonging to the genus *Flammeovirga* was selected for further investigation. The strain was isolated from an unidentified sponge collected at the Cenderawasih Bay National Park, Papua, Indonesia. However, despite the observed activity in the initial screening, the bioassay-guided isolation approach was not successful to isolate compounds with antibacterial activity produced by *Flammeovirga*. Putatively active compounds were isolated; however, in very less amount and the compounds decomposed during further analysis. Furthermore, compounds with antibacterial activity which were isolated are predicted to be medium-derived. Hence, further optimization of fermentation and purification conditions is needed. In addition, genome mining could be a way forward for the further investigation of this bacterial group.

The SeaPEPR pipeline combined phenotypic activity screening assays and metabolic fingerprinting, which allowed a fast prioritization and dereplication of

samples with the desired bioactivity for further processing. The active components of the crude extracts that should be responsible for the antimicrobial activities observed in the primary screening were successfully dereplicated. Therewith, it is possible to focus on these sponge samples that are predicted to contain new compounds for compound isolation. For the future development of sponge-derived metabolites, the production needs to be improved. For example, sponge aquaculture and cell culture to provide sponge biomass without any natural resources' overexploitation is not a standard procedure yet. These efforts should be pursued to allow harnessing the potential of this important natural resource in the near future.

Moreover, some "sponge" metabolites are in fact produced by symbiotic bacteria that live in the sponge tissue. Such sponge-associated bacteria can be regarded as the important and greatest bioresource to be used in the discovery of new active metabolites. A large number of compounds can still be detected from bacteria, due to the diversity of their secondary metabolism. Such compounds may become lead structures for the development of drugs with antibacterial, antifungal, antiviral, anticancer, and other biological activities. In this study, the percentage of active strains was less than a quarter of the total isolated bacteria. Isolates that did not display antimicrobial activities might produce compounds with other activities for which the extracts were not tested, e.g. anticancer. Furthermore, the chance is high that *in vitro* the conditions were not suitable for the activation of a biosynthetic gene cluster (BGC) that encodes for the production of any active metabolite. Laboratory conditions are a limiting factor in the expression of these BGCs. Therefore, integration of metabolic and genomic approaches is needed for further investigation of these bacteria, since the *in-silico* potential that can be identified by genome analysis will be much higher than the metabolic repertoire known. Therefore, genome sequencing is planned for selected active strains of this study. Taking this genomic information into account, increases the chance for the discovery of new metabolites. Knowledge about the genome sequence will also open the way to clone BGCs for heterologous expression or to modify, if the strains are genetically accessible, the strains to activate production of metabolites.

9. References

Albizati, K. F., John Faulkner, D., and N-h, P. (1985). Stevensine a novel alkaloid of an unidentified marine sponge. *Aust. J. Chem* 50, 220. Available at: https://pubs.acs.org/sharingguidelines [Accessed May 1, 2021].

Allard, P.-M., Péresse, T., Bisson, J., Gindro, K., Marcourt, L., Pham, V. C., et al. (2016). Integration of molecular networking and in-silico MS/MS fragmentation for natural products dereplication. *Anal. Chem.* 88, 3317–3323. doi:10.1021/acs.analchem.5b04804.

Alonso, C., Warnecke, F., Amann, R., and Pernthaler, J. (2007). High local and global diversity of *Flavobacteria* in marine plankton. *Environ. Microbiol.* 9, 1253–1266. doi:10.1111/j.1462-2920.2007.01244.x.

Anand, T. P., Bhat, A. W., Shouche, Y. S., Roy, U., Siddharth, J., and Sarma, S. P. (2006). Antimicrobial activity of marine bacteria associated with sponges from the waters off the coast of South East India. *Microbiol. Res.* 161, 252–262. doi:10.1016/j.micres.2005.09.002.

Andryukov, B., Mikhailov, V., and Besednova, N. (2019). The biotechnological potential of secondary metabolites from marine bacteria. *J. Mar. Sci. Eng.* 7, 1–16. doi:10.3390/jmse7060176.

Anteneh, Y. S., Yang, Q., Brown, M. H., and Franco, C. M. M. (2021). Antimicrobial activities of marine sponge-associated bacteria. *Microorganisms* 9, 1–19. doi:10.3390/microorganisms9010171.

Arjes, H. A., Vo, L., Marie Dunn, C., Willis, L., DeRosa, C. A., Fraser, C. L., et al. (2019). Biosurfactant production maintains viability in anoxic conditions by 1 depolarizing the membrane in *Bacillus subtilis*. *bioRxiv 720532*. doi:10.1101/720532.

Asolkar, R. N., Kirkland, T. N., Jensen, P. R., and Fenical, W. (2010). Arenimycin, an antibiotic effective against rifampin- and methicillin-resistant *Staphylococcus aureus* from the marine actinomycete *Salinispora arenicola*. *J. Antibiot. (Tokyo).* 63, 37–39. doi:10.1038/ja.2009.114.

Ávila, E., Carballo, J., and Cruz-Barraza, J. (2007). *Porifera Research Biodiversity, Innovation and Sustainability*. , eds. E. Márcio, R. Custódio, G. Lôbo-Hajdu, E. Hajdu, G. Muricy, and R. De Janeiro Rio De Janeiro Available at: www.poriferabrasil.mn.ufrj.br. [Accessed October 13, 2020].

Bakus, G. J., Targett, N. M., and Schulte, B. (1986). Chemical ecology of marine organisms: An overview. *J. Chem. Ecol.* 12.

Balansa, W., Islam, R., Gilbert, D. F., Fontaine, F., Xiao, X., Zhang, H., et al. (2013). Australian marine sponge alkaloids as a new class of glycine-gated chloride channel receptor modulator. *Bioorg. Med. Chem.* 21, 4420–4425. doi:10.1016/j.bmc.2013.04.061.

Balansa, W., Wodi, S. I. M., Rieuwpassa, F. J., and Ijong, F. G. (2020). Agelasines B, D and antimicrobial extract of a marine sponge *Agelas* sp. from Tahuna Bay, Sangihe Islands, Indonesia. *Biodiversitas J. Biol. Divers.* 21, 699–706. doi:10.13057/biodiv/d210236.

Banin, E., Hughes, D., and Kuipers, O. P. (2017). Editorial: bacterial pathogens, antibiotics and antibiotic resistance. *FEMS Microbiol. Rev.* 41, 450–452. doi:10.1093/femsre/fux016.

Barona-Gómez, F., Wong, U., Giannakopulos, A. E., Derrick, P. J., and Challis, G. L. (2004). Identification of a cluster of genes that directs desferrioxamine biosynthesis in *Streptomyces coelicolor* M145. *J. Am. Chem. Soc.* 126, 16282–16283. doi:10.1021/ja045774k.

Bauer, M., Kube, M., Teeling, H., Richter, M., Lombardot, T., Allers, E., et al. (2006). Whole genome analysis of the marine Bacteroidetes "*Gramella forsetii*" reveals adaptations to degradation of polymeric organic matter. *Environ. Microbiol.* 8, 2201–2213. doi:10.1111/j.1462-2920.2006.01152.x.

Bauermeister, A., Velasco-Alzate, K., Dias, T., Macedo, H., Ferreira, E. G., Jimenez, P. C., et al. (2018). Metabolomic fingerprinting of *Salinispora* from Atlantic Oceanic Islands. *Front. Microbiol.* 9, 3021. doi:10.3389/fmicb.2018.03021.

Becerro, M. A., Uriz, M. J., and Turon, X. (1997). Chemically-mediated interactions in benthic organisms: the chemical ecology of *Crambe crambe* (Porifera, Poecilosclerida). *Interact. Adapt. Strateg. Mar. Org.* 355, 77–89. doi:10.1007/978-94-017-1907-0_9.

Bertrand, B., and Munoz-Garay, C. (2019). Marine antimicrobial peptides: a promising source of new generation antibiotics and other bio-active molecules. *Int. J. Pept. Res. Ther.* 25, 1441–1450. doi:10.1007/s10989-018-9789-3.

Betancur, L. A., Naranjo-Gaybor, S. J., Vinchira-Villarraga, D. M., Moreno-Sarmiento, N. C., Maldonado, L. A., Suarez-Moreno, Z. R., et al. (2017). Marine *Actinobacteria* as a source of compounds for phytopathogen control: An integrative metabolic-profiling / bioactivity and taxonomical approach. *PLoS One* 12. doi:10.1371/journal.pone.0170148.

Bhakuni, D., and Rawat, D. (2005). *Bioactive Marine Natural Products*. New York: Springer.

Bialonska, D., and Zjawiony, J. (2009). Aplysinopsins - Marine indole alkaloids: Chemistry, bioactivity and ecological significance. *Mar. Drugs* 7, 166–183. doi:10.3390/md7020166.

Bibi, F., Faheem, M., Azhar, E., Yasir, M., Alvi, S., Kamal, M., et al. (2016). Bacteria from marine sponges: A source of new drugs. *Curr. Drug Metab.* 18, 11–15. doi:10.2174/1389200217666161013090610.

Bibi, F., Yasir, M., Al-Sofyani, A., Naseer, M. I., and Azhar, E. I. (2020). Antimicrobial activity of bacteria from marine sponge *Suberea mollis* and bioactive metabolites of *Vibrio* sp. EA348. *Saudi J. Biol. Sci.* 27, 1139–1147. doi:10.1016/j.sjbs.2020.02.002.

Blunt, J. W., Carroll, A. R., Copp, B. R., Davis, R. A., Keyzers, R. A., and Prinsep, M. R. (2018). Marine natural products. *Nat. Prod. Rep.* 35, 8–53. doi:10.1039/C7NP00052A.

Bohni, N., Cordero-Maldonado, M. L., Maes, J., Siverio-Mota, D., Marcourt, L., Munck, S., et al. (2013). Integration of microfractionation, qNMR and zebrafish

screening for the in vivo bioassay-guided isolation and quantitative bioactivity analysis of natural products. *PLoS One* 8, e64006. doi:10.1371/journal.pone.0064006.

Böhringer, N., Fisch, K. M., Schillo, D., Bara, R., Hertzer, C., Grein, F., et al. (2017). Antimicrobial potential of bacteria associated with marine sea slugs from North Sulawesi, Indonesia. *Front. Microbiol* 8. doi:10.3389/fmicb.2017.01092.

Bose, U., Hewavitharana, A., Ng, Y., Shaw, P., Fuerst, J., and Hodson, M. (2015). LC-MS-based metabolomics study of marine bacterial secondary metabolite and antibiotic production in *Salinispora arenicola*. *Mar. Drugs* 13, 249–266. doi:10.3390/md13010249.

Brinkmann, C. M., Marker, A., and Kurtböke, D. I. (2017). An overview on marine sponge-symbiotic bacteria as unexhausted sources for natural product discovery. *Diversity* 9, 40. doi:10.3390/d9040040.

Cai, Z. W., Ge, H. H., Yi, Z. W., Zeng, R. Y., and Zhang, G. Y. (2018). Characterization of a novel psychrophilic and halophilic β-1, 3-xylanase from deep-sea bacterium, *Flammeovirga pacifica* strain WPAGA1. *Int. J. Biol. Macromol.* 118, 2176–2184. doi:10.1016/j.ijbiomac.2018.07.090.

Calcinai, B., Bastari, A., Bavestrello, G., Bertolino, M., Horcajadas, S. B., Pansini, M., et al. (2017). Demosponge diversity from North Sulawesi, with the description of six new species. *Zookeys* 680, 105–150. doi:10.3897/zookeys.680.12135.

Cárdenas, C. A., González-Aravena, M., Font, A., Hestetun, J. T., Hajdu, E., Trefault, N., et al. (2018). High similarity in the microbiota of cold- water sponges of the genus *Mycale* from two different geographical areas. *PeerJ* 2018, 1–23. doi:10.7717/peerj.4935.

Challis, G. L., and Hopwood, D. A. (2003). Synergy and contingency as driving forces for the evolution of multiple secondary metabolite production by *Streptomyces* species. *Proc. Natl. Acad. Sci. U. S. A.* 100, 14555–14561. doi:10.1073/pnas.1934677100.

Chan, Z., Wang, R., Liu, S., Zhao, C., Yang, S., and Zeng, R. (2015). Draft genome sequence of an agar-degrading marine bacterium *Flammeovirga pacifica* WPAGA1. *Mar. Genomics* 20, 23–24. doi:10.1016/j.margen.2014.12.001.

Chen, X. H., Koumoutsi, A., Scholz, R., Eisenreich, A., Schneider, K., Heinemeyer, I., et al. (2007). Comparative analysis of the complete genome sequence of the plant growth-promoting bacterium *Bacillus amyloliquefaciens* FZB42. *Nat. Biotechnol. Vol.* 25. doi:10.1038/nbt1325.

Choi, E. J., Nam, S. J., Paul, L., Beatty, D., Kauffman, C. A., Jensen, P. R., et al. (2015). Previously uncultured marine bacteria linked to novel alkaloid production. *Chem. Biol.* 22, 1270–1279. doi:10.1016/j.chembiol.2015.07.014.

Cimino, G., De Stefano, S., and Minale, L. (1975). ent-Chromazonarol, a chroman-sesquiterpenoid from the sponge *Disidea pallescens*. *Experientia* 31, 1117–1118.

Clinical Pipeline Marine Pharmacology Available at: https://www.midwestern.edu/departments/marinepharmacology/clinical-pipeline.xml [Accessed May 10, 2021].

Costa-Lotufo, L. V., Carnevale-Neto, F., Trindade-Silva, A. E., Silva, R. R., Silva, G. G. Z., Wilke, D. V., et al. (2018). Chemical profiling of two congeneric sea mat corals along the Brazilian coast: adaptive and functional patterns. *Chem. Commun.* 54, 1952–1955. doi:10.1039/C7CC08411K.

Cottrell, M. T., and Kirchman, D. L. (2000). *Cytophaga-Flavobacter* cluster consuming low- and high-molecular-weight dissolved organic matter. *Appl. Environ. Microbiol.* 66, 1692–1697. doi:10.1128/AEM.66.4.1692-1697.2000.

Creek, D. J., Dunn, W. B., Fiehn, O., Griffin, J. L., Hall, R. D., Lei, Z., et al. (2014). Metabolite identification: are you sure? And how do your peers gauge your confidence? *Metabolomics* 10, 350–353. doi:10.1007/s11306-014-0656-8.

Crüsemann, M., O'Neill, E. C., Larson, C. B., Melnik, A. V., Floros, D. J., Da Silva, R. R., et al. (2017). Prioritizing natural product diversity in a collection of 146 bacterial strains based on growth and extraction protocols. *J. Nat. Prod.* 80, 588–597. doi:10.1021/acs.jnatprod.6b00722.

Da Silva, A. B., Silveira, E. R., Wilke, D. V., Ferreira, E. G., Costa-Lotufo, L. V., Torres, M. C. M., et al. (2019). Antibacterial salinaphthoquinones from a strain of the bacterium *Salinispora arenicola* recovered from the marine sediments of St. Peter and St. Paul Archipelago, Brazil. *J. Nat. Prod.* 82, 1831–1838. doi:10.1021/acs.jnatprod.9b00062.

Dash, S., Cuili, ·, On, J. ·, Lee, O., Xu, Y., and Qian, P.-Y. (2009). Antibacterial and antilarval-settlement potential and metabolite proWles of novel sponge-associated marine bacteria. *J Ind Microbiol Biotechnol* 36, 1047–1056. doi:10.1007/s10295-009-0588-x.

Dashti, Y., Grkovic, T., Abdelmohsen, U. R., Hentschel, U., and Quinn, R. J. (2014). Production of induced secondary metabolites by a co-culture of sponge-associated actinomycetes, *Actinokineospora* sp. EG49 and *Nocardiopsis* sp. RV163. *Mar. Drugs* 12, 3046–3059. doi:10.3390/md12053046.

De Rosa, S., Mitova, M., and Tommonaro, G. (2003). Marine bacteria associated with sponge as source of cyclic peptides. *Biomol. Eng.* 20, 311–316. doi:10.1016/S1389-0344(03)00038-8.

De Voogd, N. J., Cleary, D. F. R., Hoeksema, B. W., Noor, A., and Van Soest, R. W. M. (2006). Sponge beta diversity in the Spermonde Archipelago, SW Sulawesi, Indonesia. *Mar. Ecol. Prog. Ser.* 309, 131–142. doi:10.3354/meps309131.

Deleu, M., Bouffioux, O., Razafindralambo, H., Paquot, M., Hbid, C., Thonart, P., et al. (2003). Interaction of surfactin with membranes: a computational approach. *Langmuir* 19, 3377–3385. doi:10.1021/la026543z.

Devi, P., Wahidullah, S., Rodrigues, C., and Souza, L. D. (2010). The sponge-associated bacterium *Bacillus licheniformis* SAB1: A source of antimicrobial compounds. *Mar. Drugs* 8, 1203–1212. doi:10.3390/md8041203.

Dewi, A. S., Hadi, T. A., Fajarningsih, N. D., Blanchfield, J. T., Bernhardt, P. V., and Garson, M. J. (2014). Acanthocyclamine A from the Indonesian marine sponge *Acanthostrongylophora ingens*. *Aust. J. Chem.* 67, 1205. doi:10.1071/CH14107.

Dewi, A. S., Hadi, T. A., Januar, H. I., Pratitis, A., and Chasanah, E. (2013). Study on the effect of pollutants on the production of aaptamines and the cytotoxicity of crude extract from *Aaptos suberitoides*. *Squalen Bull. Mar. Fish. Postharvest Biotechnol.* 7, 97. doi:10.15578/squalen.v7i3.4.

Dictionary of Natural Products 29.2 Chemical Search Available at: https://dnp.chemnetbase.com/faces/chemical/ChemicalSearch.xhtml;jsessionid=DB01289ACAA79C222859E1CD8A98A894 [Accessed May 1, 2021].

Dimkic, I., Stankovic, S., Nišavic, M., Petkovic, M., Ristivojevic, P., Fira, D., et al. (2017). The profile and antimicrobial activity of *Bacillus* lipopeptide extracts of five potential biocontrol strains. *Front. Microbiol.* 8, 1–12. doi:10.3389/fmicb.2017.00925.

Dong, Q., Ruan, L., and Shi, H. (2017). Genome sequence of a high agarase-producing strain *Flammeovirga* sp. SJP92. *Stand. Genomic Sci.* 12, 2–7. doi:10.1186/s40793-017-0221-y.

Dowle, M., and Srinivasan, A. (2019). Extension of “data.frame” [R package data.table version 1.12.8]. Available at: https://cran.r-project.org/web/packages/data.table/index.html [Accessed May 11, 2020].

Dowle, M., and Srinivasan, A. (2021). data.table: Extension of “data.frame.” Available at: https://cran.r-project.org/package=data.table [Accessed May 1, 2021].

Dudler, R., and Eberl, L. (2006). Interactions between bacteria and eukaryotes via small molecules. *Curr. Opin. Biotechnol.* 17, 268–273. doi:10.1016/j.copbio.2006.04.004.

Duncan, K. R., Crüsemann, M., Lechner, A., Sarkar, A., Li, J., Ziemert, N., et al. (2015). Molecular networking and pattern-based genome mining improves discovery of biosynthetic gene clusters and their products from *Salinispora* species. *Chem. Biol.* 22, 460–471. doi:10.1016/j.chembiol.2015.03.010.

Eckert, A. (2018a). Package “parallelDist” type package title parallel distance matrix computation using multiple threads. Available at: https://github.com/alexeckert/parallelDist/issues [Accessed May 11, 2020].

Eckert, A. (2018b). parallelDist: Parallel Distance Matrix Computation using Multiple Threads. Available at: https://cran.r-project.org/package=parallelDist [Accessed May 1, 2021].

Ejje, N., Soe, C. Z., Gu, J., and Codd, R. (2013). The variable hydroxamic acid siderophore metabolome of the marine actinomycete *Salinispora tropica* CNB-440. *Metallomics* 5, 1519–1528. doi:10.1039/c3mt00230f.

El-Demerdash, A., Atanasov, A. G., Horbanczuk, O. K., Tammam, M. A., Abdel-Mogib, M., Hooper, J. N. A., et al. (2019). Chemical diversity and biological activities of marine sponges of the Genus *Suberea*: A systematic review. *Mar. Drugs* 17, 115. doi:10.3390/md17020115.

Engel, S., and Pawlik, J. R. (2005). Interactions among Florida sponges. I. Reef habitats. *Mar. Ecol. Prog. Ser.* 303, 145–152. doi:10.3354/meps303145.

English, A. L., Boufridi, A., Quinn, R. J., and Kurtböke, D. I. (2017). Evaluation of fermentation conditions triggering increased antibacterial activity from a near-

shore marine intertidal environment-associated *Streptomyces* species. *Synth. Syst. Biotechnol.* 2, 28–38. doi:10.1016/j.synbio.2016.09.005.

Esikova, T. Z., Temirov, Y. V., Sokolov, S. L., and Alakhov, Y. B. (2002). Secondary antimicrobial metabolites produced by thermophilic *Bacillus* spp. Strains VK2 and VK21. *Prikl. Biokhimiya i Mikrobiol.* 38, 266–267.

Feling, R. H., Buchanan, G. O., Mincer, T. J., Kauffman, C. A., Jensen, P. R., Fenical, W., et al. (2003). Salinosporamide A: A highly cytotoxic proteasome inhibitor from a novel microbial source, a marine bacterium of the new genus *Salinospora*. *Angew. Chem. Int.* 42, 355–357.

Fenical, W., and Jensen, P. R. (2006). Developing a new resource for drug discovery: marine actinomycete bacteria. *Nat. Chem. Biol.* 2, 666–673. doi:10.1038/nchembio841.

Fisch, K. M., Hertzer, C., Hringer, N. B., Wuisan, Z. G., Schillo, D., Bara, R., et al. (2017). The potential of Indonesian heterobranchs found around Bunaken island for the production of bioactive compounds. *Mar. Drugs* 15. doi:10.3390/md15120384.

Floss, H. G., and Yu, T.-W. (2005). Rifamycin mode of action, resistance, and biosynthesis. *Chem. Rev.* 105, 621–632. doi:10.1021/cr030112j.

Forner, D., Berrué, F., Correa, H., Duncan, K., and Kerr, R. G. (2013). Chemical dereplication of marine actinomycetes by liquid chromatography-high resolution mass spectrometry profiling and statistical analysis. *Anal. Chim. Acta* 805, 70–79. doi:10.1016/j.aca.2013.10.029.

Freel, K. C., Nam, S.-J., Fenical, W., and Jensen, P. R. (2011). Evolution of secondary metabolite genes in three closely related marine Actinomycete species. *Appl. Environ. Microbiol.* 77, 7261–7270. doi:10.1128/AEM.05943-11.

Freeman, C. J., and Thacker, R. W. (2011). Complex interactions between marine sponges and their symbiotic microbial communities. *Limnol. Oceanogr.* 56, 1577–1586. doi:10.4319/lo.2011.56.5.1577.

Freeman, C. J., Thacker, R. W., Baker, D. M., and Fogel, M. L. (2013). Quality or quantity: is nutrient transfer driven more by symbiont identity and productivity than by symbiont abundance? *ISME J.* 7, 1116–1125. doi:10.1038/ismej.2013.7.

Freitas-Silva, J., Silva-Oliveira, T., Muricy, G., Marinella, ·, and Laport, S. (2020). *Bacillus* strains associated to Homoscleromorpha sponges are highly active against multidrug resistant bacteria. *Curr. Microbiol.* 1, 3. doi:10.1007/s00284-019-01870-x.

Fuerst, J. A. (2014). Diversity and biotechnological potential of microorganisms associated with marine sponges. *Appl. Microbiol. Biotechnol.* 98, 7331–7347. doi:10.1007/s00253-014-5861-x.

Furusato, A., Kato, H., Nehira, T., Eguchi, K., Kawabata, T., Fujiwara, Y., et al. (2014). Acanthomanzamines A−E with new manzamine frameworks from the marine sponge *Acanthostrongylophora ingens*. doi:10.1021/ol5015569.

Gao, B., Jin, M., Li, L., Qu, W., and Zeng, R. (2017). Genome sequencing reveals

the complex polysaccharide-degrading ability of novel deep-sea bacterium *Flammeovirga pacifica* WPAGA1. *Front. Microbiol.* 8, 1–15. doi:10.3389/fmicb.2017.00600.

Glöckner, F. O., Fuchs, B. M., and Amann, R. (1999). Bacterioplankton compositions of lakes and oceans: A first comparison based on fluorescence in situ hybridization. *Appl. Environ. Microbiol.* 65, 3721–3726. doi:10.1128/aem.65.8.3721-3726.1999.

Gordaliza, M. (2009). Terpenyl-purines from the sea. *Mar. Drugs* 7, 833–849. doi:10.3390/md7040833.

Gordaliza, M. (2010). Cytotoxic terpene quinones from marine sponges. *Mar. Drugs* 8, 2849–2870. doi:10.3390/md8122849.

Graça, A. P., Bondoso, J., Gaspar, H., Xavier, J. R., Monteiro, M. C., de la Cruz, M., et al. (2013). Antimicrobial activity of heterotrophic bacterial communities from the marine sponge *Erylus discophorus* (Astrophorida, Geodiidae). *PLoS One* 8, e78992. doi:10.1371/journal.pone.0078992.

Graça, A. P., Viana, F., Bondoso, J., Correia, M. I., Gomes, L., Humanes, M., et al. (2015). The antimicrobial activity of heterotrophic bacteria isolated from the marine sponge *Erylus deficiens* (Astrophorida, Geodiidae). *Front. Microbiol.* 6. doi:10.3389/fmicb.2015.00389.

Griffith, O. L. (2016). Heatmap.3.R. GitHub repository. Available at: https://github.com/obigriffith/biostar-tutorials/blob/master/Heatmaps/heatmap.3.R [Accessed May 11, 2020].

Guella, G., Mancini, I., Zibrowius, H., and Pietra, F. (1989). Aplysinopsin-type alkaloids from *Dendrophyllia* sp., a scleractinian coral of the family dendrophylliidae of the philippines, facile photochemical (Z/E) photoisomerization and thermal reversal. *Helv. Chim. Acta* 72, 1444–1450. doi:10.1002/hlca.19890720703.

Gustafson, K., Roman, M., and Fenical, W. (1989). The macrolactins, a novel class of antiviral and cytotoxic macrolides from a deep-sea marine bacterium.

Gutiérrez, M., Andrianasolo, E. H., Shin, W. K., Goeger, D. E., Yokochi, A., Schemies, J., et al. (2009). Structural and synthetic investigations of tanikolide dimer, a SIRT2 selective inhibitor, and tanikolide seco -acid from the Madagascar marine Cyanobacterium *Lyngbya majuscula*. *J. Org. Chem.* 74, 5267–5275. doi:10.1021/jo900578j.

Haber, M., and Ilan, M. (2014). Diversity and antibacterial activity of bacteria cultured from Mediterranean *Axinella* spp. sponges. *J.Applied Microbiol.* 116, 519–532. doi:10.1111/jam.12401.

Han, W., Cheng, Y., Wang, D., Wang, S., Liu, H., Gu, J., et al. (2016a). Biochemical characteristics and substrate degradation pattern of a novel exo-type β-agarase from the polysaccharide-degrading marine bacterium *Flammeovirga* sp. Strain MY04. *Appl. Environ. Microbiol.* 82, 4944–4954. doi:10.1128/AEM.00393-16.

Han, W., Gu, J., Cheng, Y., Liu, H., Li, Y., and Li, F. (2016b). Novel alginate lyase (Aly5) from a polysaccharide-degrading marine bacterium, *Flammeovirga* sp. Strain MY04: Effects of module truncation on biochemical characteristics,

alginate degradation patterns, and oligosaccharide-yielding properties. *Appl. Environ. Microbiol.* 82, 364–374. doi:10.1128/AEM.03022-15.

Han, W., Gu, J., Yan, Q., Li, J., Wu, Z., Gu, Q., et al. (2012). A polysaccharide-degrading marine bacterium *Flammeovirga* sp. MY04 and its extracellular agarase system. *J. Ocean Univ. China* 11, 375–382. doi:10.1007/s11802-012-1929-3.

Hay, M. E. (1996). Marine chemical ecology: what's known and what's next?

Hay, M. E. (2009). Marine chemical ecology: Chemical signals and cues structure marine populations, communities, and ecosystems. *Ann Rev Mar Sci.* 1, 193–212.

Heerklotz, H., Wieprecht, T., and Seelig, J. (2004). Membrane perturbation by the lipopeptide surfactin and detergents as studied by deuterium NMR. *J.Phys.Chem. B* 108, 4909–4915. doi:10.1021/jp0371938.

Hentschel, U., Hopke, J., Horn, M., Friedrich, A., Wagner, M., Hacker, J., et al. (2002). Molecular evidence for a uniform microbial community in sponges from different oceans. *Appl. Environ. Microbiol* 68, 4431–4440. doi:10.1128/AEM.68.9.4431.

Hentschel, U., Piel, J., Degnan, S. M., and Taylor, M. W. (2012). Marine sponges (phylum Porifera) are functionally important members of marine benthic communities. *Nat. Publ. Gr.* 10. doi:10.1038/nrmicro2839.

Hentschel, U., Schmid, M., Wagner, M., Fieseler, L., Gernert, C., and Rg Hacker, J. « (2001). Isolation and phylogenetic analysis of bacteria with antimicrobial activities from the Mediterranean sponges *Aplysina aerophoba* and *Aplysina cavernicola*. *FEMS Microbiol. Ecol.* 35, 305–312. doi:10.1111/j.1574-6941.2001.tb00816.x.

Hentschel, U., Usher, K. M., and Taylor, M. W. (2006). Marine sponges as microbial fermenters. *FEMS Microbiol. Ecol.* 55, 167–177. doi:10.1111/j.1574-6941.2005.00046.x.

Hirsch, R., Wiesner, J., Marker, A., Pfeifer, Y., Bauer, A., Hammann, P. E., et al. (2019). Profiling antimicrobial peptides from the medical maggot *Lucilia sericata* as potential antibiotics for MDR Gram-negative bacteria. *J.Antimicrob Chemother* 74, 94–107. doi:10.1093/jac/dky386.

Hooper, J. N. A., and Van Soest, R. W. M. (2002). "Systema porifera. A guide to the classification of sponges," in *Hooper J.N.A., Van Soest R.W.M., Willenz P. (eds) Systema Porifera* (Boston, MA: Springer US). Available at: http://link.springer.com/10.1007/978-1-4615-0747-5_1 [Accessed May 13, 2020].

Hoshino, T. (1985). Description of two new species in the genus *Agelas* (Demospongia) from Zamami Island, the Ryukyus, Japan. *Jap.Soc.Syst. Zool*, 1–10.

Hosoya, S., and Yokota, A. (2007). *Flammeovirga kamogawensis* sp. nov., isolated from coastal seawater in Japan. *Int. J. Syst. Evol. Microbiol.* 57, 1327–1330. doi:10.1099/ijs.0.64977-0.

Hughes, C. C., and Fenical, W. (2010). Antibacterials from the sea. *Chem. – A Eur.*

J. 16, 12512–12525. doi:10.1002/chem.201001279.

Imai, Y., Meyer, K. J., Iinishi, A., Favre-Godal, Q., Green, R., Manuse, S., et al. (2019). A new antibiotic selectively kills Gram-negative pathogens. *Nature* 576, 459–464. doi:10.1038/s41586-019-1791-1.

Imhoff, J. F., Labes, A., and Wiese, J. (2011). Bio-mining the microbial treasures of the ocean: New natural products. doi:10.1016/j.biotechadv.2011.03.001.

Imhoff, J. F., and Stohr, R. (2003). "Sponge-associated bacteria: general overview and special aspects of bacteria associated with *Halichondria panicea*," in *Marine Molecular Biotechnology*, ed. W. Müller (Springer Verlag Berlin Heidelberg), 35–57.

Indraningrat, A. A. G., Smidt, H., and Sipkema, D. (2016). Bioprospecting sponge-associated microbes for antimicrobial compounds. *Mar. Drugs* 14, 1–66. doi:10.3390/md14050087.

Izumi, H., Gauthier, M. E. A., Degnan, B. M., Ng, Y. K., Hewavitharana, A. K., Shaw, P. N., et al. (2010). Diversity of *Mycobacterium* species from marine sponges and their sensitivity to antagonism by sponge-derived rifamycin-synthesizing actinobacterium in the genus *Salinispora*. *FEMS Microbiol. Lett.* 313, 33–40. doi:10.1111/j.1574-6968.2010.02118.x.

Izumikawa, M., Khan, S. T., Komaki, H., Takagi, M., and Shin-Ya, K. (2010). JBIR-31, a new teleocidin analog, produced by salt-requiring *Streptomyces* sp. NBRC 105896 isolated from a marine sponge. *J. Antibiot. (Tokyo).* 63, 33–36. doi:10.1038/ja.2009.113.

Izzati, F., Warsito, M. F., Bayu, A., and Prasetyoputri, A. (2021). Chemical diversity and biological activity of secondary metabolites isolated from Indonesian marine invertebrates.

Jackson, J. B. C., and Buss, L. (1975). Alleopathy and spatial competition among coral reef invertebrates. *Proc. Natl. Acad. Sci.* 72, 5160–5163. doi:10.1073/pnas.72.12.5160.

Jacques, P. (2011). "Surfactin and other lipopeptides from *Bacillus* spp.," in *Biosurfactants From Genes to Applications*, ed. G. Soberón-chávez (Heidelberg: Springer Verlag Berlin Heidelberg). doi:10.1007/978-3-642-14490-5.

Jarmusch, S. A., Lagos-Susaeta, D., Diab, E., Salazar, O., Asenjo, J. A., Ebel, R., et al. (2021). Iron-meditated fungal starvation by lupine rhizosphere-associated and extremotolerant *Streptomyces* sp. S29 desferrioxamine production. *Mol. Omi.* 17, 95–107. doi:10.1039/D0MO00084A.

Jensen, P. R., and Mafnas, C. (2006). Biogeography of the marine actinomycete *Salinispora*. *Environ. Microbiol.* 8, 1881–1888. doi:10.1111/j.1462-2920.2006.01093.x.

Jensen, P. R., Moore, B. S., and Fenical, W. (2015). The marine actinomycete genus *Salinispora*: A model organism for secondary metabolite discovery. *Nat. Prod. Rep.* 32, 738–751. doi:10.1039/C4NP00167B.

Jensen, P. R., Williams, P. G., Oh, D.-C., Zeigler, L., and Fenical, W. (2007). Species-specific secondary metabolite production in arine Actinomycetes of

the genus *Salinispora*. *Appl. Environ. Microbiol.* 73, 1146–1152. doi:10.1128/AEM.01891-06.

Jeong, Y.-S., Kang, W., Sung, H., Lee, J.-Y., Yun, J.-H., Shin, N.-R., et al. (2020). *Flammeovirga pectinis* sp. nov., isolated from the gut of the Korean scallop, *Patinopecten yessoensis*. *Int. J. Syst. Evol. Microbiol.* 70, 499–504. doi:10.1099/ijsem.0.003783.

Kamala, K., Sivaperumal, P., Kamath, S. M., Thilagaraj, W. R., and Rajaram, R. (2020). "Marine Actinobacteria as a source for emerging biopharmaceuticals," in *Encyclopedia of Marine Biotechnology* (New York: John Wiley & Sons Ltd), 2095–2105. doi:10.1002/9781119143802.ch93.

Kanagasabhapathy, M., Sasaki, H., and Nagata, S. (2008). Phylogenetic identification of epibiotic bacteria possessing antimicrobial activities isolated from red algal species of Japan. *World J. Microbiol. Biotechnol.* 24, 2315–2321. doi:10.1007/s11274-008-9746-y.

Kennedy, J., Baker, P., Piper, C., Cotter, P. D., Walsh, M., Mooij, M. J., et al. (2009). Isolation and analysis of bacteria with antimicrobial activities from the marine sponge *Haliclona simulans* collected from Irish Waters. *Mar. Biotechnol.* 11, 384–396. doi:10.1007/s10126-008-9154-1.

Kennedy, J., Codling, C. E., Jones, B. V., Dobson, A. D. W., and Marchesi, J. R. (2008). Diversity of microbes associated with the marine sponge, *Haliclona simulans* , isolated from Irish waters and identification of polyketide synthase genes from the sponge metagenome. *Environ. Microbiol.* 10, 1888–1902. doi:10.1111/j.1462-2920.2008.01614.x.

Keratosa, P. I., and Soest, R. Van (1978). Marine sponges from Curaçao and other Caribbean. *Stud. Fauna Curaçao other Caribb. Islands* 56, 1–94.

Kim, H., Kim, S., Kim, M., Lee, C., Yang, I., and Nam, S.-J. (2020). Bioactive natural products from the genus *Salinospora*: a review. *Arch. Pharm. Res.* 43, 1230–1258. doi:10.1007/s12272-020-01288-1.

Kim, K. M., Lee, J. Y., Kim, C. K., and Kang, J. S. (2009). Isolation and characterization of surfactin produced by *Bacillus polyfermenticus* KJS-2. *Arch. Pharm. Res.* 32, 711–715. doi:10.1007/s12272-009-1509-2.

Kim, T. K., and Fuerst, J. A. (2006). Diversity of polyketide synthase genes from bacteria associated with the marine sponge *Pseudoceratina clavata*: culture-dependent and culture-independent approaches. *Environ. Microbiol.* 8, 1460–1470. doi:10.1111/j.1462-2920.2006.01040.x.

Kim, T. K., Garson, M. J., and Fuerst, J. A. (2005). Marine actinomycetes related to the "*Salinospora*" group from the Great Barrier Reef sponge *Pseudoceratina clavata*. *Environ. Microbiol.* 7, 509–518. doi:10.1111/j.1462-2920.2005.00716.x.

Kim, T. K., Hewavitharana, A. K., Shaw, P. N., and Fuerst, J. A. (2006). Discovery of a new source of rifamycin antibiotics in marine sponge Actinobacteria by phylogenetic prediction. *Appl. Environ. Microbiol.* 72, 2118–2125. doi:10.1128/AEM.72.3.2118-2125.2006.

Kirchman, D. L. (2002). The ecology of *Cytophaga-Flavobacteria* in aquatic environments. *FEMS Microbiol. Ecol.* 39, 91–100. doi:10.1111/j.1574-

6941.2002.tb00910.x.

Koopmans, M., Martens, D., and Wijffels, R. H. (2009). Towards commercial production of sponge medicines. *Mar. Drugs* 7, 787–802. doi:10.3390/md7040787.

Kumar, S., Stecher, G., Li, M., Knyaz, C., and Tamura, K. (2018). MEGA X: Molecular evolutionary genetics analysis across computing platforms. *Mol. Biol. Evol.* 35, 1547–1549. doi:10.1093/molbev/msy096.

Kumar, S., Stecher, G., and Tamura, K. (2016). MEGA7: Molecular evolutionary genetics analysis version 7.0 for bigger datasets. *Mol. Biol. Evol.* 33, 1870–1874. doi:10.1093/molbev/msw054.

Kuo, J., Yang, Y. T., Lu, M. C., Wong, T. Y., Sung, P. J., and Huang, Y. Sen (2019). Antimicrobial activity and diversity of bacteria associated with Taiwanese marine sponge *Theonella swinhoei*. *Ann. Microbiol* 69, 253–265. doi:10.1007/s13213-018-1414-3.

Laatsch, H. (2017). *AntiBase: The Natural Compound Identifier*. Wiley-Vch: Weinheim, Germany Available at: https://www.lehmanns.de/shop/naturwissenschaften/38962338-9783527343591-antibase-the-natural-compound-identifier [Accessed May 1, 2021].

Laport, M. S., Santos, O. C. S., and Muricy, G. (2009). Marine sponges: potential sources of new antimicrobial drugs. *Curr. Pharm. Biotechnol.* 10, 86–105.

Letzel, A. C., Li, J., Amos, G. C. A., Millán-Aguiñaga, N., Ginigini, J., Abdelmohsen, U. R., et al. (2017). Genomic insights into specialized metabolism in the marine actinomycete *Salinispora*. *Environ. Microbiol.* 19, 3660–3673. doi:10.1111/1462-2920.13867.

Lévi, C. Sponges of the New Caledonian Lagoon. *Ed. l'Orstom, Inst. Fr. Rech. Sci. pour le Dev. en Coop. Collect. Faune flore Trop. n° XXXIII, Paris (1998)*.

Li, S. R., Chen, P. Y., Chen, L. Y., Lo, Y. F., Tsai, I. L., and Wang, E. C. (2009). Synthesis of haginin E, equol, daidzein, and formononetin from resorcinol via an isoflavene intermediate. *Tetrahedron Lett.* 50, 2121–2123. doi:10.1016/j.tetlet.2009.02.159.

Li, T., Du, Y., Cui, Q., Zhang, J., Zhu, W., Hong, K., et al. (2013). Cloning, characterization and heterologous expression of the indolocarbazole biosynthetic gene cluster from marine-derived Streptomyces sanyensis FMA. *Mar. Drugs* 11, 466–488. doi:10.3390/md11020466.

Li, W., Liu, F., and Zhang, P. (2008). Synthesis of isoflavones via base catalysed condensation reaction of deoxybenzoin. *J. Chem. Res.*, 683–685. doi:10.3184/030823408X382135.

Ling, L. L., Schneider, T., Peoples, A. J., Spoering, A. L., Engels, I., Conlon, B. P., et al. (2015). A new antibiotic kills pathogens without detectable resistance. *Nature* 517, 455–459. doi:10.1038/nature14098.

Liu, T., Wu, S., Zhang, R., Wang, D., Chen, J., and Zhao, J. (2019). Diversity and antimicrobial potential of Actinobacteria isolated from diverse marine sponges along the Beibu Gulf of the South China Sea. *FEMS Microbiol. Ecol.* 95, 89.

doi:10.1093/femsec/fiz089.

Liu, X., Ren, B., Gao, H., Liu, M., Dai, H., Song, F., et al. (2012). Optimization for the production of surfactin with a new synergistic antifungal activity. *PLoS One* 7, 1–9. doi:10.1371/journal.pone.0034430.

Liu, Y., Yi, Z., Cai, Y., and Zeng, R. (2015). Draft genome sequence of algal polysaccharides degradation bacterium, *Flammeovirga* sp. OC4. *Mar. Genomics* 21, 21–22. doi:10.1016/j.margen.2015.02.001.

Lu, X., Xu, Q., Liu, X., Cao, X., Ni, K., and Jiao, B. (2008). Marine Drugs – Macrolactins. *Chem. Biodivers.* 5, 1669–1674.

Lukowiak, M., Piser, A., and O'dea, A. (2013). Do spicules in sediments reflect the living sponge community? A test in a Caribbean shallow-water lagoon. *Palaios* 28, 373–385. doi:10.2110/palo.2012.p12-082r.

Malve, H. (2016). Exploring the ocean for new drug developments: Marine pharmacology. *J. Pharm. Bioallied Sci.* 8, 83. doi:10.4103/0975-7406.171700.

Mancini, I., Guella, G., Zibrowius, H., and Pietra, F. (2003). On the origin of quasi-racemic aplysinopsin cycloadducts, (bis)indole alkaloids isolated from scleractinian corals of the family Dendrophylliidae. Involvement of enantiodefective Diels-Alderases or asymmetric induction in artifact processes involving adve. *Tetrahedron* 59, 8757–8762. doi:10.1016/j.tet.2003.09.038.

Margassery, L. M., Kennedy, J., O'Gara, F., Dobson, A. D., and Morrissey, J. P. (2012). Diversity and antibacterial activity of bacteria isolated from the coastal marine sponges *Amphilectus fucorum* and *Eurypon major*. *Lett. Appl. Microbiol* 55, 2–8. doi:10.1111/j.1472-765X.2012.03256.x.

Marner, M., Patras, M. A., Kurz, M., Zubeil, F., Förster, F., Schuler, S., et al. (2020). Molecular networking-guided discovery and characterization of stechlisins, a group of cyclic lipopeptides from a *Pseudomonas* sp. *J. Nat. Prod.* 83, 2607–2617. doi:10.1021/acs.jnatprod.0c00263.

Matobole, R. M., Van Zyl, L. J., Parker-Nance, S., Davies-Coleman, M. T., and Trindade, M. (2017). Antibacterial activities of bacteria isolated from the marine sponges *Isodictya compressa* and *Higginsia bidentifera* collected from Algoa bay, South Africa. *Mar. Drugs* 15, 8–10. doi:10.3390/md15020047.

Meek, R. W., Vyas, H., and Piddock, L. J. V. (2015). Nonmedical uses of antibiotics: Time to restrict their use? *PLoS Biol.* 13, 1–11. doi:10.1371/journal.pbio.1002266.

Mehbub, M. F., Lei, J., Franco, C., and Zhang, W. (2014). Marine sponge derived natural products between 2001 and 2010: Trends and opportunities for discovery of bioactives. *Mar. Drugs* 12, 4539–4577. doi:10.3390/md12084539.

Melander, R. J., Liu, H.-B., Stephens, M. D., Bewley, C. A., and Melander, C. (2016). Marine sponge alkaloids as a source of anti-bacterial adjuvants. *Bioorg. Med. Chem. Lett.* 26, 5863–5866. doi:10.1016/j.bmcl.2016.11.018.

Mincer, T. J., Jensen, P. R., Kauffman, C. A., and Fenical, W. (2002). Widespread

and persistent populations of a major new marine Actinomycete taxon in ocean sediments. *Appl. Environ. Microbiol.* 68, 5005–5011. doi:10.1128/AEM.68.10.5005-5011.2002.

Mohan, G., Thangappanpillai, A. K., and Ramasamy, B. (2016). Antimicrobial activities of secondary metabolites and phylogenetic study of sponge endosymbiotic bacteria, *Bacillus* sp. at Agatti Island, Lakshadweep Archipelago. *Biotechnol. Reports* 11, 44–52. doi:10.1016/j.btre.2016.06.001.

Mohimani, H., Gurevich, A., Shlemov, A., Mikheenko, A., Korobeynikov, A., Cao, L., et al. (2018). Dereplication of microbial metabolites through database search of mass spectra. *Nat. Commun.* 9, 1–12. doi:10.1038/s41467-018-06082-8.

Mohotti, S., Rajendran, S., Muhammad, T., Strömstedt, A. A., Adhikari, A., Burman, R., et al. (2020). Screening for bioactive secondary metabolites in Sri Lankan medicinal plants by microfractionation and targeted isolation of antimicrobial flavonoids from *Derris scandens*. *J. Ethnopharmacol.* 246, 112158. doi:10.1016/j.jep.2019.112158.

Mondol, M. A. M., Shin, H. J., and Islam, M. T. (2013). Diversity of secondary metabolites from marine *Bacillus* species: Chemistry and biological activity. *Mar. Drugs* 11, 2846–2872. doi:10.3390/md11082846.

Montaser, R., and Luesch, H. (2011). Marine natural products : a new wave of drugs? *Futur. Med. Chem.* 3, 1475–1489.

Moreno-Pino, M., Cristi, A., Gillooly, J. F., and Trefault, N. (2020). Characterizing the microbiomes of Antarctic sponges: a functional metagenomic approach. *Sci. Rep.* 10, 1–12. doi:10.1038/s41598-020-57464-2.

Motohashi, K., Takagi, M., and Shin-ya, K. (2010). Tetracenoquinocin and 5-Iminoaranciamycin from a Sponge-Derived *Streptomyces* sp. Sp080513GE-26. *J. Nat. Prod.* 73, 755–758. doi:10.1021/np9007409.

Murata, M., Miyagawa-Kohshima, K., Nakanishi, K., and Naya, Y. (1986). Characterization of compounds that induce symbiosis between sea anemone and anemone fish. *Science (80-.).* 234, 585–587. doi:10.1126/science.234.4776.585.

Murthy, M. S. R., Rao, E. V., and Ward, R. S. (1986). Carbon-13 nuclear magnetic resonance spectra of isoflavones. *Magn. Reson. Chem.* 24, 225–230. doi:10.1002/mrc.1260240308.

Nagai, K., Kamigiri, K., Arao, N., Suzumura, K.-I., Kawano, Y., Yamaoka, M., et al. (2003). YM-266183 and YM-266184, novel thiopeptide antibiotics produced by *Bacillus cereus* isolated from a marine sponge. I. Taxonomy, fermentation, isolation, physico-chemical properties and biological properties. *J. Antibiot. (Tokyo).* 56, 123–128. doi:10.7164/antibiotics.56.123.

Nakamura, H., Wu, H., Kobayashi, J., Kobayashi, M., Ohizumi, Y., and Hirata, Y. (1985). Agelasidines. Novel hypotaurocyamine derivatives from the Okinawan sea sponge *Agelas nakamurai* Hoshino. *J. Org. Chem.* 50, 2494–2497. doi:10.1021/jo00214a017.

Nakamura, H., Wu, H., Ohizumi, Y., and Hirata, Y. (1984). Agelasine-A, -B, -C and -D, novel bicyclic diterpenoids with a 9-methyladeninium unit possessing

inhibitory effects on na,K-atpase from the Okinawa sea sponge *Agelas* sp. *Tetrahedron Lett.* 25, 2989–2992. doi:10.1016/S0040-4039(01)81345-9.

Nandakumar, K., Tanaka, M., and Kikuchi, T. (1993). Interspecific organisms competition in Tomioka among fouling Japan. 94, 43–50.

Neopetrosia carbonaria Available at: https://guide.poriferatreeoflife.org/sp_38.html [Accessed May 12, 2020].

Newbold, R., Jensen, P. R., Fenical, W., and Pawlik, J. R. (1999). Antimicrobial activity of Caribbean sponge extracts. *Aquat Microb Ecol* 19, 279–284.

Newman, D. J., and Cragg, G. M. (2007). Natural products as sources of new drugs over the last 25 years. *J. Nat. Prod.* 70, 461–477. doi:10.1021/np068054v.

Newman, D. J., and Cragg, G. M. (2016). Natural products as sources of new drugs from 1981 to 2014. *J. Nat. Prod.* 79, 629–661. doi:10.1021/acs.jnatprod.5b01055.

Ng, Y. K., Hodson, M. P., Hewavitharana, A. K., Bose, U., Shaw, P. N., and Fuerst, J. A. (2014). Effects of salinity on antibiotic production in sponge-derived *Salinispora* actinobacteria. *J. Appl. Microbiol.* 117, 109–125. doi:10.1111/jam.12507.

Nothias, L. F., Nothias-Esposito, M., Da Silva, R., Wang, M., Protsyuk, I., Zhang, Z., et al. (2018). Bioactivity-Based Molecular Networking for the Discovery of Drug Leads in Natural Product Bioassay-Guided Fractionation. *J. Nat. Prod.* 81, 758–767. doi:10.1021/acs.jnatprod.7b00737.

Noyer, C., Thomas, O. P., and Becerro, M. A. (2011). Patterns of chemical diversity in the Mediterranean sponge *Spongia lamella*. *PLoS One* 6. doi:10.1371/journal.pone.0020844.

O'Neill, J. (2014). Antimicrobial resistance: Tackling a crisis for the health and wealth of nations. Review on antimicrobial resistance. Available at: https://amr-review.org/Publications.html [Accessed February 20, 2020].

Oh, D.-C., Kauffman, C. A., Jensen, P. R., and Fenical, W. (2007). Induced production of emericellamides A and B from the marine-derived fungus *Emericella* sp. in competing co-culture. *J. Nat. Prod.* 70, 515–520. doi:10.1021/np060381f.

Okanya, P. W., Mohr, K. I., Gerth, K., Jansen, R., and Müller, R. (2011). Marinoquinolines A-F, pyrroloquinolines from *Ohtaekwangia kribbensis* (Bacteroidetes). *J. Nat. Prod.* 74, 603–608. doi:10.1021/np100625a.

Oku, N., Adachi, K., Matsuda, S., Kasai, H., Takatsuki, A., and Shizuri, Y. (2008). Ariakemicins A and B, novel polyketide-peptide antibiotics from a marine gliding bacterium of the genus *Rapidithrix*. *Org. Lett.* 10, 2481–2484. doi:10.1021/ol8007292.

ŌMura, S., Sasaki, Y., Iwai, Y., and Takeshima, H. (1995). Staurosporine, a potentially important gift from a Microorganism. *J. Antibiot. (Tokyo).* 48, 535–548. doi:10.7164/antibiotics.48.535.

Pabel, C. T., Vater, J., Wilde, C., Franke, P., Hofemeister, J., Adler, B., et al. (2003). Antimicrobial activities and matrix-assisted laser desorption/ionization mass spectrometry of *Bacillus* isolates from the marine sponge *Aplysina*

aerophoba. *Mar. Biotechnol.* 5, 424–434. doi:10.1007/s10126-002-0088-8.

Palanisamy, S. K., Rajendran, N. M., and Marino, A. (2017). Natural products diversity of marine Ascidians (Tunicates; Ascidiacea) and successful drugs in clinical development. *Nat. Products Bioprospect.* 7, 1–111. doi:10.1007/s13659-016-0115-5.

Palomo, S., González, I., de la Cruz, M., Martín, J., Tormo, J., Anderson, M., et al. (2013). Sponge-derived *Kocuria* and *Micrococcus* spp. as sources of the new thiazolyl peptide antibiotic kocurin. *Mar. Drugs* 11, 1071–1086. doi:10.3390/md11041071.

Patakova, P. (2013). Monascus secondary metabolites: Production and biological activity. *J. Ind. Microbiol. Biotechnol.* 40, 169–181. doi:10.1007/s10295-012-1216-8.

Patin, N. V., Duncan, K. R., Dorrestein, P. C., and Jensen, P. R. (2016). Competitive strategies differentiate closely related species of marine actinobacteria. *ISME J.* 10, 478–490. doi:10.1038/ismej.2015.128.

Pawlik, J. R., McFall, G., and Zea, S. (2002). Does the odor from sponges of the genus *Ircinia* protect them from fish predators? *J. Chem. Ecol.* 28, 1103–1115. doi:10.1023/A:1016221415028.

Pawlik, J. R., Steindler, L., Henkel, T. P., Beer, S., and Ilan, M. (2007). Chemical warfare on coral reefs: Sponge metabolites differentially affect coral symbiosis in situ. *Limnol. Oceanogr.* 52, 907–911. doi:10.4319/lo.2007.52.2.0907.

Pawlikl, J. R., and Chanasl, B. (1995). Defenses of Caribbean sponges against predatory reef fish. I. Chemical deterrency.

Pelter, A., Ward, R. S., and I, T. I. G. J. C. S. P. (1976). The carbon-13 nuclear magnetic resonance spectra of isoflavones. 666–668.

Penn, K., Jenkins, C., Nett, M., Udwary, D. W., Gontang, E. A., McGlinchey, R. P., et al. (2009). Genomic islands link secondary metabolism to functional adaptation in marine Actinobacteria. *ISME J.* 3, 1193–1203. doi:10.1038/ismej.2009.58.

Perdicaris, S., Vlachogianni, T., and Valavanidis, A. (2013). Bioactive natural substances from marine sponges: new developments and prospects for future pharmaceuticals. *Nat Prod Chem Res* 1. doi:10.4172/.

Pita, L., Rix, L., Slaby, B. M., Franke, A., and Hentschel, U. (2018). The sponge holobiont in a changing ocean: from microbes to ecosystems. *Microbiome* 6, 46. doi:10.1186/s40168-018-0428-1.

Pommier, T., Canbäck, B., Riemann, L., Boström, K. H., Simu, K., Lunberg, P., et al. (2006). Global patterns of diversity and community structure in marine bacterioplankton. *Mol. Ecol.* 16, 867–880. doi:10.1111/j.1365-294X.2006.03189.x.

Prawat, H., Mahidol, C., Kaweetripob, W., Wittayalai, S., and Ruchirawat, S. (2012). Iodo-sesquiterpene hydroquinone and brominated indole alkaloids from the Thai sponge *Smenospongia* sp. *Tetrahedron* 68, 6881–6886. doi:10.1016/j.tet.2012.06.018.

Rajasabapathy, R., Ghadi, S., … B. M.-M., and 2020, U. (2020). Antimicrobial

profiling of coral reef and sponge associated bacteria from southeast coast of India. *Microb. Pathog.* 141, 103972. Available at: https://www.sciencedirect.com/science/article/pii/S0882401019307880 [Accessed November 23, 2020].

Rampelotto, P. H. (2010). Resistance of microorganisms to extreme environmental conditions and its contribution to astrobiology. *Sustainability* 2, 1602–1623. doi:10.3390/su2061602.

Rath, J.-P., Kinast, S., and Maier, M. E. (2005). Synthesis of the fully functionalized core structure of the antibiotic abyssomicin C. *Org. Lett.* 7, 3089–3092. doi:10.1021/ol0511068.

Ravi, B., Perzanowski, H., Ross, R., Erdman, T., Scheuer, P. J., Finer, J., et al. (1979). Recent research in marine natural products: The puupehenones. *Pure Appl. Chem.* 51, 1893–1900. doi:10.1351/pac197951091893.

Reimer, A., Blohm, A., Quack, T., Grevelding, C. G., Kozjak-Pavlovic, V., Rudel, T., et al. (2015). Inhibitory activities of the marine streptomycete-derived compound SF2446A2 against *Chlamydia trachomatis* and *Schistosoma mansoni*. *J. Antibiot. (Tokyo).* 68, 674–679. doi:10.1038/ja.2015.54.

Reyes, F., Fernández, R., Rodríguez, A., Francesch, A., Taboada, S., Ávila, C., et al. (2008). Aplicyanins A-F, new cytotoxic bromoindole derivatives from the marine tunicate *Aplidium cyaneum*. *Tetrahedron* 64, 5119–5123. doi:10.1016/j.tet.2008.03.060.

Riedlinger, J., Reicke, A., Zähner, H., and Al., E. (2004). Abyssomicins, inhibitors of the paraaminobenzoic acid pathway produced by the marine *Verrucosispora* strain AB–18–032. *J. Antibiot* 5, 271–279.

Roberts, A. A., Schultz, A. W., Kersten, R. D., Dorrestein, P. C., and Moore, B. S. (2012). Iron acquisition in the marine actinomycete genus *Salinispora* is controlled by the desferrioxamine family of siderophores. *FEMS Microbiol. Lett.* 335, 95–103. doi:10.1111/j.1574-6968.2012.02641.x.

Robinson, S. J., Hoobler, E. K., Riener, M., Loveridge, S. T., Tenney, K., Valeriote, F. A., et al. (2009). Using enzyme assays to evaluate the structure and bioactivity of sponge-derived meroterpenes. *J. Nat. Prod.* 72, 1857–1863. doi:10.1021/np900465e.

Robinson, T., Singh, D., and Nigam, P. (2001). Solid-state fermentation: A promising microbial technology for secondary metabolite production. *Appl. Microbiol. Biotechnol.* 55, 284–289. doi:10.1007/s002530000565.

Rodríguez-Marconi, S., De La Iglesia, R., Díez, B., Fonseca, C. A., Hajdu, E., Trefault, N., et al. (2015). Characterization of bacterial, archaeal and eukaryote symbionts from antarctic sponges reveals a high diversity at a three-domain level and a particular signature for this ecosystem. *PLoS One* 10. doi:10.1371/journal.pone.0138837.

Roggen, H., Charnock, C., Burman, R., Felth, J., Larsson, R., Bohlin, L., et al. (2011). Antimicrobial and antineoplastic activities of agelasine analogs modified in the purine 2-position. *Arch. Pharm. (Weinheim).* 344, 50–55. doi:10.1002/ardp.201000148.

Roggen, H., and Gundersen, L.-L. (2008). Synthetic studies directed towards

agelasine analogs - synthesis, tautomerism, and alkylation of 2-substituted N -methoxy-9-methyl-9 H -purin-6-amines. *European J. Org. Chem.* 2008, 5099–5106. doi:10.1002/ejoc.200800627.

Rohde, S., Nietzer, S., and Schupp, P. J. (2015). Prevalence and mechanisms of dynamic chemical defenses in tropical sponges. *PLoS One* 10, e0132236. doi:10.1371/journal.pone.0132236.

Rohde, S., and Schupp, P. J. (2011). Allocation of chemical and structural defenses in the sponge *Melophlus sarasinorum*. *J. Exp. Mar. Bio. Ecol.* 399, 76–83. doi:10.1016/j.jembe.2011.01.012.

Romero-Tabarez, M., Jansen, R., Sylla, M., Lünsdorf, H., Häußler, S., Santosa, D. A., et al. (2006). 7-O-malonyl macrolactin A, a new macrolactin antibiotic from *Bacillus subtilis* active against Methicillin-Resistant *Staphylococcus aureus*, Vancomycin-Resistant Enterococci, and a small-colony variant of *Burkholderia cepacia*. *Antimicrob. Agents Chemother.* 50, 1701–1709. doi:10.1128/AAC.50.5.1701-1709.2006.

Sabdono, A., and Radjasa, O. K. (2008). Microbial Symbionts in Marine Songes: Marine natural product factory. *J. Coast. Dev.* 11, 57–61.

Sakai, R., and Higa, T. (1986). Manzamine A, a novel antitumor alkaloid from a sponge. *J. Acta Chem. Scand* 108, 6405–6406. Available at: https://pubs.acs.org/sharingguidelines [Accessed April 29, 2021].

Salek, R. M., Steinbeck, C., Viant, M. R., Goodacre, R., and Dunn, W. B. (2013). The role of reporting standards for metabolite annotation and identification in metabolomic studies. *Gigascience* 2, 13. doi:10.1186/2047-217X-2-13.

Sammarco, P. W., Coll, J. C., La Barre, S., and Willis, B. (1983). Competitive strategies of soft corals (Coelenterata: Octocorallia): Allelopathic effects on selected scleractinian corals. *Coral Reefs* 1, 173–178. doi:10.1007/BF00571194.

Sangnoi, Y., Sakulkeo, O., Yuenyongsawad, S., Kanjana-opas, A., Ingkaninan, K., Plubrukarn, A., et al. (2008). Acetylcholinesterase-inhibiting activity of pyrrole derivatives from a novel marine gliding bacterium, *Rapidithrix thailandica*. *Mar. Drugs* 6, 578–57886. doi:10.3390/md20080029.

Santos, O. C. S., Pontes, P. V. M. L., Santos, J. F. M., Muricy, G., Giambiagi-deMarval, M., and Laport, M. S. (2010). Isolation, characterization and phylogeny of sponge-associated bacteria with antimicrobial activities from Brazil. *Res. Microbiol.* 161, 604–612. doi:10.1016/j.resmic.2010.05.013.

Sayem, S., Manzo, E., Ciavatta, L., Tramice, A., Cordone, A., Zanfardino, A., et al. (2011). Anti-biofilm activity of an exopolysaccharide from a sponge-associated strain of *Bacillus licheniformis*. *Microb. Cell Fact.* 10, 74. doi:10.1186/1475-2859-10-74.

Schäberle, T. F., and Hack, I. M. (2014). Overcoming the current deadlock in antibiotic research. *Trends Microbiol.* 22, 165–167. doi:10.1016/j.tim.2013.12.007.

Schatz, A., Bugle, E., and Waksman, S. A. (1944). Streptomycin, a substance exhibiting antibiotic activity against Gram-positive and Gram-negative bacteria. *Exp. Biol. Med.* 55, 66–69. doi:10.3181/00379727-55-14461.

Schinke, C., Martins, T., Queiroz, S. C. N., Melo, I. S., and Reyes, F. G. R. (2017). Antibacterial compounds from marine bacteria, 2010-2015. *J. Nat. Prod.* 80, 1215–1228. doi:10.1021/acs.jnatprod.6b00235.

Schirmer, A., Gadkari, R., Reeves, C. D., Ibrahim, F., Delong, E. F., Hutchinsonl, C. R., et al. (2005). Metagenomic analysis reveals diverse polyketide synthase gene clusters in microorganisms associated with the marine sponge *Discodermia dissoluta*. *Appl. Environ. Microbiol* 71, 4840–4849. doi:10.1128/AEM.71.8.4840.

Schmidt, D., and Heckendorf (2019). Co-Operation: Fast Covariance, correlation, and cosine similarity operations. Available at: https://cran.r-project.org/web/packages/coop/citation.html [Accessed May 11, 2020].

Schmidt, E. W. (2008). Trading molecules and tracking targets in symbiotic interactions. *Nat. Chem. Biol.* 4, 466–473. doi:10.1038/nchembio.101.

Schmidt, M., Priemé, A., and Stougaard, P. (2006). Rhodonellum psychrophilum gen. nov., sp. nov., a novel psychrophilic and alkaliphilic bacterium of the phylum Bacteroidetes isolated from Greenland. *Int. J. Syst. Evol. Microbiol.* 56, 2887–2892. doi:10.1099/ijs.0.64450-0.

Schneemann, I., Nagel, K., Kajahn, I., Labes, A., Wiese, J., and Imhoff, J. F. (2010). Comprehensive investigation of marine *Actinobacteria* associated with the sponge *Halichondria panicea*. *Appl. Environ. Microbiol.* 76, 3702–3714. doi:10.1128/AEM.00780-10.

SciFinder SciFinder. Redistributed with Permission.Copyright © 2020 American Chemical Society (ACS). All rights reserved.

Selvin, J., Kennedy, J., Lejon, D. P. H., Kiran, G., and Dobson, A. D. W. (2012). Isolation identification and biochemical characterization of a novel halo-tolerant lipase from the metagenome of the marine sponge *Haliclona simulans*. *Microb. Cell Fact.* 11, 72. doi:10.1186/1475-2859-11-72.

Selvin, J., Shanmughapriya, S., Gandhimathi, R., Seghal Kiran, G., Rajeetha Ravji, T., Natarajaseenivasan, K., et al. (2009). Optimization and production of novel antimicrobial agents from sponge associated marine actinomycetes *Nocardiopsis dassonvillei* MAD08. *Appl. Microbiol. Biotechnol.* 83, 435–445. doi:10.1007/s00253-009-1878-y.

Sidebottom, A. M., Johnson, A. R., Karty, J. A., Trader, D. J., and Carlson, E. E. (2013). Integrated metabolomics approach facilitates discovery of an unpredicted natural product suite from *Streptomyces coelicolor* M145. *ACS Chem. Biol.* 8, 2009–2016. doi:10.1021/cb4002798.

Singh, A., and Thakur, N. L. (2016). Significance of investigating allelopathic interactions of marine organisms in the discovery and development of cytotoxic compounds. *Chem. Biol. Interact.* 243, 135–147. doi:10.1016/j.cbi.2015.09.009.

Spyere, A., Rowley, D. C., Jensen, P. R., and Fenical, W. (2003). New neoverrucosane diterpenoids produced by the marine gliding bacterium *Saprospira grandis*. *J. Nat. Prod.* 66, 818–822. doi:10.1021/np0205351.

Stout, E. P., Yu, L. C., and Molinski, T. F. (2012). Antifungal diterpene alkaloids from the Caribbean sponge *Agelas citrina*: Unified configurational

assignments of agelasidines and agelasines. *European J. Org. Chem.* 2012, 5131–5135. doi:10.1002/ejoc.201200572.

Stylissa flabelliformis – Sponges of Polynesia Available at: https://sponges-tahiti.ird.fr/?p=899 [Accessed May 13, 2020].

Subagio, I. B., Setiawan, E., Hariyanto, S., and Irawan, B. (2017). Spicule size variation in *Xestospongia testudinaria* Lamarck, 1815 at Probolinggo-Situbondo coastal. *AIP Conf. Proc.* 1854. doi:10.1063/1.4985425.

Sudarmono, P., Wibisana, A., Listriyani, L. W., and Sungkar, S. (2019). Characterization and synergistic antimicrobial evaluation of lipopeptides from *Bacillus amyloliquefaciens* isolated from oil-contaminated soil. *Int. J. Microbiol.* 2019. doi:10.1155/2019/3704198.

Sullivan, B., Faulkner, D. J., and Webb, L. (1983). Siphonodictidine, a metabolite of the burrowing sponge *Siphonodictyon* sp. that tnhibits coral growth. *Science (80-.).* 221, 1175–1176. doi:10.1126/science.221.4616.1175.

Sun, W., Dai, S., Jiang, S., Wang, G., Liu, G., Wu, H., et al. (2010). Culture-dependent and culture-independent diversity of *Actinobacteria* associated with the marine sponge *Hymeniacidon perleve* from the South China Sea. *Antonie Van Leeuwenhoek* 98, 65–75. doi:10.1007/s10482-010-9430-8.

Sung, J. H., Choi, S. J., Lee, S. W., Park, K. H., and Moon, T. W. (2004). Isoflavones found in Korean soybean paste as 3-hydroxy-3-methylglutaryl coenzyme a reductase inhibitors. *Biosci. Biotechnol. Biochem.* 68, 1051–1058. doi:10.1271/bbb.68.1051.

Suzumura, K.-I., Yokoi, T., Funatsu, M., Nagai, K., Tanaka, K., Zhang, H., et al. (2003). YM-266183 and YM-266184, novel thiopeptide antibiotics produced by *Bacillus cereus* isolated from a marine sponge. II. Structure elucidation. *J. Antibiot. (Tokyo).* 56, 129–134. doi:10.7164/antibiotics.56.129.

Tacconelli, E., Carrara, E., Savoldi, A., Harbarth, S., Mendelson, M., Monnet, D. L., et al. (2018). Discovery, research, and development of new antibiotics: the WHO priority list of antibiotic-resistant bacteria and tuberculosis. *Lancet Infect. Dis.* 18, 318–327. doi:10.1016/S1473-3099(17)30753-3.

Takahashi, M., Suzuki, K.-I., and Nakagawa, Y. (2006). Emendation of the genus *Flammeovirga* and *Flammeovirga aprica* with the proposal of *Flammeovirga arenaria* nom. rev., comb. nov. and *Flammeovirga yaeyamensis* sp. nov. *Int. J. Syst. Evol. Microbiol.* 56, 2095–2100. doi:10.1099/ijs.0.64324-0.

Tangerina, M. M. P., Correa, H., Haltli, B., Vilegas, W., and Kerr, R. G. (2017). Bioprospecting from cultivable bacterial communities of marine sediment and invertebrates from the underexplored Ubatuba region of Brazil. *Arch. Microbiol.* 199, 155–169. doi:10.1007/s00203-016-1290-9.

Tawfike, A., Attia, E. Z., Desoukey, S. Y., Hajjar, D., Makki, A. A., Schupp, P. J., et al. (2019). New bioactive metabolites from the elicited marine sponge-derived bacterium *Actinokineospora spheciospongiae* sp. nov. *AMB Express* 9. doi:10.1186/s13568-018-0730-0.

Taylor, M. W., Radax, R., Steger, D., and Wagner, M. (2007). Sponge-associated microorganisms: evolution, ecology, and biotechnological potential. *Microbiol. Mol. Biol. Rev.* 71, 295–347. doi:10.1128/mmbr.00040-06.

Team, R. C. (2019). R: The R project for statistical computing. Available at: https://www.r-project.org/ [Accessed May 11, 2020].

Thacker, R. W., Becerro, M. A., Lumbang, W. A., and Paul, V. J. (1998). Allelopathic interactions between sponges on a tropical reef. *Ecology* 79, 1740–1750. doi:10.1890/0012-9658(1998)079[1740:AIBSOA]2.0.CO;2.

Thakur, N. L., and Singh, A. (2016). "Marine sponges: Chemicobiological and biomedical applications," in *Marine Sponges: Chemicobiological and Biomedical Applications* (Springer India), 1–381. doi:10.1007/978-81-322-2794-6.

Thiel, V., Neulinger, S. C., Staufenberger, T., Schmaljohann, R., and Imhoff, J. F. (2006). Spatial distribution of sponge-associated bacteria in the Mediterranean sponge *Tethya aurantium*. *FEMS Microbiol. Ecol.* 59, 47–63. doi:10.1111/j.1574-6941.2006.00217.x.

Thomas, T. R. A., Kavlekar, D. P., and LokaBharathi, P. A. (2010). Marine drugs from sponge-microbe association - A review. *Mar. Drugs* 8, 1417–1468. doi:10.3390/md8041417.

Torriani, S. F. F., Melichar, J. P. E., Mills, C., Pain, N., Sierotzki, H., and Courbot, M. (2015). *Zymoseptoria tritici*: A major threat to wheat production, integrated approaches to control. *Fungal Genet. Biol.* 79, 8–12. doi:10.1016/j.fgb.2015.04.010.

Ueda, K., Ogi, T., and Sato, A. (2007). Cytotoxic haterumadienone congeners from the Okinawan marine sponge *Dysidea* sp. *Heterocycles* 72, 655–663. Available at: https://ci.nii.ac.jp/naid/40015348835 [Accessed May 1, 2021].

Ueda, K., Ueta, T., Siwu, E. R. O., Kita, M., and Uemura, D. (2005). Haterumadienone: A new puupehenone congener from an Okinawan marine sponge, *Dysidea* sp. *Chem. Lett.* 34, 1530–1531. doi:10.1246/cl.2005.1530.

Van Soest, R. W. M., Boury-Esnault, N., Vacelet, J., Dohrmann, M., Erpenbeck, D., De Voogd, N. J., et al. (2012). Global diversity of sponges (Porifera). *PLoS One* 7, e35105. doi:10.1371/journal.pone.0035105.

Van Soest, R. W. M., Erpenbeck, D., and Alvarez, B. (2002). "Family Dictyonellidae Van Soest, Diaz & Pomponi, 1990," in *Systema Porifera: A Guide to the Classification of Sponges,* eds. J. N. A. Hooper and R. W. M. Van Soest (New York: Kluwer Academic/Plenum Publishers), 773–786. doi:10.1007/978-1-4615-0747-5_83.

Versalovic, J. (2005). Microbial DNA typing by automated repetitive-sequence-based PCR. *Artic. J. Clin. Microbiol.* doi:10.1128/JCM.43.1.199-207.2005.

Vicente, J., Ríos, J. A., Zea, S., and Toonen, R. J. (2019). Molecular and morphological congruence of three new cryptic *Neopetrosia* spp. in the Caribbean. *PeerJ* 7, e6371. doi:10.7717/peerj.6371.

Vidgen, M. E., Hooper, J. N. A., and Fuerst, J. A. (2012). Diversity and distribution of the bioactive actinobacterial genus *Salinispora* from sponges along the Great Barrier Reef. *Antonie van Leeuwenhoek, Int. J. Gen. Mol. Microbiol.* doi:10.1007/s10482-011-9676-9.

Wang, C., Lu, Y., and Cao, S. (2020). Antimicrobial compounds from marine

actinomycetes. *Arch. Pharm. Res* 43, 677–704. doi:10.1007/s12272-020-01251-0.

Wang, C., Mei, X., Wang, D., and Zhu, W. (2019). “Marine natural products from marine sponge microorganisms,” in *Symbiotic microbiomes of coral reefs sponges and corals* (Switzerland: Springer Natur), 263–310. doi:10.1007/978-94-024-1612-1.

Wang, M., Carver, J. J., Phelan, V. V., Sanchez, L. M., Garg, N., Peng, Y., et al. (2016). Sharing and community curation of mass spectrometry data with Global Natural Products Social Molecular Networking. *Nat. Biotechnol.* 34, 828–837. doi:10.1038/nbt.3597.

Warnes, G., Bolker, B., Bonebakke, L., Gentleman, R., Huber, W., Liaw, A., et al. (2020). Various R Programming Tools for Plotting Data [R package gplots version 3.1.1]. Available at: https://cran.r-project.org/package=gplots [Accessed May 1, 2021].

Warnes, G. R., Bolker, B., Bonebakke, L., Gentleman, R., Huber, W., Liaw, A., et al. (2019). gplots: Various R programming tools for plotting data version 3.0.3 from CRAN. Available at: https://rdrr.io/cran/gplots/ [Accessed May 11, 2020].

Webster, N. S., and Taylor, M. W. (2012). Marine sponges and their microbial symbionts: Love and other relationships. *Environ. Microbiol.* 14, 335–346. doi:10.1111/j.1462-2920.2011.02460.x.

Webster, N. S., and Thomas, T. (2016). The sponge hologenome. *MBio* 7, 1–14. doi:10.1128/mBio.00135-16.

Wehrl, M., Steinert, M., and Hentschel, U. (2007). Bacterial uptake by the marine sponge *Aplysina aerophoba*. *Microb. Ecol.* 53, 355–365. doi:10.1007/s00248-006-9090-4.

Wickham, H. (2017). Easily install and load the “Tidyverse” [R package tidyverse version 1.3.0]. Available at: https://cran.r-project.org/package=tidyverse [Accessed May 11, 2020].

Wickham, H., Hester, J., and Chang, W. (2020a). Tools to make developing R packages easier [R package devtools version 2.3.0]. Available at: https://cran.r-project.org/package=devtools%0A%0A [Accessed May 11, 2020].

Wickham, H., Hester, J., and Chang, W. (2021). *devtools: Tools to Make Developing R Packages Easier*. Comprehensive R Archive Network (CRAN) Available at: https://cran.r-project.org/package=devtools [Accessed May 1, 2021].

Wickham, H., Hester, J., and Francois, R. (2020b). readr: Read Rectangular Text Data. Available at: https://cran.r-project.org/web/packages/readr/index.html [Accessed May 1, 2021].

Wiedenmayer, F. (1977). *Shallow-water sponges of the western Bahamas*. Basel: Springer.

Wilkinson, C., Garrone, R., and Vacelet, J. (1984). Marine sponges discriminate between food bacteria and bacterial symbionts: electron microscope radioautography and in situ evidence. *Proc R Soc L B*, 519–528.

Wilkinson, C. R. (1987). Productivity and abundance of large sponge populations on Flinders Reef flats, Coral Sea. *Coral Reefs* 5, 183–188. doi:10.1007/BF00300961.

Williams, P. G., Asolkar, R. N., Kondratyuk, T., Pezzuto, J. M., Jensen, P. R., and Fenical, W. (2007). Saliniketals A and B, bicyclic polyketides from the marine actinomycete *Salinispora arenicola*. *J. Nat. Prod.* 70, 83–88. doi:10.1021/np0604580.

Williams, P. G., Buchanan, G. O., Feling, R. H., Kauffman, C. A., Jensen, P. R., and Fenical, W. (2005). New cytotoxic salinosporamides from the marine actinomycete *Salinispora tropica*. doi:10.1021/jo050511.

Wilson, D. M., Puyana, M., Fenical, W., and Pawlik, J. R. (1999). Chemical defense of the Caribbean reef sponge *Axinella corrugata* against predatory fishes. *J. Chem. Ecol.* 25, 2811–2823. doi:10.1023/A:1020811810223.

Wilson, M. C., Mori, T., Rückert, C., Uria, A. R., Helf, M. J., Takada, K., et al. (2014). An environmental bacterial taxon with a large and distinct metabolic repertoire. *Nature*. doi:10.1038/nature12959.

Wulff, J. L. (1995). Sponge-feeding by the Caribbean starfish *Omaster reticulatus*. *Mar. Biol.* 123, 313–325.

Xiao, F., Li, H., Xu, M., Li, T., Wang, J., Sun, C., et al. (2018). Staurosporine derivatives generated by pathway engineering in a heterologous host and their cytotoxic selectivity. *J. Nat. Prod.* 81, 1745–1751. doi:10.1021/acs.jnatprod.8b00103.

Xu, H., Fu, Y., Yang, N., Ding, Z., Lai, Q., and Zeng, R. (2012). *Flammeovirga pacifica* sp. nov., isolated from deep-sea sediment. *Int. J. Syst. Evol. Microbiol.* 62, 937–941. doi:10.1099/ijs.0.030676-0.

Yamanaka, K., Oikawa, H., Ogawa, H.-O., Hosono, K., Shinmachi, F., Takano, H., et al. (2005). Desferrioxamine E produced by *Streptomyces griseus* stimulates growth and development of *Streptomyces tanashiensis*. *Microbiology* 151, 2899–2905. doi:10.1099/mic.0.28139-0.

Yang, J. Y., Sanchez, L. M., Rath, C. M., Liu, X., Boudreau, P. D., Bruns, N., et al. (2013). Molecular networking as a dereplication strategy. *J. Nat. Prod.* 76, 1686–1699. doi:10.1021/np400413s.

Yoo, J.-S., Zheng, C.-J., Lee, S., Kwak, J.-H., and Kim, W.-G. (2006). Macrolactin N, a new peptide deformylase inhibitor produced by *Bacillus subtilis*. *Bioorg. Med. Chem. Lett.* 16, 4889–4892. doi:10.1016/j.bmcl.2006.06.058.

Yu, M., Li, Y., Banakar, S. P., Liu, L., Shao, C., Li, Z., et al. (2019). New metabolites from the Co-culture of marine-derived actinomycete *Streptomyces rochei* MB037 and fungus *Rhinocladiella similis* 35. *Front. Microbiol* 10, 1–11. doi:10.3389/fmicb.2019.00915.

Zheng, C.-J., Lee, S., Lee, C.-H., and Kim, W.-G. (2007). Macrolactins O–R, glycosylated 24-membered lactones from *Bacillus* sp. AH159-1. *J. Nat. Prod.* 70, 1632–1635. doi:10.1021/np0701327.

10. APPENDIX

Supplementary Methods

Sponge spicule preparation and measurement

To obtain spicules, a small piece (1 cm^3) of each sponge was dried in the oven at 105°C for 1-2 h to completely remove water and subsequently left to cool down for 15 minutes. Maceration was performed in 5.0 mL commercial bleach (Bayclin, which 5% sodium hypochlorite) for 15 min. to 2 h, depending on toughness of specimens with the hard sponge normally requiring longer time. The sample was washed four times with distilled water and rinsed with alcohol (70%) to remove organic materials including sponge's fibers. Following the maceration, the free spicules of each sponge were mounted on a microscope slide, air dried for few minutes and observed under a binocular microscope (Olympus, XSZ107BN) with 16x and 40x magnification for the ocular and objective lens, respectively. All spicule's pictures were taken with a Samsung J4+ 13-megapixel camerathrough the microscope ocular. The length and width of every spicule was determined by dividing its length and width—measured by the Corel Draw X6 (64-Bit) in cm on the spicule's picture taken previously by the camera—with the total magnification value of the microscope (640 total magnification resulting from a 4x magnification of ocular and 60x of objective lens) and then multiplying the value by 10,000 to get the final value of the measurement in micrometre (µm) as indicated in the following spicule's pictures Table 10.2.

	1	2	3	4	5	6	7	8	9	10	11	12	13	14	15	16	17	18	19	20	21	22	23	24
A					1	2	3	4	5	6	7	8	9	10	11	12	13	14	15	16	17	18	19	20
B					40	39	38	37	36	35	34	33	32	31	30	29	28	27	26	25	24	23	22	21
C					41	42	43	44	45	46	47	48	49	50	51	52	53	54	55	56	57	58	59	60
D					80	79	78	77	76	75	74	73	72	71	70	69	68	67	66	65	64	63	62	61
E					81	82	83	84	85	86	87	88	89	90	91	92	93	94	95	96	97	98	99	100
F					120	119	118	117	116	115	114	113	112	111	110	109	108	107	106	105	104	103	102	101
G					121	122	123	124	125	126	127	128	129	130	131	132	133	134	135	136	137	138	139	140
H					Pos.con.	159	158	157	156	155	154	153	152	151	150	149	148	147	146	145	144	143	142	141
I					1	2	3	4	5	6	7	8	9	10	11	12	13	14	15	16	17	18	19	20
J					40	39	38	37	36	35	34	33	32	31	30	29	28	27	26	25	24	23	22	21
K					41	42	43	44	45	46	47	48	49	50	51	52	53	54	55	56	57	58	59	60
L					80	79	78	77	76	75	74	73	72	71	70	69	68	67	66	65	64	63	62	61
M					81	82	83	84	85	86	87	88	89	90	91	92	93	94	95	96	97	98	99	100
N					120	119	118	117	116	115	114	113	112	111	110	109	108	107	106	105	104	103	102	101
O					121	122	123	124	125	126	127	128	129	130	131	132	133	134	135	136	137	138	139	140
P					Pos.con.	159	158	157	156	155	154	153	152	151	150	149	148	147	146	145	144	143	142	141

Figure 10.1. Microfractionation: General µ-fractionation plate layout. Column 1 contains cation adjusted Mueller Hinton II Medium without test strain as contamination control; Columns 2+3 contain antibiotic standard; Column 4 contains cells/spores in medium without antibiotic or extract fractions as growth control; Area AH05- AH24: Collected fractions from the first injection replicate; Area IP05- IP24: Collected fractions from the second injection replicate. Numbers indicate fraction count for the two injection replicates.

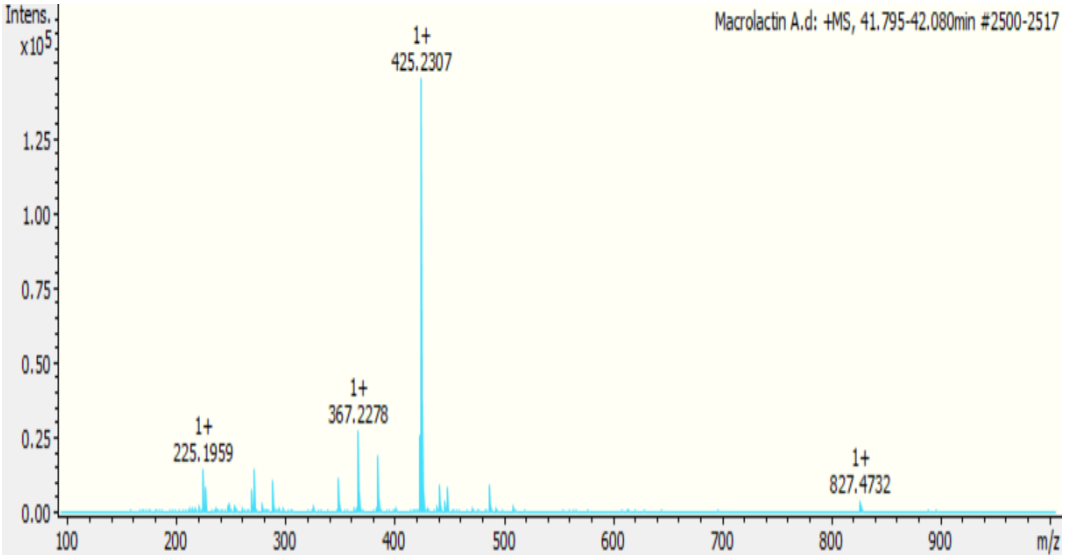

Figure 10.2. LCHRMS of macrolactin A

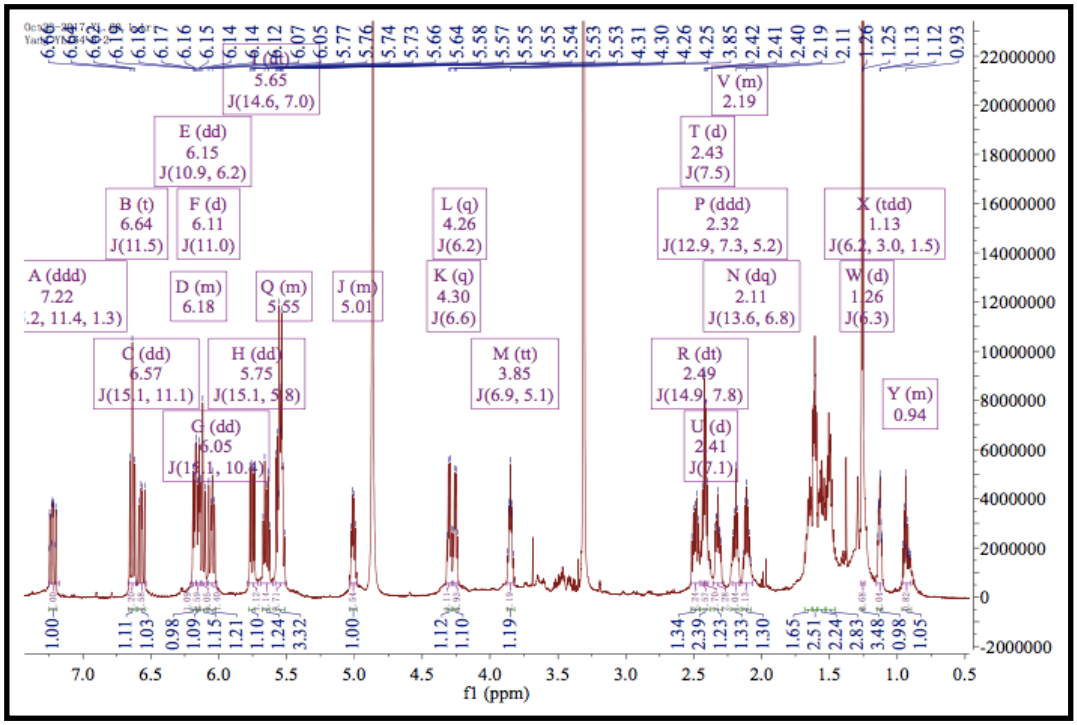

Figure 10.3. ^{1}H NMR spectrum of macrolactin A

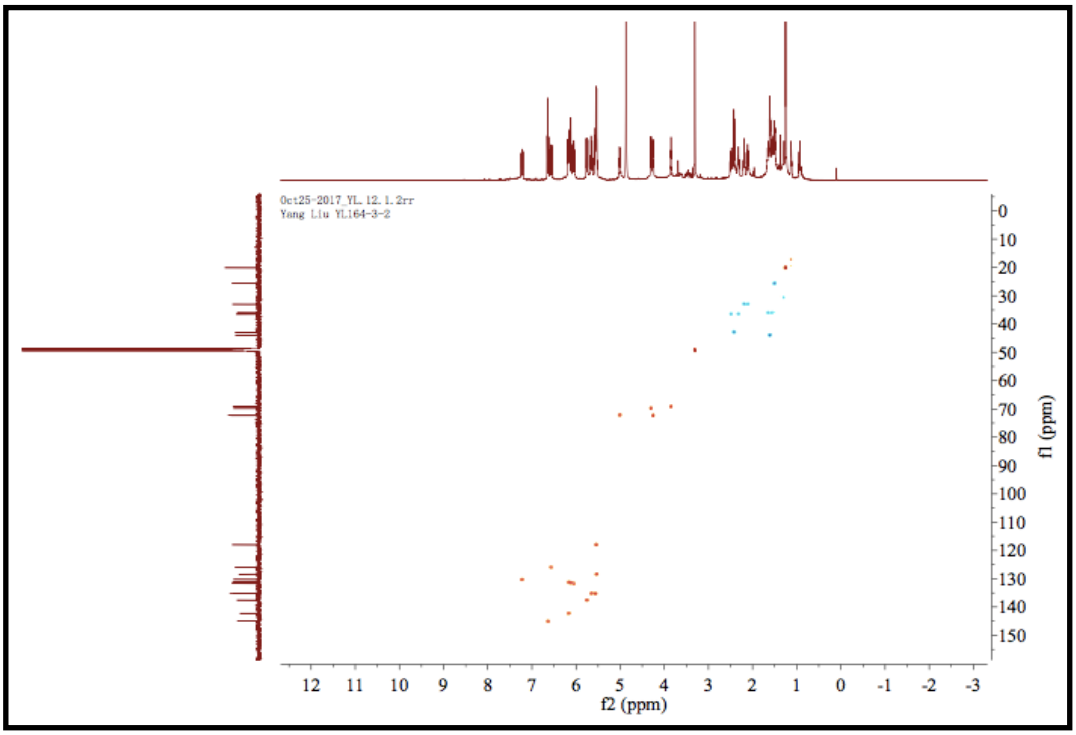

Figure 10.4. HSQC spectrum of macrolactin A

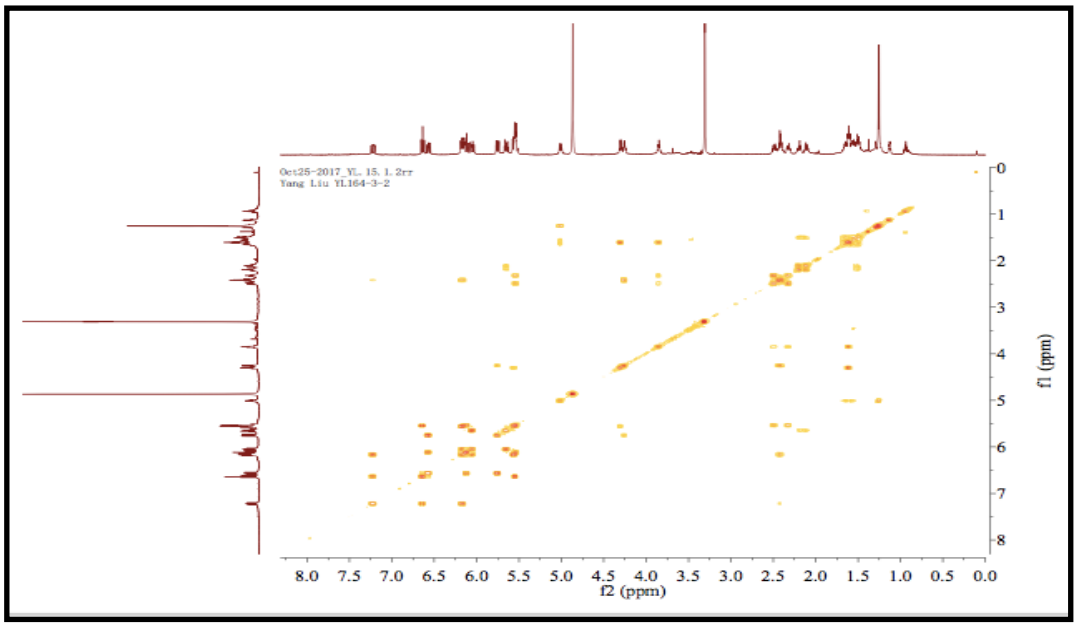

Figure 10.5. COSY correlations of macrolactin A

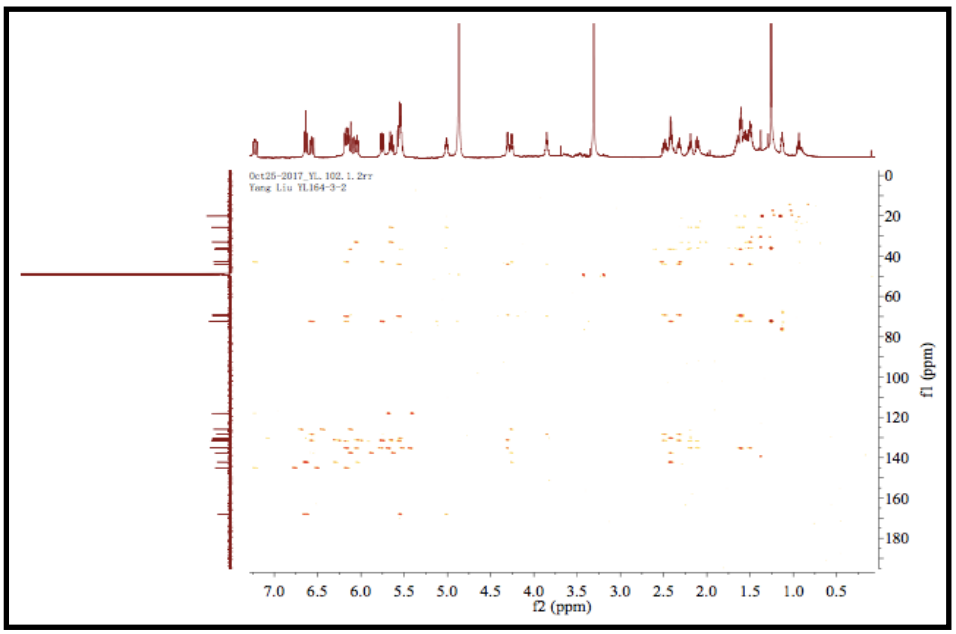

Figure 10.6. HMBC spectrum of macrolactin A

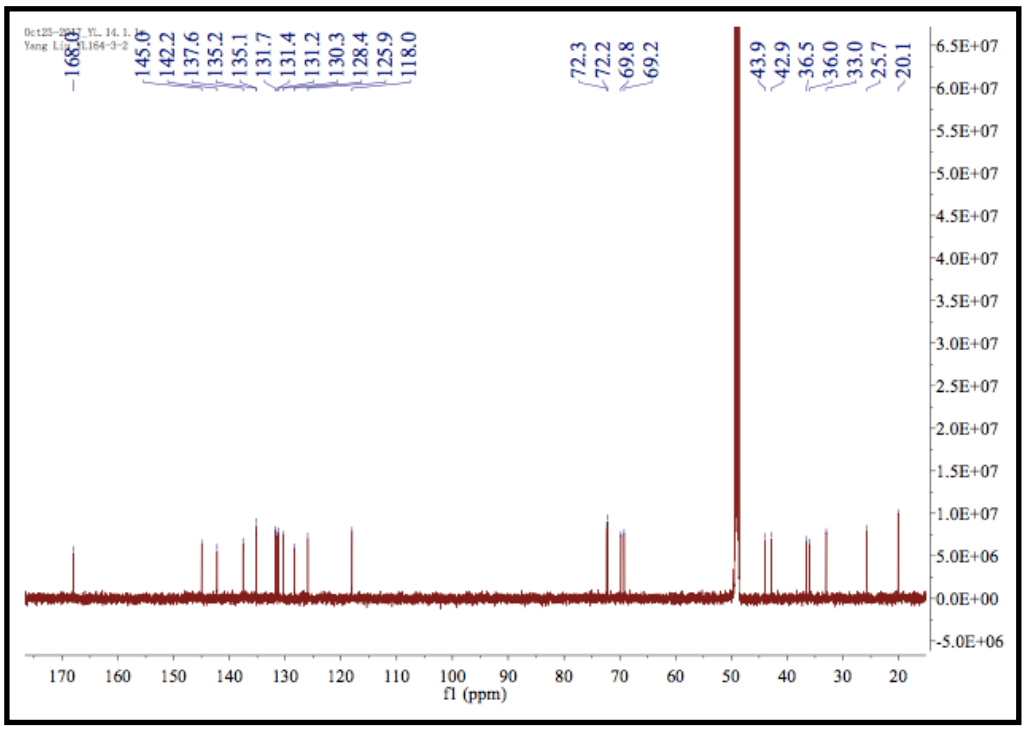

Figure 10.7. ^{13}C NMR spectrum of macrolactin A

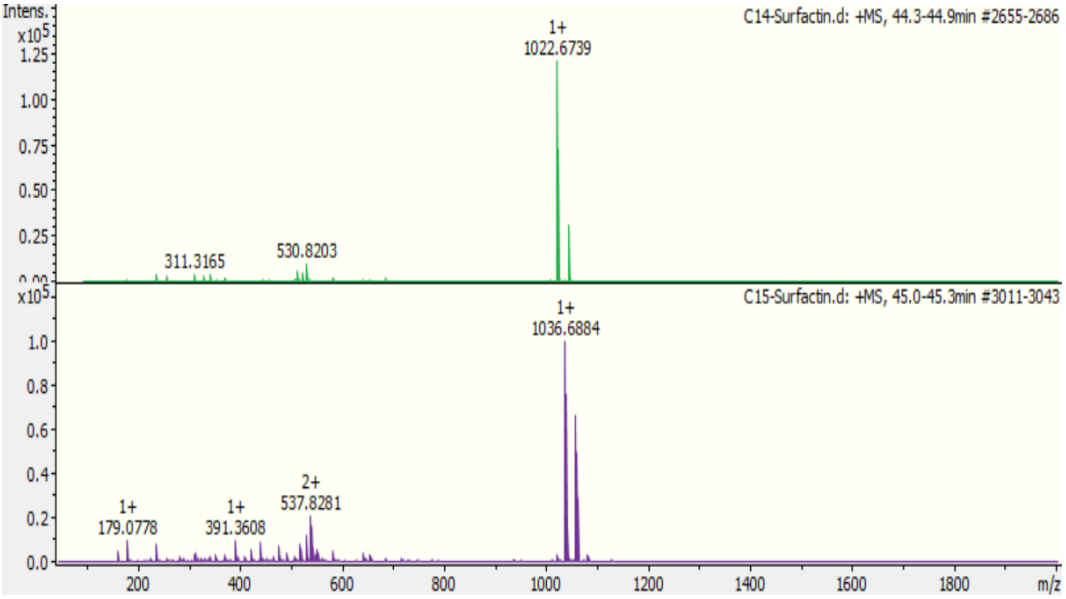

Figure 10.8. LCHRMS of C14surfactin and C15 surfactin

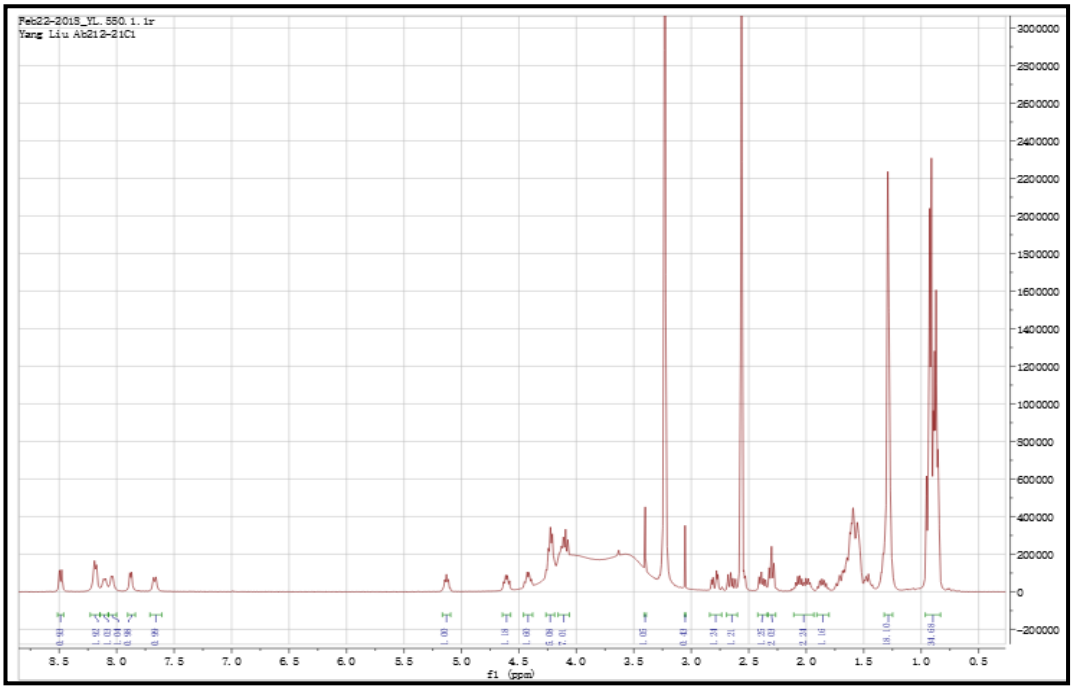

Figure 10.9. ^{1}H NMR spectrum of C14 surfactin

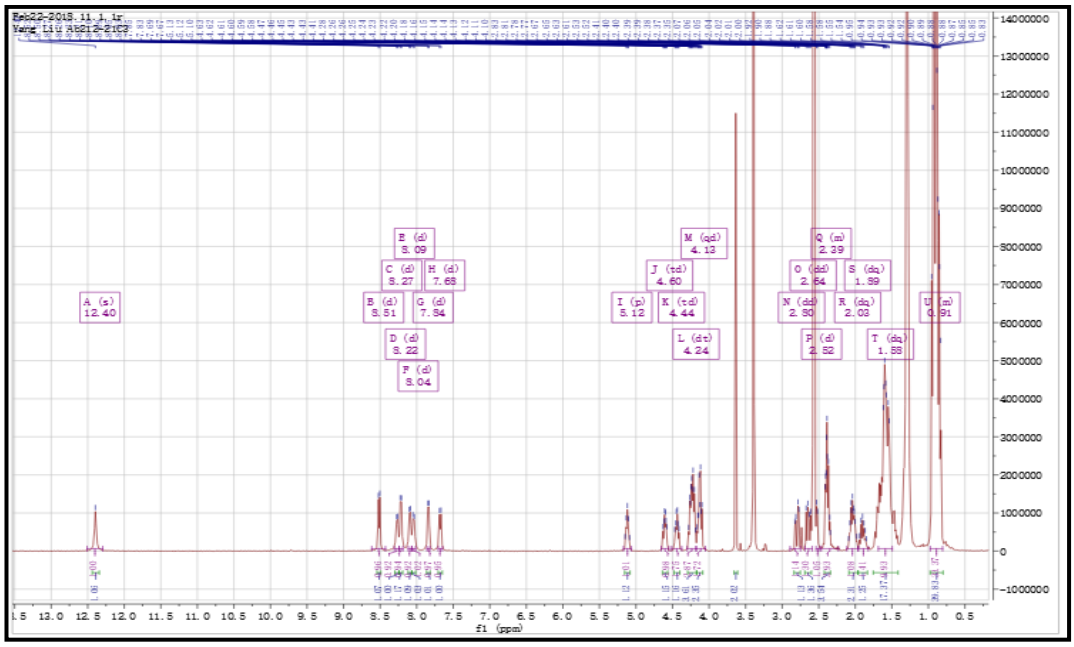

Figure 10.10. ^{1}H NMR spectrum of C15 surfactin

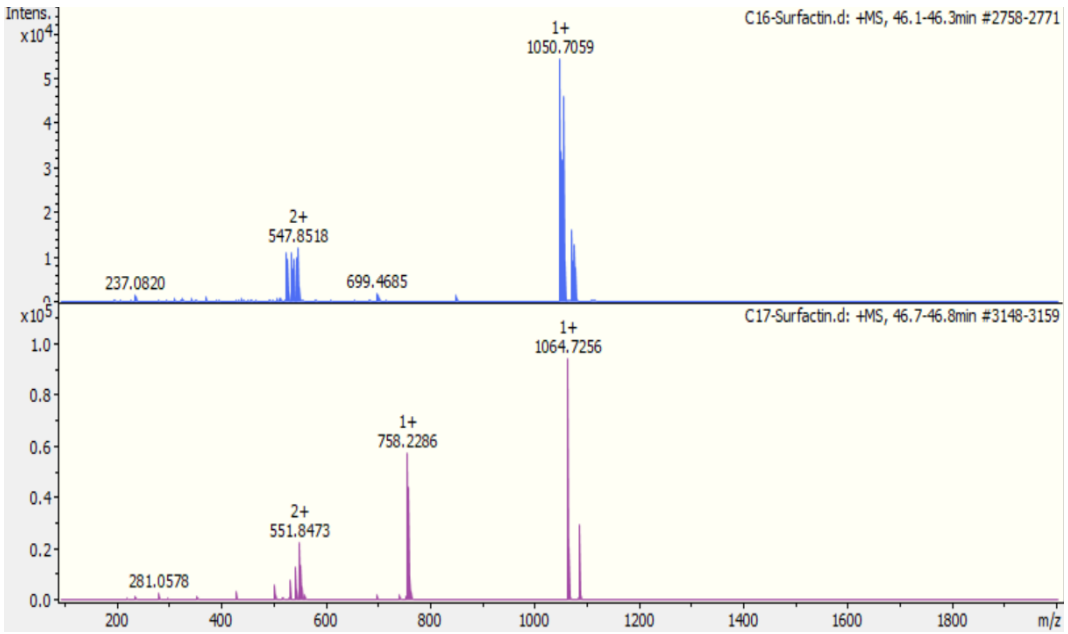

Figure 10.11. LCHRMS of C16 surfactin and C17 surfacti

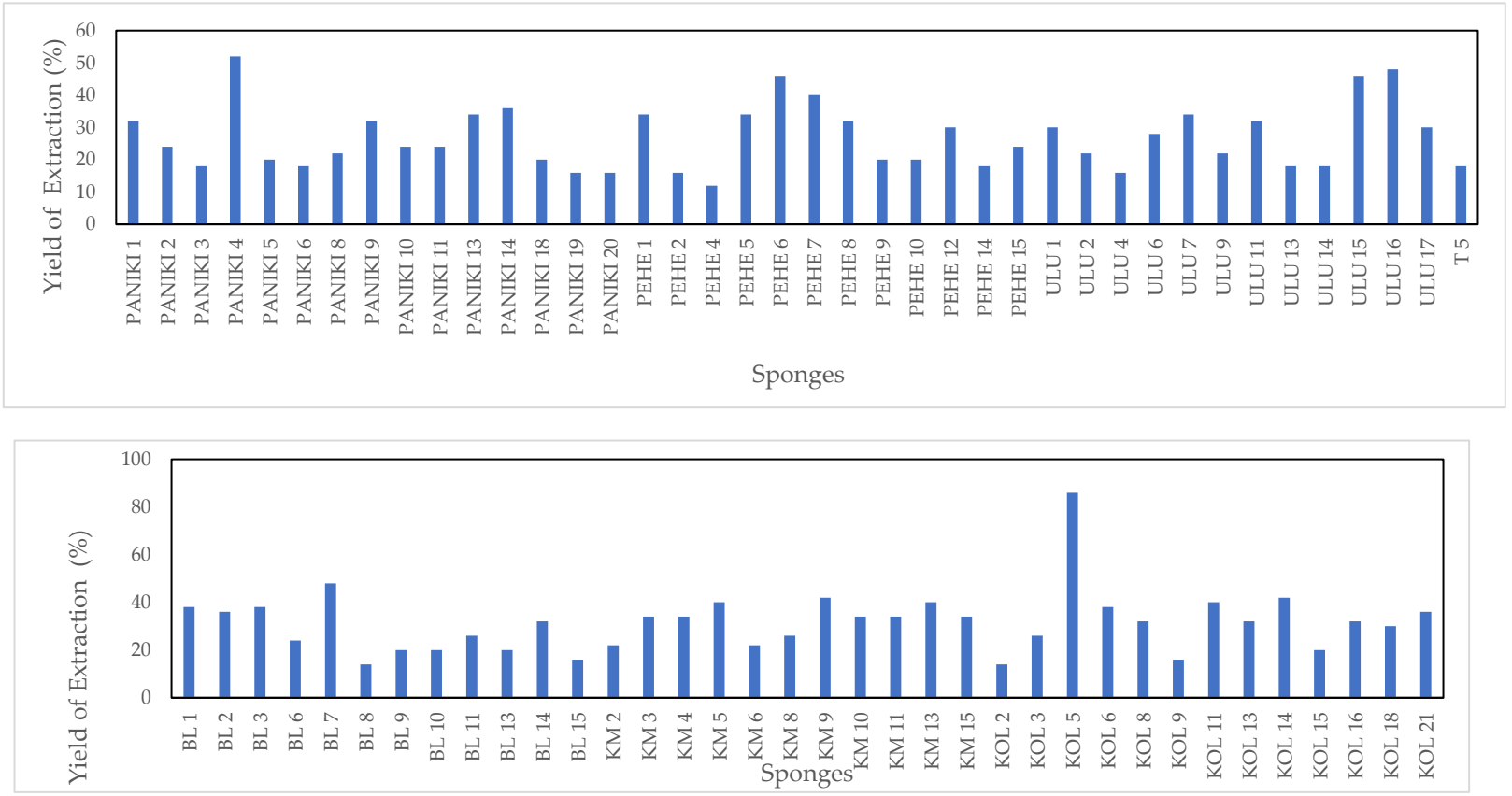

Figure 10.12. Sponges investigated in this study and extraction yield

	1	2	3	4	5	6	7	8	9	10	11	12	13	14	15	16	17	18	19	20	21	22	23	24
A	100	100	100	22	14	17	14	21	21	18	18	5	17	17	10	6	5	14	-12	15	2	-7	-2	-6
B	100	102	102	27	-10	31	15	20	19	10	40	14	20	13	26	9	4	16	28	5	-1	-7	-9	-39
C	100	101	100	24	2	-1	10	-4	0	3	0	-11	-8	-14	-20	-18	-24	-20	-45	-44	-41	-23	-35	-9
D	101	103	103	-8	100	-3	-17	3	9	-23	-17	-3	-5	-17	-20	-21	-3	-38	-24	-20	-16	-33	-42	-42
E	100	100	101	14	100	-3	100	100	4	6	4	-23	3	-7	-12	-14	-9	5	-5	-6	-5	-35	-39	-15
F	97	102	102	-6	1	-37	-24	-12	20	-11	-6	-5	18	-11	3	1	3	-21	-10	-20	-8	-35	-19	-50
G	100	100	99	-3	8	-9	7	0	-28	12	-11	-1	10	-1	-24	-5	-24	-24	-24	-30	-38	-34	-37	-40
H	100	97	98	-14	-2	7	-13	-2	-16	22	-13	21	13	-4	11	13	-11	10	1	-2	-10	-14	-17	-48
I	100	101	101	-6	-4	-31	-31	-39	-37	-37	-42	-45	-45	-48	-50	-62	-60	-60	-61	-66	-69	-83	-76	-61
J	100	13	11	5	-21	-27	-18	-9	-15	-13	-26	-15	-18	-12	-41	-26	-33	-31	-34	-24	-53	-55	-85	-63
K	97	-11	-11	-8	-37	-11	-17	-29	-49	-42	-52	-29	-49	-44	-53	-46	-55	-40	-56	-50	-61	-40	-70	-71
L	101	7	4	-7	102	-7	-5	-14	-6	-10	-13	-10	-14	-3	-30	-16	-11	-14	-21	-21	-33	-36	-41	-42
M	100	-11	-10	-12	101	-19	101	102	-31	-26	-44	-37	-27	-20	-38	-28	-21	-16	-26	-24	-31	-24	-35	-53
N	101	-15	-7	-15	-18	-18	-13	-1	-36	-22	-17	-26	-20	-26	-17	-30	-35	-29	-37	-34	-40	-40	-42	-53
O	101	-9	-18	3	-15	1	-9	-12	-12	-23	-14	-15	-9	-19	-19	-8	-46	-42	-16	-24	-23	-35	-39	-53
P	102	-7	-6	-16	-79	-3	-13	-10	-26	-24	-35	-12	-31	-27	-20	-25	-15	-7	-33	-16	-21	-39	-45	-7

(a)

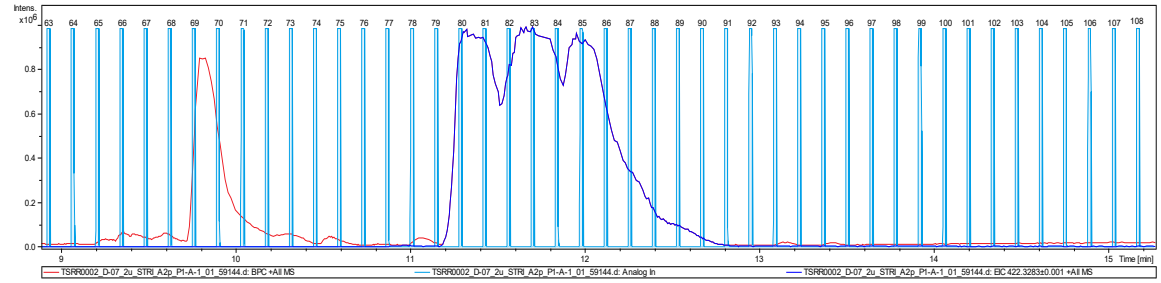

(b)

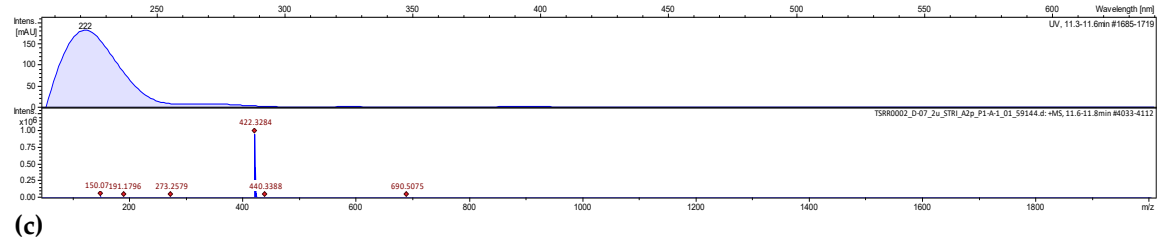

(c)

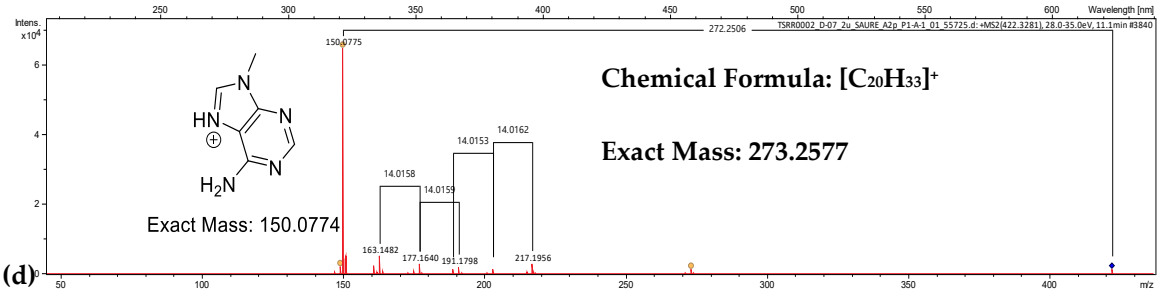

(d)

Figure 10.13. Microfractionation: Bioassay and dereplication results plate KOL_18 against *S. aureus* **(a)** Assay read-out of microfractionation plate KOL_18 against *S. aureus*. Numbers indicate the relative growth inhibition of the test strain. Fractions causing at least 70% rel. growth inhibition were considered “active”. Column 1: Medium control; Columns 2 + 3 antibiotic standard (Gentamycin 64 - 0.002 µg/mL); Column 4: Growth control. Area AH05- AH24: 1 µL injection volume replicate showing activity in fractions 80-81 and 83-84; Area IP05- IP24: 2 µL injection volume replicate showing activity in fractions 80-81 and 83-84; **(b)** Overlaid base peak chromatogram (red), fraction collector analog signal (light blue bars) and extracted ion chromatogram of *m/z* 422.3281 ± 0.001 $[M]^+$ (dark blue) of the 1 mg/mL (in MeOH) with 2 µL injection volume; **(c)** UV chromatogram and MS spectrum of fractions 80-84; **(d)** MS/MS fragmentation of the precursor ion at *m/z* 422.3281 $[M]^+$ (dereplicated as agelasine A-F), manual annotation of the neutral losses and proposed structure of the base peak ion.

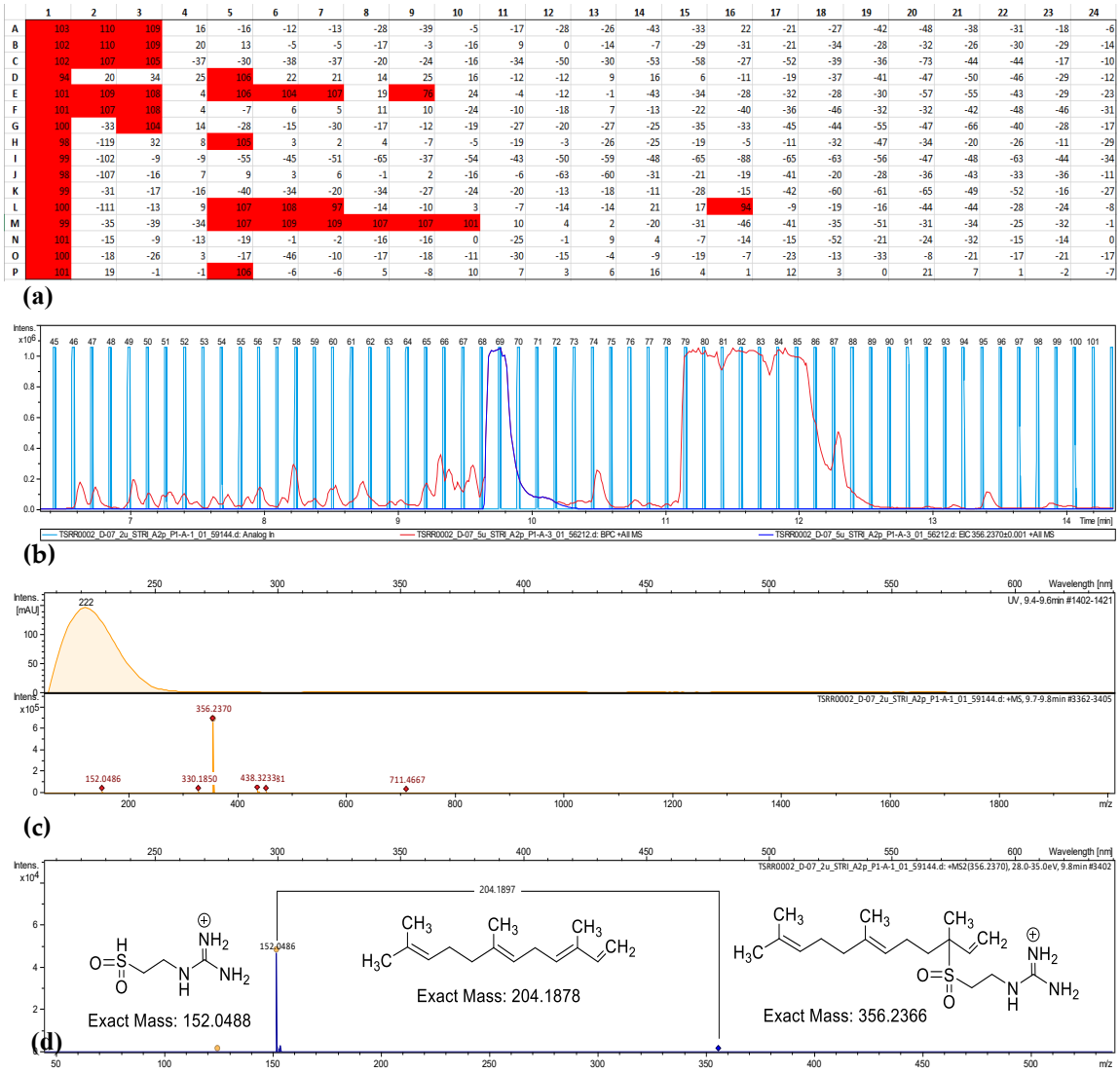

Figure 10.14. Microfractionation: Bioassay and dereplication results plate KOL_18 against *S. triciti* (a) Assay read-out of the microfractionation plate KOL_18 against *S. triciti*. Numbers indicate the relative growth inhibition of the test strain. Fractions causing at least 70% rel. growth inhibition were considered “active”. Column 1: Medium control; Columns 2 + 3 antibiotic standard (Nystatin 25.6 – 0.0008 µg/mL); Column 4: Growth control. Area AH05- AH24: 2 µL injection volume replicate showing activity in fractions 80-83 and 85; Area IP05- IP24: 5 µL injection volume replicate showing activity in fractions 69 and 80-85; H5 and P5: unfractionated extract control **(b)** Overlaid base peak chromatogram (red), fraction collector analog signal (light blue bars) and extracted ion chromatogram of *m/z* 355.2370 ± 0.001 $[M+H]^+$ (dark blue) of the 1 mg/mL (in MeOH) with 5 µL injection volume; **(c)** UV chromatogram and MS spectrum of fraction 69; **(d)** MS/MS fragmentation of the precursor ion at *m/z* 356.2370 $[M+H]^+$ (dereplicated as agelasidine A), manual annotation of the neutral loss and proposed structure of the base peak ion.

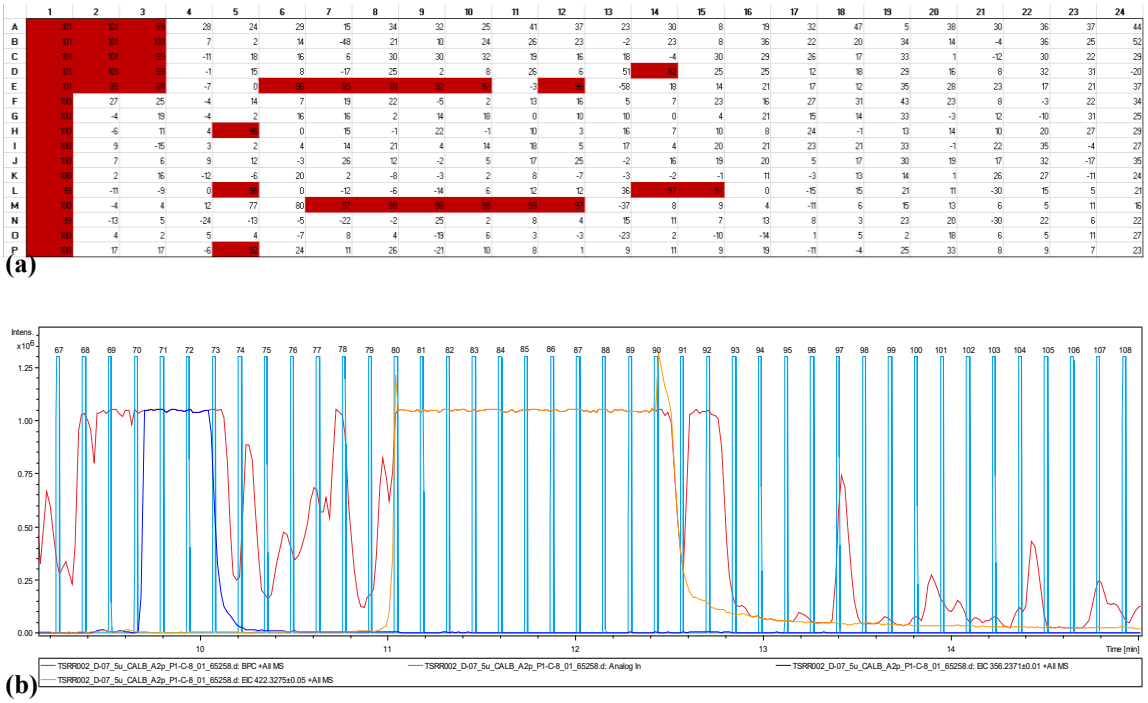

Figure 10.15. Microfractionation: Bioassay and dereplication results plate KOL_18 against *C. albicans* (a) Assay read-out of the microfractionation plate KOL_18 against *C. albicans*. Numbers indicate the relative growth inhibition of the test strain. Fractions causing at least 70% rel. growth inhibition were considered “active”. Column 1: Medium control; Columns 2 + 3 antibiotic standard (Nystatin 64 - 0.002 µg/mL); Column 4: Growth control. Area AH05- AH24: 2 µL injection volume replicate showing activity in fractions 71, 82-86 and 88; Area IP05- IP24: 5 µL injection volume replicate showing activity in fractions 70-71, 80 and 83-88; H5 and P5: Unfractionated extract control **(b)** Overlaid base peak chromatogram (red), fraction collector analog signal (light blue bars), extracted ion chromatogram of *m/z* 355.2370 ± 0.001 $[M+H]^+$ (dark blue)-dereplicated as agelasidine A and extracted ion chromatogram of *m/z* 422.3281 ± 0.005 $[M]^+$ (orange)-dereplicated as agelasine (A-F) of the 2 mg/mL (in MeOH) with 5 µL injection volume.

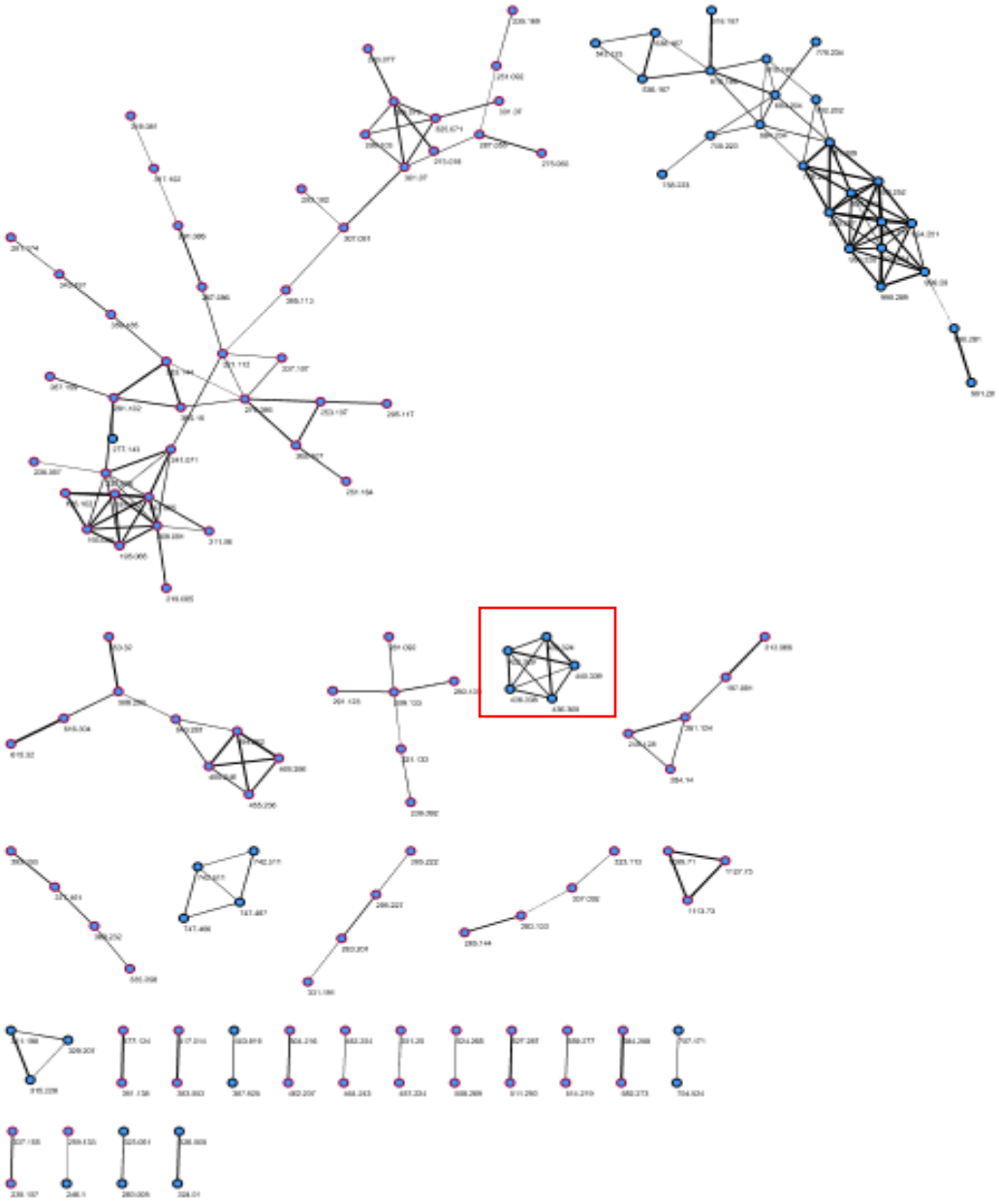

Figure 10.16. Molecular networking of the analyzed sponge sample set. The cluster of the agelasine family is framed in red.

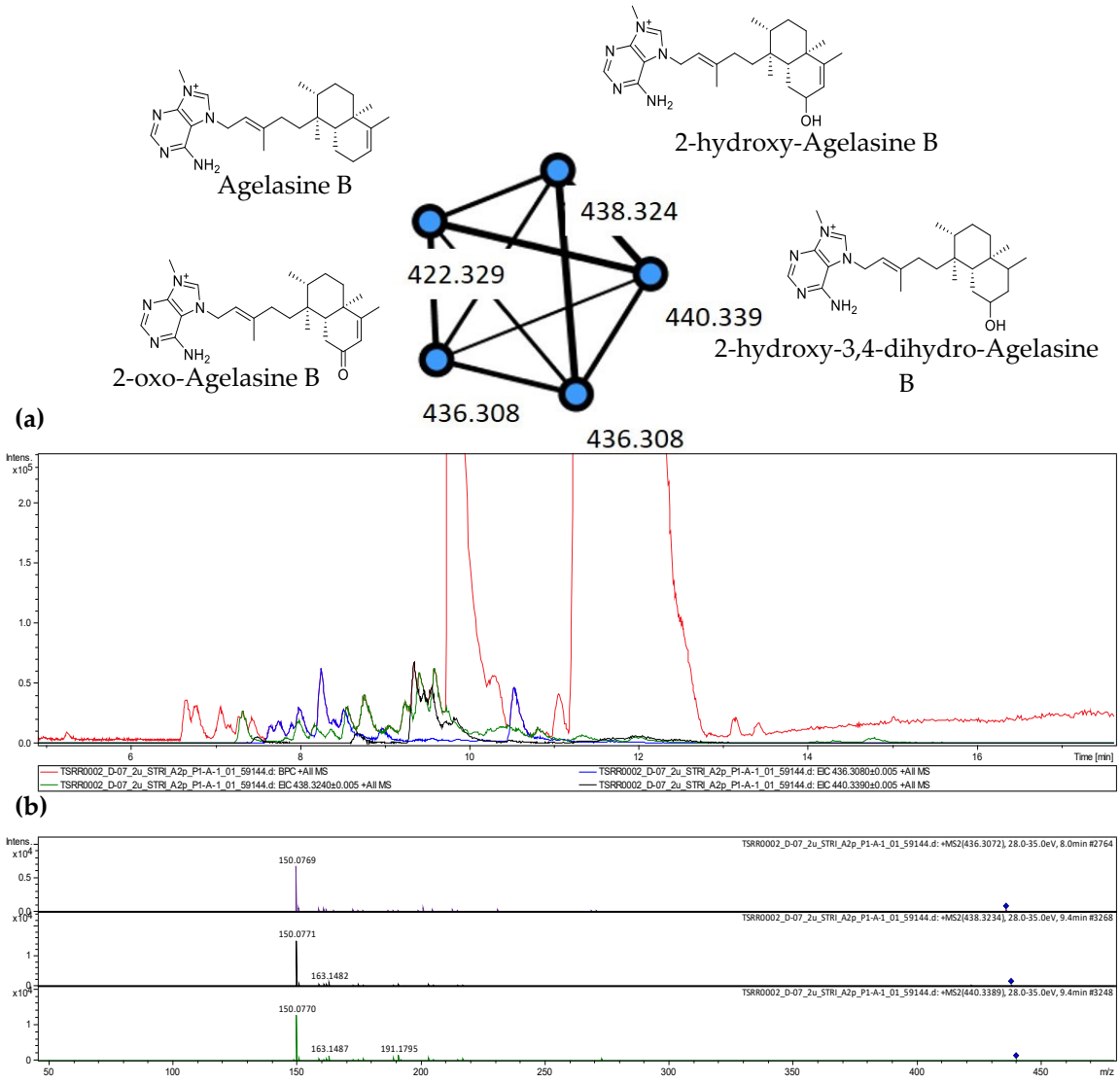

Figure 10.17. Enlarged cluster of agelasine derivatives and MS/MS fragmentation analysis (a) Cluster of agelasine derivatives present in the extract of KOL_18 with selected structures corresponding to the precursor ions (framework of agelasine B was chosen as example); **(b)** Overlaid base peak chromatogram (red) of the KOL_18 extract, extracted ion chromatogram, of *m/z* 436.3080 ± 0.005 (blue), *m/z* 438.3240 ± 0.005 (green) and *m/z* 440.3390 ± 0.005 (black); **(c)** MS/MS fragmentation of the selected precursor ions.

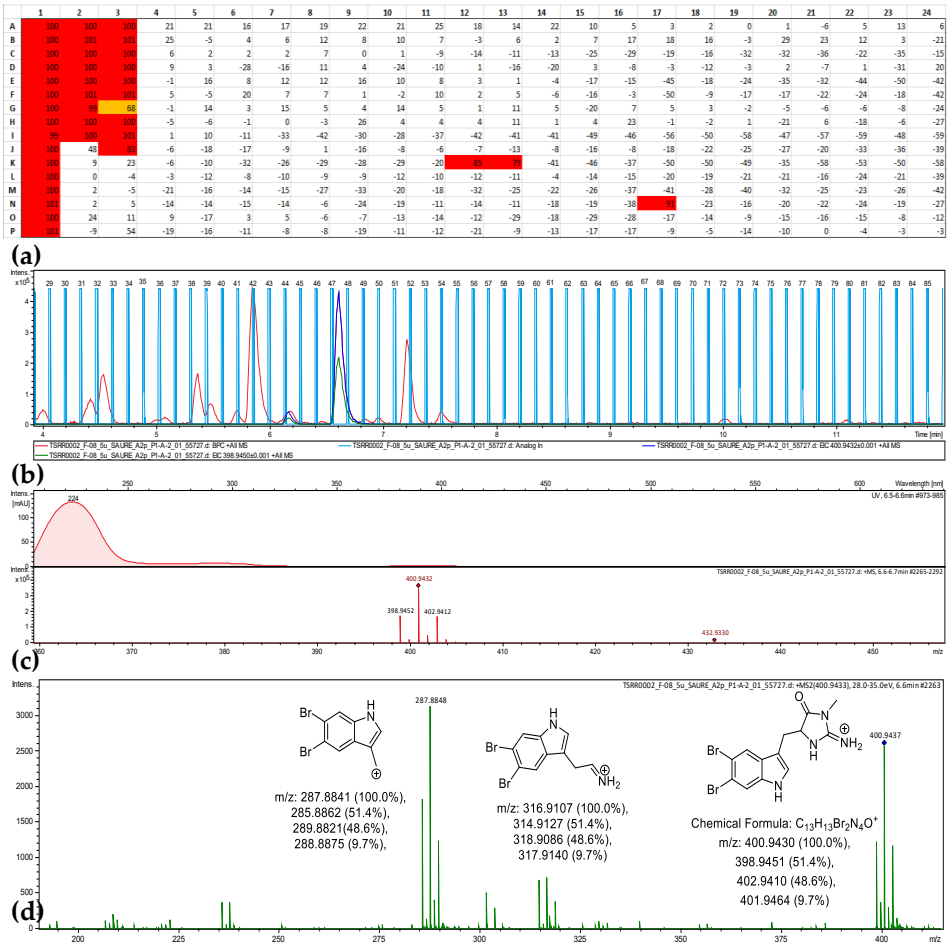

Figure 10.18. Microfractionation: Bioassay and dereplication results plate PEHE_5 against *S. aureus* fractions 47-48 (a) Assay read-out of microfractionation plate PEHE_5 against *S. aureus*. Numbers indicate the relative growth inhibition of the test strain. Fractions causing at least 70% rel. growth inhibition were considered “active”. Column 1: Medium control; Columns 2 + 3 antibiotic standard; Column 4: Growth control. Area AH05- AH24: 2µL injection volume; Area IP05- IP24 : 5 µL injection; **(b)** Overlaid base peak chromatogram (red), fraction collector analog signal (light blue bars) and extracted ion chromatogram of *m/z* 398.9450 ± 0.001 $[M+H]^+$ (dark blue) and 400.9432 ± 0.001 $[M+H]^+$ (green) of the 1 mg/mL (in MeOH) with 5 µL injection volume; **(c)** UV chromatogram and MS spectrum of fractions 47-48; **(d)** MS/MS fragmentation of the precursor ion at *m/z* 400.9432 $[M+H]^+$

(dereplicated as 5,6-dibromo-1',8-dihydro-2'-demethylaplysinopsin), and proposed structures of the fragment ions.

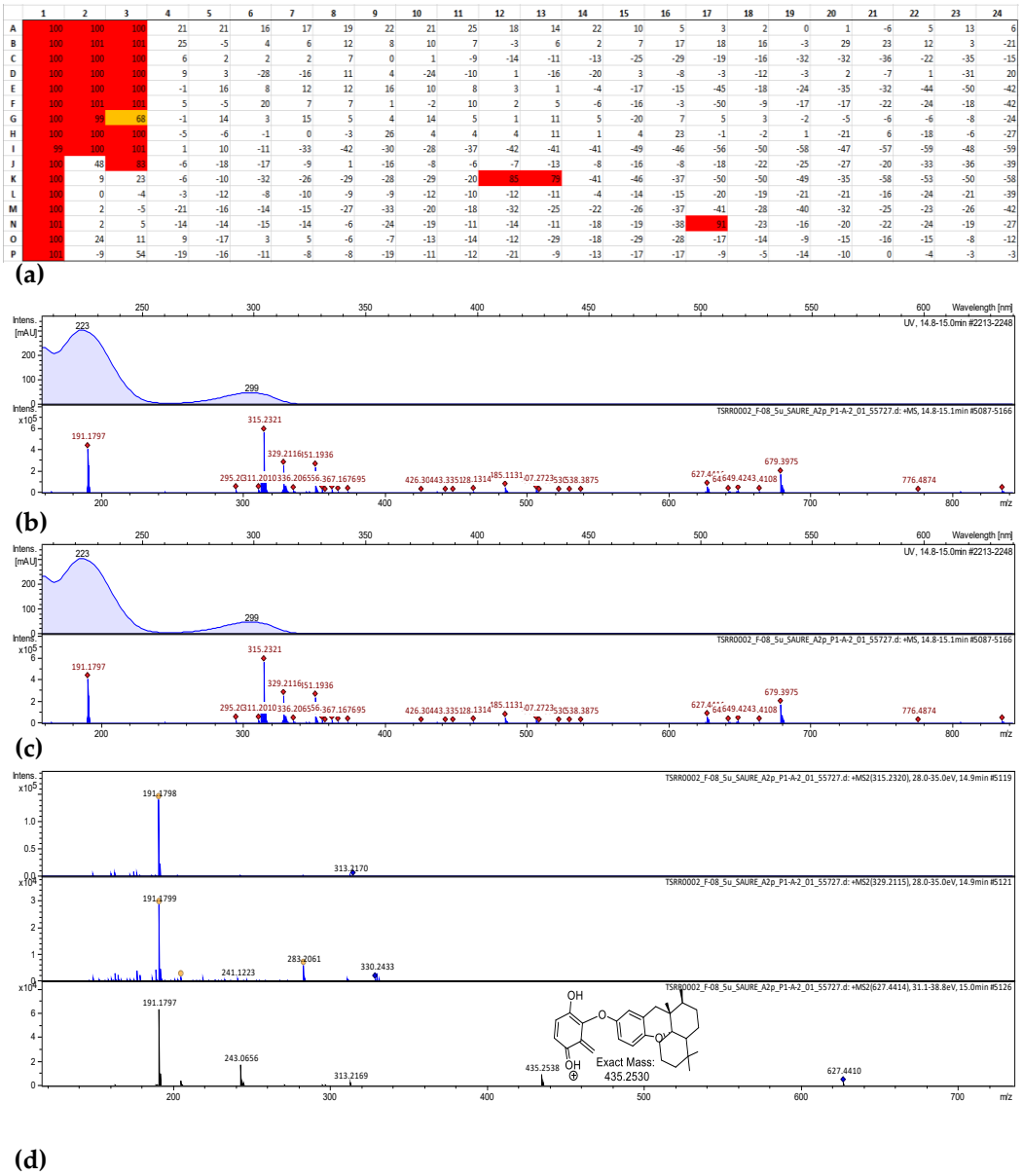

Figure 10.19. Microfractionation: Bioassay and dereplication results plate PEHE_5 against *S. aureus* fraction 108 (a) Assay read-out of µ-fractionation plate PEHE_5 against *S. aureus.* Numbers indicate the relative growth inhibition of the test strain. Fractions causing at least 70% rel. growth inhibition were considered "active". Column 1: Medium control; Columns 2 + 3 antibiotic standard; Column 4: Growth control. Area AH05- AH24: 2 µL injection volume; Area IP05- IP24 : 5 µL injection; **(b)** Overlaid base peak chromatogram (red), fraction collector analog signal (light blue bars) and extracted ion chromatogram of *m/z* 315.2321±0.001 $[M+H]^+$ (dark blue), *m/z* 329.2115 ± 0.001 $[M+H]^+$ (green) and *m/z* 627.4414 $[M+H]^+$ of the 1 mg/mL (in MeOH) with 5 µL injection volume; **(c)** UV chromatogram and MS spectrum of fraction 108; **(d)** MS/MS fragmentation of the precursor ions at *m/z* 315.2321 $[M+H]^+$, *m/z* 329.2115 $[M+H]^+$ and *m/z* 627.4414 $[M+H]^+$, tentatively assigned to the group of sesquiterpene hydroquinones.

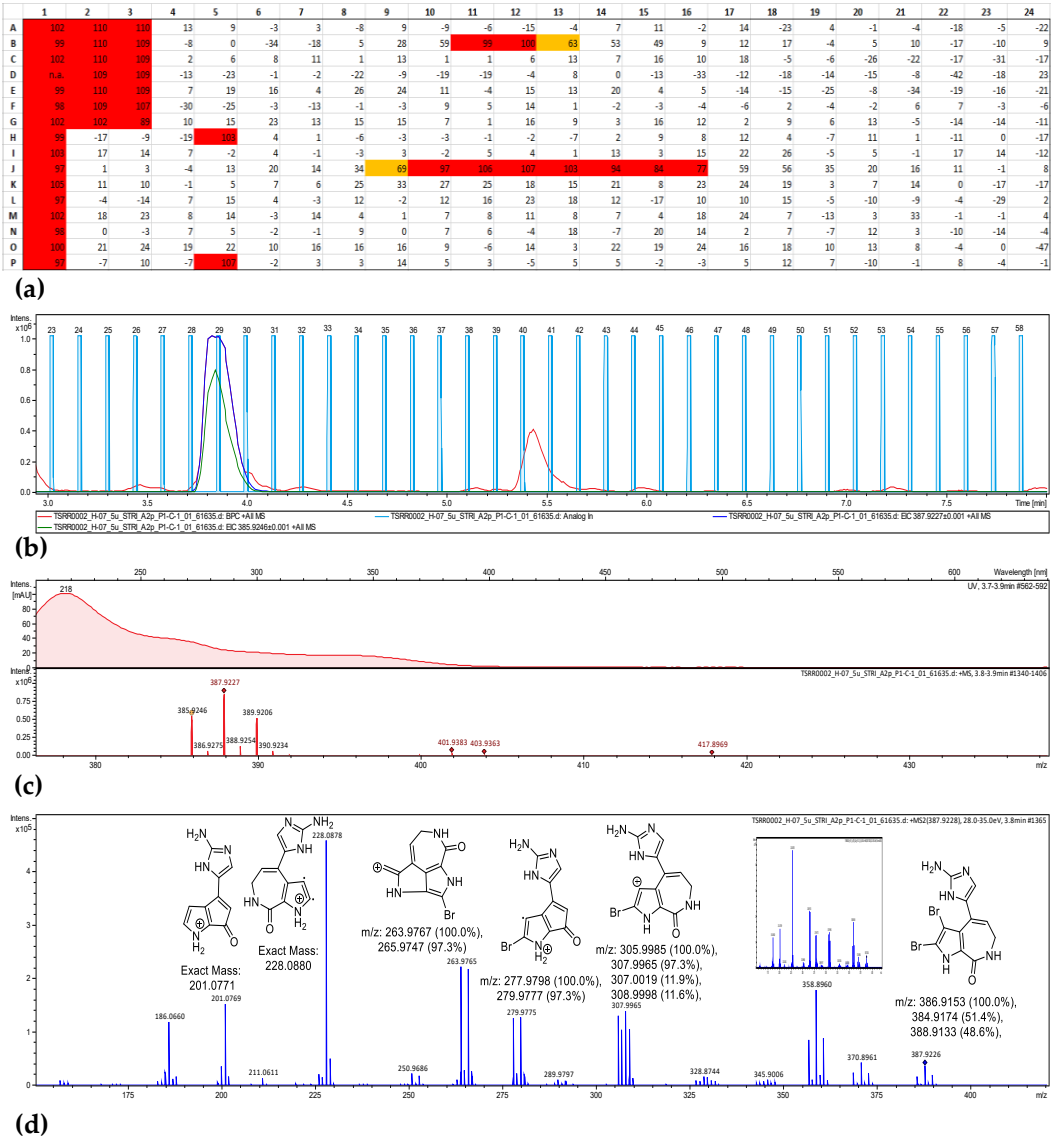

Figure 10.20. Microfractionation: Bioassay and dereplication results plate ULU_16 against *S. triciti* (a) Assay read-out of µ-fractionation plate ULU_16 against *S. triciti.* Numbers indicate the relative growth inhibition of the test strain. Fractions causing at least 70% rel. growth inhibition were considered “active”. Column 1: Medium control; Column 2 + 3 antibiotic standard; Column 4: growth control. Area AH05- AH24: 2µL injection volume; Area IP05- IP24 : 5 µL injection; H5 and P5 unfractionated extract control **(b)** Overlaid base peak chromatogram (red), fraction collector analog signal (light blue bars) and extracted ion chromatogram of *m/z* 385.9249 ± 0.001 $[M+H]^+$ (green) and 387.9227 ± 0.001 $[M+H]^+$ (dark blue) of the 1 mg/mL (in MeOH) with 5 µL injection volume; **(c)** UV chromatogram and MS spectrum of fractions 29-30; **(d)** MS/MS fragmentation of the precursor ion at *m/z* 387.9227 $[M+H]^+$ (dereplicated as stevensine/odiline), and proposed structures of the fragment ions.

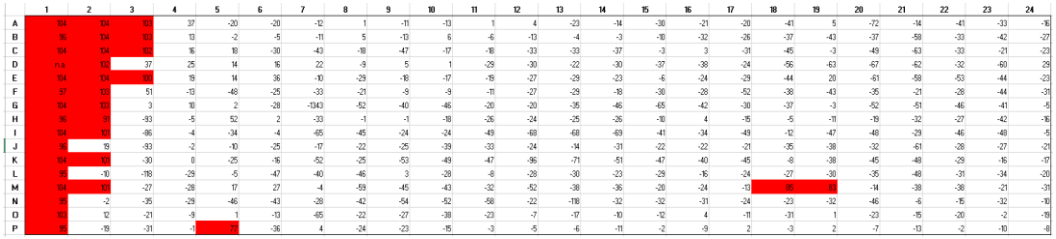

(a)

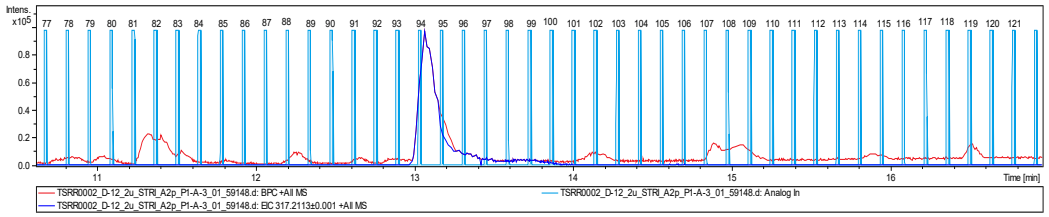

(b)

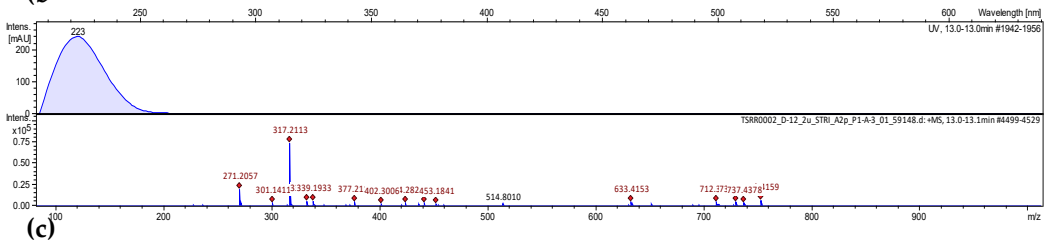

(c)

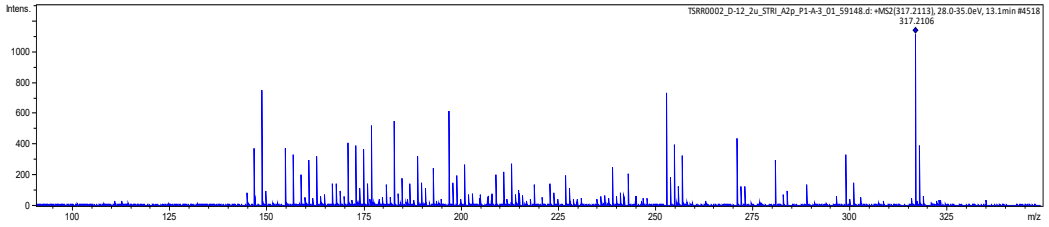

(d)

Figure 10.21. Microfractionation: Bioassay and dereplication results plate PANIKI_4 against *S. triciti* (a) Assay read-out of µ-fractionation plate PANIKI_4 against *S. triciti*. Numbers indicate the relative growth inhibition of the test strain. Fractions causing at least 70% rel. growth inhibition were considered “active”. Column 1: Medium control; Column 2 + 3 antibiotic standard; Column 4: growth control. Area AH05- AH24: 2µL injection volume; Area IP05- IP24 : 5 µL injection; **(b)** Overlaid base peak chromatogram (red), fraction collector analog signal (light blue bars) and extracted ion chromatogram of *m/z* 317.2112 ± 0.001 $[M+H]^+$ (dark blue) of the 1 mg/mL (in MeOH) with 5 µL injection volume; **(c)** UV chromatogram and MS spectrum of fractions 94-95; **(d)** MS/MS fragmentation of the precursor ion at *m/z* 317.2112 $[M+H]^+$ (tentatively assigned the structure of 20-hydroxyhaterumadienone).

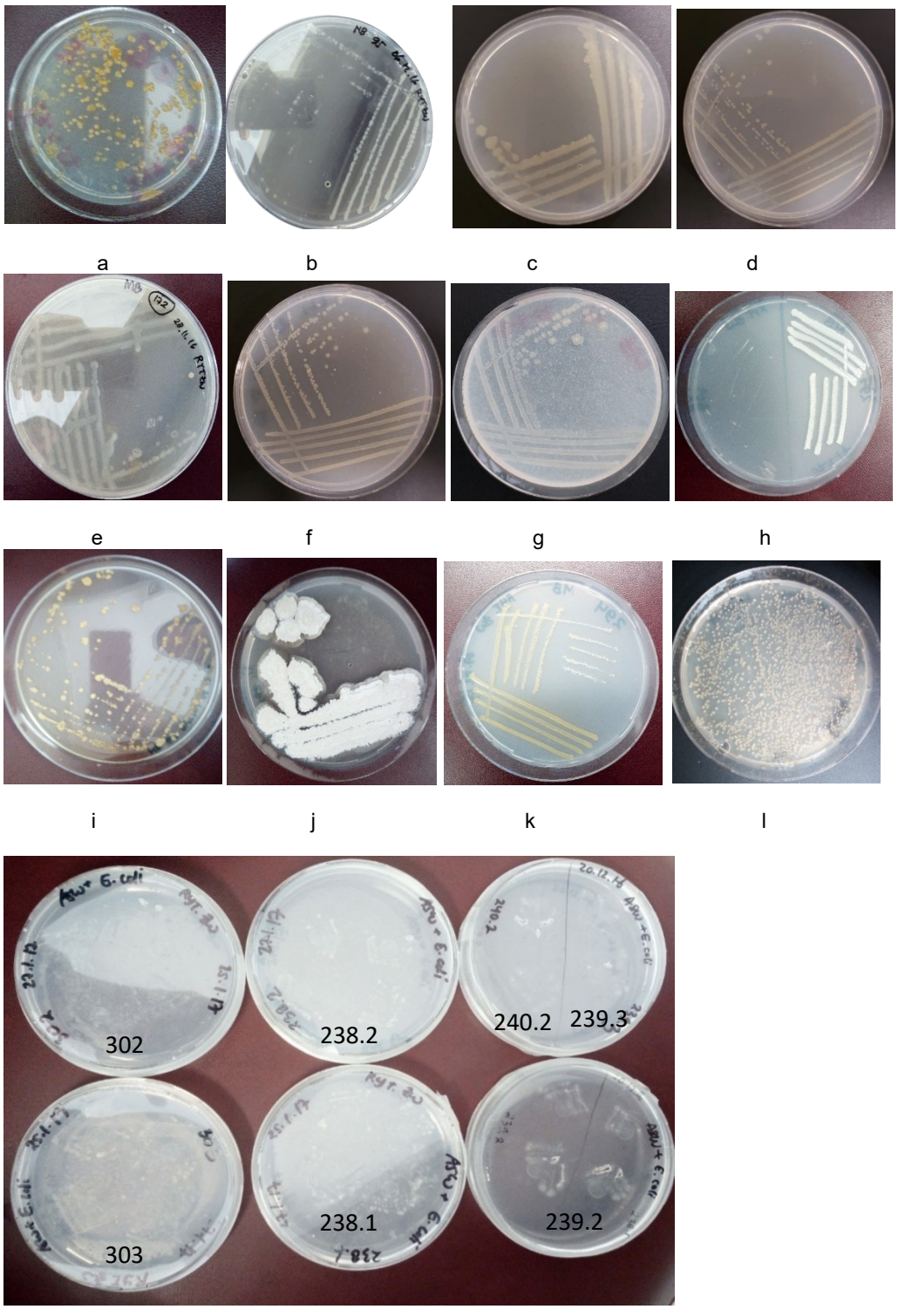

Figure 10.22. The axenic culture some active bacteria (a) *Bacillus cibi* 68 (b) *Bacillus amyloliquefaciens* 95 (c) *Bacillus pumilus* 161 (d) *B. pumilus* 165 (e) *Bacillus* sp. *172* (f) *Bacillus firmus* 277 (g) *Bacillus xiamenensis* 278 (h) *Bacillus thuringiensis* 295 (i) *Psychrobacter pacificensis* 118 (j) *Nocardiopsis synnemataformans* 290 (k) *Microbacterium arborescens* 294 (l) *Salinispora* sp. 301 (m) *Salinispora* strains collection-

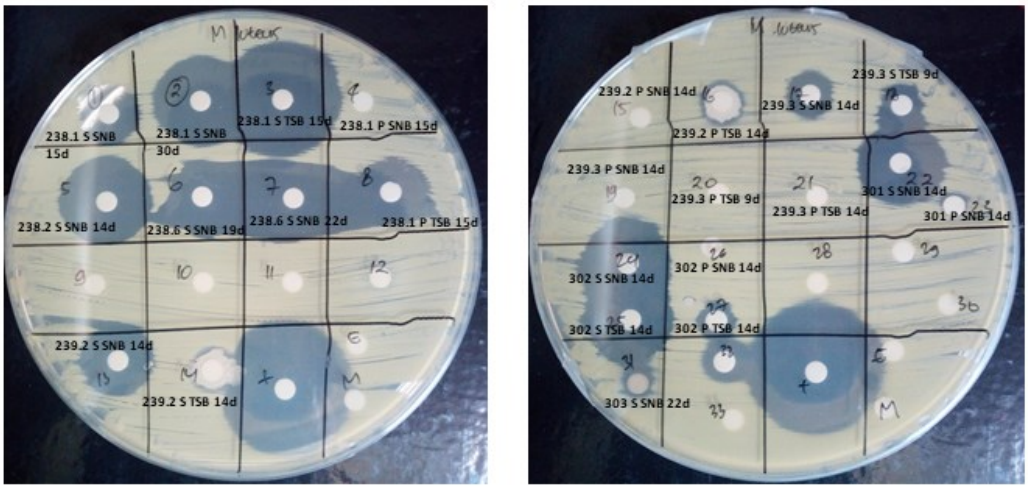

Figure 10.23. Activities *Salinispora* sp. against *M. lute*us

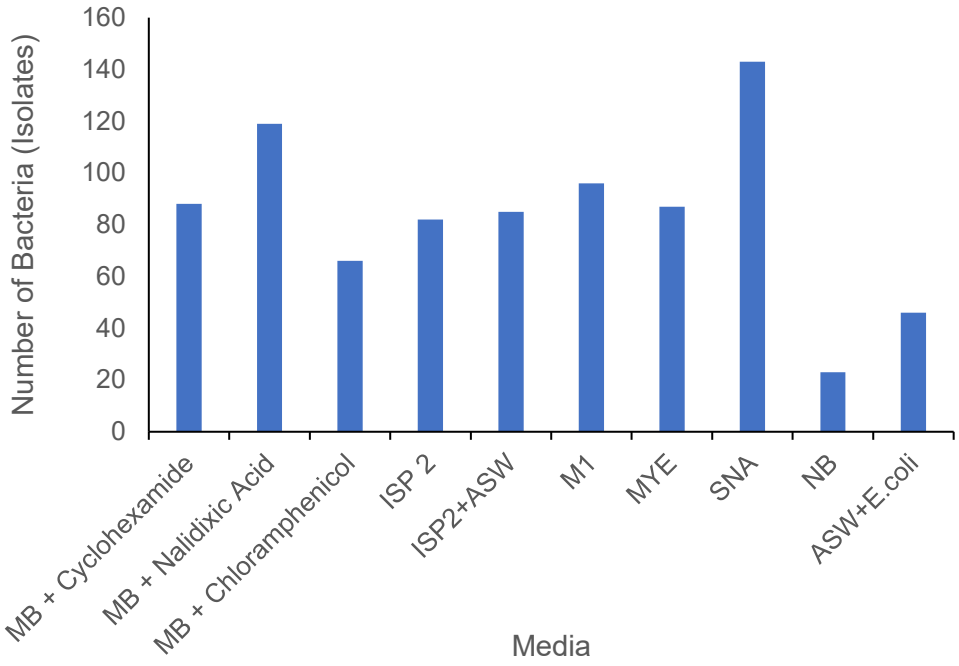

b

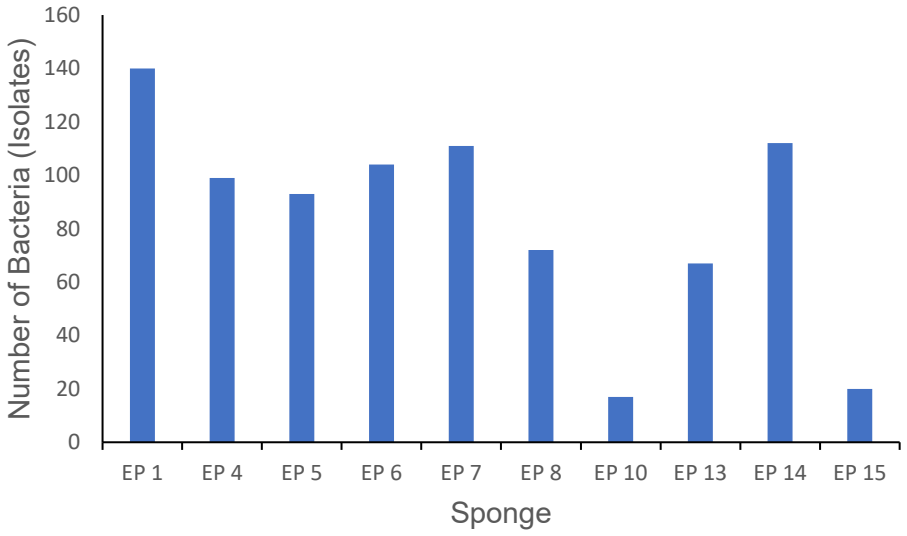

Figure 10.24. Number of strains isolated from 10 sponges collected from Sangihe Island, Indonesia based on media (a) and host sponges (b).

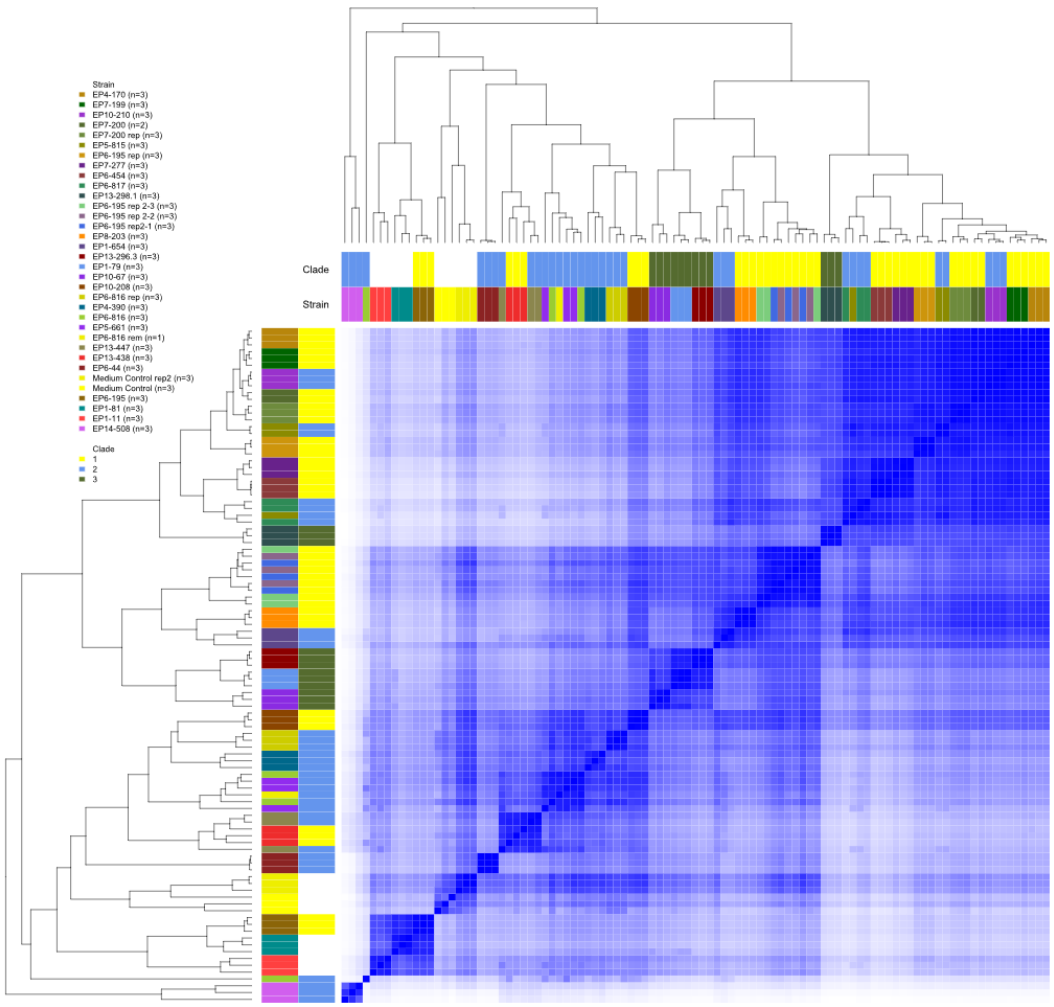

Figure 10.25. Cosine similarities of chemical fingerprints from 25 strains and medium control. All MS-runs performed are represented. Strain-IDs and clades (according to box-plot in figure 4) are color-coded in the sidebars. Clustering is based on cosine similarity profiles.

In Figure 10.25 the complete dataset is shown. One sample was remeasured (strain 186 rem) after storage and a couple of lipophilic peaks vanished, likely due to precipitation. It subsequently clustered in a different group. In first fermentation of EP7-200 one extract was lost, the refermentation was highly similar and is used for main analysis. EP6-816 was repeated to corroborate the clustering behaviour, the second round resulted in higher compound concentrations (and therefore clustered differently) but showed very similar pattern to first fermentation in visual MS-Data inspection. The second fermentation of EP6-816 is used for main analysis.

Strain EP6-195 was fermented in three batches. In the first fermentation it was highly similar to strain EP1-81. In the second round it clustered with the complete metabolic group 1, making contamination likely. For the third fermentation three cryo-stored starter cultures were used to ferment triplicates each, no other strain was handled in the vicinity during that time. All three triplicates are highly similar to each other, making the result trustworthy. The strain has a metabolomics profile similar to strains EP8-203 and EP1-654. However, these were not handled during third fermentation of EP6-195.

These results show that the strongest competitor approach needs careful handling to conserve diversity, and that a combination of genetic and metabolomic analysis helps in analysis of the results.

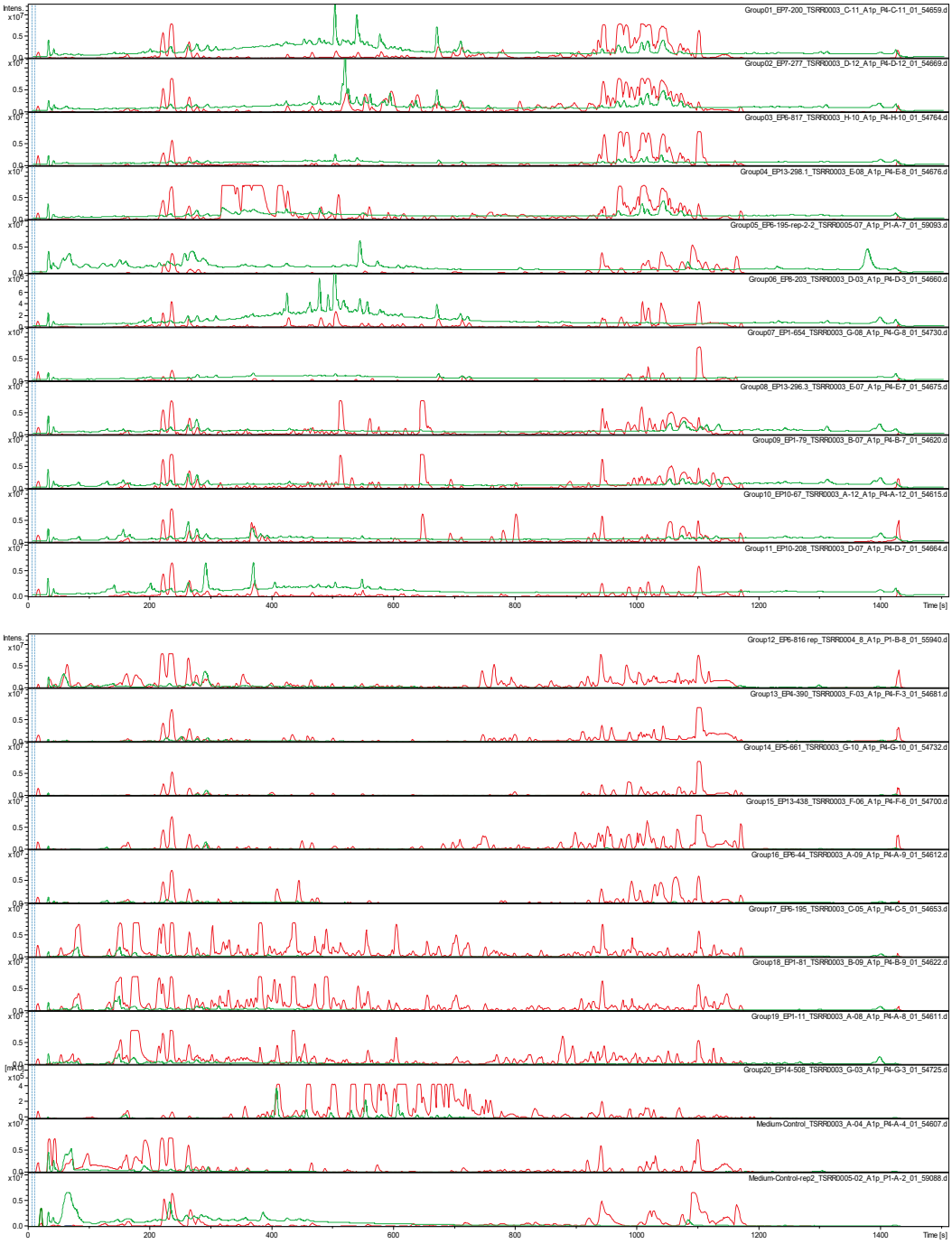

Figure 10.26. Metabolome verification of one sample each metabolic group from 25 selected bacterial strains and medium control. Group 17 is represented by the first fermentation of *Bacillus* sp. EP6-195, which is deemed to be a co-culture and excluded in Figure 6.5.

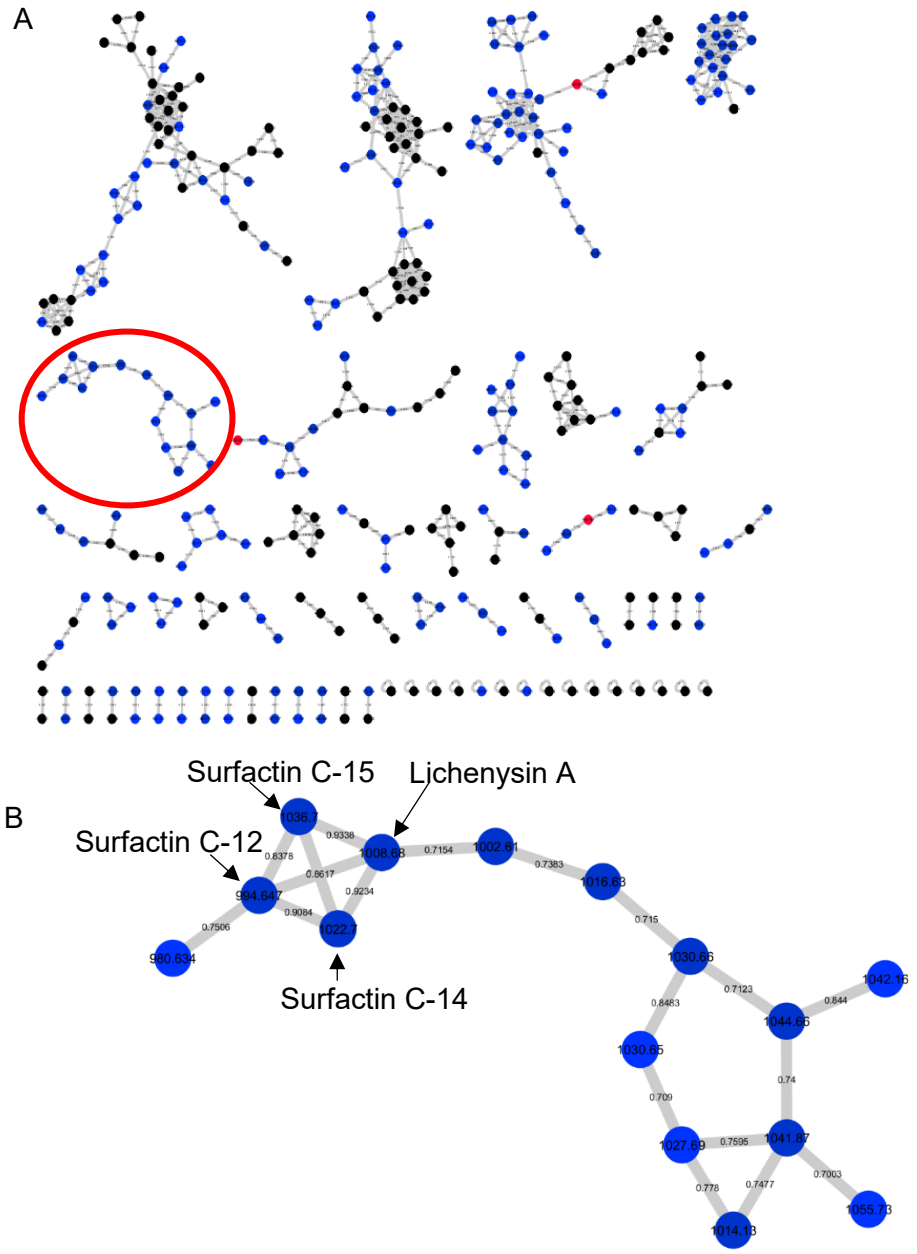

Figure 10.27. Molecular networking analysis of strain *Bacillus* sp. EP7-200

(A) Colours indicate media and conditions when the respective ion was detected: Media background (black), present in all media (blue) and solely in ISP2 medium (red), of which the extract showed activity against *E. coli*. (B) Enlarged cluster of surfactins and lichenysin A, which were dereplicated.

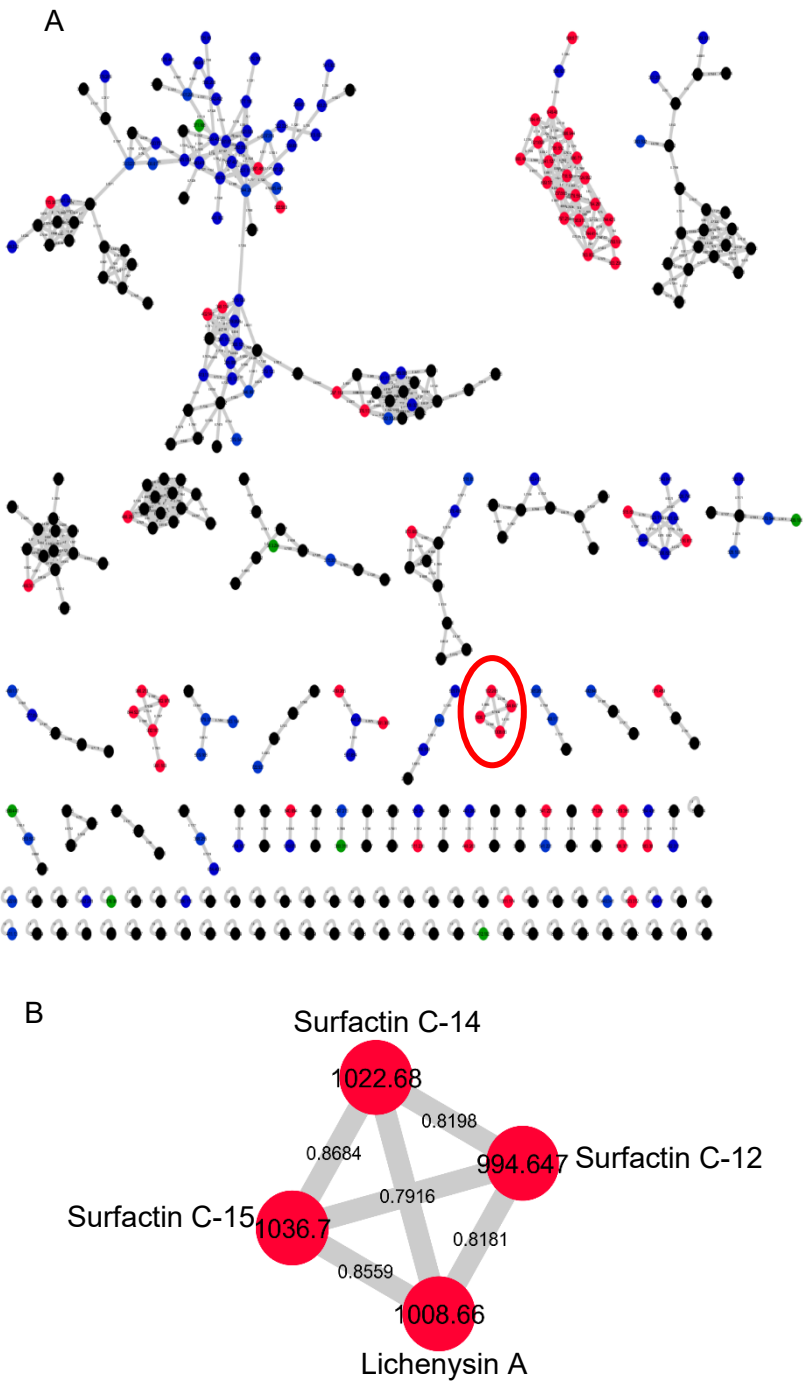

Figure 10.28. Molecular networking analysis of strain *Bacillus* sp. EP5-815. (A) Colours indicate the media and conditions when the respective ion was detected. Media (black), present in all media (blue), solely present in LB and NB media (green), of which the extract showed activity against *E. coli*, and MB medium (red). (B) Enlarged cluster of surfactins and lichenysin A, which were produced by *Bacillus* sp. EP5-815 in MB medium only.

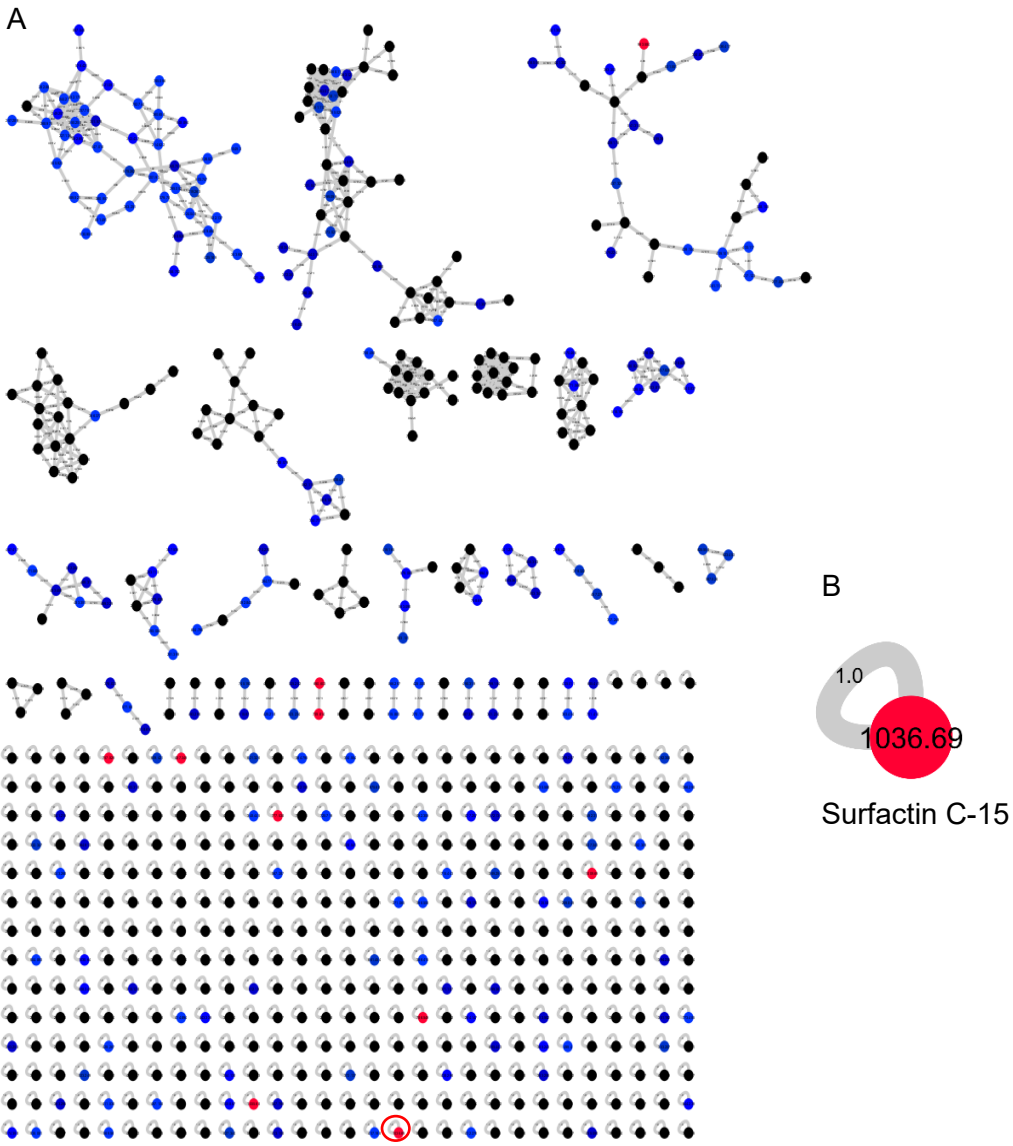

Figure 10.29. Molecular networking analysis of strain *Bacillus* sp. EP6-816. (A) Colours indicate the media and conditions when the respective ion was detected. Media (black), present in all media (blue), tryptone and yeast extract medium with ASW (red). (B) Enlarged cluster of C15 surfactin.

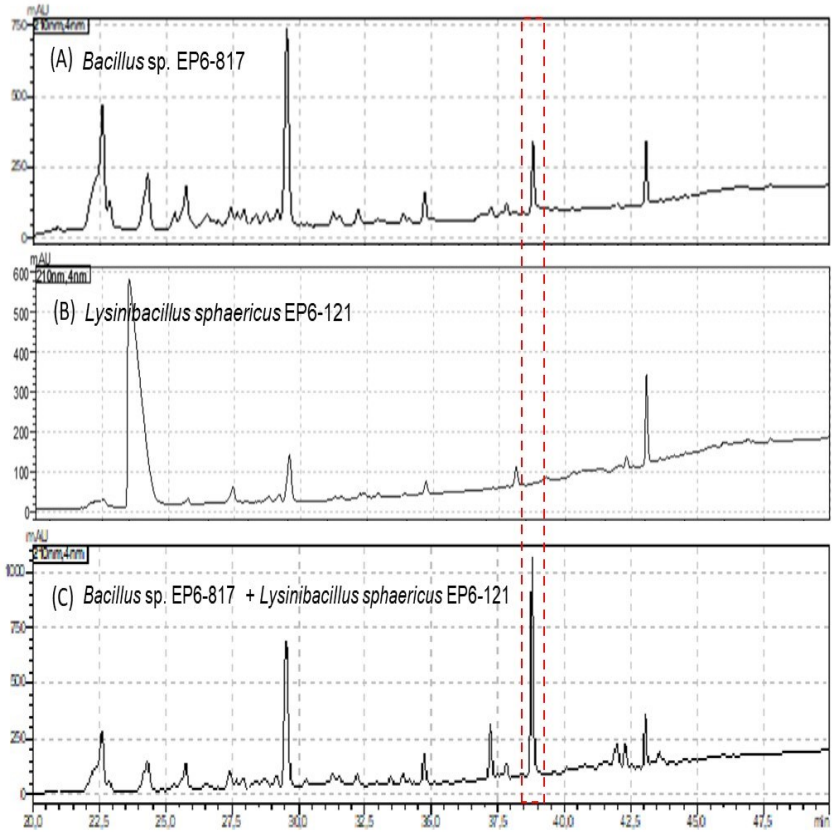

Figure 10.30. High performance liquid chromatography (HPLC) profiles of the EtOAc extract of different culture approaches pure culture of *Bacillus* sp. EP6-817 (A), pure culture of *L. sphaericus* EP6-121 (B) and co-culture *Bacillus* sp. EP6-817 and *L. sphaericus* EP6-121 (C). A clear increase in the production of one compound was observed during co culture (red line).

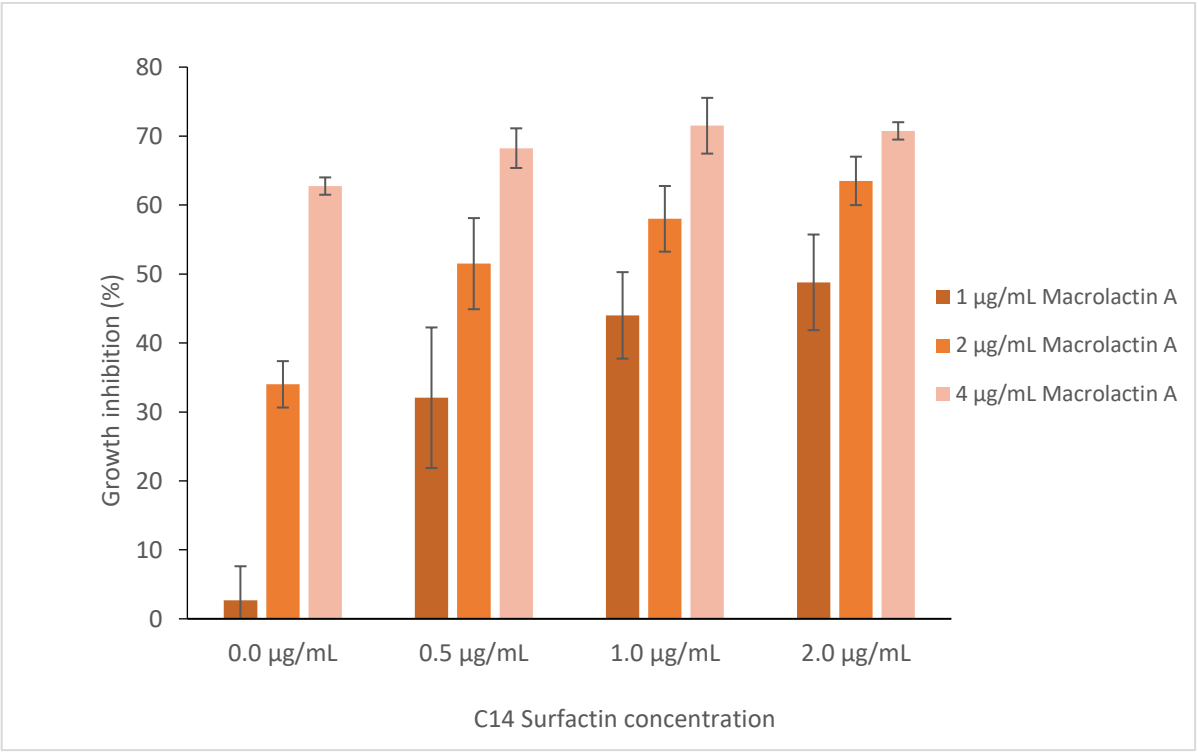

Figure 10.31. Combination effect between macrolactin A and C14 surfactin against *Staphylococcus aureus* (ATCC 33592, MRSA). Data shows average values from 4 measurements ± 1x standard deviations.

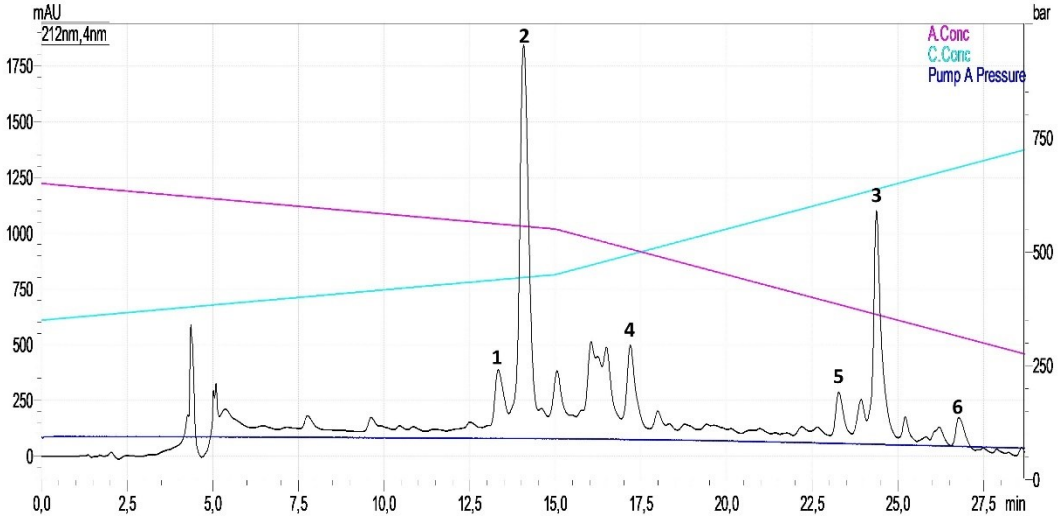

Figure 10.32. HPLC chromatogram of purification fraction 12 (compound **1** - **6**)

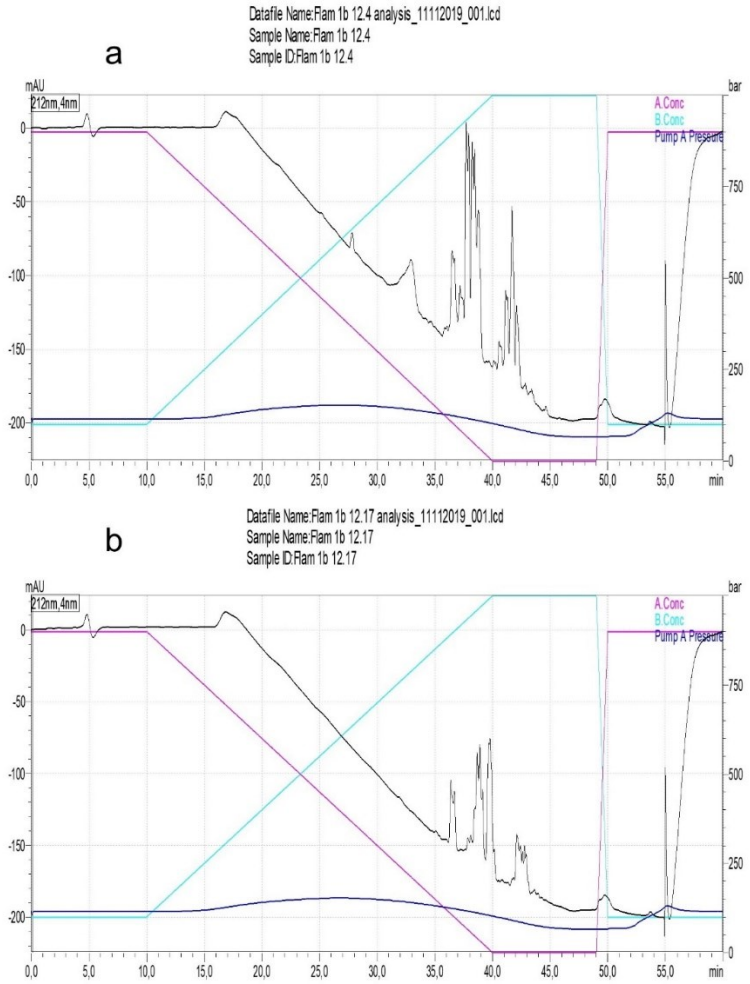

Figure 10.33. HPLC chromatogram of analysis compound **2** (a) and **3** (b).

Intensity of masses show only in Fraction 8.1

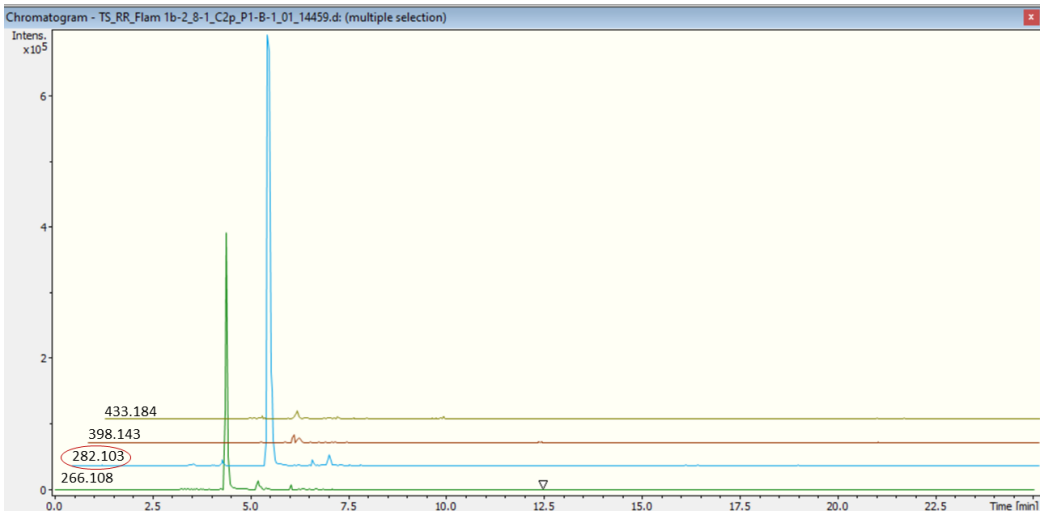

Intensity of masses show in Fraction 8.1 and others fraction

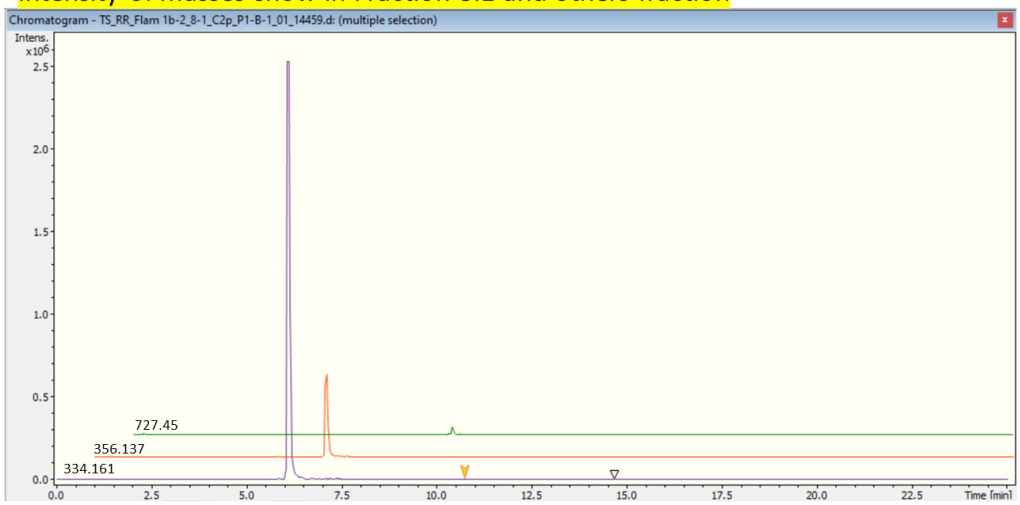

Figure 10.34. LC-HRMS of fraction 8.1 (5.3 mg)

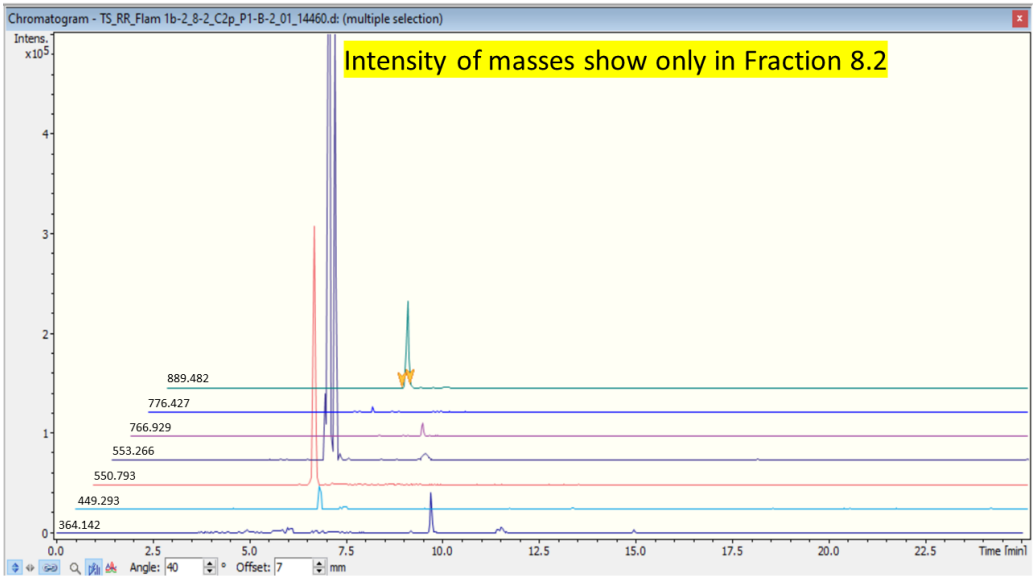

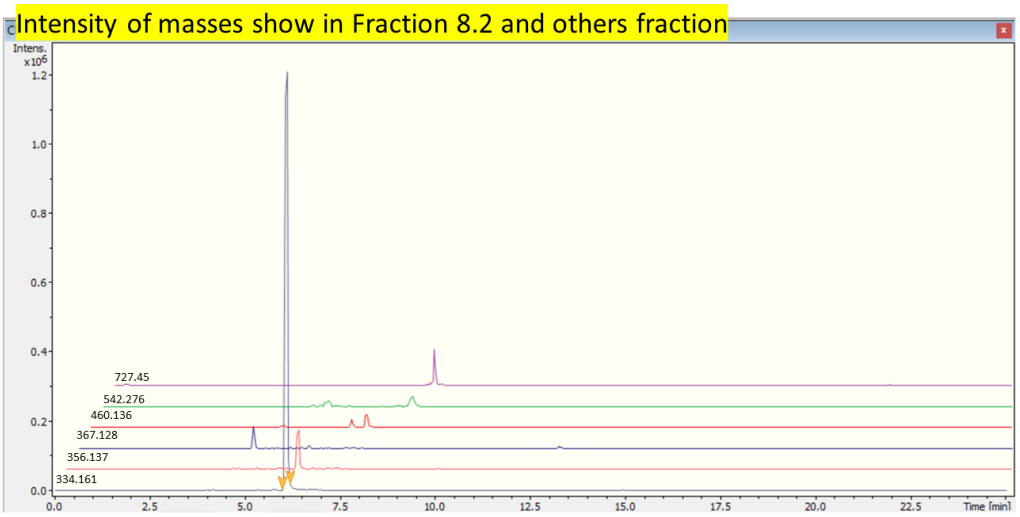

Figure 10.35. LC-HRMS fraction 8.2 (1.5 mg)

Intensity of masses show only in Fraction 8.3

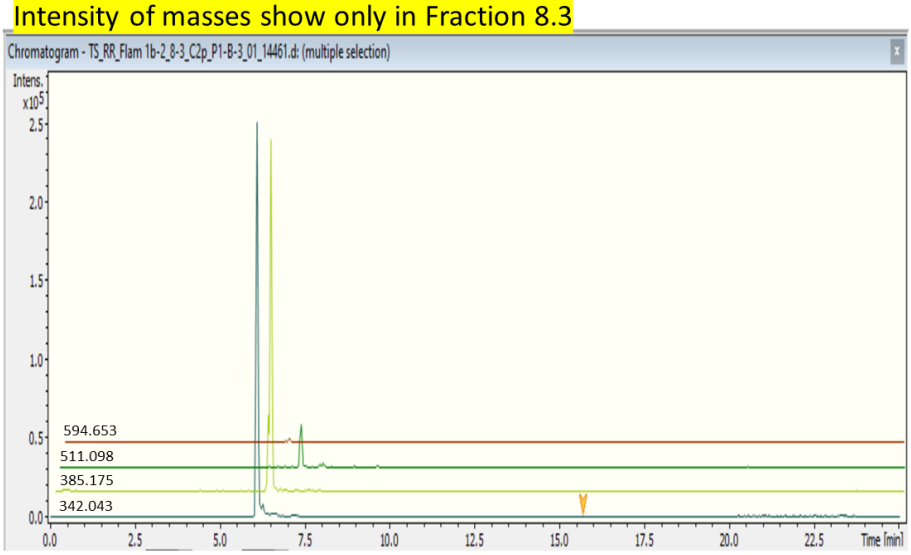

Intensity of masses show in Fraction 8.3 and others fraction

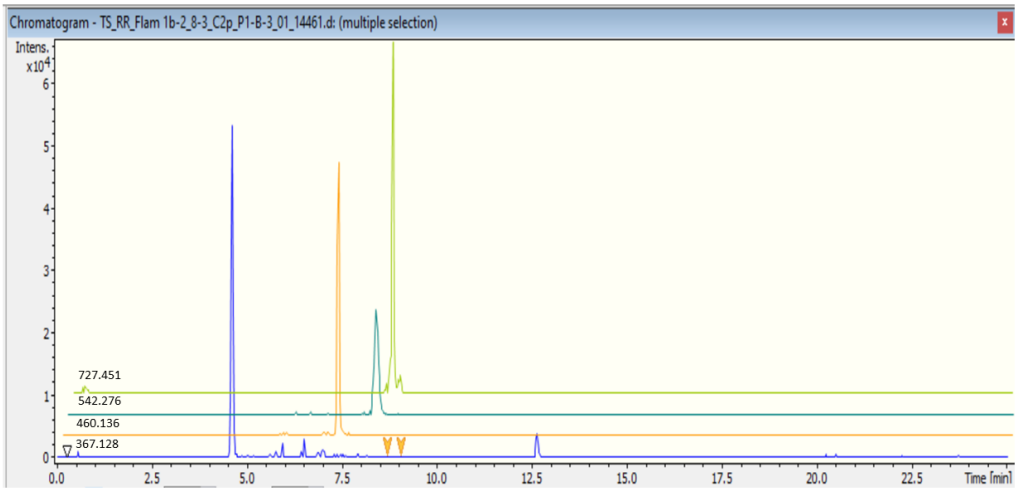

Figure 10.36. LC-HRMS fraction 8.3 (5.4 mg)

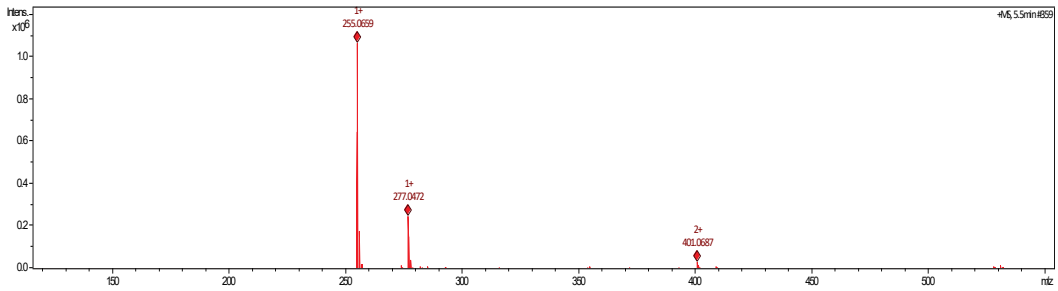

Figure 10.37. LCHRMS of compound **6.4** (daidzein)

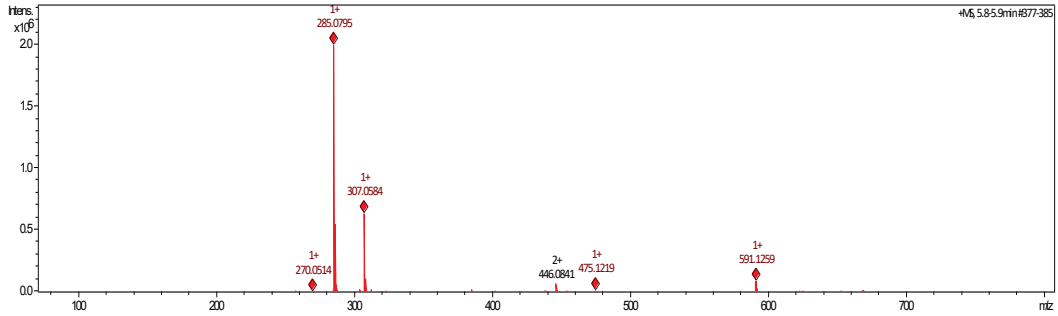

Figure 10.38. LCHRMS of compound **6.5** (glycitein)

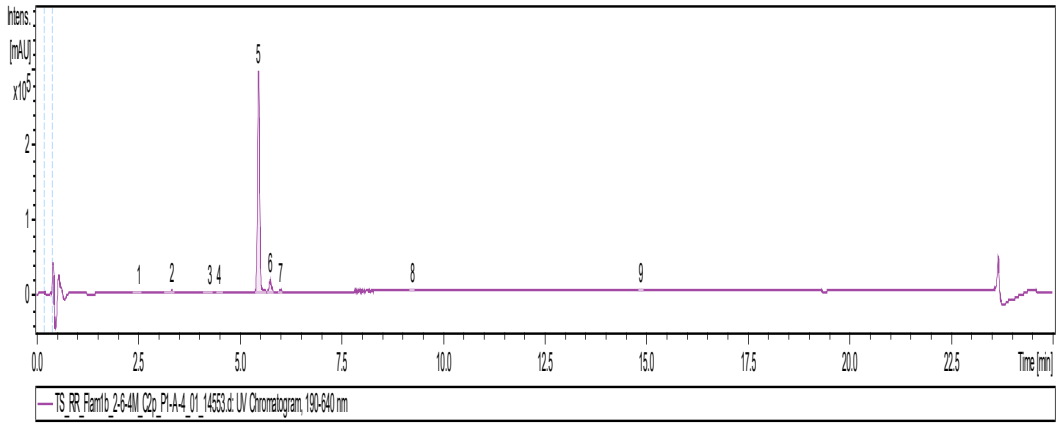

Figure 10.39. LCHRMS compound **6.4** which was detected 1 major peak (peak 5) as daidzein and 8 peaks as minor compounds.

Table 10.1. Five sponge samples collected from Bunake National Park, Manado, North Sulawesi, Indonesia campaign1

Sample Code	Image
Phva16Sa-49	
Phpu16Sa-88-S	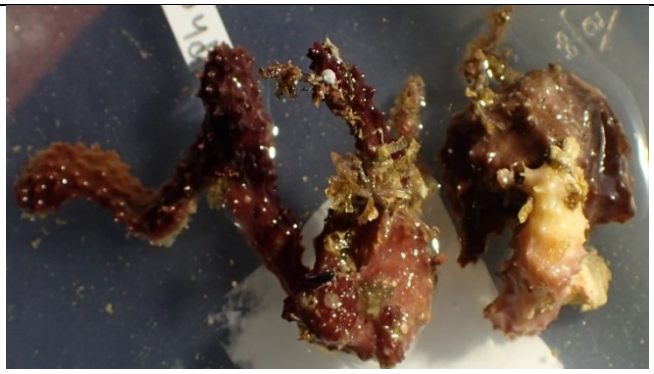
Phli16Sa-7-S	
Phpu16Sa-47S	

Phva16Sa-43,44-S	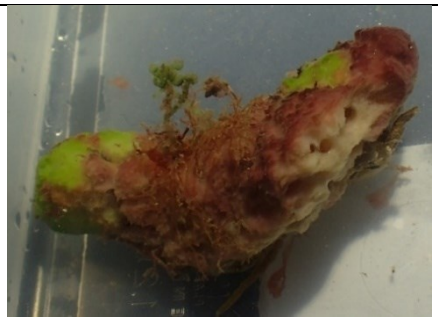 

Table 10.2. Morphological description of sponges and underwater documentation

Code	Morphological features	Image	Type of Spicule	Ref
EP1	Sponge orange coloured underwater (a) and also after exposure to air (b); soft, with a foliaceous (leaf like shaped) growth form and corrugated surface structure. Morphological appearance and spicule type (c) suggest assignment to *Stylissa flabelliformis*. Collected in shallow water (~1 m) of a coral reef from a rocky bottom.	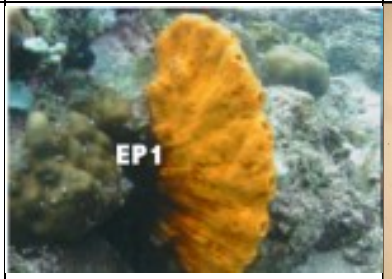 *a* 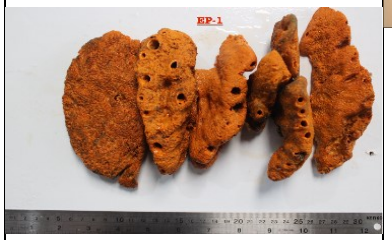 *b* *Stylissa flabelliformis*	 *c* Megascleres, type Style (with one end pointed and the other end round) (277.65 - 286.33 µm)	(Hooper and Van Soest, 2002) (Van Soest et al., 2002) (Stylissa flabelliformis – Sponges of Polynesia)

EP4	Sponge dark orange coloured underwater and encrusting (a), very small conulate or cone-shaped projections. Morphological appearance and spicule type (b) suggest assignment to *Petrosia* sp. Collected at ~4 m, spreading over rocky bottom.	 *a* *Petrosia* sp.	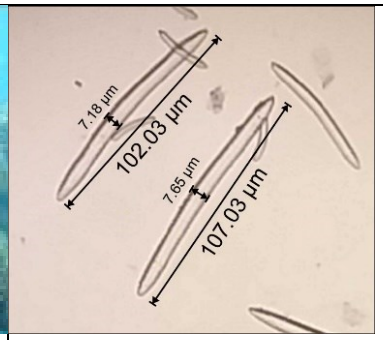 *b* Megascleres, type Oxea with both ends pointed (102.03 x 7.18 – 107.03 x 7.65); Microscleres of Oxea type are also present.	

EP5	Sponge large and barrel-shaped, with ribbed surface and a deep cavity in the centre; incompressible (hard) (a). Morphological appearance and spicule type (b) suggest assignment to *Xestospongia testudinaria.* Collected at ~7 m.	 *a* 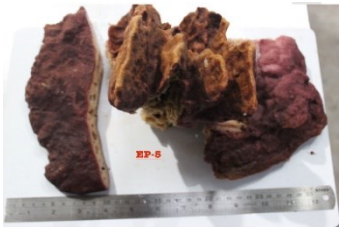 *b* *Xestospongia testudinaria*	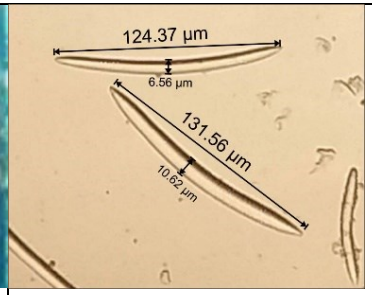 *b* Megascleres, type Oxea (124.37 x 6.56–131.56 x 10.62 µm)	(Subagio et al., 2017)

EP6	Sponge black coloured underwater, shape amorphous (a). Morphological appearance and spicule type (b) suggest assignment to *Neopetrosia sp*. Collected at ~5 m.	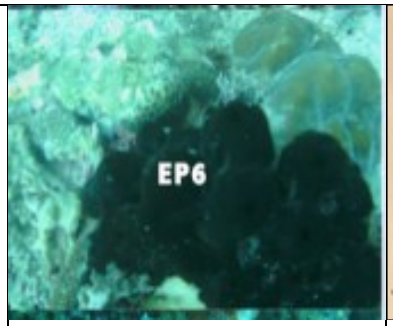 *a* *Neopetrosia* sp.	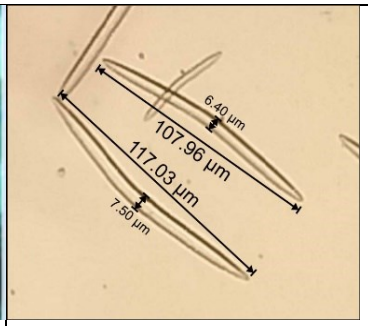 *b* Megascleres, type Oxea (107.96 x 6.40-117.03 – 117.03 x 7.50 µm); microscleres of Oxea type also present	

EP7	Large sponge of grey color underwater (a), dark grey (b) and light brown (c) when exposed to air; body shape spherical with a spiny fibrous exterior surface structure, but soft interior; very tough, like rubber, and very smelly. Morphological appearance and lack of any spicules suggest assignment to *Ircinia strobilina.* Collected at ~6 m on a rocky bottom.	 *a*  *b*  *c Ircinia strobilina*	Mineral spicules absent.	(Pawlik et al., 2002) (Wiedenmayer, 1977) (Keratosa and Soest, 1978)

EP8	Sponge black; shape encrusting, lobate and fragile; (a), producing slime, which is typically released as a black and purple exudate when damaged (b). Morphological appearance and spicule type (not figured) suggest assignment to *Neopetrosia* sp. Collected at ~4 m.	 *a*  *b* *Neopetrosia* sp.	Three types of Megascleres, type Strongyles (thin, with both ends blunt or round), type Style, and a very thin type (107.03 x 5.46-107.3 x 5.62 µm).	(Lukowiak et al., 2013) (Neopetrosia carbonaria) (Vicente et al., 2019)
EP10	Sponge reddish to black exteriorly and bright yellow inside; massive, with bluntly lobate form (a). Morphological appearance and spicule type (b) suggest assignment to *Aaptos*	 *a* *Aaptos suberitoides*	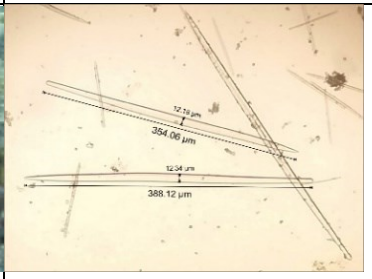 *b*	(Dewi et al., 2013) (Calcinai et al., 2017)

	suberitoides. Collected at ~5 m.		Megascleres, type Strongyloxea (379.83-416.66 µm)	
EP13	Sponge greenish brown, soft, with massive oscular chimneys (fistules); surface structure uneven and brittle (a). Collected at ~5 m on coral sandy bottom. Morphological appearance and spicule type suggest assignment to *Spechiosponiga vagabunda*. (*<u>Remark</u>: Morph. appearance would also fit to* A. ingens; *however, subtylostyle megascleres are not described for the latter.)*	 *a* *Spechiosponiga vagabund*	 b Megascleres, type Subtylostyle (265.16 -281.33 µm)	(Dewi et al., 2014) (Lévi)

EP14	Sponge light brown underwater, redish brown when exposed to air (a); egg-shaped with a large osculum in the middle. Morphological appearance and spicule type (b) suggest assignment to *Melophus sarasinorum*. Collected at a depth of ~5 meter.	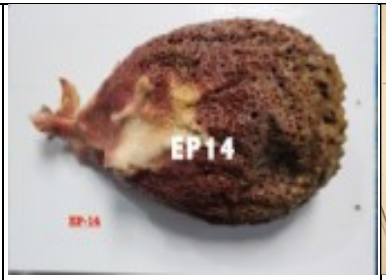 *a* *Melophlus/Asteropus sarasinorum*	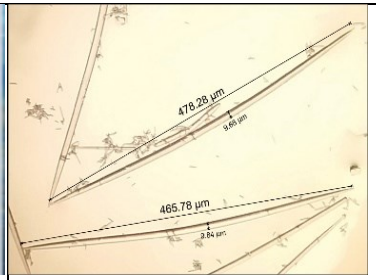 b Megascleres, type Oxea, very thin (498.22-515.16 µm)	(Rohde and Schupp, 2011)
EP15	Sponge reddish-brown to brick red, with the interior of similar, but lighter colour, especially when dry; massive and round in shape, with encrusting growth form; hardly compressible (a). Based on DNA barcoding analysis Balansa *et al*. (2020) identified this specimen as	 a *Agelas nakamurai*	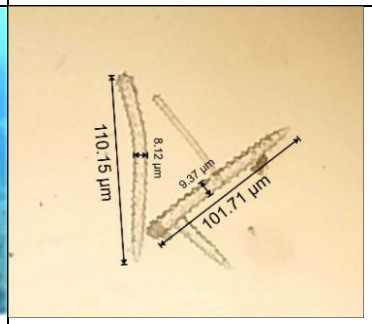 b Megascleres, type Acanthostyle (101.71 x 9.37-110.15 x 8.12 µm)	(Hoshino, 1985)

	Agelas sp. Morphological appearance and spicule type (b) suggest assignment to *Agelas nakamurai*.			

Table 10.3. Morphological description of sponges KOL_08, KOL_16, KOL_18 and ULU_13 and underwater documentation

Code	Morphological Features	Image	Type of Spicule
KOL_8	Massive orange sponge. Hard, compressible with seemingly corrugated surface and acanthostyle typed spicule. Collected at 4 m growing on rubble in Kolongan's coral reef Sangihe Island, Indonesia. Morphological and spicule characteristics suggest assignment to *Agelas nakamurai*. It is likely that this sponge was newly grown *A. nakamurai*.	 *Agelas nakamurai*	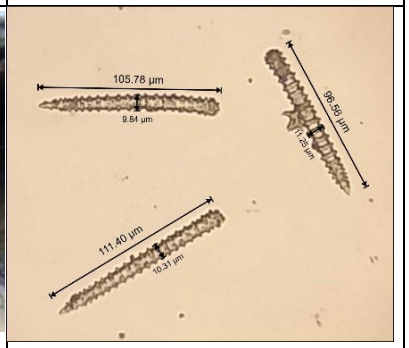 Type of spicule megascleres acanthostyle (96.56x11.25-111.40x10.31) µm.

KOL_16	Thick encrusting orange sponge. Soft, compressible with bumpy surface and acanthostyle typed spicule. Collected at ~5 m growing on corals from Kolongan's coral reef Sangihe Island, Indonesia. Morphological and spicule characteristics suggest assignment to *Agelas nakamurai*.	 *Agelas nakamurai*	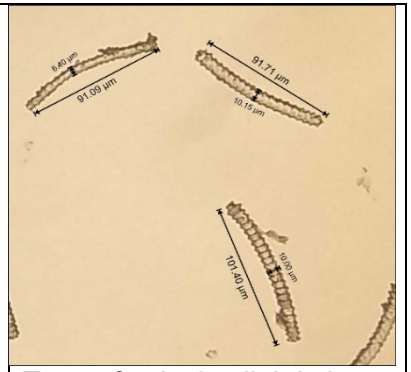 Type of spicule slightly bent megascleres acanthostyle (91.09x6.40-101.40) µm
KOL_18	Thick encrusting orange sponge. Compressible, cavernous with megascleres acanthostyle typed spicule. Collected at ~4 m growing on corals in Kolongan beach Sangihe Island. Morphological and spicule characteristics suggest assignment to *Agelas nakamurai*.	 *Agelas nakamurai*	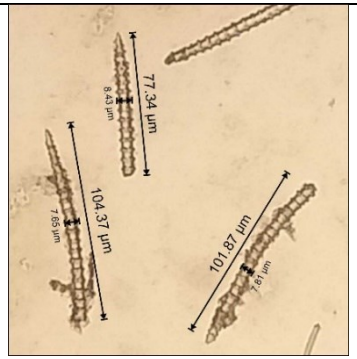 Type of spicule megascleres acanthostyle (77.34x8.34-104.37x7.65) µm.

ULU_13	Thick encrusting orange sponge. Soft, compressible (resilient) with bumpy surface, coanosome of 0.4-1.0 cm in diameter and acanthostyle typed spicule similar to KOL-8 and KOL-18 coded sponges. Collected at ~9 m from Ulu Sea port, Siau Island, Indonesia. Morphological and spicule characteristics as well as comparison with those for KOL-8, and KOL-18 suggest assignment to *Agelas nakamurai*.	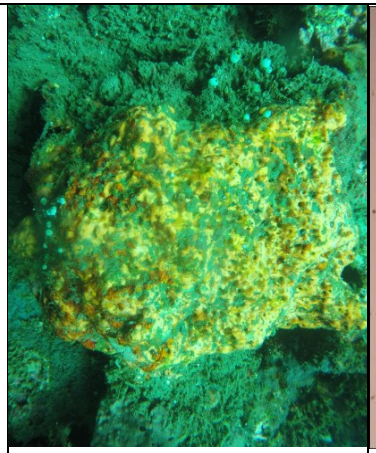 *Agelas nakamurai*	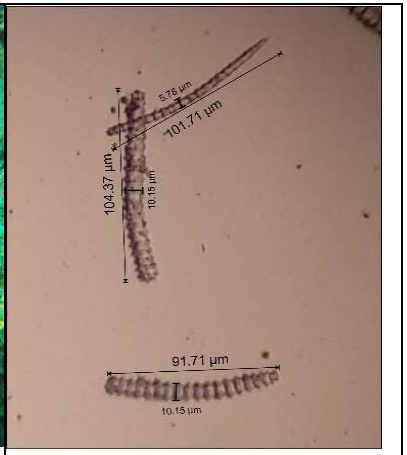 Type of spicule megascleres acanthostyle wide (91.71x10.15-104.37x10.15) µm and thin (101.71x5.78) µm

Table 10.4. The GenBank accession number for the sequence reported in this paper

Strain	Accession Number
Bacillus sp. EP1-11	MT314037
Bacillus thuringiensis EP6-44	MT314038
Bacillus tequilensis EP5-661	MT314039
Bacillus stratosphericus EP1-79	MT314040
Bacillus sp. EP7-277	MT314041
Bacillus sp. EP8-203	MT314042
Bacillus sp. EP10-208	MT314043
Bacillus sp. EP6-195	MT314044
Bacillus subtilis EP7-199	MT314045
Bacillus subtilis EP7-200	MT314046
Bacillus sp. EP13-438	MT314047
Bacillus sp. EP1-654	MT314048
Bacillus subtilis EP4-170	MT314049
Bacillus sp. EP13-296.3	MT314050
Bacillus sonorensis EP13-298.1	MT314051
Leclercia sp. EP4-390	MT314052
Brevibacterium sp. EP14-508	MT314053
Pseudomonas balearica EP13-447	MT314054
Bacillus sp. EP10-67	MT314055
Bacillus sp. EP6-454	MT314056
Bacillus sp. EP5-815	MT314057
Bacillus sp. EP6-816	MT314058
Bacillus sp. EP6-817	MT314059
Verrucosispora sp. EP6-325	MT314060
Lysinibacillus sphaericus EP6-121	MT314061

Table 10.5 Pairwise similarities of clustered samples and resulting metabolic grouping

Sample	Pairwise cosine	Metabolic group (0.7)	Sample ID
X:\2019-12-05_Schaeberle_A1p_10k_SN0\TSRR0002_F-04_A1p_P2-F-7_01_53159.d	0	1	T_5
X:\2019-12-05_Schaeberle_A1p_10k_SN0\TSRR0002_G-07_A1p_P2-B-2_01_53173.d	0.845572753	1	ULU_1
X:\2019-12-05_Schaeberle_A1p_10k_SN0\TSRR0002_E-03_A1p_P2-E-5_01_53144.d	0.817301893	1	PANIKI_5
X:\2019-12-05_Schaeberle_A1p_10k_SN0\TSRR0002_E-11_A1p_P2-F-4_01_53156.d	0.804278199	1	PANIKI_18
X:\2019-12-05_Schaeberle_A1p_10k_SN0\TSRR0002_H-06_A1p_P2-C-2_01_53182.d	0.846885255	1	ULU_15
X:\2019-12-05_Schaeberle_A1p_10k_SN0\TSRR0002_D-11_A1p_P2-E-3_01_53142.d	0.930428595	1	PANIKI_3
X:\2019-12-05_Schaeberle_A1p_10k_SN0\TSRR0002_G-03_A1p_P2-A-7_01_53169.d	0.833846083	1	PEHE_10
X:\2019-12-05_Schaeberle_A1p_10k_SN0\TSRR0002_D-03_A1p_P2-D-4_01_53133.d	0.803911482	1	KOL_13
X:\2019-12-05_Schaeberle_A1p_10k_SN0\TSRR0002_F-11_A1p_P2-A-5_01_53167.d	0.735445223	1	PEHE_8
X:\2019-12-05_Schaeberle_A1p_10k_SN0\TSRR0002_A-03_A1p_P2-A-1_01_53101.d	0.659071771	2	BL_1
X:\2019-12-05_Schaeberle_A1p_10k_SN0\TSRR0002_E-07_A1p_P2-E-9_01_53150.d	0.637927943	3	PANIKI_10
X:\2019-12-05_Schaeberle_A1p_10k_SN0\TSRR0002_E-04_A1p_P2-E-6_01_53145.d	0.690402335	4	PANIKI_6
X:\2019-12-05_Schaeberle_A1p_10k_SN0\TSRR0002_F-12_A1p_P2-A-6_01_53168.d	0.9172631	4	PEHE_9
X:\2019-12-05_Schaeberle_A1p_10k_SN0\TSRR0002_D-09_A1p_P2-E-1_01_53140.d	0.678517726	5	PANIKI_1
X:\2019-12-05_Schaeberle_A1p_10k_SN0\TSRR0002_F-03_A1p_P2-F-6_01_53158.d	0.895923176	5	PANIKI_20
X:\2019-12-05_Schaeberle_A1p_10k_SN0\TSRR0002_E-12_A1p_P2-F-5_01_53157.d	0.834843678	5	PANIKI_19
X:\2019-12-05_Schaeberle_A1p_10k_SN0\TSRR0002_G-05_A1p_P2-A-9_01_53171.d	0.677195099	6	PEHE_14
X:\2019-12-05_Schaeberle_A1p_10k_SN0\TSRR0002_E-05_A1p_P2-E-7_01_53148.d	0.622802274	7	PANIKI_8

X:\2019-12-05_Schaeberle_A1p_10k_SN0\TSRR0002_G-09_A1p_P2-B-4_01_53175.d	0.495296877	8	ULU_4
X:\2019-12-05_Schaeberle_A1p_10k_SN0\TSRR0002_G-12_A1p_P2-B-7_01_53178.d	0.441072394	9	ULU_9
X:\2019-12-05_Schaeberle_A1p_10k_SN0\TSRR0002_F-06_A1p_P2-F-9_01_53161.d	0.528518763	10	PEHE_2
X:\2019-12-05_Schaeberle_A1p_10k_SN0\TSRR0002_G-08_A1p_P2-B-3_01_53174.d	0.287752804	11	ULU_2
X:\2019-12-05_Schaeberle_A1p_10k_SN0\TSRR0002_C-03_A1p_P2-C-3_01_53122.d	0.16868076	12	KM_11
X:\2019-12-05_Schaeberle_A1p_10k_SN0\TSRR0002_G-04_A1p_P2-A-8_01_53170.d	0.147234059	13	PEHE_12
X:\2019-12-05_Schaeberle_A1p_10k_SN0\TSRR0002_G-06_A1p_P2-B-1_01_53172.d	0.266894781	14	PEHE_15
X:\2019-12-05_Schaeberle_A1p_10k_SN0\TSRR0002_H-08_A1p_P2-C-4_01_53184.d	0.047730056	15	ULU_17
X:\2019-12-05_Schaeberle_A1p_10k_SN0\TSRR0002_H-03_A1p_P2-B-8_01_53179.d	0.878330315	15	ULU_11
X:\2019-12-05_Schaeberle_A1p_10k_SN0\TSRR0002_F-08_A1p_P2-A-2_01_53164.d	0.020499965	16	PEHE_5
X:\2019-12-05_Schaeberle_A1p_10k_SN0\TSRR0002_B-09_A1p_P2-B-8_01_53117.d	0.487292669	17	KM_6
X:\2019-12-05_Schaeberle_A1p_10k_SN0\TSRR0002_C-12_A1p_P2-D-3_01_53132.d	0.039901317	18	KOL_11
X:\2019-12-05_Schaeberle_A1p_10k_SN0\TSRR0002_B-10_A1p_P2-B-9_01_53118.d	0.641326389	19	KM_8
X:\2019-12-05_Schaeberle_A1p_10k_SN0\TSRR0002_F-07_A1p_P2-A-1_01_53163.d	0.01406283	20	PEHE_4
X:\2019-12-05_Schaeberle_A1p_10k_SN0\TSRR0002_D-10_A1p_P2-E-2_01_53141.d	0.962507941	20	PANIKI_2
X:\2019-12-05_Schaeberle_A1p_10k_SN0\TSRR0002_C-08_A1p_P2-C-8_01_53127.d	0.747722085	20	KOL_5
X:\2019-12-05_Schaeberle_A1p_10k_SN0\TSRR0002_G-10_A1p_P2-B-5_01_53176.d	0.241174937	21	ULU_6
X:\2019-12-05_Schaeberle_A1p_10k_SN0\TSRR0002_G-11_A1p_P2-B-6_01_53177.d	0.973911588	21	ULU_7
X:\2019-12-05_Schaeberle_A1p_10k_SN0\TSRR0002_F-09_A1p_P2-A-3_01_53165.d	0.877792718	21	PEHE_6
X:\2019-12-05_Schaeberle_A1p_10k_SN0\TSRR0002_C-04_A1p_P2-C-4_01_53123.d	0.600764918	22	KM_13
X:\2019-12-05_Schaeberle_A1p_10k_SN0\TSRR0002_D-05_A1p_P2-D-6_01_53135.d	0.427158951	23	KOL_15

X:\2019-12-05_Schaeberle_A1p_10k_SN0\TSRR0002_A-09_A1p_P2-A-7_01_53107.d	0.722789893	23	BL_9
X:\2019-12-05_Schaeberle_A1p_10k_SN0\TSRR0002_B-05_A1p_P2-B-4_01_53113.d	0.719881971	23	KM_2
X:\2019-12-05_Schaeberle_A1p_10k_SN0\TSRR0002_H-07_A1p_P2-C-3_01_53183.d	0.30835053	24	ULU_16
X:\2019-12-05_Schaeberle_A1p_10k_SN0\TSRR0002_B-04_A1p_P2-B-3_01_53112.d	0.282645433	25	BL_15
X:\2019-12-05_Schaeberle_A1p_10k_SN0\TSRR0002_C-11_A1p_P2-D-2_01_53131.d	0.733995291	25	KOL_9
X:\2019-12-05_Schaeberle_A1p_10k_SN0\TSRR0002_A-10_A1p_P2-A-8_01_53108.d	0.535876053	26	BL_10
X:\2019-12-05_Schaeberle_A1p_10k_SN0\TSRR0002_E-10_A1p_P2-F-3_01_53155.d	0.023532767	27	PANIKI_14
X:\2019-12-05_Schaeberle_A1p_10k_SN0\TSRR0002_C-09_A1p_P2-C-9_01_53128.d	0.076270264	28	KOL_6
X:\2019-12-05_Schaeberle_A1p_10k_SN0\TSRR0002_A-12_A1p_P2-B-1_01_53110.d	0.721063739	28	BL_13
X:\2019-12-05_Schaeberle_A1p_10k_SN0\TSRR0002_C-07_A1p_P2-C-7_01_53126.d	0.620897476	29	KOL_3
X:\2019-12-05_Schaeberle_A1p_10k_SN0\TSRR0002_H-05_A1p_P2-C-1_01_53181.d	0.524667283	30	ULU_14
X:\2019-12-05_Schaeberle_A1p_10k_SN0\TSRR0002_E-08_A1p_P2-F-1_01_53153.d	0.348892857	31	PANIKI_11
X:\2019-12-05_Schaeberle_A1p_10k_SN0\TSRR0002_B-12_A1p_P2-C-2_01_53121.d	0.945814485	31	KM_10
X:\2019-12-05_Schaeberle_A1p_10k_SN0\TSRR0002_B-06_A1p_P2-B-5_01_53114.d	0.927905842	31	KM_3
X:\2019-12-05_Schaeberle_A1p_10k_SN0\TSRR0002_B-11_A1p_P2-C-1_01_53120.d	0.074030661	32	KM_9
X:\2019-12-05_Schaeberle_A1p_10k_SN0\TSRR0002_C-05_A1p_P2-C-5_01_53124.d	0.966532397	32	KM_15
X:\2019-12-05_Schaeberle_A1p_10k_SN0\TSRR0002_F-10_A1p_P2-A-4_01_53166.d	0.036839827	33	PEHE_7
X:\2019-12-05_Schaeberle_A1p_10k_SN0\TSRR0002_D-04_A1p_P2-D-5_01_53134.d	0.760303799	33	KOL_14
X:\2019-12-05_Schaeberle_A1p_10k_SN0\TSRR0002_E-06_A1p_P2-E-8_01_53149.d	0.027309927	34	PANIKI_9
X:\2019-12-05_Schaeberle_A1p_10k_SN0\TSRR0002_A-08_A1p_P2-A-6_01_53106.d	0.775760877	34	BL_8
X:\2019-12-05_Schaeberle_A1p_10k_SN0\TSRR0002_C-06_A1p_P2-C-6_01_53125.d	0.571533934	35	KOL_2

X:\2019-12-05_Schaeberle_A1p_10k_SN0\TSRR0002_A-11_A1p_P2-A-9_01_53109.d	0.02062157	36	BL_11
X:\2019-12-05_Schaeberle_A1p_10k_SN0\TSRR0002_D-12_A1p_P2-E-4_01_53143.d	0.005422886	37	PANIKI_4
X:\2019-12-05_Schaeberle_A1p_10k_SN0\TSRR0002_B-07_A1p_P2-B-6_01_53115.d	0.620588253	38	KM_4
X:\2019-12-05_Schaeberle_A1p_10k_SN0\TSRR0002_H-04_A1p_P2-B-9_01_53180.d	0.00171338	39	ULU_13
X:\2019-12-05_Schaeberle_A1p_10k_SN0\TSRR0002_D-07_A1p_P2-D-8_01_53137.d	0.832556165	39	KOL_18
X:\2019-12-05_Schaeberle_A1p_10k_SN0\TSRR0002_D-06_A1p_P2-D-7_01_53136.d	0.757141862	39	KOL_16
X:\2019-12-05_Schaeberle_A1p_10k_SN0\TSRR0002_C-10_A1p_P2-D-1_01_53129.d	0.728148087	39	KOL_8
X:\2019-12-05_Schaeberle_A1p_10k_SN0\TSRR0002_A-04_A1p_P2-A-2_01_53102.d	0	40	BL_2
X:\2019-12-05_Schaeberle_A1p_10k_SN0\TSRR0002_E-09_A1p_P2-F-2_01_53154.d	0	41	PANIKI_13
X:\2019-12-05_Schaeberle_A1p_10k_SN0\TSRR0002_A-05_A1p_P2-A-3_01_53103.d	0.920690168	41	BL_3
X:\2019-12-05_Schaeberle_A1p_10k_SN0\TSRR0002_A-06_A1p_P2-A-4_01_53104.d	0.034280319	42	BL_6
X:\2019-12-05_Schaeberle_A1p_10k_SN0\TSRR0002_B-03_A1p_P2-B-2_01_53111.d	0	43	BL_14
X:\2019-12-05_Schaeberle_A1p_10k_SN0\TSRR0002_F-05_A1p_P2-F-8_01_53160.d	0.609542211	44	PEHE_1
X:\2019-12-05_Schaeberle_A1p_10k_SN0\TSRR0002_A-07_A1p_P2-A-5_01_53105.d	0.712116419	44	BL_7
X:\2019-12-05_Schaeberle_A1p_10k_SN0\TSRR0002_D-08_A1p_P2-D-9_01_53138.d	0.01357126	45	KOL_21
X:\2019-12-05_Schaeberle_A1p_10k_SN0\TSRR0002_B-08_A1p_P2-B-7_01_53116.d	0.833021679	45	KM_5

Table 10.6. Antibacterial activity bacteria associated with sponge campaign 1

No	Bacteria	Activity	
		E. coli	***M. luteus***
1	*Bacillus cibi* 68	-	+
2	*Bacillus amyloliquefaciens* 95	+	++
3	*Psychrobacter pacificensis* 118	-	+
4	*Bacillus pumilus* 161	-	+
5	*Bacillus pumilus* 165	+	+
6	*Bacillus thuringiensis* 172	+	++
7	*Salinispora arenicola* 238.1	-	++
8	*Salinispora arenicola* 238.2	+	+++
9	*Salinispora arenicola* 238.6	-	++
10	*Salinispora arenicola* 239.2	+	++
11	*Salinispora arenicola* 239.3	+	++
12	*Salinispora arenicola* 240.2	+	+++
13	*Bacillus firmus* 277	-	++
14	*Bacillus xiamenensis* 278	-	++
15	*Nocardiopsis synnemataformans* 290	-	+++
16	*Microbacterium arborescens* 294	+	+++
17	*Bacillus* sp. *295*	++	+
18	*Salinispora arenicola* 301	-	+
19	*Salinispora arenicola* 302	-	+
20	*Salinispora arenicola* 303	-	++++
21	*Bacillus nanhaiisediminis* 306	++	++++
22	*Bacillus vallismortis* 308	++	+
23	*Microbacterium arborescens* 296	+	+++
24	*Microbacterium arborescens* 297	+	+++

Table 10.7. Primary screening of antibacterial activity of 108 isolates against Gram-negative (*Eschericia coli*) and Gram-positive bacteria (*Micrococcus luteus*)

No	Bacteria	Activity	
		E. coli	***M. luteus***
1	*Bacillus* sp. EP1-11	-	+++
2	*Bacillus cereus* EP4-29	-	+++
3	*Pseudomonas balearica* EP4-31	-	+++
4	*Bacillus* sp. EP6-35	-	+
5	*Pseudomonas* sp. EP6-36	-	++
6	*Bacillus thuringiensis* EP6-44	-	+
7	*Bacillus aerius* EP10-66	-	++
8	*Bacillus* sp. EP10-67	++	-
9	*Bacillus* sp. EP13-69	-	++
10	*Bacillus stratosphericus* EP1-79	-	++
11	*Lysinibacillus* sp. EP1-81	-	++
12	*Lysinibacillus sphaericus* EP1-82	-	++
13	*Bacillus altitudinis* EP5-102	-	+
14	*Serratia* sp. EP5-103.1	-	+
15	*Bacillus subtilis* EP5-103.2	-	+
16	*Lysinibacillus sphaericus* EP5-105	-	+++
17	*Bacillus indicus* EP4-109	-	+
18	*Bacillus* sp. EP4-112	-	++
19	*Pseudomonas* sp. EP4-113	-	+++
20	*Staphylococcus* sp. EP6-114	-	+
21	*Bacillus safensis* EP6-119	-	+
22	*Bacillus altitudinis* EP6-120	-	+
23	*Lysinibacillus sphaericus* EP6-121	-	+
24	*Bacillus stratosphericus* EP6-122	-	+
25	*Bacillus aerius* EP6-123	-	+
26	*Bacillus aerius* EP6-124	-	+
27	*Staphylococcus* sp. EP6-125	-	+
28	*Bacillus cereus* EP7-128	-	++
29	*Bacillus cereus* EP7-133	-	+++
30	*Bacillus aerophilus* EP10-141	-	+
31	*Pseudomonas* sp. EP10-142	-	+
32	*Bacillus altitudinis* EP13-159	-	++
33	*Bacillus* sp. EP1-163	-	+++
34	*Bacillus* sp. EP1-164	-	+++
35	*Bacillus subtilis* EP4-170	-	+
36	*Bacillus* sp. EP5-180	-	++
37	*Bacillus* sp. EP5-181	-	++
38	*Bacillus* sp. EP6-195	+	+++

39	*Bacillus subtilis* EP7-199	+++	+++
40	*Bacillus subtilis* EP7-200	+++	+++
41	*Bacillus subtilis* EP7-202	-	++
42	*Bacillus* sp. EP8-203	-	+++
43	*Bacillus* sp. EP10-208	+++	+++
44	*Lysinibacillus fusiformis* EP10-209	-	+
45	*Bacillus subtilis* EP10-210	-	+
46	*Enterobacter* sp. EP4-251	-	+
47	*Enterobacter* sp. EP4-255	-	+
48	*Bacillus zhangzhouensis* EP5-268	-	+
49	*Staphylococcus kloosii* EP5-270	-	+
50	*Bacillus amyloliquefaciens* EP7-273	-	+
51	*Bacillus* sp. EP7-274	-	+
52	*Bacillus* sp. EP7-277	-	+
53	*Bacillus velezensis* EP7-278	-	++
54	*Staphylococcus* sp. EP10-289	-	+
55	*Staphylococcus* sp. EP14-293	-	+
56	*Cronobacter sakazakii* EP13-296.3	-	+
57	*Bacillus sonorensis* EP13-298.1	-	++
58	*Bacillus* sp. EP4-304	-	+++
59	*Bacillus* sp. EP4-309	-	+
60	*Enterobacter* sp. EP4-311	-	+
61	*Bacillus* sp. EP5-314	-	+
62	*Serratia* sp. EP5-317	-	++
63	*Staphylococcus* sp. EP6-323	+	-
64	*Bacillus* sp. EP6-324	+	-
65	*Verrucosispora* sp. EP6-325	+	-
66	*Bacillus cereus* EP7-334	-	+++
67	*Bacillus* sp. EP13-345	-	+++
68	*Bacillus stratosphericus* EP13-347	-	+++
69	*Citrobacter sedlakii* EP4-372	-	+
70	*Bacillus* sp. EP1-379	+	+
71	*Serratia* sp. EP1-388	+	+
72	*Leclercia* sp. EP4-390	-	++
73	*Bacillus* sp. EP4-391	+	+++
74	*Bacillus altitudinis* EP6-405	-	+
75	*Bacillus tequilensis* EP6-407	-	+
76	*Citrobacter sedlakii* EP6-409	-	+
77	*Bacillus altitudinis* EP6-410	-	+
78	*Bacillus velezensis* EP7-417	++	++
79	*Bacillus aerius* EP7-419	++	-
80	*Bacillus amyloliquefaciens* EP7-424	+	++
81	*Bacillus* sp. EP7-428	-	+

82	*Bacillus* sp. EP13-438	-	+++
83	*Pseudomonas balearica* EP13-447	-	++
84	*Citrobacter sedlakii* EP13-449	-	+
85	*Bacillus* sp. EP6-454	+	++
86	*Brevibacterium* sp. EP14-508	-	+
87	*Bacillus subtilis* EP1-652	-	++
88	*Bacillus* sp. EP1-653	-	++
89	*Bacillus* sp. EP1-654	-	+++
90	*Bacillus velezensis* EP1-655	+	+++
91	*Bacillus velezensis* EP1-656	+	+++
92	*Bacillus velezensis* EP1-655.1	+	+++
93	*Bacillus velezensis* EP1-657	+	+++
94	*Bacillus* sp. EP1-658	-	++
95	*Bacillus tequilensis* EP5-661	-	++
96	*Bacillus velezensis* EP7-663	-	+++
97	*Bacillus* sp. EP7-664	-	++
98	*Pseudomonas balearica* EP8-741	-	+
99	*Pseudomonas* sp. EP8-742	-	+
100	*Bacillus* sp. EP5-815	-	++
101	*Bacillus* sp. EP6-816	-	+++
102	*Bacillus* sp. EP6-817	-	+++
103	*Solwaraspora* sp. EP8-524	++	+++
104	*Solwaraspora* sp. EP8-525	++	++
105	*Solwaraspora* sp. EP8-532	++	++
106	*Solwaraspora* sp. EP8-533	++	++
107	*Solwaraspora* sp. EP8-540	-	++
108	*Cellulosimicrobium* sp. EP1-15	-	++

- : no activity + : weak activity

++ : moderate activity +++ : strong activity

Table 10.8. Competition assay between 25 high competitor strains originating from different sponges (diameter inhibition zone in mm red colour)

Sponge	Sponge	EP 1				EP 4		EP 5		EP 6					EP 7			EP 8	EP 10			EP 13				EP 14
	Strain[a]	11	79	81	654	170	390	661	815	44	195	454	816	817	199	200	277	203	67	208	210	296	298	438	447	508
EP 1	11	x			10,0					11,0		10,0														
	79		X	10,0	9,0							13,0														
	81			x					10,0	11,0			11,0						11,0	12,0						12,0
	654	13,3	13,3	20,0	x	13,0		12,0		12,0	20,0	9,0		10,0			9,0		20,0		9,0	14,3	10,0	12,0		22,0
EP 4	170				17,0	x			10,7	14,0	11,0								16,0			10,0				17,0
	390						X																			
EP 5	661							x																		
	815	9,3	10,7	9,0	18,0	9,0			x	9,0	15,0								11,3			12,7		15,3	15,3	19,0
EP 6	44									x						9,0					9,0	9,0				
	195								12,0		x		8,0	8,0	9,0		10,0			12,0						10,0
	454										x	14,0										9,0				17,0
	816	9,0	9,0	9,0	17,0	9,0		9,0			17,0		x						17,0			11,0		16,7	14,7	19,0
	817	9,0		10,0		9,0					17,0			x					15,0			11,0		10,0	14,0	18,3
EP 7	199	9,0	9,0	9,0	17,3	9,0		10,0			12,0				x				13,0			11,0				17,0
	200	10,0	10,0	10,0	20,0	10,0		10,0		9,0	14,0			9,0		x			18,0			13,0				19,0
	277									12,0							x									12,3
EP 8	203	11,7	12,3	12,0	17,0	12,0		12,0			13,0			9,0				x	18,3			12,0		9,0		20,0
EP 10	67																		x							
	208	10,0		9,0		9,0														x						19,3
	210	9,0				9,0															x					21,0
EP 13	296,3																					x				11,0
	298,1	9,0	9,3	9,0		9,0																	x			13,0
	438									14,0				11,0	15,0	13,0	14,0	12,0					15,3	x		
	447																						20,3		x	
EP 14	508																									x

[a]In the horizontal line the inoculated strains are given and in the vertical line the ones that were added as agar plug

Table 10.9. Grouping output of the complete dataset, 25 selected bacterial strains and the medium control

Name	Samples Code	File	Similarity	Group 0.9	Group 0.8	Group 0.7
Bacillus subtilis EP4-170	EP4-170	TSRR0003_C-03_A1p_P4-C-3_01_54627.d	0	1	1	1
Bacillus subtilis EP4-170	EP4-170	TSRR0003_B-11_A1p_P4-B-11_01_54624.d	0.989176	1	1	1
Bacillus subtilis EP4-170	EP4-170	TSRR0003_B-12_A1p_P4-B-12_01_54625.d	0.986345	1	1	1
Bacillus subtilis EP7-199	EP7-199	TSRR0003_C-07_A1p_P4-C-7_01_54655.d	0.974909	1	1	1
Bacillus subtilis EP7-199	EP7-199	TSRR0003_C-09_A1p_P4-C-9_01_54657.d	0.989418	1	1	1
Bacillus subtilis EP7-199	EP7-199	TSRR0003_C-08_A1p_P4-C-8_01_54656.d	0.985179	1	1	1
Bacillus subtilis EP10-210	EP10-210	TSRR0003_D-09_A1p_P4-D-9_01_54666.d	0.9628	1	1	1
Bacillus subtilis EP10-210	EP10-210	TSRR0003_D-11_A1p_P4-D-11_01_54668.d	0.995425	1	1	1
Bacillus subtilis EP10-210	EP10-210	TSRR0003_D-10_A1p_P4-D-10_01_54667.d	0.9902	1	1	1
Bacillus subtilis EP7-200	EP7-200	TSRR0003_C-11_A1p_P4-C-11_01_54659.d	0.973238	1	1	1
Bacillus subtilis EP7-200	EP7-200	TSRR0003_C-10_A1p_P4-C-10_01_54658.d	0.984451	1	1	1
Bacillus subtilis EP7-200	EP7-200 rep	TSRR0004_5_A1p_P1-B-5_01_55937.d	0.931136	1	1	1
Bacillus subtilis EP7-200	EP7-200 rep	TSRR0004_6_A1p_P1-B-6_01_55938.d	0.986411	1	1	1
Bacillus subtilis EP7-200	EP7-200 rep	TSRR0004_4_A1p_P1-B-4_01_55936.d	0.975506	1	1	1
Bacillus sp. EP5-815	EP5-815	TSRR0003_H-04_A1p_P4-H-4_01_54755.d	0.909907	1	1	1
Bacillus sp. EP5-815	EP5-815	TSRR0003_H-03_A1p_P4-H-3_01_54736.d	0.992662	1	1	1
Bacillus sp. EP6-195	EP6-195 rep	TSRR0004_3_A1p_P1-B-3_01_55935.d	0.898818	2	1	1
Bacillus sp. EP6-195	EP6-195 rep	TSRR0004_2_A1p_P1-B-2_01_55934.d	0.996361	2	1	1
Bacillus sp. EP6-195	EP6-195 rep	TSRR0004_1_A1p_P1-B-1_01_55933.d	0.974596	2	1	1
Bacillus sp. EP7-277	EP7-277	TSRR0003_E-04_A1p_P4-E-4_01_54672.d	0.791775	3	2	1
Bacillus sp. EP7-277	EP7-277	TSRR0003_E-03_A1p_P4-E-3_01_54671.d	0.990296	3	2	1
Bacillus sp. EP7-277	EP7-277	TSRR0003_D-12_A1p_P4-D-12_01_54669.d	0.966299	3	2	1

Bacillus sp. EP6-454	EP6-454	TSRR0003_F-12_A1p_P4-F-12_01_54724.d	0.95822	3	2	1
Bacillus sp. EP6-454	EP6-454	TSRR0003_F-10_A1p_P4-F-10_01_54722.d	0.997127	3	2	1
Bacillus sp. EP6-454	EP6-454	TSRR0003_F-11_A1p_P4-F-11_01_54723.d	0.996348	3	2	1
Bacillus sp. EP6-817	EP6-817	TSRR0003_H-09_A1p_P4-H-9_01_54763.d	0.848704	4	2	1
Bacillus sp. EP6-817	EP6-817	TSRR0003_H-10_A1p_P4-H-10_01_54764.d	0.970872	4	2	1
Bacillus sp. EP5-815	EP5-815	TSRR0003_G-12_A1p_P4-G-12_01_54734.d	0.935064	4	2	1
Bacillus sp. EP6-817	EP6-817	TSRR0003_H-08_A1p_P4-H-8_01_54762.d	0.941439	4	2	1
Bacillus sonorensis EP13-298.1	EP13-298.1	TSRR0003_E-10_A1p_P4-E-10_01_54678.d	0.699325	5	3	2
Bacillus sonorensis EP13-298.1	EP13-298.1	TSRR0003_E-08_A1p_P4-E-8_01_54676.d	0.980143	5	3	2
Bacillus sonorensis EP13-298.1	EP13-298.1	TSRR0003_E-09_A1p_P4-E-9_01_54677.d	0.968988	5	3	2
Bacillus sp. EP6-195	EP6-195 rep 2-3	TSRR0005-12_A1p_P1-B-3_01_59098.d	0.574131	6	4	3
Bacillus sp. EP6-195	EP6-195 rep 2-2	TSRR0005-08_A1p_P1-A-8_01_59094.d	0.963742	6	4	3
Bacillus sp. EP6-195	EP6-195 rep2-1	TSRR0005-06_A1p_P1-A-6_01_59092.d	0.945458	6	4	3
Bacillus sp. EP6-195	EP6-195 rep 2-2	TSRR0005-07_A1p_P1-A-7_01_59093.d	0.963381	6	4	3
Bacillus sp. EP6-195	EP6-195 rep2-1	TSRR0005-04_A1p_P1-A-4_01_59090.d	0.960878	6	4	3
Bacillus sp. EP6-195	EP6-195 rep 2-2	TSRR0005-09_A1p_P1-A-9_01_59095.d	0.934307	6	4	3
Bacillus sp. EP6-195	EP6-195 rep2-1	TSRR0005-05_A1p_P1-A-5_01_59091.d	0.987616	6	4	3
Bacillus sp. EP6-195	EP6-195 rep 2-3	TSRR0005-10_A1p_P1-B-1_01_59096.d	0.949749	6	4	3
Bacillus sp. EP6-195	EP6-195 rep 2-3	TSRR0005-11_A1p_P1-B-2_01_59097.d	0.976218	6	4	3
Bacillus sp. EP8-203	EP8-203	TSRR0003_D-04_A1p_P4-D-4_01_54661.d	0.84143	7	4	3
Bacillus sp. EP8-203	EP8-203	TSRR0003_D-03_A1p_P4-D-3_01_54660.d	0.989255	7	4	3
Bacillus sp. EP8-203	EP8-203	TSRR0003_D-05_A1p_P4-D-5_01_54662.d	0.972721	7	4	3
Bacillus sp. EP1-654	EP1-654	TSRR0003_G-07_A1p_P4-G-7_01_54729.d	0.853457	8	4	3
Bacillus sp. EP1-654	EP1-654	TSRR0003_G-08_A1p_P4-G-8_01_54730.d	0.942051	8	4	3
Bacillus sp. EP1-654	EP1-654	TSRR0003_G-06_A1p_P4-G-6_01_54728.d	0.848986	9	4	3
Bacillus sp. EP13-296.3	EP13-296.3	TSRR0003_E-05_A1p_P4-E-5_01_54673.d	0.616547	10	5	4

Bacillus sp. EP13-296.3	EP13-296.3	TSRR0003_E-07_A1p_P4-E-7_01_54675.d	0.990675	10	5	4
Bacillus sp. EP13-296.3	EP13-296.3	TSRR0003_E-06_A1p_P4-E-6_01_54674.d	0.982615	10	5	4
Bacillus stratosphericus EP1-79	EP1-79	TSRR0003_B-05_A1p_P4-B-5_01_54618.d	0.875983	11	5	4
Bacillus stratosphericus EP1-79	EP1-79	TSRR0003_B-07_A1p_P4-B-7_01_54620.d	0.988461	11	5	4
Bacillus stratosphericus EP1-79	EP1-79	TSRR0003_B-06_A1p_P4-B-6_01_54619.d	0.969844	11	5	4
Bacillus sp. EP10-67	EP10-67	TSRR0003_B-04_A1p_P4-B-4_01_54617.d	0.802926	12	5	4
Bacillus sp. EP10-67	EP10-67	TSRR0003_A-12_A1p_P4-A-12_01_54615.d	0.963492	12	5	4
Bacillus sp. EP10-67	EP10-67	TSRR0003_B-03_A1p_P4-B-3_01_54616.d	0.93112	12	5	4
Bacillus sp. EP10-208	EP10-208	TSRR0003_D-06_A1p_P4-D-6_01_54663.d	0.627381	13	6	5
Bacillus sp. EP10-208	EP10-208	TSRR0003_D-07_A1p_P4-D-7_01_54664.d	0.985177	13	6	5
Bacillus sp. EP10-208	EP10-208	TSRR0003_D-08_A1p_P4-D-8_01_54665.d	0.984266	13	6	5
Bacillus sp. EP6-816	EP6-816 rep	TSRR0004_9_A1p_P1-B-9_01_55941.d	0.730369	14	7	5
Bacillus sp. EP6-816	EP6-816 rep	TSRR0004_8_A1p_P1-B-8_01_55940.d	0.965884	14	7	5
Bacillus sp. EP6-816	EP6-816 rep	TSRR0004_7_A1p_P1-B-7_01_55939.d	0.957094	14	7	5
Leclercia sp. EP4-390	EP4-390	TSRR0003_E-12_A1p_P4-E-12_01_54680.d	0.729582	15	8	5
Leclercia sp. EP4-390	EP4-390	TSRR0003_F-03_A1p_P4-F-3_01_54681.d	0.892871	16	8	5
Leclercia sp. EP4-390	EP4-390	TSRR0003_E-11_A1p_P4-E-11_01_54679.d	0.8741	17	8	5
Bacillus sp. EP6-816	EP6-816	TSRR0003_H-05_A1p_P4-H-5_01_54756.d	0.782622	18	9	5
Bacillus tequilensis EP5-661	EP5-661	TSRR0003_G-09_A1p_P4-G-9_01_54731.d	0.956815	18	9	5
Bacillus tequilensis EP5-661	EP5-661	TSRR0003_G-10_A1p_P4-G-10_01_54732.d	0.946889	18	9	5
Bacillus sp. EP6-816	EP6-816 rem	TSRR0003_H-07_rem_A1p_P4-H-7_01_55570.d	0.900967	18	9	5
Bacillus sp. EP6-816	EP6-816	TSRR0003_H-06_A1p_P4-H-6_01_54760.d	0.876308	19	9	5
Bacillus tequilensis EP5-661	EP5-661	TSRR0003_G-11_A1p_P4-G-11_01_54733.d	0.79211	20	10	5
Pseudomonas balearica EP13-447	EP13-447	TSRR0003_F-07_A1p_P4-F-7_01_54702.d	0.611993	21	11	6
Pseudomonas balearica EP13-447	EP13-447	TSRR0003_F-08_A1p_P4-F-8_01_54703.d	0.970532	21	11	6
Bacillus sp. EP13-438	EP13-438	TSRR0003_F-06_A1p_P4-F-6_01_54700.d	0.912345	21	11	6

Bacillus sp. EP13-438	EP13-438	TSRR0003_F-04_A1p_P4-F-4_01_54696.d	0.849307	22	11	6
Bacillus sp. EP13-438	EP13-438	TSRR0003_F-05_A1p_P4-F-5_01_54697.d	0.897763	23	11	6
Pseudomonas balearica EP13-447	EP13-447	TSRR0003_F-09_A1p_P4-F-9_01_54705.d	0.808288	24	11	6
Bacillus thuringiensis EP6-44	EP6-44	TSRR0003_A-10_A1p_P4-A-10_01_54613.d	0.416388	25	12	7
Bacillus thuringiensis EP6-44	EP6-44	TSRR0003_A-09_A1p_P4-A-9_01_54612.d	0.995294	25	12	7
Bacillus thuringiensis EP6-44	EP6-44	TSRR0003_A-11_A1p_P4-A-11_01_54614.d	0.991094	25	12	7
Medium Control	Medium Control rep2	TSRR0005-03_A1p_P1-A-3_01_59089.d	0.562337	26	13	8
Medium Control	Medium Control rep2	TSRR0005-02_A1p_P1-A-2_01_59088.d	0.989265	26	13	8
Medium Control	Medium Control rep2	TSRR0005-01_A1p_P1-A-1_01_59087.d	0.92888	26	13	8
Medium Control	Medium Control	TSRR0003_A-05_A1p_P4-A-5_01_54608.d	0.702332	27	14	8
Medium Control	Medium Control	TSRR0003_A-04_A1p_P4-A-4_01_54607.d	0.57114	28	15	9
Medium Control	Medium Control	TSRR0003_A-03_A1p_P4-A-3_01_54606.d	0.810841	29	15	9
Bacillus sp. EP6-195	EP6-195	TSRR0003_C-06_A1p_P4-C-6_01_54654.d	0.242599	30	16	10
Bacillus sp. EP6-195	EP6-195	TSRR0003_C-05_A1p_P4-C-5_01_54653.d	0.982618	30	16	10
Bacillus sp. EP6-195	EP6-195	TSRR0003_C-04_A1p_P4-C-4_01_54628.d	0.978819	30	16	10
Lysinibacillus sp. EP1-81	EP1-81	TSRR0003_B-10_A1p_P4-B-10_01_54623.d	0.888261	31	16	10
Lysinibacillus sp. EP1-81	EP1-81	TSRR0003_B-09_A1p_P4-B-9_01_54622.d	0.962261	31	16	10
Lysinibacillus sp. EP1-81	EP1-81	TSRR0003_B-08_A1p_P4-B-8_01_54621.d	0.886927	32	16	10
Bacillus sp. EP1-11	EP1-11	TSRR0003_A-07_A1p_P4-A-7_01_54610.d	0.693656	33	17	11
Bacillus sp. EP1-11	EP1-11	TSRR0003_A-08_A1p_P4-A-8_01_54611.d	0.912174	33	17	11
Bacillus sp. EP1-11	EP1-11	TSRR0003_A-06_A1p_P4-A-6_01_54609.d	0.875067	34	17	11
Bacillus sp. EP6-816	EP6-816	TSRR0003_H-07_A1p_P4-H-7_01_54761.d	0.179614	35	18	12
Brevibacterium sp. EP14-508	EP14-508	TSRR0003_G-05_A1p_P4-G-5_01_54727.d	0.074954	36	19	13
Brevibacterium sp. EP14-508	EP14-508	TSRR0003_G-03_A1p_P4-G-3_01_54725.d	0.854807	37	19	13
Brevibacterium sp. EP14-508	EP14-508	TSRR0003_G-04_A1p_P4-G-4_01_54726.d	0.822315	38	19	13

Strains are indicated by their internal identifier. Metabolic groups according to the chemical diversity are given for a similarity threshold of 0.9, 0.8 and 0.7, respectively

Table 10.10. Inspected metabolic groups (n=3)

Strain	Metabolic group
EP4-170	1
EP7-199	1
EP10-210	1
EP7-200 rep	1
EP5-815	1
EP7-277	2
EP6-454	2
EP6-817	3
EP13-298.1	4
EP6-195 rep2-1	5
EP8-203	6
EP1-654	7
EP13-296.3	8
EP1-79	9
EP10-67	10
EP10-208	11
EP6-816 rep	12
EP4-390	13
EP6-816	14
EP5-661	14
EP13-447	15
EP13-438	15
EP6-44	16
Medium Control	
EP1-81	17
EP1-11	18
EP14-508	19

Table 10.11. Antibacterial activity of selected strains against Gram-negative (*E. coli*) and Gram-positive bacteria (*M. luteus*) in 10 different media

No	Strain	200				203				654				815				816			
		1		2		1		2		1		2		1		2		1		2	
	Media	**Ec**	**Ml**	**Ec**	**Ml**	**Ec**	**Ml**	**Ec**	**Ml**	**Ec**	**Ml**	**Ec**	**Ml**	**Ec**	**Ml**	**Ec**	**Ml**	**Ec**	**Ml**	**Ec**	**Ml**
1	Flam+Asw	NT	NT	-	+++	NT	NT	-	++	NT	NT	-	-	NT	NT	-	+++	NT	NT	-	+++
2	ISP2+NaCl	+++	++	-	+++	-	+++	-	+++	NT	NT	-	+++	NT	NT	-	+	NT	NT	-	+
3	LB	NT	NT	-	+++	NT	NT	-	+++	NT	NT	-	+	NT	NT	+	+++	NT	NT	-	+++
4	LB+ASW	NT	NT	-	16	NT	NT	-	+++	NT	NT	-	++	NT	NT	-	+++	NT	NT	-	+++
5	MB	NT	NT	-	-	NT	NT	-	+++	NT	NT	-	-	NT	NT	-	+	NT	NT	-	+
6	MYE	NT	NT	-	++	NT	NT	-	+++	NT	NT	+++	++	NT	NT	-	++	NT	NT	-	+
7	NA	NT	NT	-	++	NT	NT	-	++	-	++++	-	++	-	++	+	+++	-	+++	-	+++
8	SNA+ASW	NT	NT	-	+	NT	NT	-	-	NT	NT	-	-	NT	NT	-	+	NT	NT	-	++
9	TSA	NT	NT	-	+++	NT	NT	-	++	NT	NT	-	-	NT	NT	-	+++	NT	NT	-	++
10	ISP2	NT	NT	+	+++	NT	NT	++	+++	NT	NT	-	+	NT	NT	-	++	NT	NT	-	++

1 : First screening + : weak activity - : no activity Ml : *Micrococcus luteus*

2 : Second screening ++ : moderate activity NT : Not tested Ec : *Escherichia coli*

+++ : strong activity

Table 10.12. MIC values of surfactins and macrolactin A (all MIC values were obtained from three independent measurements, n = 3).

Tested cpd	MIC (µg/mL)					
	E. coli **ATCC 25922 wild type**	***E. coli*** **ATCC 25922 ΔTolC**	***B. subtilis*** **DSM 10 wild type**	***S. aureus*** **ATCC 25923 MSSA**	***S. aureus*** **ATCC 33592 MRSA**	***L. monocytogenes*** **DSM 20600 wild type**
1: C14 surfactin (n=3)	> 128	> 128	> 128	> 128	> 128	> 128
2: C15 surfactin (n=3)	> 128	> 128	> 128	> 128	> 128	> 128
3: C16 surfactin (n=3)	> 128	> 128	> 128	> 128	> 128	> 128
4: C17surfactin (n=3)	> 128	> 128	> 128	> 128	> 128	> 128
5: Macrolactin A (n=3)	> 128	> 128	> 128	4-8	2-4	2-32
Gentamycin control (n=3)	0.25-1	0.125-0.5	≤ 0.063	0.125	0.125-0.25	0.063

Table 10.13. Combination effect between macrolactin A and C14 surfactin

Cpd	***E. coli* ATCC25922**	***B. subtilis* DSM10**	***S. aureus* ATCC33592(MRSA)**
C14 surfactin	Not active	Not active	Not active
Macrolactin A	Not active	Not active	Active
Combination	No effect	No effect	Synergistic effect

Table 10.14. ^{1}H, HSQC and HMBC for compound 6.4 (AV 400, DMSO-d6)

δ H [ppm]	Multiplicity	J [Hz]	Integral	δ C [ppm]	Signal phase HSQC	Assignment of **CH**	HMBC coupling with	Assignment of $\mathbf{C_q}$
8.27	s	/	1H	152.7 (from HMBC; not visible in HSQC)	/ (152.7 from HMBC; not visible in HSQC)	2	174.7, 157.5, 123.4	4, 8a, 3
7.94	d	8.76	1H	127.2	+ → CH	5	174.7, 163.2, 157.5	4, 7, 8a
7.38	d	8.60	2H	130.1	+ → 2 x CH	2' + 6'	157.1, 130.1, 123.4	4', 2' + 6', 3
6.91	dd	8.78 2.02	1H	115.4	+ → CH	6	102.1, 116.3	8, 4a
6.83	d	2.00	1H	102.1	+ → CH	8	~~(114.9),~~ 163.2, (157.5)	~~(3' + 5'),~~ 7, (8a)
6.80	d	8.56	2H	114.9	+ → 2 x CH	3' + 5'	157.1, 122.6, 114.9	4', 1', 3' + 5'

Table 10.15. ^{1}H, HSQC, COSY, HMBC for compound 6.5 (AV 400. DMSO-d6)

δ H [ppm]	Multiplicity	J [Hz]	Integral	δ C [ppm]	Signal phase HSQC	COSY coupling with	Assignment of **CH**	HMBC coupling with	Assignment of **C_q**
8.11	s	/	1 H	/	/	/	OH?	/	
7.36	d	7.26	2 H	130.5	+ → 2 x CH	d (= 6.78)	6', 2'	157.4; 130.6; 123.9	4', 6' & 2', 1' (or 3)
7.26	s	/	1 H	104.2	+ → CH	/	5? (or8??)	/	
6.78	d	7.56	2 H	115.4	+ → 2 x CH	b (= 7.36)	5', 3'	123.9	1'
3.80	s	/	3 H	55.8	+ → CH_3	/	9	149.3	6
3.75	s	/	1 H	59.0	+ → CH	/	Unknown compound	/	Unknown compound
~~1.88~~	~~d (oder m?)~~	~~6.18~~	~~1 H~~	~~38.2; 18.7~~	~~+ → CH~~	~~k (= 0.93); 2.20~~	Unknown compound	~~/~~	Unknown compound
1.44	s	/	1 H	21.4	+ → CH	/	Unknown compound	139.5; 128.4; (40.1)	Unknown compound
~~1.23~~	~~s~~	~~/~~	~~1 H~~	~~29.4~~	~~- → CH_2~~	~~/~~	Unknown compound	~~/~~	Unknown compound
1.04	s	/	1 H	29.4	+ → CH	/	Unknown compound	139.4; 48.2; 36.2; 30.1	Unknown compound
0.93	d	6.90	1 H	15.5	+ → CH	/	Unknown compound	59.0; 38.3; 24.9	Unknown compound
0.87	s	/	1 H	30.0	+ → CH	/	Unknown compound	139.4; 48.2; 36.2; 29.6	Unknown compound
0.84	t?	7.47	1 H	12.4	+ → CH	/	Unknown compound	38.3	Unknown compound

Curriculum Vitae

The curriculum vitae was removed from the electronic version of the paper.

PUBLICATIONS

Riyanti; Marner, M.; Hartwig, C.; Patras, M.; Wodi, S.; Rieuwpassa, F.; Ijong, F.; Balansa, W.; Schäberle, T. Sustainable Low-Volume Analysis of Environmental Samples by Semi-Automated Prioritization of Extracts for Natural Product Research (SeaPEPR)**.** *Mar. Drugs* 2020, *18*, 649, doi:10.3390/md18120649.

Riyanti; Balansa, W.; Liu, Y.; Sharma, A.; Mihajlovic, S.; Hartwig, C.; Leis, B.; Rieuwpassa, F.J.; Ijong, F.G.; Wägele, H.; et al. Selection of sponge-associated bacteria with high potential for the production of antibacterial compounds. *Sci Rep* 2020, *10*, 19614, doi:10.1038/s41598-020-76256-2.

Sabdaningsih, A.; Liu, Y.; Mettal, U.; Heep, J.; **Riyanti**; Wang, L.; Cristianawati, O.; Nuryadi, H.; Triandala Sibero, M.; Marner, M.; Radjasa, O.K.; Sabdono, A.; Trianto, A.; Schäberle, T.F. A New Citrinin Derivative from the Indonesian Marine Sponge-Associated Fungus *Penicillium citrinum*. *Mar. Drugs* 2020, *18*, 227. DOI: 10.3390/md18040227.

Ayuningrum D, Liu Y, **Riyanti**, Sibero MT, Kristiana R, Asagabaldan MA, Wuisan ZG, Trianto A, Radjasa OK, Sabdono A, Schäberle TF (2019). Tunicate-associated bacteria show a great potential for the discovery of antimicrobial compounds. PLoS ONE 2019, 14(3). DOI: 10.1371/journal.pone.0213797.

Syakti, A. D., Lestari, P., Simanora, S., Sari, L. K., Lestari, F., Idris, F., Agustiadi, T, Akhlus, S, Hidayati, N.V, **Riyanti** (2019). Culturable hydrocarbonoclastic marine bacterial isolates from Indonesian seawater in the Lombok Strait and Indian Ocean. *Heliyon* 5. doi:10.1016/j.heliyon.2019.e01594.

Riyanti, Rahmawati, M., Hidayati, N. V., Syakti, A. D., and Radjasa, O. K. (2018). Analysis of Carotenoids and Identification of Mangrove Sediment Bacteria of. *Indones. J. Mar. Sci.* 23, 163–170. doi:10.14710/ik.ijms.23.4.163-170.

Riyanti, R., Nurkhasanah, W., and Radjasa, O. K. (2016). Diversity and Antifungal Activity of Actinomycetes Symbiont Hard Coral Mucus of Genera Goniopora and Porites. *Makara J. Sci.* 20, 193–198. doi:10.7454/mss.v20i4.6707.

Riyanti, J., Widada, O.K. Radjasa. 2009. Isolation and Screening of Antimicrobial Producing-Actinomycetes Symbiont in Nudibranch. *Indon. J. Biotechnol,* 14(1): 11321138.

PROJECTS

Diversity of Secondary Metabolite Biosynthetic Genes of Cultivable Marine Actinomycetes Isolated from Segara Anakan Cilacap. Indonesian Toray Science Foundation. 2015.

Screening of Natural Antibiotic from marine actinomycetes symbiont in marine sediment Segara Anakan Waters, Cilacap, Central Java. 2013-2014.RISIN-DIPA UNSOED.

Cloning and Sequensing PKS I/NRPS gene of Marine Actinomycetes Producing Antioxidant Activity. 2012-2013.PEKERTI GRANT-DIKTI.

Genetic Diversity of Actinomycetes Symbiont in Soft Coral, Seagrass and Seaweed. 2011.DIPA UNSOED.

Bleaching of Coral *Goniopora* sp. on Different Salinity and Lighting. 2007. YOUNG SCIENTIST DIKTI.

SEMINARS

Riyanti et al. 2019. Isolation and Screening of Antimicrobial Compounds Producing Bacteria Associated with Sponges. Biology of Microorganisms Producing Natural Product. International VAAM Workshop.

Riyanti et al. 2018. Co-culture Marine Sponge-Associated Bacteria as Resource for Novel Antibiotics. On the Biology of Bacteria Producing Natural Products International VAAM Workshop

Riyanti et al. 2017. Marine Sponge-Associated Bacteria as Resource for Novel Antibiotics. Biology of Bacteria Producing Natural Products International VAAM Workshop.

Riyanti., Hidayati, NV., Danny, RB., Radjasa, OK. 2013. Antibacterial potency of Actinomycete Symbionts in Seagrasses *Enhalus acoroides* Second International Conference on Alfred Russel Wallace and the Wallacea Wakatobi.

Riyanti and Hidayati, NV. 2011. Genetic Diversity of Actinomycetes Symbiont Soft Coral isolated from Pangandaran Coastal, West Java. National Seminar LPPM Unsoed.

Riyanti., Widada, J, Radjasa, OK. 2010. Utilization of Actinomycetes Associate with nudibranchs as a producer of antimicrobial. National Seminar “Marine and Fisheries. Development Strategy based on Environmental” (December 9, 2010). Pancasakti University,Tegal, Indonesia.